

Some pages of this thesis may have been removed for copyright restrictions.

If you have discovered material in AURA which is unlawful e.g. breaches copyright, (either yours or that of a third party) or any other law, including but not limited to those relating to patent, trademark, confidentiality, data protection, obscenity, defamation, libel, then please read our [Takedown Policy](#) and [contact the service](#) immediately

NITRIC OXIDE IN THE RAT GASTROINTESTINAL TRACT

KENNETH JOHN PRICE

**A thesis submitted for the degree of
DOCTOR OF PHILOSOPHY**

**THE UNIVERSITY OF ASTON IN BIRMINGHAM
January 1997**

This copy of the thesis has been supplied on condition that anyone who consults it is understood to recognise that its copyright rests with its author and that no quotation from the thesis and no information derived from it may be published without proper acknowledgment.

UNIVERSITY OF ASTON IN BIRMINGHAM
NITRIC OXIDE IN THE RAT GASTROINTESTINAL TRACT

by

KENNETH JOHN PRICE

**A thesis submitted for the degree of
DOCTOR OF PHILOSOPHY - 1997**

This study concerns the nature of nitric oxide synthase (NOS) and the role of nitric oxide (NO) in the rat gastrointestinal tract. The major objectives were (i) to characterise NOS isoforms in the gastric glandular mucosa, (ii) to localise NOS isoforms in the rat gastric glandular mucosa, (iii) to investigate the role of NO in carbachol-stimulated gastric mucus secretion, (iv) to investigate the nature of NOS activity induced by intravenous injection of lipopolysaccharide (LPS) in rat large and small intestine.

Immunoblotting was performed using polyclonal antisera raised against two peptides found in the rat brain NOS sequence and commercial monoclonal antibodies directed against neuronal and endothelial isoforms of NOS. A 160kDa band was detected in brain and gastric mucosal samples with antibodies and antisera directed against neuronal NOS sequences, and a 140kDa band was detected in gastric mucosal samples using an anti-endothelial NOS antibody. An intense 160kDa neuronal NOS band was detected in a high-density fraction of gastric mucosal cells separated on a Percoll gradient. Detection of neuronal NOS by a carboxyl-terminal antiserum in samples of brain, but not of gastric mucosa, could be blocked by the peptide (20µg/ml) against which the antibody was raised. After affinity purification, recognition of gastric mucosal NOS was blocked by peptide.

Particulate neuronal NOS was found in the brain by immunoblotting while 94% of gastric mucosal enzyme was soluble. Gastric mucosal endothelial NOS was 95% particulate. 95% of NOS activity in the gastric mucosa was due to neuronal NOS.

Paraformaldehyde- and acetone-fixed gastric mucosal sections were subject to immunocytochemistry using the above antibodies. Neuronal NOS was localised to the surface mucosal epithelial cells while endothelial NOS was associated with microvessels at the base of the mucosa and to larger vessels in the submucosa.

Intragastric administration of carbachol or 16, 16-dimethyl prostaglandin E₂ increased the thickness of the rat gastric mucus layer. The NOS inhibitor N^G-nitro-L-arginine methyl ester dose-dependently, and selectively, prevented the stimulatory effect of carbachol.

Ca²⁺-independent NOS activity in rat ileal, jejunal and colonic muscle was increased after LPS induction. Ca²⁺-dependent activity was not affected. Distribution of inducible NOS protein paralleled Ca²⁺-independent activity. LPS treatment did not affect the content of neuronal NOS in colonic muscle.

Key words: Nitric oxide, NO, nitric oxide synthase, gastric mucosa, mucus, lipopolysaccharide, colon, small intestine.

To my parents.

ACKNOWLEDGEMENTS

I would like to sincerely thank my supervisor, Dr Peter Hanson, for his help and guidance both in the preparation of this thesis and throughout the course of my studies at Aston.

I would also like to thank all the technical and animal house staff who have helped to ensure the smooth progress of my laboratory work and Clare Byrne for preparation of isolated cells and also for her company and good humour in the lab. Thanks also to all my other friends and colleagues at Aston for making my time at Aston an enjoyable one.

Finally I would like to thank my family for the support and encouragement they have given me throughout my academic career and also Alison for helping me through the preparation of this thesis.

TABLE OF CONTENTS

	<u>Page</u>
THESIS SUMMARY	2
DEDICATION	3
ACKNOWLEDGEMENTS	4
TABLE OF CONTENTS	5
LIST OF FIGURES	7
LIST OF TABLES	10
LIST OF PLATES	11
<u>CHAPTER 1: INTRODUCTION</u>	13
1.1 NITRIC OXIDE: GENERAL ASPECTS	14
1.2 STRUCTURE OF THE INTESTINAL TRACT	21
1.3 EFFECTS OF NITRIC OXIDE ON FUNCTIONS OF THE STOMACH	26
1.4 FUNCTIONING OF NITRIC OXIDE IN THE INTESTINE	34
1.5 SUMMARY OF AIMS OF THIS THESIS	35
<u>CHAPTER 2: GENERAL METHODOLOGY</u>	37
2.1 ASSAYS OF PROTEIN	38
2.2 ASSAYS FOR NOS ACTIVITY	40
2.3 POLYACRYLAMIDE GEL ELECTROPHORESIS	45
2.4 RAISING ANTIPEPTIDE ANTIBODIES	54
2.5 ISOLATION AND FRACTIONATION OF GASTRIC MUCOSAL CELLS	60
<u>CHAPTER 3: GASTRIC MUCOSAL NITRIC OXIDE SYNTHASES: ISOFORMS AND LOCALISATION</u>	61
3.1 INTRODUCTION	62
3.2 METHODS	70
3.3 RESULTS	75
3.4 DISCUSSION	100
<u>CHAPTER 4: LOCALISATION OF CONSTITUTIVE NITRIC OXIDE SYNTHASE IN THE GASTRIC GLANDULAR MUCOSA</u>	107
4.1 INTRODUCTION	108
4.2 METHODS	116

	<u>Page</u>
4.3 RESULTS	123
4.4 DISCUSSION	140
<u>CHAPTER 5: EFFECT OF NITRIC OXIDE ON MUCUS</u>	145
SECRETION IN THE STOMACH	
5.1 INTRODUCTION	146
5.2 METHODS	147
5.3 RESULTS	150
5.4 DISCUSSION	152
<u>CHAPTER 6: INDUCIBLE NITRIC OXIDE SYNTHASE IN THE</u>	155
COLON AND SMALL INTESTINE	
6.1 INTRODUCTION	156
6.2 METHODS	158
6.3 RESULTS	162
6.4 DISCUSSION	175
CHAPTER 7: GENERAL CONCLUSIONS	178
REFERENCES	182
APPENDICES	202
A1: ABBREVIATIONS	203
A2: SOURCE OF REAGENTS	204
A3: EQUIPMENT	206
A4: ANIMALS	207
A5: PILE UP OF AMINO ACIDS IN ISOFORMS OF NOS	207
A6: STATISTICAL TESTS USED TO COMPARE MUCUS	212
THICKNESS RESULTS	
A7: PUBLICATIONS RESULTING FROM THIS WORK	215

LIST OF FIGURES

<u>Figure</u>	<u>Page</u>
1.1 A: Schematic representation of cofactor recognition sites on NOS isoforms	16
1.1 B: Biosynthesis of NO	18
1.1 C: NOS inhibitors	19
1.2 A: Stomach	22
1.2 B: Gastric gland	23
1.3 A: Schematic illustration of gastric acid secretion	26
1.3 B: Bicarbonate secretion in gastric epithelial Cells (adapted from Allen et al., 1993)	29
2.1: Bicinchoninic acid protein assay reaction scheme	38
2.3 A: Electrophoretic transfer unit	49
2.3 B: ECL development reaction scheme	50
2.3 C: Oxidation of luminol by peroxidase to produce light	50
2.3 D: Densitometric analysis of immunoblots	53
2.4 Peptide-Bovine Serum Albumin conjugation reaction scheme	58
3.2: Peptide immobilisation on Sulpholink gel	73
3.3.1 A: Titres for antisera against an internal peptide of nNOS	75
3.3.1 B: Titres for antisera against a carboxyl-terminal peptide of nNOS	76
3.3.2.A: Immunoblotting with monoclonal anti-nNOS antibody	77
3.3.2.B: Immunoblotting with monoclonal anti-nNOS antibody	77
3.3.2 C: Immunoblotting with monoclonal anti-nNOS and anti-eNOS antibodies	78
3.3.2 D: Immunoblotting with monoclonal anti-eNOS antibody	79
3.3.3 A Immunoblotting with antiserum to carboxyl-terminal peptide of NOS \pm peptide (20 μ g/ml)	80
3.3.3 B: Immunoblotting with antiserum to carboxyl-terminal peptide of NOS \pm peptide (100 μ g/ml)	80
3.3.3 C: Immunoblotting with antiserum to carboxyl-terminal peptide of NOS \pm peptide (20 μ g/ml) on isolated cells	81

	<u>Page</u>
3.3.3 D: Immunoblotting with antiserum to carboxyl-terminal peptide of NOS \pm peptide (20 μ g/ml) on recombinant rat brain NOS	82
3.3.3 E: Immunoblotting with antiserum to carboxyl-terminal peptide of NOS on tissue homogenates showing removal of NOS after 2', 5' - ADP agarose	83
3.3.4 A: Immunoblotting with antiserum to carboxyl-terminal peptide of NOS \pm peptide (20 μ g/ml) on brain and pancreatic samples	84
3.3.4 B: Immunoblotting with antiserum to carboxyl-terminal peptide of NOS and monoclonal anti-nNOS antibody on gastric mucosal and pancreatic tissue homogenates	85
3.3.5 A: Immunoblot of brain versus gastric mucosa using monoclonal anti-nNOS antibody and anti-peptide antisera	86
3.3.5 B: Immunoblot of brain versus pancreas using monoclonal anti-nNOS antibody and anti-peptide antisera	87
3.3.6: Immunoblotting with antiserum to carboxyl-terminal peptide of NOS pretreated with a peptide-agarose or a cysteine-agarose affinity matrix	88
3.3.7 A: Immunoblotting with antiserum to carboxyl-terminal peptide of NOS \pm peptide (20 μ g/ml) using partially purified NOS	89
3.3.7 B: Quantification of block by the peptide of recognition of the 160kDa band by the antiserum directed against a carboxyl-terminal peptide of nNOS on crude tissue extracts or partially purified preparations of NOS	90
3.3.7 C: Immunoblotting with antiserum to carboxyl-terminal peptide of NOS \pm peptide (20 μ g/ml) on samples prepared over different time courses	92
3.3.8 A: Immunoblotting with anti-nNOS and anti-eNOS antibodies on subcellular fractions of tissue homogenates	96
3.3.8 B: Amount of nNOS or eNOS in subcellular fractions of tissue homogenates (% of total NOS) measured by densitometric analysis of immunoblots	95
3.3.8 C: NOS activity in subcellular tissue fractions (nmol/min/ml homogenate)	96
3.3.8 D: NOS activity in subcellular tissue fractions (nmol/min/mg protein)	97
3.3.8 E: NOS activity in subcellular tissue fractions (% of total activity)	98

	<u>Page</u>
3.3.8 F Proportions of NOS Activity in the whole gastric mucosa by the constitutive isoforms of NOS	99
3.4: Hypothesis to explain lack of peptide block of recognition by carboxyl-terminal antiserum of gastric mucosal nNOS	103
4.1: ABC method of immunocytochemistry	114
4.2: Mounting of gastric mucosal tissue on cryostat chuck	117
5.2: Measurement of gastric mucus thickness	149
5.3 A: Mucus thickness in gastric glandular mucosa after administration of various agents	151
5.3 B: Dose-response curve of the effect of L-NAME on the increase of mucus secretion by carbachol	152
6.3.1 A: Effect of EGTA in homogenisation buffer on Ca^{2+} -dependency of NOS activity induced by NOS in the colonic mucosa	163
6.3.1 B Effect of EGTA at various concentrations in homogenisation buffer on NOS Activity Induced by LPS in Colonic Mucosa	164
6.3.1 C: Investigation of the effect of the presence of EDTA, during homogenisation, on Ca^{2+} Dependence of NOS Activity in colonic mucosa from rats induced with LPS	165
6.3.2 A: Total and Ca^{2+} -independent NOS activity in muscles of the intestinal tract	166
6.3.2 B: Graph showing Ca^{2+} -dependent NOS Activity in muscles of intestinal tract	167
6.3.2 C: Proportion of Ca^{2+} -dependent NOS activity in muscles of the gastrointestinal Tract	168
6.3.2 D: Immunoblotting with monoclonal anti-iNOS antibody	169
6.3.2 E: Immunoblotting with monoclonal anti-nNOS antibody	170
6.3.2 F: Standard curve for NOS content from immunoblotting	171
6.3.2 G: NOS protein content in colonic mucosa	172
6.3.2 H: Correlation of nNOS content with Ca^{2+} -dependent NOS activity in colon	173
6.3.2 I: Protein content in samples of muscles from the intestinal tract	174

LIST OF TABLES

Table	<u>Page</u>
2.2: Constituents of assay buffers used for assays of NOS activity	43
2.3 A: Make up of separating gel	47
2.3 B: Make up of stacking gel	47
2.4: Immunisation timetable	55
3.1 A: Tissues/cells giving positive results on immunoblotting with antibodies/antisera directed against nNOS	62
3.1 B: Tissues/cells giving positive results on immunoblotting with antibodies/antisera directed against eNOS	65
3.1 C: Tissues/cells giving positive results on immunoblotting with antibodies/antisera directed against iNOS	66
3.1 D: Sequences of peptides used in raising antisera	69
3.3.7 A: Effect of preparation procedures on the ability of the peptide to block the 160kDa band recognised by carboxyl-terminal antiserum in gastric mucosal material	91
3.3.7 B: Effect of protein phosphatase inhibitors on block by peptide of recognition of the 160kDa band by carboxyl-terminal antiserum in 100,000 x g_{av} supernatant of gastric mucosal homogenates	93
4.1 A: Summary of major studies localising NOS thought to be the neuronal Form	108
4.1 B: Summary of major studies localising NOS thought to be the endothelial Form	111
6.1: Ca^{2+} chelators in homogenisation buffers used by previous studies	157
6.2 A: Variation of EGTA concentration in homogenisation buffer	159
6.2 B: [EGTA] and [Ca^{2+}] values calculated to give an equal free [Ca^{2+}] in assay mixtures for homogenates of different [EGTA]-Experiment 1	160
6.2 C: Variation of [Ca^{2+}] in Assay Buffer - Experiment 1	160
6.2 D: [EGTA] and [Ca^{2+}] values calculated to give an equal free [Ca^{2+}] in assay mixtures for different homogenates - Experiment 2	161

LIST OF PLATES

<u>Series/ Plate</u>	<u>Page</u>
<u>4.3.1:</u> <u>Immunocytochemistry with antiserum to the internal peptide of nNOS and controls (acetone-fixed)</u>	127
4.3.1 A: Antiserum to the internal peptide of nNOS - Gastric Mucosa	127
4.3.1 B: Pre-immune serum - Gastric Mucosa	127
4.3.1. C: Antiserum to the internal peptide of nNOS+ peptide - Gastric Mucosa	127
4.3.1.D: Affinity column wash - Gastric Mucosa	128
<u>4.3.2</u> <u>Antiserum to the carboxyl-terminal peptide of nNOS and controls (acetone-fixed)</u>	129
4.3.2 A: Carboxyl-terminal antiserum - gastric mucosa	129
4.3.2 B: Pre-immune serum - Gastric Mucosa	129
4.3.2 C: Carboxyl-terminal antiserum + peptide - Gastric Mucosa	129
4.3.2 D: Carboxyl-terminal antiserum - Duodenum	130
<u>4.3.3:</u> <u>Polyclonal anti-nNOS antibody, control and validation (acetone-fixed)</u>	131
4.3.3 A: Polyclonal anti-nNOS antibody - Gastric Mucosa	131
4.3.3 B: Rabbit IgG - Gastric Mucosa	131
4.3.3 C: Polyclonal anti-nNOS antibody - Brain	131
<u>4.3.4 :</u> <u>Monoclonal anti-nNOS antibody and controls (acetone Fixed)</u>	132
4.3.4 A: Monoclonal anti-nNOS antibody - Gastric Mucosa	132
4.3.4 B: Mouse IgG - Gastric Mucosa	132
4.3.4 C: Monoclonal anti-nNOS antibody - Duodenum	133
4.3.4 D: Monoclonal anti-nNOS antibody - Isolated Gastric Mucosal cells	133
<u>4.3.5:</u> <u>Monoclonal anti-nNOS antibody and controls (paraformaldehyde fixed)</u>	134
4.3.5 A: Monoclonal anti-nNOS antibody - Gastric Mucosa	134
4.3.5 B: Monoclonal anti-nNOS antibody - Gastric Mucosa	134
4.3.5 C: Monoclonal anti-nNOS antibody - Gastric Mucosa	134
4.3.5 D: Monoclonal anti-nNOS antibody + recombinant NOS - Gastric Mucosa	134
4.3.5 E: Monoclonal anti-nNOS antibody - Gastric Muscle	135
4.3.5 F: Monoclonal anti-nNOS antibody - Duodenum	135
<u>4.3.6:</u> <u>Anti-eNOS antibody and Controls (paraformaldehyde fixed)</u>	136
4.3.6 A: Anti-eNOS antibody - Gastric Mucosa	136

	<u>Page</u>
4.3.6 B: Anti-eNOS antibody - Gastric Mucosa	136
4.3.6 C: Anti-eNOS antibody - Gastric Mucosa	136
4.3.6 D: Anti-eNOS antibody - Gastric Muscle	136
4.3.6 E: Anti-eNOS antibody - Aorta	137
4.3.6 F: Mouse IgG - Aorta	137
<u>4.3.7:</u> <u>Anti iNOS antibody</u>	138
<u>4.3.8:</u> <u>NADPH Diaphorase staining</u>	139
4.3.8 A: NADPH Diaphorase on acetone fixed gastric mucosa	139
4.3.8 B: NADPH Diaphorase on paraformaldehyde fixed gastric mucosa	139
4.3.8 C: Anti-nNOS monoclonal antibody - Gastric Mucosa	139
4.3.8 D: Anti-mucin antibody - Gastric Mucosa	139

CHAPTER 1

GENERAL INTRODUCTION

This chapter is intended as a general introduction to nitric oxide and gastrointestinal function. Chapters 3-6, which describe studies carried out to investigate various aspects of nitric oxide in the gastrointestinal tract, contain short introductory sections which relate more specifically to the work carried out in each study. Since most of the work carried out in this thesis investigates nitric oxide in the gastric glandular mucosa the structure and function of the stomach is described below in more detail than that of the rest of the gastrointestinal tract. Specific aims of the thesis are summarised at the end of this chapter and are also restated in the appropriate place in the chapters which follow.

1.1 NITRIC OXIDE: GENERAL ASPECTS

Where specific references are not given, information can be found in the following reviews: Moncada et al. (1991), Stark et al. (1992), Schmidt et al. (1993), Feldman et al. (1993), Bredt and Snyder (1994), Nathan and Xie (1994), Marletta (1993), Stamler, (1994), Aoki et al. (1995), and Forstermann et al. (1995)

1.1.1 Introduction

Nitric oxide (NO) is a small molecule and an unstable free radical gas with a large and expanding range of biological activities. NO exhibits the lowest molecular weight of any mammalian cell secretory product with biological activity. NO is an unusual mediator in that it is not stored, being manufactured and secreted on demand, nor does it exert its actions via typical membrane-bound receptors. NO has a half-life of only a few seconds being oxidised by reaction with oxygen to nitrite or nitrate and therefore uptake mechanisms are not necessary to control removal of NO. NO is membrane-permeable and therefore can readily diffuse into target cells and because of its short half-life probably has very local actions although some estimates have suggested actions over 200µm (Wood and Garthwaite, 1996). NO is also able to act as a neurotransmitter in both the central and peripheral nervous systems and is involved in the regulation of blood pressure as

endothelium-derived relaxing factor and has an immunological role in destroying pathogens when released from activated macrophages.

1.1.2 NO Biosynthesis

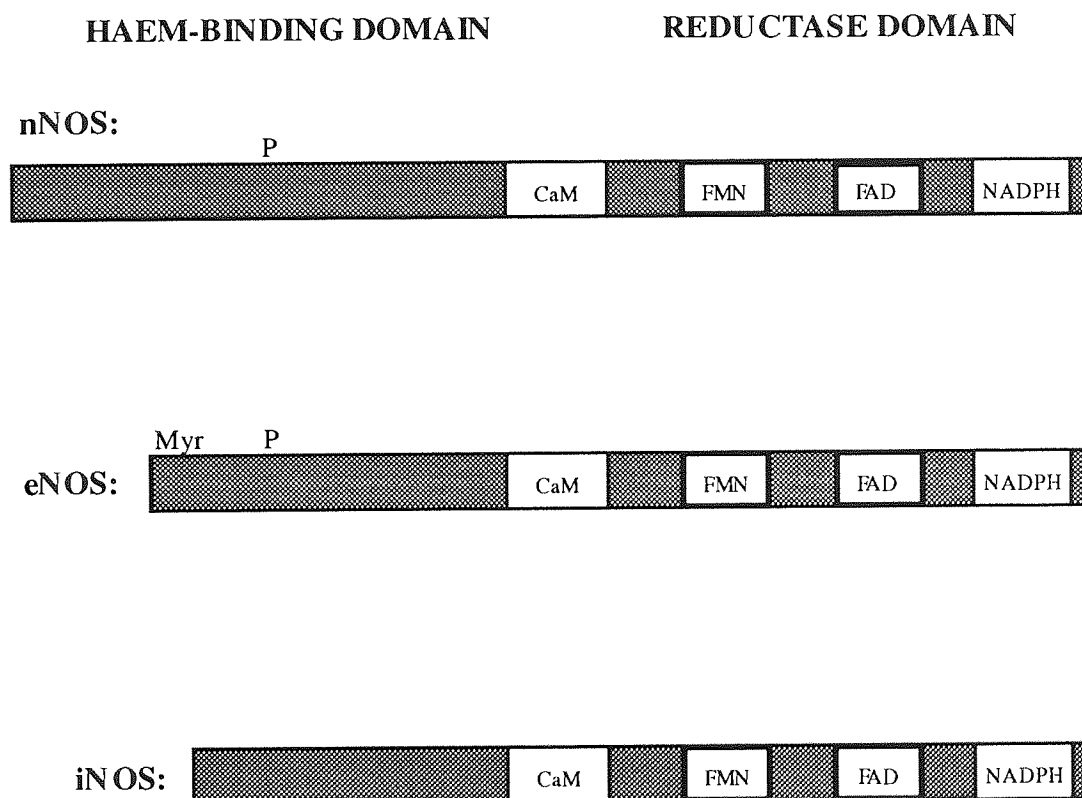
1.1.2.1 NOS isoforms

NO is synthesised *in vivo* by one of three NO-synthase (NOS) isoforms. While a variety of naming schemes are used to identify the three isoforms of NOS (Forstermann et al., 1995), in this study the enzymes will be referred to as nNOS, eNOS and iNOS. nNOS and eNOS are constitutively expressed and Ca^{2+} -dependent, produce low levels of NO (pmoles) and are so named because the prototypical enzymes are present in neurons and vascular endothelial cells respectively. iNOS is not normally present in cells but expression is induced by cytokines, bacterial lipopolysaccharide or *Propionibacterium acnes*. iNOS is largely or completely Ca^{2+} -independent and produces high levels of NO (nmoles). The prototypical iNOS enzyme is expressed in murine macrophages and therefore it is also commonly described as macNOS.

nNOS has a molecular mass of 155-160kDa and was first purified from rat and porcine cerebellum (Bredt et al., 1990). nNOS was initially thought of as a predominantly soluble enzyme in brain (Forstermann et al., 1991b; Schmidt et al., 1991; Bredt et al., 1990) although more recently some particulate activity has been detected in the presence of FAD in brain (Hiki et al., 1992; Hecker et al., 1994), and nNOS in skeletal muscle is largely membrane bound (Kobzik et al., 1994). eNOS has a molecular mass of approximately 135kDa and is predominantly particulate (Forstermann et al., 1991a; Hecker et al., 1991) due to myristoylation at the N-terminal glycine and nearby palmitoylation (Robinson & Michel 1995) which anchors the enzyme to membranes. eNOS was first cloned from bovine and human endothelial cells (Lamas et al., 1992; Marsden et al., 1992) and shares 60% homology with nNOS. iNOS, which is also a predominantly soluble enzyme was first isolated from murine macrophages (Hevel et al., 1991; Stuehr et al., 1991), has

a molecular mass of approximately 130kDa and shares 50% homology with nNOS. One aim of this thesis was to identify the forms of NOS and their localisation in rat gastric mucosa.

Figure 1.1 A: Schematic representation of cofactor recognition Sites on NOS isoforms



Legend to Figure 1.1 A

Cofactor recognition sites on the three isoforms of NOS. CaM = Calmodulin binding site. FMN, FAD, NADPH = binding sites for these cofactors. P = Protein kinase A phosphorylation site. Myr = Myristoylation site.

All NOS isoforms consist of two domains, a reductase domain which is similar to cytochrome P-450 reductase and a haem-binding or oxygenase domain. All three isoforms of NOS have flavin adenine dinucleotide (FAD), flavin mononucleotide

(FMN) and haem iron bound as prosthetic groups. The cofactor recognition sites for FMN and FAD are illustrated diagrammatically in Figure 1.1 A. The haem binding site is not shown but is found in the haem-binding domain. Also shown in Figure 1.1 A are binding sites for calmodulin (CaM) and β -nicotinamide adenine dinucleotide (β -NADPH). Also shown in Figure 1.1 A is the position of the consensus protein kinase A phosphorylation site in nNOS and eNOS and the myristoylation site in eNOS. Binding sites also exist in NOS protein for L-arginine and tetrahydrobiopterin.

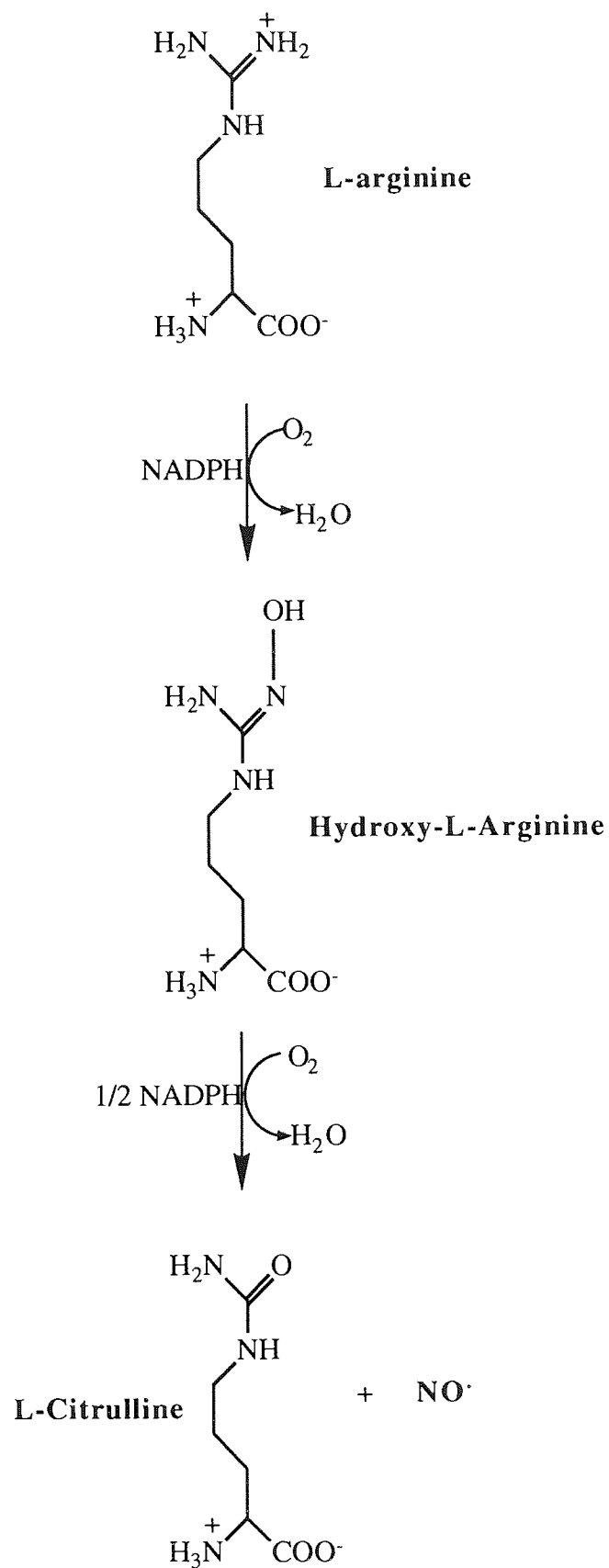
Aligned amino acid sequences for the various NOS isoforms are given in Appendix A5.

1.1.2.2 NO formation

NOS produces NO by a five electron oxidation of the guanido-nitrogen of L-arginine with L-citrulline produced as a co-product. The reaction is shown in Figure 1.1 B and involves two steps. The first step is a two electron oxidation of L-arginine to L-hydroxyarginine and the second step is a three electron conversion of L-hydroxyarginine producing NO and L-citrulline. L-arginine, β -NADPH, and O_2 and the cofactors/prosthetic groups FAD, FMN, calmodulin, tetrahydrobiopterin and haem are all required for NO synthesis.

Before activation by calmodulin, and in the presence of sufficient levels of substrates and cofactors, all three isoforms of NOS exist as homodimers (head to tail orientation). Calmodulin binding which induces a conformational change in the NOS homodimer is the critical factor in NOS activation (Su et al., 1995). Thus binding of calmodulin, which allows electron flow to take place, to the two constitutive isoforms of NOS takes place due to a rise in intracellular Ca^{2+} concentration whereas calmodulin is tightly bound to iNOS even at resting Ca^{2+} concentrations. Therefore the main switch for eNOS and nNOS activation is the concentration of intracellular Ca^{2+} whereas the main switch for iNOS activity is the level of its mRNA. Thus, once iNOS expression is induced by LPS or cytokines

Figure 1. 1 B: Biosynthesis of NO



the concentration of Ca^{2+} in resting cells is sufficient to maintain NO synthesis by the enzyme. The expression of iNOS can be prevented by dexamethasone.

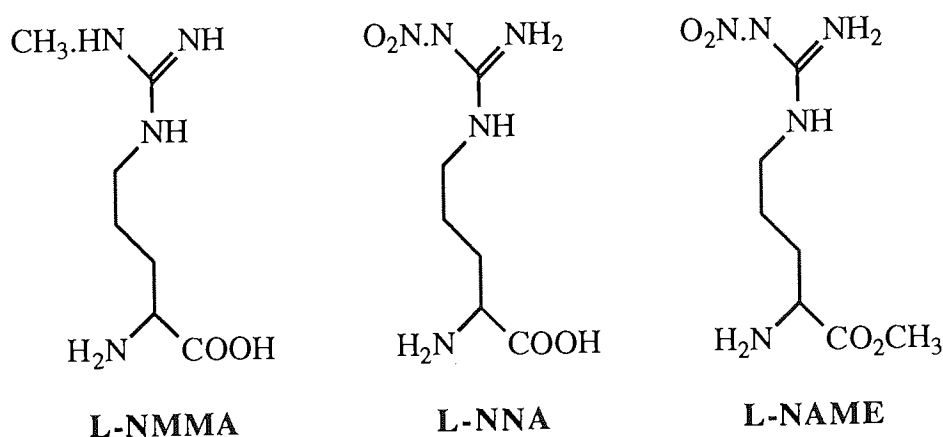
1.1.2.3 Regulation of NO activity by phosphorylation

Phosphorylation is another method of regulating NOS activity. Phosphorylation of nNOS by cAMP-dependent protein kinase, protein kinase C, cGMP-dependent protein kinase, and Ca^{2+} /calmodulin-dependent protein kinase has been shown to decrease enzyme catalytic activity (Bredt et al., 1990; Nakane et al., 1991; Brune et al., 1991). Furthermore, phosphorylation of eNOS is associated with both translocation of the enzyme from the soluble to the particulate fraction and a decrease in activity of the enzyme (Michel et al., 1993).

1.1.2.3 Inhibition of NOS

All isoforms of NOS can be inhibited by analogues of L-arginine such as N^G -monomethyl-L-arginine (L-NMMA), N^G -nitro-L-arginine (L-NNA), and the methyl ester of L-NNA (L-NAME) the structures of which are shown in Figure 1.1 C. The effect of these inhibitors can be overcome by L-arginine itself.

Figure 1.1 C: NOS inhibitors



1.1.3 Targets for action of NO

NO reacts in biological systems with O_2 , the superoxide radical ($O_2^{\cdot -}$) and transition metals. The products of these reactions support further nitrosative reactions, i.e. S-nitrosothiol formation. Major targets for NO are signalling proteins, ion channels, receptors, transcription factors and enzymes which contain either transition metals or thiols strategically located at either allosteric or active sites.

The main physiological target for NO produced by eNOS and nNOS is soluble guanylate cyclase which catalyses the conversion of guanosine triphosphate (GTP) to the cellular second messenger cyclic guanosine monophosphate (cGMP). NO activates soluble guanylate cyclase by binding to the haem iron in its active site and causing a conformational alteration. The cGMP produced by soluble guanylate cyclase after activation by NO can act to alter cellular responses by regulation of cGMP-gated cation channels, regulation of cAMP-phosphodiesterases or activation of cGMP-dependent protein kinases.

The higher amounts of NO produced by iNOS are cytotoxic mainly due to oxidation of lipids and thiols in key enzymes by NO itself, or by peroxynitrite ($ONOO^-$) formed from the reaction of NO with $O_2^{\cdot -}$. The importance of peroxynitrite in the cytotoxic actions of NOS is apparent when cytotoxicity is attenuated by superoxide dismutase which removes the superoxide radicals necessary for formation of peroxynitrite. Major targets in the cytotoxicity due to NO are aconitase, an important enzyme in the Krebs cycle, and complex I and II of the mitochondrial electron transport chain all of which are inhibited therefore severely disrupting the target cells' energy supply. NO also acts to inhibit ribonucleotide reductase, therefore preventing the formation of precursors for DNA synthesis.

1.2 STRUCTURE OF THE GASTROINTESTINAL TRACT

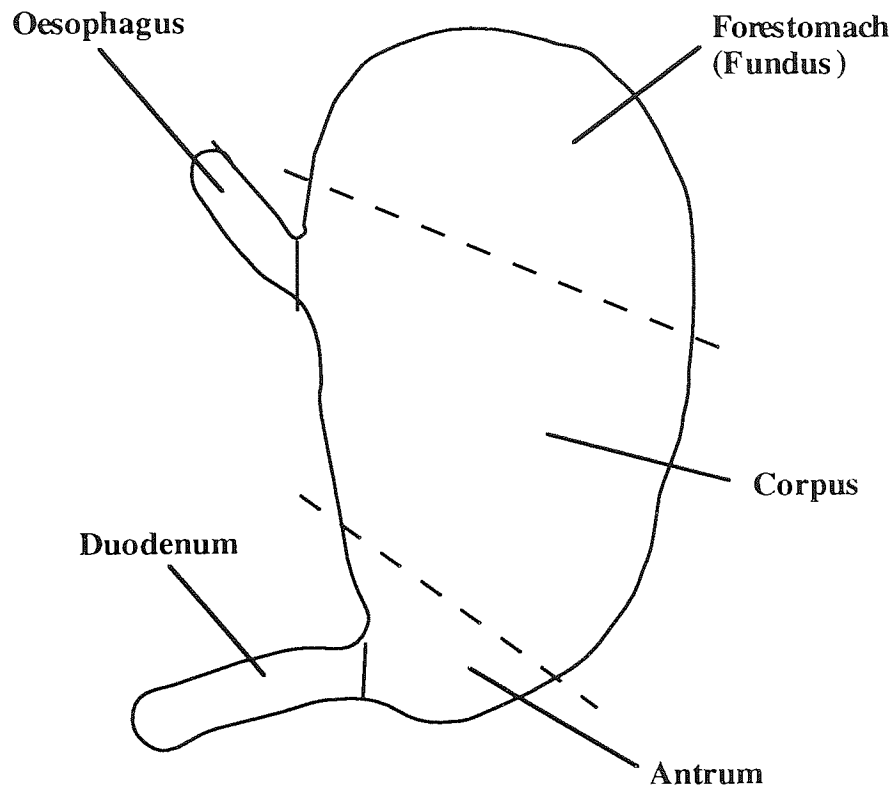
1.2.1 Basic structure

The entire length of the gastrointestinal tract has the same basic structure. The first layer on the luminal side of the gastrointestinal wall is the mucosa. The mucosa consists of an epithelium which covers the entire luminal surface of the intestine and contains both exocrine and endocrine cells, below which is the lamina propria which is a layer of connective tissue throughout which small blood vessels, lymphatic ducts and nerve fibres pass. The lamina propria sits on a thin layer of smooth muscle called the muscularis mucosa. The next layer is the submucosa which is also a connective tissue layer and contains a network of nerve cells called the submucous plexus and also major blood and lymphatic vessels. Below the submucosa is the muscularis externa which is a layer of circular smooth muscle followed by a thinner layer of longitudinal smooth muscle. Between the two muscle layers is another network of nerve cells known as the myenteric plexus. The final, outer layer of the gastrointestinal wall is a layer of connective tissue called the serosa.

The mammalian stomach is an expanded region of the gastrointestinal tract which receives food from the oesophagus and processes it into chyme. The structure and function of the stomach is well described in a number of reviews and textbooks such as Ito (1987), Ross and Romrell (1989), Johnson (1991) and Vander et al. (1990).

The rat stomach can be divided into three areas (Figure 1.2 A). The forestomach or fundus is referred to as the non-glandular region since no acid or pepsinogen is secreted in this region. The epithelium of the forestomach is of the stratified squamous type and differs from the epithelium of the rest of the stomach. The body or corpus and the antrum have a simple (i.e. one cell thick) columnar epithelium. The corpus contains gastric glands which secrete acid and pepsinogen (Figure 1.2 B). Glands in the antrum secrete gastrin into the blood from the endocrine cells found there.

Figure 1.2 A: Stomach



1.2.2 Cell-types of the gastric glandular mucosa

1.2.2.1 Surface mucous cells

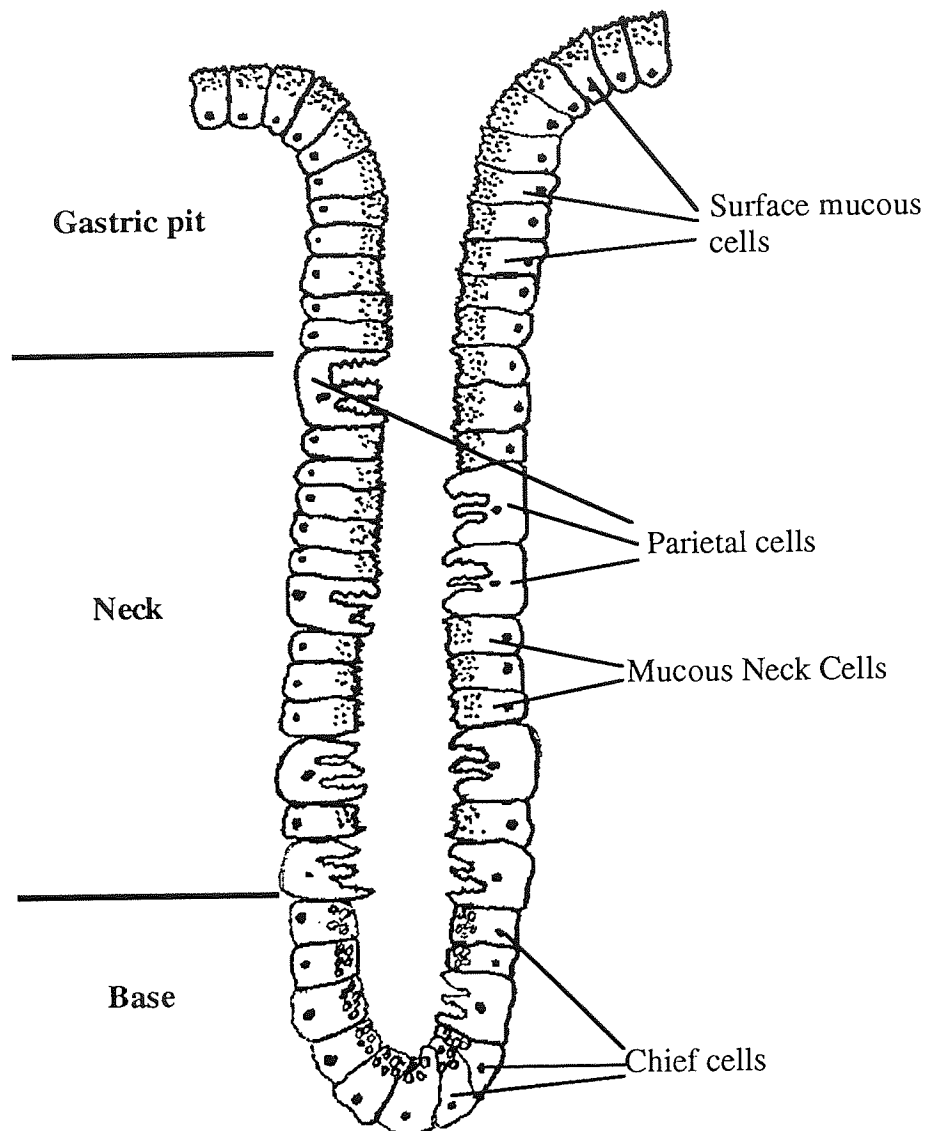
Surface mucous cells cover the entire surface of the glandular mucosa and are involved in the secretion of mucus and bicarbonate which gives rise to an adherent mucus gel layer which protects the gastric mucosa from digestion by acid and pepsin. The luminal surface of gastric mucous cells has short microvilli and the apical cytoplasm is packed with mucin granules.

1.2.2.2 Mucous neck cells

Mucous neck cells are similar in appearance to surface mucous cells and are found in the neck regions of the gastric glands. They also secrete mucus and are frequently found adjacent to parietal cells. The mucin granules in mucous neck cells are larger than those in surface mucous cells and are often found in the paranuclear region. The mucous neck cell population also includes undifferentiated

cells which can either migrate up the gland to become surface mucous cells or down the gland to become parietal cells.

Figure 1.2 B: Gastric gland (Not drawn to scale)



1.2.2.3 Parietal cells

Parietal cells, which are located in the neck and base regions of gastric glands, are also known as oxyntic cells and secrete hydrochloric acid. Parietal cells have intracellular secretory canaliculi which communicate with the lumen of the gland, microvilli which line the canaliculi, a tubovesicular system under the microvilli and numerous mitochondria. In the resting cell the tubovesicular system predominates

and canaliculi are less numerous. However upon stimulation of acid secretion the tubovesicular system diminishes and secretory canaliculi are more numerous.

1.2.2.4 Chief cells

Chief cells are located in the base of gastric glands and are typical protein secreting cells. They contain zymogen granules full of pepsinogen at the apical cell surface and abundant endoplasmic reticulum at the base. Pepsinogen is secreted from chief cells by exocytosis.

1.2.2.5 Endocrine cells

A number of endocrine cells also exist in the gastric mucosa. G cells are found predominately in the antrum and secrete gastrin which is a stimulant of gastric acid secretion. Release of gastrin from G cells can be inhibited by the release of somatostatin from D cells. Two other important endocrine cells of the stomach are enterochromaffin cells which secrete 5-HT and enterochromaffin-like (ECL) cells which secrete histamine.

1.2.3 Small intestine

The final stages of digestion and absorption of nutrients takes place in the small intestine which is a long tubular part of the gastrointestinal tract. The small intestine can be divided into three sections, the initial short segment is the duodenum, followed by the major sections, the jejunum and the ileum. The surface of the small intestine is convoluted and the surface area is amplified to aid absorption by the presence of villi. Crypts are present at the base of the villi and cells formed at this site migrate up the villi to be shed from the tip.

The cell-types and secretions of the small intestine differ from those of the stomach. The intestinal epithelium is of the simple columnar type and contains a number of cell-types. Enterocytes, which are also referred to as intestinal absorptive cells are tall columnar cells which cover the surface of the villi. They contain numerous microvilli at the apical surface. While the main purpose of enterocytes is absorption they can also synthesise digestive enzymes. Goblet cells are found interspersed throughout the other cells of the intestinal epithelium and are

the mucus secreting cells of the small intestine. A variety of endocrine cells are also found in the small intestinal epithelium which secrete cholecystokinin (CCK) secretin and gastric inhibitory peptide (GIP). CCK is related to gastrin and its release is stimulated by the presence of amino and fatty acids in the small intestine. It acts physiologically to increase pancreatic bicarbonate and enzyme secretion and to increase contraction of the gall bladder to release bile salts into the intestine. Secretin release is stimulated by the presence of acid in the small intestine and acts to inhibit gastric acid secretion and also to increase pancreatic release of bicarbonate. GIP release is stimulated by the presence of glucose and fat in the small intestine and stimulates insulin release and inhibits gastric acid secretion.

1.2.4 Colon

The colon does not contain villi nor is the luminal surface convoluted. The role of the colon is to remove water and salts from the intestinal contents prior to defaecation. The colonic mucosa contains numerous straight tubular glands that extend throughout the thickness of the mucosa. The colonic epithelium is of the simple columnar type and the major epithelial cell is the columnar absorptive cell. Goblet cells are more numerous in the colon than in the small intestine because the mucus they secrete is required to lubricate the passage of the increasingly more solid colonic contents.

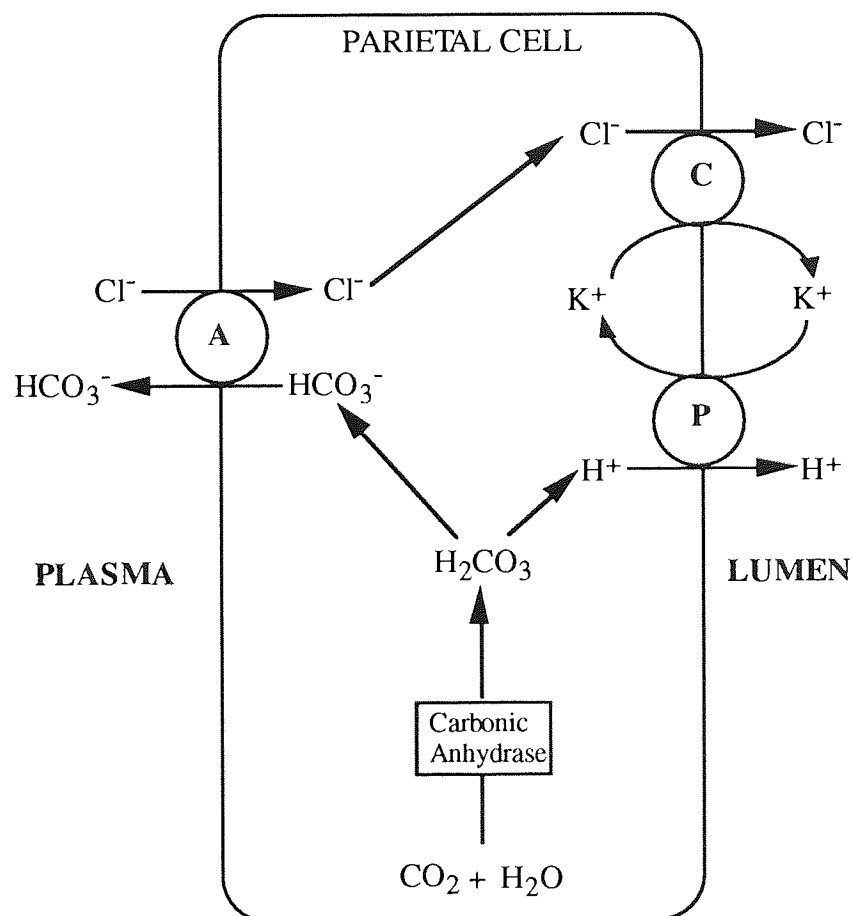
1.3 EFFECT OF NITRIC OXIDE ON FUNCTIONS OF THE STOMACH

1.3.1 Gastric acid secretion

1.3.1.1 Mechanism of acid secretion

The process of acid secretion by parietal cells is illustrated in Figure 1.3 A. H^+ ions are actively pumped into the gastric lumen while Cl^- ions are carried into the lumen via a symport carrier with K^+ .

Figure 1.3 A: Schematic illustration of gastric acid secretion



Legend to Figure 1.2 B

P = H^+/K^+ ATPase proton pump. C = Symport carrier for K^+ and Cl^- . A = Antiport which exchanges Cl^- and HCO_3^- .

The three main stimuli which act on parietal cells to stimulate acid secretion are gastrin, histamine and acetylcholine (ACh). The 17 amino acid form of gastrin (G17) is the main form involved in the control of gastric secretion and is released from G cells in the gastric antrum to act on specific receptors on the parietal cell. Histamine is released from histamine containing (ECL) cells to act on H₂ histamine receptors and ACh is released from cholinergic nerve endings to act on muscarinic receptors on the parietal cell. Gastrin and ACh can both act on ECL cells to increase histamine release and therefore to increase acid secretion. Gastrin release is dependent on the presence of peptides formed by the digestive action of pepsin and on the pH of the gastric lumen. Peptides in the stomach lead to gastrin secretion and therefore increased acid secretion. Furthermore, gastrin secretion is inhibited by a low luminal [H⁺] so when food enters the stomach and binds hydrogen ions the [H⁺] decreases and therefore the inhibition of gastrin secretion and consequently acid secretion is removed. Somatostatin released by D cells is the inhibitory mediator which acts on G-cells to inhibit gastrin release. Gastric acid secretion is inhibited directly by the action of prostaglandin E₂ on the parietal cells.

1.3.1.2 Effects of NO on acid secretion

NO does not directly affect basal acid secretion or acid secretion stimulated by pentagastrin *in vivo* since L-NMMA does not change acid secretion in either case (Pique et al., 1992). However, the role of NO in gastric mucosal blood flow may have an indirect effect on acid secretion because at a high dose of L-NMMA a decrease in secretion is observed presumably due to the associated inhibition of hyperemia which reduces the delivery of metabolic requirements to parietal cells (Whittle et al., 1994). Takeuchi et al. (1995) found no evidence for inhibition of pentagastrin or histamine-stimulated acid secretion by NOS-inhibitors *in vivo* although NO donors could decrease histamine-stimulated acid secretion. Brown et al. (1993) showed that histamine-stimulated acid secretion in isolated parietal cells could be inhibited by high concentrations of NO-donors.

Barrachina et al. (1994) showed that NO donors could inhibit neuronally-stimulated gastric acid secretion *in vivo* and suggested the possibility of a nervous reflex which, under pathological conditions, triggers release of NO and leads to inhibition of acid secretion.

Another suggestion, that the role of NO in gastric acid secretion may be more pathological than physiological, is the report that L-NAME prevents the decrease in acid secretion seen after exposure to mild irritants (Takeuchi et al., 1994 a & b). Furthermore, Esplugues et al. (1993) showed that the inhibition of pentagastrin-stimulated gastric acid secretion by interleukin-1 β is mediated by NO and Martinez-Cuesta et al. (1992) described the NO-dependence of the endotoxin-mediated inhibition of the secretory response to pentagastrin, an effect which was not due to the NO from the iNOS isoform.

The involvement of NO in gastric acid secretion is therefore complicated and has not yet been fully understood.

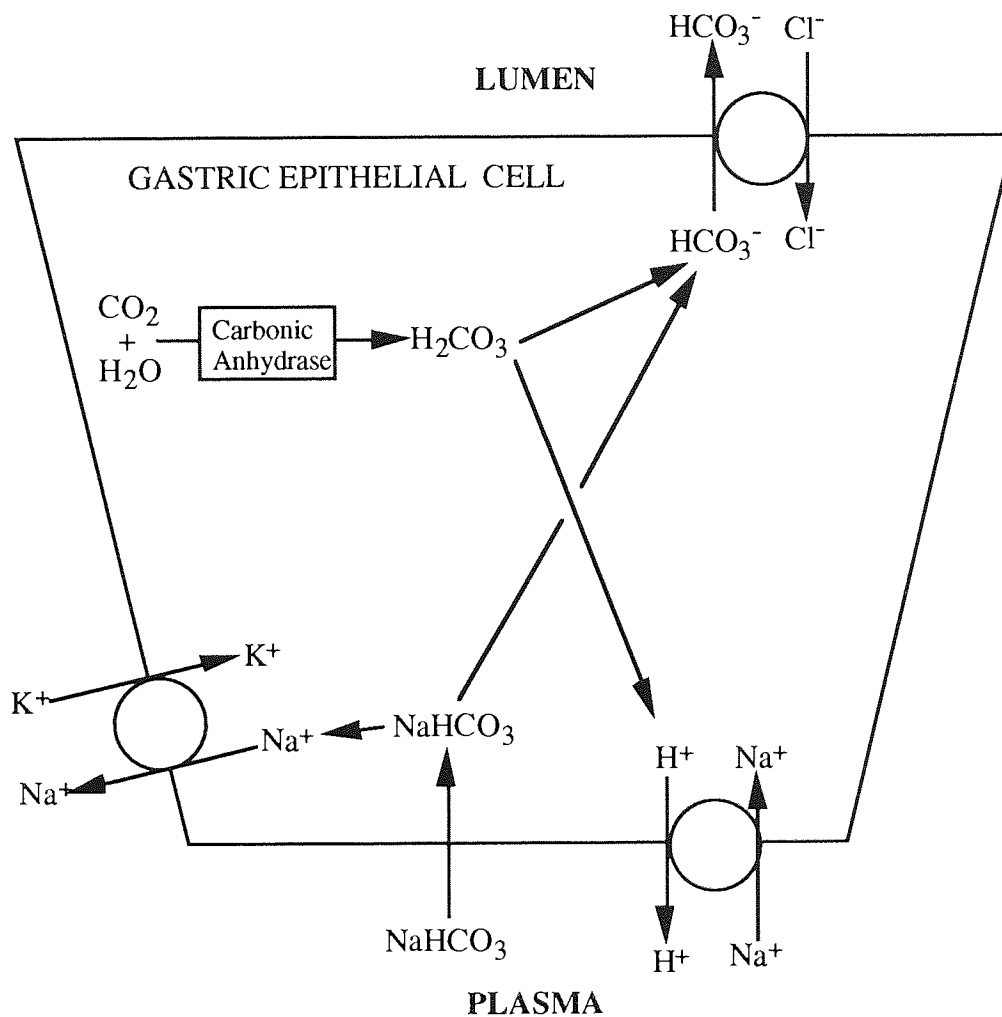
1.3.2 Mucus and bicarbonate

1.3.2.1 Nature of the mucus gel

The process of mucous and bicarbonate secretion is described by Allen et al. (1993) and Flemstrom et al. (1994). Mucous and bicarbonate secretion by the surface mucous cells gives rise to an adherent, unstirred, alkaline mucus gel layer which provides protection to the gastric mucosa against digestion by acid and pepsin. Mucous is secreted by surface mucous cells. The mucous secretion contains protein, lipid and nucleic acid, much of which is derived from exfoliated cells and bacteria, however the adherent and gel-forming properties are due to the presence of mucin. Gastrointestinal mucins are glycoproteins of large molecular weight (approximately 10×10^6 Da) with a composition of > 80% carbohydrate. Structural subunits of mucin glycoproteins consist of a protein core with glycosylated and non-glycosylated regions. The glycosylated region consists of many carbohydrate side chains (up to nineteen sugars per chain) attached by O-glycosidic linkages to

serine and threonine residues in the protein core. Non-glycosylated regions form interchain disulphide bridges that link subunits and are necessary for formation of a gel. The mucus gel layer formed tends to be of variable thickness but is continuous, continuity being essential to provide an effective barrier.

Figure 1.3 B: Bicarbonate secretion in gastric epithelial cells (adapted from Allen et al., 1993)



1.3.2.2 Bicarbonate secretion

Bicarbonate secretion from gastric epithelial cells alkalinises the mucus gel layer providing a first line defence against luminal acid. The process of bicarbonate secretion is energy-dependent and involves exchange of bicarbonate for chloride ions and is illustrated in Figure 1.2 C. Bicarbonate is either synthesised in the gastric epithelial cell or enters the cell via the serosal surface. Bicarbonate is carried to the serosal surface from the parietal cells where it originates via arterioles and capillaries in a so called "alkaline tide".

1.3.2.3 Role of NO in mucus secretion

One aim of this work was to provide information on the involvement of NO in gastric mucus secretion and this topic is dealt with in depth in chapter 5.

1.3.2.4 Role of NO in bicarbonate secretion

Gastric bicarbonate secretion is known to be stimulated by cGMP (Flemstrom, 1994) which could imply a role for NO in this process. Some studies however (Takeuchi et al., 1992 & 1993) imply a physiological depressant role for NO on vagal or other neuronal activity that regulates bicarbonate secretion. Takeuchi et al. (1994) showed that the decrease in acid secretion seen after damage by NaCl was NO-dependent but the increase in luminal bicarbonate was not. This implies that the decrease in acid secretion unmasks luminal alkalinisation seen around the damaged area but that NO was not involved. In the small intestine L-NAME produces an increase in bicarbonate secretion (Miller et al., 1993). However, rather than a direct effect on bicarbonate secretion this is likely to be due to increased epithelial permeability since L-NAME is known to increase the permeability of the intestinal epithelium (see 1.4).

1.3.3 Gastric mucosal protection

1.3.3.1 Mechanisms

Mechanisms of gastric mucosal protection have been reviewed by Allen et al. (1993) and Wallace and Bell (1995) and the regulation of the gastric microcirculation has been reviewed by Whittle (1993).

The first line of defence against gastric acid and pepsin is the continuous adherent alkaline mucus gel layer. Bicarbonate neutralises luminal acid within the matrix of the mucus gel. The mucus gel provides an unstirred layer at the mucosal surface that restricts the movement of newly secreted bicarbonate and prevents it from being overwhelmed by acid. The mucus gel layer dramatically slows down the movement of pepsin and although pepsin digests mucus at the surface of the gel this process is slow and the mucus digested is replaced by *de novo* synthesis and secretion. Mucus also plays a key role in the protection of damaged areas of the gastric mucosa by forming a thick protective mucoid cap over the damaged area which allows restitution to take place.

Another key factor in the maintenance of gastric mucosal integrity is the gastric microcirculation. In normal conditions most hydrogen ions are buffered in the mucus-bicarbonate barrier and any that do get through are either neutralised by the alkaline tide or are removed in the blood stream. When the gastric barrier is damaged, either by increased acid load or by topical irritants such as bile salts, ethanol or nonsteroidal anti-inflammatory drugs (NSAIDs), hydrogen ions enter the mucosa, a process known as acid back-diffusion. In such cases the blood vessels of the gastric microcirculation dilate, blood flow is increased and the extra hydrogen ions are removed in the blood. If this hyperemic response to acid back-diffusion is impaired in some way so that the excess hydrogen ions cannot be removed, tissue damage results.

The gastric microcirculation is regulated by a number of vasoactive substances. NO is released from the vascular endothelium to dilate blood vessels and another vasodilator, calcitonin gene related peptide (CGRP), is released from sensory

afferent neurons . An interaction between NO and CGRP is described below. Prostacyclin is also released from the vascular endothelium to act as a vasodilator. Vasoconstriction can be caused by substances such as noradrenaline, neuropeptide Y and endothelin.

1.3.3.2 The role of NO in gastroprotection and in regulating the gastric microcirculation

A clear role for NO has been established in the maintenance of gastric mucosal integrity. Treatment of rats with indomethacin followed by L-NMMA caused gastric mucosal damage (Whittle et al., 1990) while either agent alone had no effect. Gislason et al. (1996) reported that L-NMMA increased gastric mucosal damage and decreased the hyperemic response to damage by NaCl in the corpus and fundus but not in the antrum. The extensive gastric damage induced by the vasoconstrictor endothelin can be prevented by administration of NO donors (Lopez-Belmonte et al., 1993; Lazaratos et al., 1995). Also Kitagawa et al. (1990) reported that NO donors protect against damage by hydrochloric acid and MacNaughton et al. (1989) showed that NO donors decrease the level of gastric mucosal damage produced by ethanol. This latter gastroprotective effect of NO does not appear to involve prostaglandins because indomethacin does not decrease these protective properties (MacNaughton et al., 1989). Overall, these results imply that the gastroprotective action of NO is likely to be due to its ability to improve gastric mucosal blood flow by causing vasodilatation.

Pretreatment of rats with luminal capsaicin has a protective effect on the stomach and this is an NO-dependent process (Whittle et al., 1992; Podolsky et al., 1994; Merchant et al., 1994 and 1995). This effect is due to the stimulation of afferent sensory nerves, release of CGRP and subsequent endothelial NO release and vasodilatation. It is also possible that neuronally derived NO is in a capsaicin-stimulated nervous reflex that leads to release of sensory neuropeptides.

The gastroprotective effects of CCK-8 and pentagastrin are NO-dependent however they may or may not be mediated by CGRP release. Konturek et al. (1995 a & b)

reported that gastrin and CCK-8 can protect the mucosa from damage by an NO-dependent mechanism which does not involve sensory nerve fibres. However, Heinemann et al (1996) suggest a vagovagal reflex on CCK-8/gastrin administration which involves release of ACh and CGRP with NO as the final messenger. Heinemann's results are similar to those obtained by Kiraly et al. (1993) which showed that central vagal stimulation is gastroprotective due to ACh, CGRP and NO. The implication of NO in gastric vasodilatation by CGRP is not mirrored elsewhere in the body. Holzer et al. (1994) reported that this interaction occurred in the gastric but not in the cutaneous microcirculation. Lippe and Holzer (1992) reported that the hyperemia due to acid back-diffusion involved NO but not prostacyclin.

NO has been implicated in the mechanism of action of a number of anti-ulcer agents. Mobarak-Ali (1995) reported that L-NAME attenuates the protective effect of sodium chromoglycate. Furthermore Konturek et al (1992, -93, -94 and -95) described the involvement of NO in the cytoprotective effects of sucralfate, Maalox and $\text{Al}(\text{OH})_3$.

Epidermal growth factor (EGF), which is secreted by salivary gland and can be gastroprotective might interact with NO *in vivo* to exert its gastroprotective actions because gastric damage caused by HCl in sialoadenectomised rats is exacerbated by L-NAME administration. Treatment of sialoadenectomised rats with EGF prevented the damaging effects of L-NAME on the gastric mucosa (Tepperman and Soper, 1993).

Finally, NO appears to be involved in the formation of the mucoid cap which forms over an area of gastric damage and is vital in the repair and restitution of the mucosa (Yanaka et al., 1995).

1.3.4 Pepsin

1.3.4.1 Secretion

Pepsin is secreted from chief cells as the inactive precursor pepsinogen. The low luminal pH in the stomach converts pepsinogen to pepsin. Pepsin is an aspartate endoproteinase of broad specificity which breaks down proteins to peptide fragments. Peptide fragments produced by pepsin activity are a stimulus for acid secretion. The strongest stimulus of pepsinogen secretion is ACh from cholinergic nerves. Gastrin also stimulates pepsinogen secretion.

1.3.4.2 Effect of NO

The effect of NO on pepsinogen secretion has not been widely studied and recent publications are conflicting. All studies have used isolated guinea pig chief cells. Fiorucci et al. (1995 a & b and 1996) have detected NO release from isolated chief cells on stimulation of pepsinogen secretion by various agonists. Fiorucci et al. (1995 a) also showed that carbachol-stimulated pepsinogen secretion could be inhibited by L-NAME. A possible role for NO in stimulating pepsinogen secretion is suggested by these results. However, another recent study (Okayama et al., 1995) using cultured chief cells showed that carbachol-stimulated pepsinogen secretion could be inhibited by NO donors and an analogue of cGMP. The role of NO in pepsinogen secretion is, therefore, unclear. Moreover, all studies have been carried out on isolated cells so the involvement of NO *in vivo* is not known at all.

1.4 FUNCTIONING OF NITRIC OXIDE IN THE INTESTINE

The gastrointestinal tract is densely innervated by nonadrenergic noncholinergic (NANC) nerve fibres. Many of the NANC fibres in the stomach and intestine release NO as a neurotransmitter (Sanders and Ward, 1992). NANC nerve fibres can be inhibitory and cause relaxation throughout the gastrointestinal tract (Whittle, 1994; Sanders and Ward, 1992). NO has been implicated in NANC relaxation of

the oesophagus, the stomach, the small intestine and the colon and anus (Whittle, 1994; Sanders and Ward, 1992)

NO is also important in the intestine because it regulates the intestinal barrier. NO decreases the epithelial permeability in the intestine by a process which is not a direct result of increased blood flow (Alican and Kubes, 1996; Miller et al., 1993). A role for NO in the protection of intestinal integrity as well as that of the stomach is, therefore, implied because decreased intestinal permeability is characteristic of the restitution process (Miller et al., 1993). The potent vasodilator actions of NO may also play a role in maintenance of intestinal integrity (Whittle et al., 1994).

The induction of iNOS in macrophages in the intestine is important in protection against microorganisms (Whittle et al. 1994). Moreover, in inflammation of the intestinal tract in both animal and human models there is evidence for an involvement of iNOS (Boughton-Smith et al., 1992 and 1993 a & b). The characteristics of NOS induced in both the muscle and mucosal layer of the small intestine and colon is described in detail in chapter 6 and one aim of this thesis (Chapter 6) was to investigate the changes in NOS induced by LPS in the small and large intestine with particular reference to the Ca^{2+} -dependency of the enzyme in muscle and mucosal layers.

1.5 SUMMARY OF AIMS OF THIS THESIS

The main aims of this thesis were as follows:

- 1:** To raise a polyclonal antiserum to rat nNOS and use it, and commercially produced antibodies, to characterise the isoforms of NOS found in the rat gastric glandular mucosa.
- 2:** To localise the isoforms of NOS found in the rat gastric glandular mucosa to specific regions and cell-types.
- 3:** To investigate the subcellular localisation of nNOS and eNOS in the rat gastric glandular mucosa and to quantify the relative activities of the two isoforms.

- 4:** To investigate the role of NO in gastric mucus secretion stimulated by carbachol and a prostaglandin analogue.
- 5:** To investigate the Ca^{2+} -dependency of NOS activity in mucosal and muscle layers of rat jejunum, ileum and colon after treatment of rats with intravenous lipopolysaccharide.

CHAPTER 2:
GENERAL METHODOLOGY

This chapter contains descriptions of general methods used throughout the thesis. Techniques associated only with a particular chapter are described therein.

2.1 ASSAYS OF PROTEIN

Two protein assays were used to measure the protein content of samples prepared during the course of this project. The assay used for any particular sample was chosen in regard to the expected protein content of the sample and, more importantly, the presence of substances in the sample likely to interfere with the assay .

2.1.1 Bicinchoninic acid protein assay

The Bicinchoninic Acid (BCA) protein assay is a colorimetric assay that combines the reduction of Cu^{2+} to Cu^+ by protein in an alkaline medium (the biuret reaction) with the colorimetric detection of the cuprous cation (Cu^+) by BCA. The purple-coloured reaction product of the assay is formed by the chelation of two molecules of BCA with one cuprous ion. (Figure 2.1).

Figure 2.1: Bicinchoninic acid protein assay reaction scheme

- 1: Protein (peptide bonds) + Cu^{2+} \rightarrow tetradentate- Cu^+ complex
- 2: $\text{Cu}^+ + 2 \text{BCA} \rightarrow \text{BCA-Cu}^+$ -ternary complex (purple-coloured)

The BCA protein assay was carried out by using the Pierce BCA protein assay reagent kit. The working assay solution was prepared by mixing 50ml of reagent A from the kit with 1ml of reagent B. Reagent A contained sodium carbonate, sodium bicarbonate, bicinchoninic acid and sodium tartrate (unknown concentrations) in 0.2M sodium hydroxide. Samples for assay were prepared by dilution in double-distilled water. Samples for the standard curve of the protein assay were prepared by diluting Bovine Serum Albumin (2mg/ml) in double-distilled water to give a range of samples with concentrations ranging from 20-

100µg/ml. The standard curve tubes, and blanks (double-distilled water) also contained an appropriate dilution of the medium in which the samples had been prepared. This precaution was to ensure that the conditions in all tubes in the assay were identical.

To perform the assay 2ml of the working solution was added to 100µl of dilute sample, protein standard or blank in polystyrene tubes and incubated for 30 min at 37°C in a water bath. The absorbance of each sample was then measured at 562nm in a double beam spectrophotometer with the reagent blank as the reference. A standard curve was prepared and protein concentration values were calculated.

The BCA reagent does not reach a true end point and colour development will continue even after cooling to room temperature so absorbance measurements were carried out as quickly as possible in order to ensure that no significant error was introduced. The main interfering substances that affect the BCA assay are reducing agents, in particular dithiothreitol (DTT, >1mM) and 2-mercaptoethanol(>0.01% v/v).

2.1.2 Coomassie blue protein assay

The Coomassie Blue Protein assay is a dye-binding assay that is based on the shift of the absorbance maximum of an acidic solution of Coomassie Brilliant Blue G250 from 465nm to 595nm when binding to protein occurs. The main interfering substances affecting this assay are detergents (e.g. SDS) in concentrations greater than about 0.1g/100ml. The Coomassie Blue assay therefore cannot be used to measure the protein content of samples in electrophoresis sample buffer. Two different assay procedures were used depending on the expected protein content of the samples being assayed.

2.1.2.1 Microassay procedure

This assay procedure is used to detect 1-20µg of total protein in a sample. Samples were diluted in the same buffer as that used for their preparation and protein standard dilutions (2-20µg Bovine Serum Albumin in the assay tube) were also

prepared in the same buffer. Blank tubes contained sample buffer alone. The assay was carried out by adding 0.4ml of sample, protein standard or blank buffer to 0.4ml of distilled water in polystyrene tubes, adding 0.2ml of Coomassie Blue dye reagent concentrate (Sigma) to each tube and incubating for 5min at room temperature. The absorbance of each sample was measured against the reagent blank at 595nm and protein concentrations were calculated from the standard curve.

2.1.2.3 Standard assay procedure

The standard assay procedure is used to detect 20-140µg total protein in a sample and is similar to the microassay but for the volumes of sample and reagent used. Samples and standards were prepared in the same way but the dye reagent was diluted (1:4, dye:distilled water). The assay was carried out by adding 2.5ml of diluted dye reagent to 50µl sample, standard or blank, and incubating for 5min at room temperature. Absorbance at 595nm was measured as before and the protein concentrations of samples calculated.

2.2 ASSAY FOR NOS ACTIVITY

2.2.1 Principle

NOS activity is measured in this assay as the conversion of L-[¹⁴C]arginine to L-[¹⁴C]citrulline (Bredt & Snyder, 1990). L-arginine has a net positive charge at the pH at which the assay is carried out while L-citrulline is neutral. When a tissue sample containing NOS is added to the assay buffer L-[¹⁴C]arginine is converted to NO and L-[¹⁴C]citrulline. The reaction is stopped after a set period of time by addition of the cationic exchange resin DOWEX (AG 50-W8, Na⁺-activated) which binds L-[¹⁴C]arginine and settles out in the assay tube. The L-[¹⁴C]citrulline is left in solution and a fraction of the solution is removed for scintillation counting to determine the amount of L-[¹⁴C]citrulline present in the supernatant and therefore the activity of NO synthase in the tissue sample. To ensure that all the L-[¹⁴C]citrulline equates with NO formation samples to which the NOS inhibitor L-

NMMA had been added were also counted and the mean value of inhibited samples was subtracted from the mean values from uninhibited samples.

2.2.2 Protocol

2.2.2.1 Activation of DOWEX

The cationic exchange resin, DOWEX AG 50-W8 was activated by addition of 200ml of 1M NaOH to 50g of DOWEX in a beaker, gently swirling to suspend the DOWEX, and then leaving to settle. After 1h the aqueous layer was then carefully decanted, another 200ml of 1M NaOH was added, the DOWEX was resuspended, and was allowed to settle for 1h as before. The aqueous layer was then decanted off, 300ml of double-distilled water was added, the DOWEX was resuspended in the water and was allowed to settle before the aqueous layer was decanted off and the process repeated. Washing continued until the pH of the DOWEX suspension was approximately 6.8. The aqueous layer was then poured off and a 1:1 suspension of DOWEX with distilled water was prepared. The container was covered with sealing film and left at 4°C until required.

2.2.2.2 Preparation of gastric mucosal homogenate for assay of NOS

Male Wistar rats were anaesthetised with sodium pentobarbitone (60mg/kg i.p.). Their stomachs were removed via a midline incision and were plunged into ice-cold saline (NaCl, 9g/l). The non-glandular region of the stomach was then removed and discarded and the stomach was opened out by cutting along the greater curvature. The stomach was rinsed thoroughly in ice-cold saline by holding it by the stump of the oesophagus. The stomach was then placed on a glass plate over ice, luminal surface upwards, was carefully blotted dry using filter paper and the mucosa was carefully scraped away from the muscle layer using a scalpel. The mucosa was placed in a clean pre-weighed glass scintillation vial, which was weighed again, and 5ml of NOS homogenisation buffer (10µg/ml soybean trypsin inhibitor, 10µg/ml leupeptin, 6µg/ml aprotinin, 0.1mg/ml PMSF in 10mM HEPES, 320mM sucrose, 1mM dithiothreitol, 0.1mM EDTA, pH 7.5) was added per 1g and

the tissue was homogenised on ice for 30s by using an Ultraturrax homogeniser running at maximum speed. A 1ml sample of each homogenate was transferred to a 1.5ml microfuge tube and homogenates were spun for 20 min at $10,000 \times g_{av}$ at 4°C. The supernatant was removed and stored on ice until used for a maximum of 1h. Samples of other tissues for NOS assay were prepared in a similar way.

2.2.2.3 Standard assay protocol

For each sample nine assay tubes were prepared to measure NOS. Three tubes contained uninhibited assay buffer, three tubes contained assay buffer with the NOS inhibitor L-NMMA included and a further three tubes contained assay buffer with the calcium chelator EGTA added. The composition of 1ml of each assay buffer is shown in table 2.2. The basic assay buffer contained 40mM $KH_2PO_4 \cdot H_2O$, 0.20mM $CaCl_2$, 1mM $MgCl_2$ (pH 7.4). Each 1.5ml assay tube contained 50µl of appropriate buffer and tubes were pre-warmed to 37°C in a water bath. The assay was carried out by sequentially adding 20µl of sample to each assay tube and incubating for 10min at 37°C. Enzyme activity was stopped by addition of 0.5ml of DOWEX (1:1 suspension) followed by 1.0ml of double-distilled water. The tubes were allowed to stand for the DOWEX to settle after which 975µl of supernatant from each tube was removed and transferred to plastic scintillation vials to which 5ml of scintillation fluid (Optiphase HiSafe II) was added. The vials were capped, shaken and the amount of radiolabelled citrulline in the supernatants was determined by scintillation counting with reference to a blank vial containing only scintillation fluid to take account of background radiation.

2.2.2.4 Assay of NOS in subcellular fractions

The assay used for NOS activity in subcellular fractions was based on that used by Hecker et al. (1994). The principle of the assay was the same as described for the standard assay however it differed in the volumes used and in some of the assay constituents (Table 2.2). The basic assay buffer used was different (50mM HEPES, 1mM DTT, 1mM EDTA, 1.25mM $CaCl_2$) and Flavin

Table 2.2: Constituents of assay buffers used for assays of NOS activity

	STANDARD ASSAY		ASSAY OF NOS IN SUBCELLULAR FRACTIONS	
Reagent Stock	Final Conc. in Assay Buffer	Final Conc. after Addition of Sample	Final Conc. in Assay Buffer	Final Conc. after Addition of Sample
β NADPH (50mM)	1mM	0.714mM	1mM	0.8mM
L-[14 C]arginine (297mCi/mmol, 50 μ Ci/ml)	1.515 μ M	1.082 μ M	1.515 μ M	1.212 μ M
L-Arginine (5mM)	20 μ M	14.28 μ M	20 μ M	16 μ M
L-Valine (500mM)	10mM	7.14mM	10mM	8 μ M
L-NMMA (50mM)	1mM when added	0.714mM when added	1mM when added	0.8mM when added
EGTA (50mM)	1mM where added	0.714mM when added	NA	NA
FAD (1mM)	NA	NA	1 μ M	0.8 μ M
6R BH ₄ (15mM)	NA	NA	15 μ M	12 μ M
Calmodulin (100 μ M)	NA	NA	1 μ M	0.8 μ M

Adenine Dinucleotide (FAD), tetrahydrobiopterin and calmodulin were present in the final assay buffer.

The assay was started by adding 25µl of sample to 100µl of either uninhibited or L-NMMA inhibited, final assay buffer in microfuge tubes and was stopped by adding 0.5ml of a 1:1 suspension of DOWEX followed by 0.5ml of double-distilled water. Assay tubes were subjected to centrifugation for 5min at 10,000 x g_{av} at room temperature, to settle the DOWEX and particulate material in relevant samples, and 0.5ml was removed from each tube for scintillation counting as described in 2.2.2.3.

2.2.2.5 Calculation of NOS activity

An average value (dpm) was calculated from the triplicate results for each sample under the three conditions (uninhibited, L-NMMA and EDTA). The specific activity of L-[¹⁴C]arginine was calculated as follows:

Concentration of L-arginine in 1ml of assay buffer = 21.515 nmol/ml

Concentration of radioactivity = 10⁶ dpm/ml

∴ Specific Activity = 10⁶/21.515 = 46479 dpm/nmol

NOS activity, as citrulline formation could be calculated using the following formula:

$$\text{NOS Activity} = \frac{\text{dpm above background}}{\text{specific activity (dpm/nmol)}} \times \frac{\text{Volume supernatant in assay tube (ml)}}{\text{Volume supernatant counted (ml)}} \times \frac{\text{Correction Factor to give activity/ml}}{\text{Time of assay (min)}}$$

e.g.:

$$\text{NOS Activity} = \frac{\text{dpm above background}}{46479} \times \frac{1320}{975} \times \frac{50}{10} \quad (\text{nmol/min/ml homogenate})$$

To express NOS activity as nmol/min/mg protein, the activity per ml homogenate was divided by the protein concentration of homogenates (in mg/ml), measured by the BCA protein assay. NOS activity was also expressed per g wet weight. If 1g of

tissue was homogenised in 5ml of buffer, and assuming 80% of the tissue is water, then there is 1g wet weight in 5.8ml. The activity per ml homogenate is therefore divided by 5.8 to express activity as nmol/min/g wet weight. The total NOS activity in a tissue is expressed as the mean activity measured from uninhibited tubes minus the activity measured in L-NMMA inhibited tubes. Calcium-independent activity is expressed as the activity in EGTA inhibited tubes minus the activity in L-NMMA inhibited tubes.

2.3 POLYACRYLAMIDE GEL ELECTROPHORESIS

Proteins in homogenates were separated by sodium dodecyl sulphate-polyacrylamide gel electrophoresis (SDS-PAGE) on gels made with 8% acrylamide, and identified by immunoblotting and Enhanced Chemiluminescence (ECL) detection.

2.3.1 Preparation of samples and markers for SDS-PAGE

2.3.1.1 Homogenisation of tissue in electrophoresis sample buffer

Tissues were removed from male Wistar rats (200-300g) under terminal anaesthesia (60mg/kg sodium pentobarbitone i.p.). The stomach was removed and the mucosa scraped off as described in 2.2.2.2. To remove the brain the animal was decapitated, the skull was opened and the brain was removed, rinsed in ice-cold saline and the rear portion (mainly cerebellum) was removed for homogenisation. Pancreas was simply removed from the animal and rinsed in ice-cold isotonic saline. The tissues were then placed in separate pre-weighed glass scintillation vials and were weighed. 5ml of boiling 1x electrophoresis sample buffer without DTT (62.5mM Tris.HCl pH 6.8, 10%v/v glycerol, 2%w/v SDS, 0.0125mg/ml bromophenol blue) was added per 1g of tissue, and the tissues were homogenised for 30s using an UltraTurrax homogeniser at full speed. A 1ml sample of each homogenised tissue was then removed, was boiled in a 1.5 ml microfuge tube for

5min and then centrifuged at $10,000 \times g_{av}$ for 5min at room temperature. A 50 μ l sample was then removed for protein determination (BCA assay) and 50 μ l of 1M DTT was added to 450 μ l to make the sample 0.1M with respect to DTT. The mixture was then boiled and centrifuged as before. After cooling to room temperature the sample could then be loaded onto a gel directly or stored frozen at -20°C.

2.3.1.2 Molecular mass markers

"Rainbow" molecular mass markers (Amersham) consist of a series of individually coloured and purified proteins which give a series of coloured bands of known molecular mass when run on a polyacrylamide gel. By measuring the distance travelled by each coloured band a calibration curve of electrophoretic mobility versus molecular mass can be drawn allowing accurate measurement of the molecular mass of bands of interest on a gel. "Rainbow" markers are also useful because they provide a visual check that electrophoretic transfer from the gel to the blotting membrane is complete.

"Rainbow" markers were prepared for running on a gel by adding 10 μ l of the mixture to 10 μ l of complete 2x electrophoresis sample buffer (125mM Tris.HCl pH6.8, 20% v/v glycerol, 4%w/v SDS, 0.2M DTT, 0.025mg/ml bromophenol blue). This mixture was boiled for 2min, centrifuged for a few seconds to collect it at the bottom of the tube and allowed to cool before loading onto the gel.

2.3.2 Preparation of gel

Two glass plates were separated with spacers (0.75mm or 1.0mm) at the sides and clamped to form a gel sandwich which was placed in a stand and clamped down onto a rubber seal at the base of the plates. The separating gel was prepared as shown in table 2.3 A, N, N, N', N'-tetramethylenediamine (TEMED) was the last reagent added to initiate the polymerisation reaction, and the mixture was mixed gently using a magnetic stirrer before pouring between the plates, using a syringe, to a marked level. The separating gel was then overlaid with a 1cm layer of

water:methanol (1:1) and allowed to set. The water/methanol overlay was the poured off and the residue removed by using folded filter paper and the stacking gel (Table 2.3 B) was prepared, poured on top of the separating gel and a comb was inserted between the plates to form either 10 or 15 sample wells.

Table 2.3 A: Make up of separating gel

Stock/Reagent	Volume	Final Concentration
1.5M Tris.HCl (pH 8.8)	5ml	375mM
10% (w/v) SDS	0.2ml	0.1%
Acrylamide/N, N'-bisacrylamide(30%/0.8% respectively)	5.34ml	8% (acrylamide)
Distilled water	9.36ml	NA
Fresh ammonium persulphate (100mg/ml).	0.1ml	0.5mg/ml
N, N, N', N'-tetramethylenediamine	7.5 μ l	NA

Table 2.3 B: Make up of stacking gel

Stock/Reagent	Volume	Final Concentration
0.5M TRIS.HCl. (pH 6.8)	2.5ml	125mM
10% (w/v) SDS	0.1ml	0.1%
Acrylamide/N, N'-bisacrylamide(30%/0.8% respectively)	1.0ml	3% (acrylamide)
Distilled water	6.35ml	NA
Fresh ammonium persulphate (100mg/ml).	0.05ml	0.5mg/ml
N, N, N', N'-tetramethylenediamine	5 μ l	NA

After the stacking gel had set the comb was removed and the wells rinsed with 125mM TRIS, 0.1% SDS. The wells were then filled with running buffer (0.025M TRIS, 0.2M glycine, 0.1% (w/v) SDS, pH 8.3) ready for loading of samples and running of the gel.

2.3.3 Loading and running of gels

Samples containing a known amount of protein in electrophoresis sample buffer, or rainbow markers (see 2.3.1) were loaded into wells using flat ended micropipette tips. Wells were topped up with complete 2 x electrophoresis sample buffer so that each well contained the same final volume in order to ensure the smooth running of the gel. The upper buffer reservoir was clamped to the top of the gel sandwich and filled with running buffer so that the upper electrode was covered. The remaining running buffer was used to fill the gel tank and the gel sandwich/upper reservoir assembly was lowered into the tank and the safety lid fitted. The heat exchange unit was attached to a thermostatic circulator which passed water through it at 10°C in order to prevent the gel from overheating. The electrodes were then attached to the power supply and a constant current of 25mA was applied across the gel with maximum voltage set at 500V. The gel was stopped running when the leading edge of the samples had reached 1-2cm from the bottom of the gel.

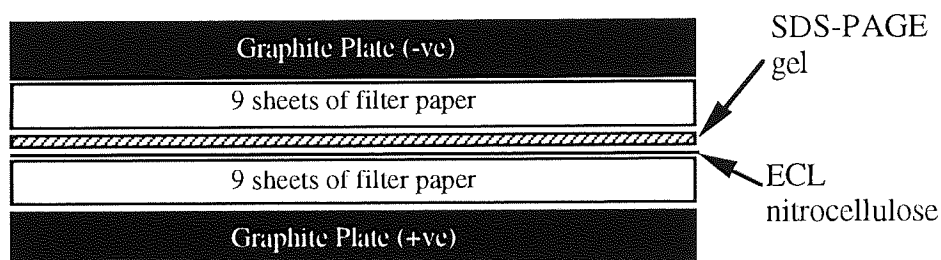
2.3.4 Immunoblotting

Electrophoretic transfer of the proteins on the gel onto the blotting membrane was performed using an LKB electrophoresis transfer unit (Multiphor II) which consists of two graphite plates which can be connected to a power supply and between which the transfer unit can be assembled (Figure 2.3 A).

The lower graphite plate was soaked with distilled water and the excess was wiped off. Eighteen sheets of filter paper (Whatman, 3MM) and one sheet of ECL nitrocellulose (Amersham) were cut to the same size as the separating gel. Nine sheets of filter paper were soaked in transfer buffer (39mM glycine, 0.0375% w/v

SDS, 48mM TRIS in methanol:distilled water(1:4)) and placed exactly on top of one another on the electrode taking care to avoid bubbles. The gel sandwich was carefully disassembled, the stacking gel was cut away and removed and the separating gel was transferred to the nitrocellulose sheet also soaked in transfer buffer. The nitrocellulose sheet and gel were placed on top of the stack of filter paper and another nine sheets of soaked filter paper were stacked on top. The upper graphite plate was then placed on top of the transfer unit after being soaked with distilled water and a constant current (0.8mA per cm²) was applied across the transfer unit for 1h. After transfer was complete the nitrocellulose membrane was either processed immediately or stored desiccated overnight at 4°C.

Figure 2.3 A: Electrophoretic transfer unit



2.3.5 ECL immunodetection

2.3.5.1 Principle

Enhanced chemiluminescence (ECL) is a light-emitting method for the detection of specific antigens on nitrocellulose. A commercial ECL kit from Amersham was used. A primary antibody to the protein being studied is added to the membrane followed by an anti-species IgG secondary antibody conjugated with horseradish peroxidase (HRP). ECL is initiated when detection reagents, consisting of luminol, hydrogen peroxide and a chemical enhancer (unknown concentrations), are added to the membrane and HRP catalyses the oxidation of luminol (Figure 2.3 B) in the presence of a chemical enhancer (e.g. a phenol). Light (maximum wavelength of

428nm) is produced by the oxidation of luminol (Figure 2.3 C) which is detected by exposure to blue-light sensitive autoradiography film (Hyperfilm ECL).

Figure 2.3 B: ECL development reaction scheme

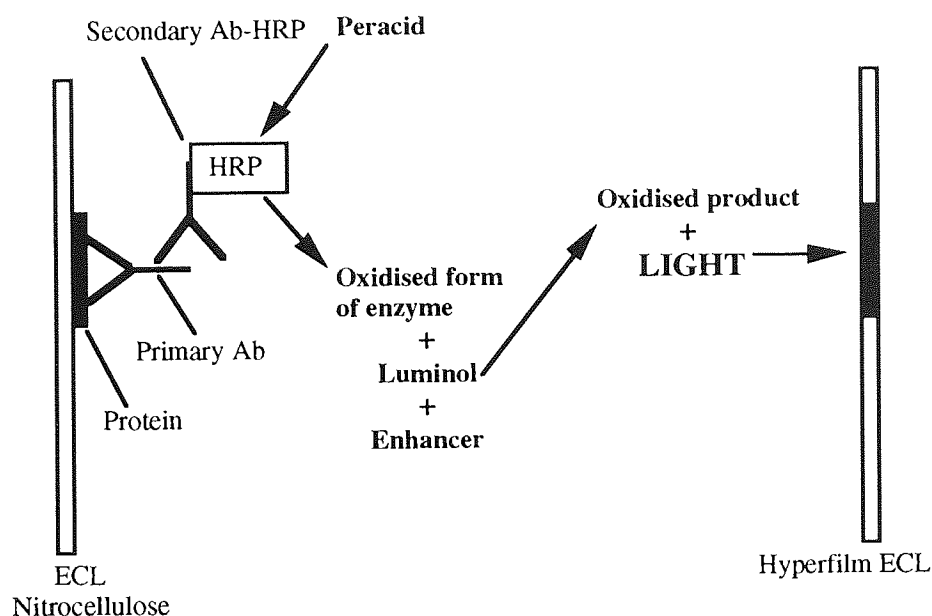
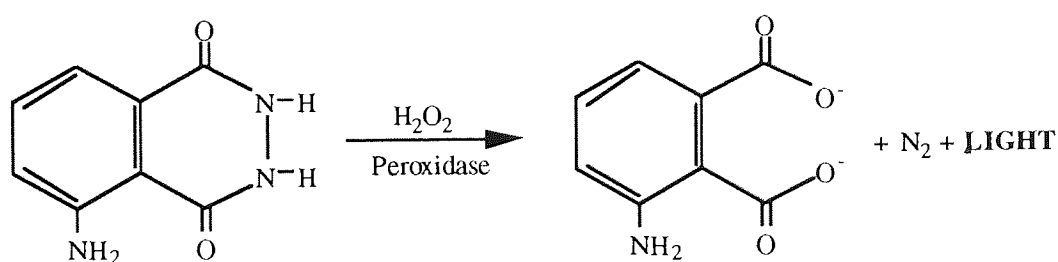


Figure 2.3 C: Oxidation of luminol by peroxidase to produce Light



2.3.5.2 Processing of immunoblots in rolling tubs

Individual nitrocellulose blots were cut using rainbow markers as a guide to allow different lanes on a single blot to be probed with different antibodies, and the position of markers was recorded. Blots were placed in screw topped polystyrene tubs, the surface with protein bound facing the inside of the tub. The various

incubations and washing steps in the processing procedure took place at room temperature with the tubs on a roller at low speed (40rpm).

Non-specific binding sites on the blots were blocked by incubating with 10ml of 5% (w/v) defatted milk in Tris buffered saline/Tween (TBS/Tween: 0.1%v/v Tween 20 in 10mM Tris, 100mM NaCl, pH 7.5) for 1 h. The blots were then incubated for 1h with primary antibody or antiserum (various antibodies and concentrations) dissolved in 2.5ml of TBS/Tween/milk. In experiments where peptide was added with an antiserum the antiserum was pre-incubated in 100 μ l of the peptide solution for 10min following which the solution was transferred to 2.4ml of TBS/Tween/milk. Excess antibody was removed after the 1h incubation period by washing the blots once for 1min and three times for 10min with 25ml of TBS/Tween. HRP-conjugated secondary antibody (anti-mouse or anti-rabbit) was then diluted in TBS/Tween/milk and added to each tub at a dilution of 1:1000 (5 μ l in 5ml) and incubated for 1h. Excess secondary antibody was removed by one wash of 1min and four washes of 10min with TBS/Tween.

2.3.5.3 Detection by ECL

Nitrocellulose was placed, protein surface upwards, on a sheet of cling film (Saran Wrap) in a dark room. An equal volume of ECL detection solution 1 was added to ECL detection solution 2 to give sufficient to cover the blot (0.125ml/cm²) and the mixture was poured over the blot and incubated for 1min at room temperature without agitation. The excess detection reagent was drained off by pipette and the blot wrapped in plastic film. The blot was then exposed to a sheet of autoradiography film (Hyperfilm-ECL) for between 15s and 5min. The film was then removed from the blot and placed in developer (Kodak) until bands appeared, was then rinsed in water and then placed in fixer (Kodak). Once fixed the film was rinsed in water and allowed to dry naturally. If no bands, or very light bands appeared at the development step or if bands were too dark then the time course of exposure to the autoradiography film was altered.

2.3.5.4 Stripping of antibodies from immunoblots in preparation for reprobing

Immunoblots, already probed and developed could be stripped of both primary and secondary antibodies and reprobed using different antibodies by the following procedure.

The immunoblot was placed in 200ml of stripping buffer (100mM 2-mercaptoethanol, 2% w/v SDS, 62.5mM Tris, pH 6.7) at 50°C and was incubated at the same temperature for 30min with occasional agitation. The immunoblot was then washed for 2 x 10min in 200ml of TBS/Tween (see 2.3.5.2). At this stage the immunoblots could then be reprobed by ECL immunodetection as desired.

2.3.6 Scanning and densitometric analysis of immunoblots

2.3.6.1 Scanning

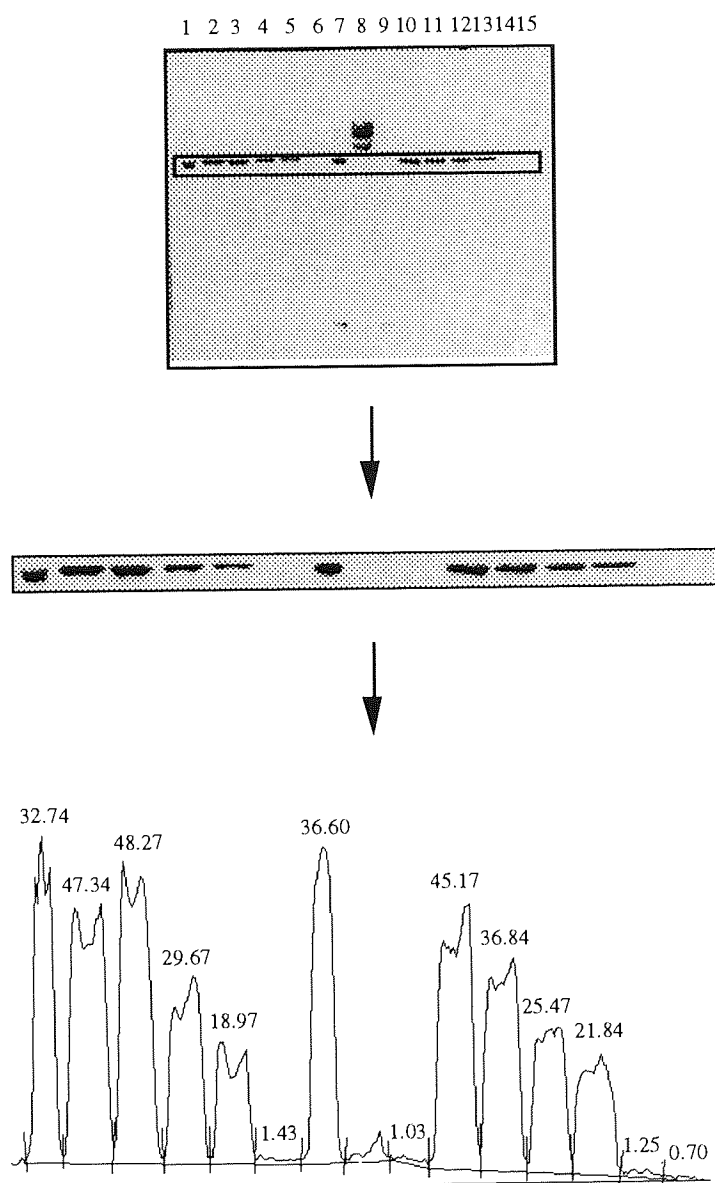
Immunoblots were scanned using an Agfa Focus Color Scanner attached to an Apple Macintosh Computer running the scanning software, M.C. colorview. Scanning was performed in grey-scale mode at a resolution between 100 and 200 dpi (dots per inch) and scans were saved as both TIFF and PICT files in order that they could be both analysed, by densitometric analysis using NIH Image (version 1.58), and could be prepared as figures using Macdraw Pro.

2.3.6.2 Densitometric analysis

TIFF files of scans were loaded into NIH Image (version 1.58). The bands to be analysed were surrounded by a box (Figure 2.3 D) and selected as the zone for which results were required. Calibration was carried out by simply selecting uncalibrated optical density. A plot was then produced of the optical density across the zone selected. Because the background optical density across the original immunoblot scan may not have been constant, a baseline was drawn in manually using the line control from the tool box menu. The peaks on the optical density curve were then separated manually with reference to the image of the original blot and the peaks for which values were required were selected using a specific tool from the tool box menu (See Figure 2.3 D). Values for areas under the peaks

selected could then be displayed on the graph (arbitrary units), and semiquantitative comparisons* could be made between bands of samples on the same immunoblot. For direct quantitation a standard curve was generated using known amounts of NOS protein.

Figure 2.3 D: Densitometric analysis of immunoblots



* N.B.: O.D. is not necessarily linearly related to protein on the gel especially if overloaded.

2.4 RAISING ANTIPEPTIDE ANTIBODIES

2.4.1 Background

When the study described in this chapter was initiated no commercial antibodies to nNOS were available therefore antibodies in antisera were raised in rabbits against two peptides, the sequences of which are found in the rat brain NOS (Bredt et al, 1990). The sequences of the two peptides used are shown in table 3.1D (Chapter 3).

Both peptides were produced commercially (Affiniti, Exeter, U.K.), and were conjugated to keyhole-limpet haemocyanin (KLH) via reaction with the cysteine sulphhydryl by the manufacturer. Conjugation to KLH was carried out because the immune response in the animals to the conjugate was likely to be much better than to the peptide alone. The immune response was also enhanced by using Freund's adjuvant (complete and incomplete) as an immunopotentiator in which the peptide-KLH conjugates were prepared before injection. Freund's adjuvant (incomplete) is a mineral oil with an emulsifier included to yield stable water-in-oil emulsions of the immunogen. Complete Freund's adjuvant contains, in addition, a dispersion of dried, heat killed, *Mycobacterium tuberculosis* in the oil phase (0.5mg/ml). Complete Freund's adjuvant causes local formation of granulomas which are rich in macrophages and immunocompetent cells. Because complete Freund's adjuvant causes granulomas at the site of subcutaneous injection it is only used for the first immunisation and all boost injections are carried out using the incomplete form.

2.4.2 Methods

2.4.2.1 Immunisation protocol

Each peptide was used to immunise two rabbits over a ten week period. The immunisation timetable and protocol is shown in table 2.4 Rabbits coded A and B were immunised with the internal peptide of nNOS and rabbits coded C and D were immunised with the carboxyl-terminal peptide of nNOS.

Table 2.4: Immunisation timetable

Week Number	Procedure
-1	Test bleed rabbits to prepare pre-immune serum (5-10ml per rabbit).
0	Inject 1.0ml of Freund's complete adjuvant:Peptide, 1:1 emulsion, at four sites subcutaneously (0.25ml per site). 100µg peptide in total per rabbit.
2	Boost using the same procedure as in week 0 but using Freund's incomplete adjuvant.
4	Boost.
6	Boost.
7	Test bleed (5ml per rabbit) to assay for antibody titre.
8	Boost.
9	Test bleed (5ml per rabbit) to assay for antibody titre.
10	Boost.
11	Bleed rabbits out (approximately 60ml blood per rabbit)

The emulsion of adjuvant and peptide was prepared by repeatedly forcing the mixture between two syringes connected by a three-way stopcock. Thus, peptide conjugates were stored frozen in 100µl aliquots (250 µg conjugate). Just before emulsion the conjugates were thawed and 1.15ml of sterile isotonic saline was added and the solution mixed gently. Freund's adjuvant was brought to room temperature and whirlmixed. Two labelled syringes were prepared and 1.2ml of adjuvant was taken up into one syringe and 0.4ml of antigen into the other. The two syringes were then fitted onto a three-way tap. Antigen was first pushed into the adjuvant through the three-way tap and the emulsion was then pushed back and forward between the two syringes for 1 minute after which the emulsion was

pushed back into the syringe labelled for adjuvant, the antigen syringe refilled as before and the process repeated. The emulsification process was completed using the final quantity of antigen in the same way. The quality of the emulsion produced was tested by expelling a drop onto the surface of cold water through an 18 gauge needle. A discrete white drop on or below the waters surface indicated that the water phase was well established within the oil drop. Any dispersion indicated that the emulsion was not adequately stable, adjuvant action would be decreased and the emulsion would require further mixing.

2.4.2.2 Preparation of serum from whole blood

In test bleeds, blood was collected from the ear vein of each rabbit, while restrained, by piercing the vein with a sterile scalpel and collecting the blood in a sterile universal container . The final bleed was carried out by collecting the blood via cardiac puncture under vacuum with the rabbits anaesthetised (halothane/nitrous oxide).

Blood was left on the bench at room temperature for 1h to clot and then left overnight at 4°C. The following morning the liquid from the clots was poured off into clean tubes and this serum spun in an ultracentrifuge at 15000 x g for 30 minutes at 4°C. The final serum supernatant after the centrifugation was then stored in 1ml aliquots at -70°C.

2.4.3 ELISA to monitor antibody titre

2.4.3.1 Background

To test for the presence of anti-peptide antibodies against peptides in the serum of the animals, separate Enzyme Linked Immunosorbent Assays (ELISAs) were carried out using peptides or peptide-bovine serum albumin conjugates since this structure more closely resembles the material used as antigen. Peptides or peptide-bovine serum albumin conjugates were used to coat 96-well plates which were then probed with various dilutions of serum to check for recognition.

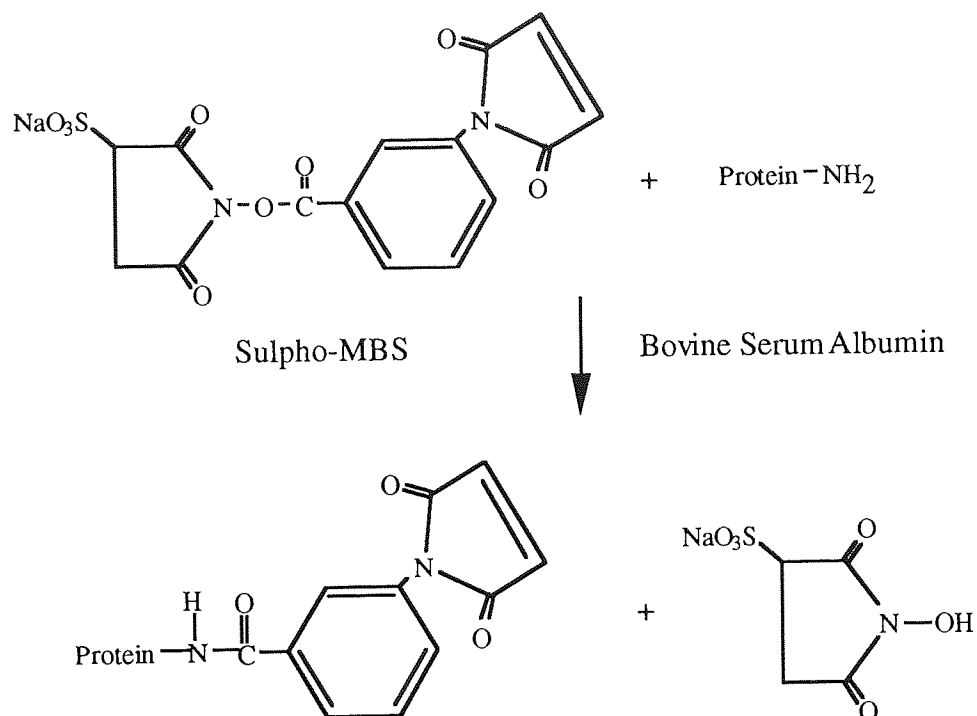
2.4.3.2 Conjugation of peptides to bovine serum albumin

Peptides were conjugated to bovine serum albumin via a Pierce sulphy-MBS heterobifunctional cross linker. The reaction scheme is shown in Figure 2.4

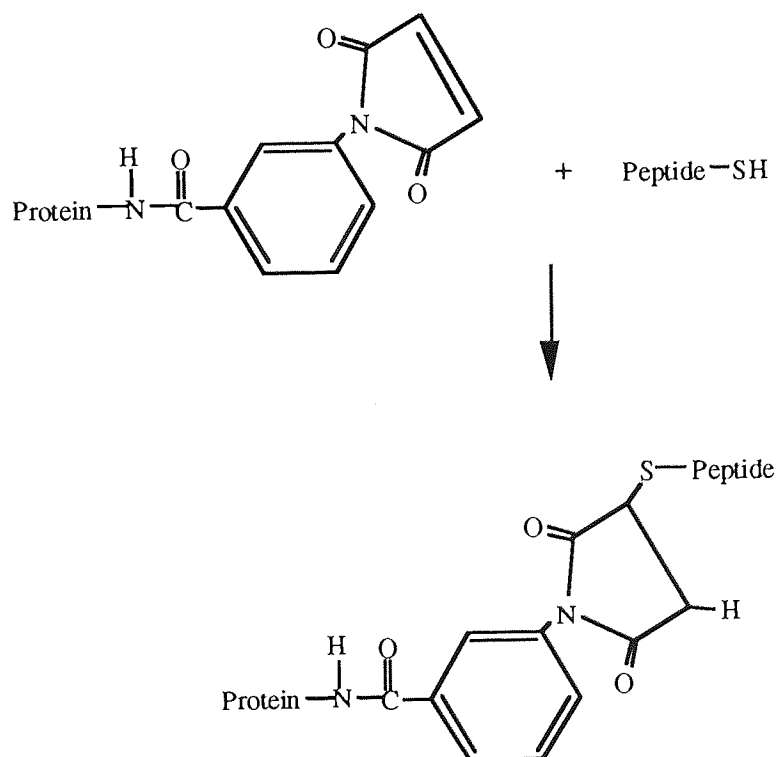
20mg of bovine serum albumin was dissolved in 1ml of PBS (10 mM NaH_2PO_4 , 9g/l NaCl, pH 7.5) and 2mg of sulphy-MBS was dissolved in 1ml of PBS. 200 μl of the sulphy-MBS solution and 200 μl of the bovine serum albumin solution were then added to a 1.5ml microfuge tube and the mixture was left at room temperature for 1h with occasional inversion. The solution was then filtered through a 14ml Sephadex-G25 column, was collected in fractions using a fraction collector (45 drops per fraction) and the absorbance of each fraction at 280nm was measured using a U.V. spectrophotometer. The concentration of protein in the peak protein fraction (i.e. the fraction with the highest absorbance value) was calculated from the absorbance value (A_{280} of 1.0 = 1.8mg/ml protein) and was then diluted to give a concentration of 1mg/ml. Peptide was dissolved (1mg/ml in PBS) and the absorbance of the resulting solution at 280nm was measured. A 1mg/ml cysteine solution in PBS was also prepared. 500 μl of the activated albumin solution (1mg/ml) from the peak protein fraction was added to 500 μl of peptide solution (1mg/ml in PBS) or 500 μl of cysteine solution in 1.5ml microfuge tubes which were left for 2h at room temperature with occasional inversion. The contents of each tube were transferred into the top chamber of a centricon 30 microconcentrator and were subjected to centrifugation for 30min at 5000 $\times g_{av}$. Microconcentrators consist of a capped tube with two chambers separated by an ultrafilter (cut off $M_r=30,000$). The absorbance of the filtrate from the reaction tube containing peptide was measured (280nm) and since the absorbance of the initial peptide solution was known the proportion of peptide which had reacted with the activated albumin was calculated. The filtrates from both microconcentrators were then discarded. The microconcentrators were then everted and subjected to centrifugation for 2min at 5000 $\times g_{av}$ and the material collected was diluted to give an appropriate working solution of conjugate.

Figure 2.4: Peptide-bovine serum albumin conjugation reaction scheme

Step 1: Hydrolysis of ester to attach bovine serum albumin to cross-linker.



Step 2: Reaction of maleimide group on cross-linker with sulphydryl group on peptide.



2.4.3.3 ELISA protocol

Both peptides and bovine serum albumin conjugates were dissolved in carbonate buffer (15mM Na₂CO₃, 35mM NaHCO₃, pH 9.6). Peptides were dissolved to make 2.5μM solutions and peptide-bovine serum albumin conjugates were dissolved to give an estimated final protein concentration of 5μg/ml. Peptide, peptide-bovine serum albumin conjugate or carbonate buffer blank were added to wells on a 96-well plate according to a predetermined plan (100μl per well). The plate was covered with cling film and left overnight at 4°C.

The following morning the plate was emptied and washed by banging it top down on a paper wad, flooding the plate with PBS/Tween (1.5mM KH₂PO₄, 8.1mM Na₂HPO₄, 0.14M NaCl, 2.7mM KCl pH 7.4, 0.1% Tween 20) and standing for 3 minutes. This wash was repeated two times and finally the plate was emptied.

To prevent non-specific binding of antibodies to the plate, all of the wells were then blocked by adding 100μl of a freshly prepared solution of bovine serum albumin in PBS (80mg/ml). After an hour at room temperature the plate was emptied and washed as before.

Nine serial dilutions of rabbit sera were prepared in PBS, from 1/100 to 1/25600. Sera dilutions were mixed by inversion, not by whirlimixing. The 50μl of diluted sera were added to the appropriate wells on the plate. PBS controls of 50μl per well for each initial coating were also added to the plate. The plate was then covered and left for an hour at room temperature and then washed as before.

Protein A-alkaline phosphatase binds selectively to IgG molecules and was the detector-enzyme conjugate used in this ELISA. Protein A-alkaline phosphatase conjugate(6μg) was dissolved in 6ml of TBS, mixed and 50μl/well was added to all wells on the plate with the exception of one column used as a control.

The plate was then covered and left for an hour at room temperature. The plate was then emptied and washed as before but at this stage TBS/Tween (20mM Tris, 0.14MNaCl, 2.7mM KCl pH 7.4, 0.1% Tween 20) was used for the wash because

the phosphate in PBS/Tween has an inhibitory effect on protein A-alkaline phosphatase.

The final step was to incubate the plate with the substrate of the detector enzyme to produce a yellow product. One 15 mg tablet of para-nitrophenylphosphate was dissolved in 16 ml of diethanolamine buffer (1M diethanolamine, 0.5mM MgCl₂, pH 9.8) and 150µl of this solution was added to each well on the plate. After 1 hour at room temperature the reaction was stopped by the addition of 50µl of 3M NaOH to all wells on the plate and the absorbance was read at 405nm using a plate reader.

2.5 ISOLATION AND FRACTIONATION OF GASTRIC MUCOSAL CELLS

Gastric mucosal cells were isolated and fractionated by a colleague (see acknowledgements). Isolated gastric mucosal cells were prepared by digestion of everted sacs of rat corpus with pronase and intermittent chelation of Ca²⁺ with EDTA (Hatt and Hanson, 1989). Cells were separated into two fractions on a self-forming Percoll gradient (36ml/100ml isotonic Percoll, 12mM HEPES, 0.6mg/ml Bovine Serum Albumin, 0.3mM DTT, 1.8mM EDTA in Eagle's minimum essential medium). Unenriched cells were resuspended in the Percoll gradient solution and centrifuged at 30,000 *g*_{av} at 4°C using a 20° rotor in an ultracentrifuge for 13min. Two main zones of cells were produced, the low-density layer containing mainly parietal cells (around 80%) and the high-density layer containing mucous and other cells.

CHAPTER 3
ISOFORMS AND SUBCELLULAR LOCALISATION
GASTRIC MUCOSAL NITRIC OXIDE SYNTHASES:

3.1 INTRODUCTION

3.1.1 Aims

The various isoforms of NOS have been detected in a number of tissues and species. Ca^{2+} -dependent NOS activity was found in the stomach of fed rats by Salter et al. (1991), and this activity is possibly associated with mucus-containing epithelial cells (Brown et al. 1992). Aims of the work presented in this chapter were to use immunoblotting to characterise the Ca^{2+} -dependent NOS activity present in the rat gastric glandular mucosa by determining which isoforms were present, to investigate their subcellular distribution and, if more than one form was present, to determine their relative catalytic activity.

3.1.2 Immunoblotting for NOS isoforms

Immunoblotting with has been used to investigate the presence of the three isoforms of NOS in a variety of different tissues and cell-types. Summaries of recent and major studies are shown in tables 3.1 A, B and C.

Table 3.1 A: Tissues/cells giving positive results on immunoblotting with antibodies/antisera directed against nNOS

Tissue	Source	Antibody/ Antiserum	Band Recognition	Authors
BRAIN	Partially purified by 2', 5' ADP- Sephrose (Rat)	Polyclonal antisera to cerebellar NOS and to peptides from rat NOS	Only a single band detected - Size not shown	Springall et al. (1992)

Tissue	Source	Antibody/ Antiserum	Band Recognition	Authors
BRAIN	Cerebellum (Rat) direct into electrophoresis sample buffer.	Polyclonal antiserum to porcine cerebellar NOS	~160kDa	Kugler et al. (1994)
	Partially purified by 2', 5' ADP- Sephrose (Rat)	Polyclonal antiserum to rat cerebellar NOS	160kDa	Schmidt et al. (1992a)
	Brain (Rat) homogenised in sample buffer	Monoclonal anti- nNOS antibody	160kDa	Silvagno et al. (1996)
	100,000 x g _{av} supernatant from cerebellar homogenate (Rat)	Polyclonal antiserum to rat cerebellar NOS	160kDa	Schmidt et al. (1992b)
STOMACH	Homogenates of cardiac mucosa and oxyntic mucosa(Rat) in sample buffer.	Polyclonal antiserum to porcine cerebellar NOS	Band in cardiac mucosa but not oxyntic mucosa. ~160kDa	Kugler et al. (1994)
KIDNEY	100,000 x g _{av} supernatant from homogenate (Rat)	Polyclonal antiserum to rat cerebellar NOS	150-165kDa	Schmidt et al. (1992a)
PANCREAS	100,000 x g _{av} supernatant from homogenate (Rat)	Polyclonal antiserum to rat cerebellar NOS	150-165kDa	Schmidt et al. (1992a)

Tissue	Source	Antibody/ Antiserum	Band Recognition	Authors
PANCREAS	100,000 x g _{av} supernatant from homogenate of HIT-T15 pancreatic β cells (Hamster)	Polyclonal antiserum to rat cerebellar NOS	150kDa	Schmidt et al. (1992b)
LUNG	100,000 x g _{av} supernatant from homogenate (Rat)	Polyclonal antiserum to rat cerebellar NOS	150-165kDa	Schmidt et al. (1992a)
SKELETAL MUSCLE	Muscle (Rat) homogenised in sample buffer	Monoclonal anti- nNOS antibody	164kDa (splice variant)	Silvagno et al. (1996)
UTERUS	100,000 x g _{av} supernatant from homogenate (Rat)	Polyclonal antiserum to rat cerebellar NOS	150-165kDa	Schmidt et al. (1992a)
CARTILAGE	Extracts from Osteoarthritic chondrocytes (Human)	Polyclonal antibody to human nNOS	150kDa	Amin et al. (1995)

Table 3.1 B: Tissues/cells giving positive results on immunoblotting with antibodies/antisera directed against eNOS

Tissue	Source	Antibody/ Antiserum	Band Recognition	Authors
KIDNEY	Partially purified by 2', 5' ADP- Sephadex(LLC- PK ₁ tubular epithelial cells)	Monoclonal anti - eNOS antibody	~140kDa	Tracey et al. (1994)
AORTA	Partially purified by 2', 5' ADP- Sephadex, and tissue homogenates (Bovine from cultured or native endothelial cells)	Monoclonal anti - eNOS antibody	135kDa	Pollock et al. (1993)
	Homogenate (Porcine native cells)	Monoclonal anti - eNOS antibody	135kDa	Pollock et al. (1993)
SMALL INTESTINAL MESENTERY	Homogenate (Rat)	Monoclonal anti - eNOS antibody	135kDa	Pollock et al. (1993)

Table 3.1 C: Tissues/cells giving positive results on immunoblotting with antibodies directed against iNOS

Tissue	Source	Antibody/ Antiserum	Band Recognition	Authors
LIVER	Partially purified by 2',5' ADP- Agarose (Rat- Induced*)	Polyclonal anti- iNOS antiserum	125kDa	Oguchi et al. (1992)
	3T3 cells transfected with human hepatocyte iNOS, prepared in sample buffer	Polyclonal and Monoclonal anti- mouse iNOS antibodies	133kDa	Amin et al. (1995)
LUNG	Partially purified by 2',5' ADP- Agarose (Rat- Induced)	Polyclonal anti- iNOS antiserum	125kDa	Oguchi et al. (1992)
SPLEEN	Partially purified by 2',5' ADP- Agarose (Rat- Induced)	Polyclonal anti- iNOS antiserum	125kDa	Oguchi et al. (1992)
MACROPHAGE	Cell line induced and then prepared in sample buffer.	Polyclonal and monoclonal anti- mouse iNOS antibodies	133kDa	Amin et al. (1995)

* The term "induced" indicates treatment of animals or cells with lipopolysaccharide or *Propionibacterium acnes* to initiate iNOS expression.

The above tables indicate that the three isoforms of NOS have been detected by immunoblotting in a large number of tissues in different species. The sequence of a NOS isoform in one tissue may however be slightly different from that of another. There is evidence of alternative splicing of the primary transcript between exons 16 and 17 in nNOS from skeletal muscle (Silvagno et al., 1996), penis and urinary tract (Magee et al., 1996) with the resulting enzyme containing a 34 amino acid insert between the calmodulin and FMN binding domains. Alternative splicing of the primary transcript has also been observed in the promoter region (Xie et al., 1995). Evidence of heterogeneity of nNOS is also suggested by immunohistochemical studies where one antibody to nNOS known to stain neuronal NOS has been shown to recognise NOS in pancreatic islets of Langerhans (Schmidt et al., 1992a) whereas another antibody does not (Worl et al. 1994).

3.1.3 Subcellular distribution

3.1.3.1 eNOS

eNOS in bovine endothelial cells is found predominantly in the particulate fraction (Forstermann et al., 1991a; Hecker et al., 1991). Binding of eNOS to membranes was initially explained as due to a post-translational myristoylation at the N-terminus which allowed the enzyme to anchor to the membrane (Pollock et al., 1992; Lamas et al., 1992). More recently eNOS has been shown to be palmitoylated on cys-15 and cys-26 and mutagenesis of the palmitoylation sites reduced membrane association (Robinson & Michel, 1995). It seems likely that both myristoylation and palmitoylation are important for association with membranes.

3.1.3.2 nNOS

Early studies found nNOS to be predominantly soluble (Forstermann et al., 1991b; Schmidt et al., 1991; Bredt et al. 1990). The lack of membrane localisation was presumed to be due to a lack of a myristoylation site (Bredt et al., 1991). However, particulate rat brain NOS activity has been described in more recent studies by Hiki

et al. (1992), Matsumoto et al. (1993) and Hecker et al. (1994), who detected NOS activity in an endoplasmic reticulum fraction of rat cerebellum. No difference was found between soluble and particulate forms with respect to specific activity, Ca^{2+} - and pH-dependency, inhibitor sensitivity or immunoreactivity. A 155kDa band was recognised in both soluble and particulate fractions by an antiserum directed against rat cerebellar NOS indicating that the NOS activity in the particulate fraction is nNOS. The more recent studies assays of NOS activity were carried out in the presence of FAD, while this was not the case in earlier studies indicating that detection of particulate NOS activity from rat brain requires added FAD. Particulate nNOS has also been shown in the sarcolemma of skeletal muscle (Kobzik et al., 1994). In skeletal muscle nNOS associates with dystrophin (Brenman et al., 1995) by binding to α 1-syntrophin (Brenman et al., 1996), a protein which is a constituent of the dystrophin complex. Binding involves interaction of a PDZ protein motif in the amino-terminus of nNOS with a similar domain on α 1-syntrophin. In the brain nNOS binds, again by PDZ domain interactions, to two proteins related to syntrophin, namely PSD 95 and PSD 93 (Brenman et al., 1996).

No studies have investigated the subcellular localisation of NOS in rat gastric glandular mucosa.

3.1.4 Practical considerations

3.1.4.1 Antisera and antibodies

As described in Chapter 2, two antisera were raised to peptides from rat brain NOS. The internal peptide corresponds to residues 252-267 of rat brain NOS and the carboxyl-terminal peptide corresponds to residues 1414-1429 of the same enzyme with a cysteine residue added to, respectively, the carboxyl-terminal and amino-terminal ends, and to which keyhole limpet haemocyanin was conjugated. The sequences of the two peptides used are shown in table 3.1D.

Table 3.1 D Sequences of peptides used in raising antisera

Peptide	N-Terminus	Peptide Sequence	C-Terminus
Internal	Ac-	D-N-D-R-V-F-N-D-L-W-G-K-D-N-V-P-C	-NH ₂
C-terminal	H-	C-A-F-I-E-E-S-K-K-D-A-D-E-V-F-S-S	-NH ₂

The two peptides used were chosen for a variety of reasons. Firstly, with these sequences the antisera produced were likely to be isoform specific (see Appendix A5). Secondly, evaluation by Riveros -Moreno et al. (1993) of a number of peptides from the rat brain NOS sequence pointed to these peptides being suitably antigenic. Thus, antibody titre from rabbits immunised with sequences similar to the internal and the carboxyl-terminal peptides was high in relation to many of the other peptides used and antisera to both peptides recognised a 160kDa band by immunoblotting of partially purified rat brain NOS but did not cross react with macrophage iNOS. Thirdly, an internal peptide was used as well as the carboxyl-terminal peptide because of the possibility of proteolytic cleavage at the carboxyl-terminus removing the peptide in homogenates.

During the course of the project a monoclonal and a polyclonal antibody to nNOS became available commercially both raised against a protein fragment corresponding to residues 1095-1289 of human nNOS. This region showed 97% homology with rat nNOS. An antibody to eNOS was also available raised against residues 1030-1209 of human eNOS. The sequences of the NOS isoforms are given in Appendix A5, and the relevant sequences against which the various antibodies and antisera were raised are highlighted.

3.2 METHODS

3.2.1 Samples for SDS-PAGE

The basic protocol for preparation of samples is given in 2.3.1.1. Modifications are described as appropriate in the results section.

3.2.2 Removal of NOS from a gastric mucosal homogenate by affinity adsorption

NOS adsorbs onto 2', 5'-ADP agarose by virtue of its ability to bind β -NADPH. The following procedure was used to provide evidence that bands obtained on immunoblots were due to NOS by showing that pretreatment of samples with 2', 5'-ADP agarose and centrifugation could remove the immunoreactive material.

Gastric mucosa, obtained as described in 2.2.2.2, was placed in a glass scintillation vial and was homogenised in purification buffer (0.57mM PMSF, 10 μ g/ml aprotinin, 10 μ g/ml leupeptin, 10 μ g/ml pepstatin, 1mM benzamidine, 5 μ M 2-mercaptoethanol, 1mM EDTA in 50mM Tris.HCl pH 7.5) using 5ml buffer per 1g tissue. The homogenate was then centrifuged for 30min at 100,000 x g_{av} at 4°C. A sample of the supernatant was saved for assay of protein (Coomassie Blue procedure, 2.1.2). A control sample was prepared for electrophoresis by adding 250 μ l of supernatant to 250 μ l of boiling whole 2x electrophoresis sample buffer in a 1.5ml microfuge tube, boiling for 5min then centrifuging for 5min at 10,000 x g_{av} in a microcentrifuge. The remaining supernatant was retained for the NOS removal experiment.

2', 5'-ADP agarose was prepared by swelling 1ml of gel in 5ml of purification buffer and washing twice with the same buffer by allowing the ADP agarose to settle, decanting the buffer off and adding more of the same buffer. One half of the ADP agarose was then resuspended in purification buffer to give a 50:50 suspension and the other half was resuspended in the same buffer containing 10mM β NADPH, again to give a 50:50 suspension. 200 μ l of each suspension was added to separate 1.5ml microfuge tubes (i.e. 100 μ l of ADP agarose) and 500 μ l of gastric

mucosal supernatant was added to each tube. The tubes were incubated for 15min at 4°C on a roller (40rpm) and then centrifuged for 30s in a microcentrifuge at room temperature to pellet the ADP agarose. Samples for electrophoresis were prepared by removing 250µl of the supernatants from the tube and boiling for 5min with 250µl of 2x electrophoresis sample buffer.

3.2.3 Partial purification of NOS

Stomachs and brains (cerebella) from five male Wistar rats (200-300g) were removed under terminal anaesthesia and were homogenised separately in purification buffer using an Ultraturrax homogeniser at full speed for 30s. The five homogenates were pooled and were centrifuged at 100,000 x g_{av} for 30min at 4°C. 2', 5'-ADP agarose was prepared as above (3.2.2), and 1ml of 2', 5'-ADP agarose was added to each of two 1cm x 30cm polystyrene columns, one for brain and one for gastric mucosa. Supernatants of each homogenate were then added to the appropriate columns and run through (Flow rate=1-2ml/min). Each column was then washed with 25ml of purification buffer containing 0.5M NaCl. This step was to remove proteins unrelated to NOS which might be binding to the column via weak ionic reactions. The columns were then washed again with purification buffer (10ml per column). NOS was finally eluted from each column with 4ml of purification buffer containing 10mM βNADPH. A sample of each eluate was retained for protein assay (Coomassie Blue procedure, 2.1.2) and the remaining eluates were freeze-dried overnight in 1ml aliquots. The freeze-dried samples were reconstituted in boiling 2x electrophoresis sample buffer (to give a concentration of 10µg protein per 40µl) and boiled for 5min.

3.2.4 Variation in treatment of tissue homogenates before preparation for electrophoresis

Gastric mucosa was removed and homogenised in NOS purification buffer (see 3.2.2). The homogenate was then split into fractions to be treated in three different ways. One fraction was prepared for electrophoresis as described for homogenate in 2.3.1.1. This sample was then stored at -20°C. The remaining two fractions were centrifuged at 100,000 x g_{av} for 30 minutes at 4°C. The supernatant of one of the fractions was immediately prepared for electrophoresis as above while the supernatant of the remaining fraction was stored overnight at 4°C before preparation for electrophoresis.

3.2.5 Inclusion of protein phosphatase inhibitors during preparation of samples

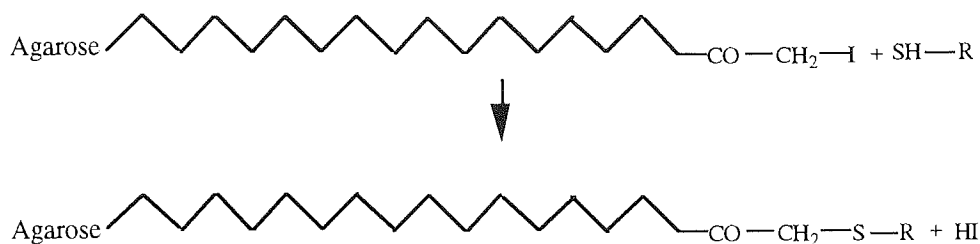
Rat gastric mucosa was removed under terminal anaesthesia and was homogenised in purification buffer (see 3.2.2). The homogenate was then diluted 1:1 in NOS purification buffer containing one of the following phosphatase inhibitors: okadaic acid, 0.5-10µM; calyculin A, 50nM; NaF, 100mM, and was then centrifuged for 100,000 x g_{av} for 30min at 4°C. 500µl of supernatant was then removed and prepared for electrophoresis by boiling for 5min in the same volume of 2 x sample buffer.

3.2.6 Affinity adsorption of antiserum raised against the carboxyl-terminal peptide of rat brain NOS with the immobilised peptide.

3.2.6.1 Coupling of peptide to agarose gel

A peptide-affinity matrix was prepared by using SulphoLink gel which reacts specifically with sulphhydryls via the iodoacetyl group (figure 3.1 A, SH-R represents the peptide) and therefore the carboxyl-terminal peptide was immobilised on the gel via the terminal cysteine residue.

Figure 3.2: Peptide immobilisation on Sulpholink gel



Coupling gel (SulphoLink) was brought to room temperature and was added to two capped tubes (1ml gel in each tube). The gel was washed twice with 3ml of column buffer (50mM Tris, 5mM EDTA, pH 8.5) by adding the buffer to the tube, mixing for 2min on a slow roller (40rpm) and allowing the gel to settle before removing the buffer by pipette and repeating the wash. The carboxyl-terminal peptide of NOS was coupled to the gel in one tube by adding 1ml of the peptide solution (1mg/ml in PBS). The control gel in the other tube was prepared by adding 1ml of column buffer. Both tubes were incubated at room temperature for 15min on a slow roller (40rpm) and were then allowed to settle for 30min at room temperature. The supernatant was then removed from each tube and the gel was washed with 3ml of column buffer as before. Unreacted iodoacetyl sites were blocked in both tubes by adding 1ml of cysteine solution (50mM in column buffer) to each tube, incubating at room temperature for 15min on a slow roller (40rpm) and allowing to settle for 30min at room temperature. The contents of each tube were then transferred to two plastic columns (5ml in volume) and 16ml of TBS (10mM Tris, 100mM NaCl, pH 7.5) was washed through each column.

3.2.6.2 Adsorption of antiserum

The coupling gel in the two columns was resuspended in two tubes in TBS/Tween to give 1:1 suspensions. 400µl of each suspension (200µl of affinity matrix) was transferred to two 1.5ml microfuge tubes. A third tube was prepared containing only 200µl of TBS/Tween. 4µl of the antiserum raised against the carboxyl-

terminal peptide of rat brain NOS was added to each tube. The three tubes were incubated at room temperature for 30min on a slow roller (40rpm). The tubes were then subjected to centrifugation for 1min at $10,000 \times g_{av}$. 100 μ l of the supernatant from each tube was added to three tubes containing 2.4ml of TBS/Tween/Milk which were then whirlmixed before applying the contents to protein blots on nitrocellulose.

3.2.7 Subcellular fractionation

Cerebellum and gastric mucosa were homogenised separately in homogenisation buffer (10 μ g/ml soybean trypsin inhibitor, 10 μ g/ml leupeptin, 6 μ g/ml aprotinin, 0.1mg/ml PMSF in 10mM HEPES, 320mM sucrose, 1mM Dithiothreitol, 0.1mM EDTA, pH 7.5) using an Ultraturrax homogeniser at full speed for 30s on ice. The homogenates were centrifuged at $100,000 \times g_{av}$ for 30 minutes at 4°C in an ultracentrifuge. The supernatants were removed and kept on ice. The pellets were transferred to 1.5ml microfuge tubes to be resuspended. Homogenisation buffer containing 10% (v/v) glycerol was added to each pellet. The volume of buffer added equalled the initial volume of homogenate that had been centrifuged. The pellets were resuspended in this buffer by homogenising with an Ultra-turrax microhomogeniser for 30s at full speed on ice. The resuspended pellets were then returned to ice. Both supernatant and pellet samples were used immediately, either in an assay to measure NOS activity or to make samples for electrophoresis (Hecker et al., 1994), or both.

3.2.8 NOS assay

To measure NOS activity in pellet and supernatant fractions of brain and gastric mucosal tissue the NOS assay for subcellular fractions described in 2.2.2 was used which was a modification of the procedure used by Hecker et al. (1994).

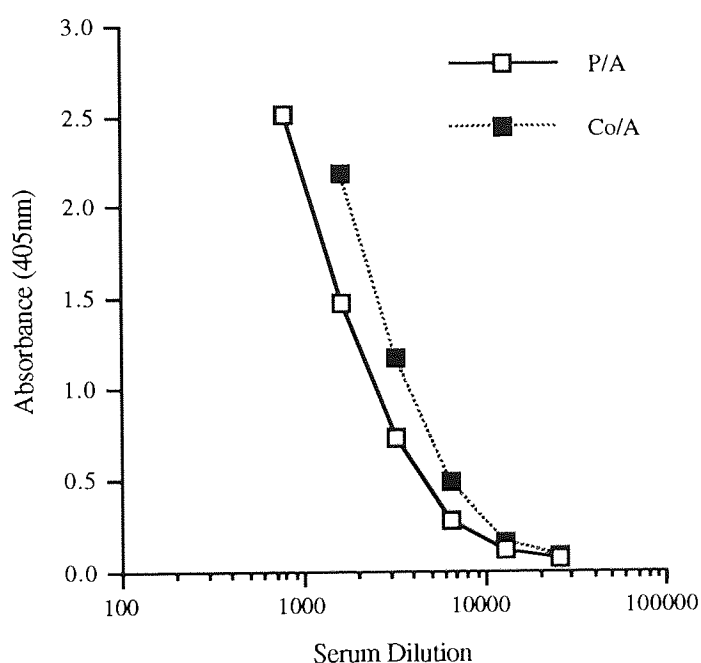
3.3 RESULTS

All the immunoblotting results presented in this chapter derive from experiments repeated at least three times.

3.3.1 Measurement of antibody titre in anti-peptide antisera

Figures 3.3.1 A and 3.3.1 B show the results obtained from ELISAs for recognition of peptides using sera obtained from 2 rabbits in the week 9 test bleed of the immunisation procedure.

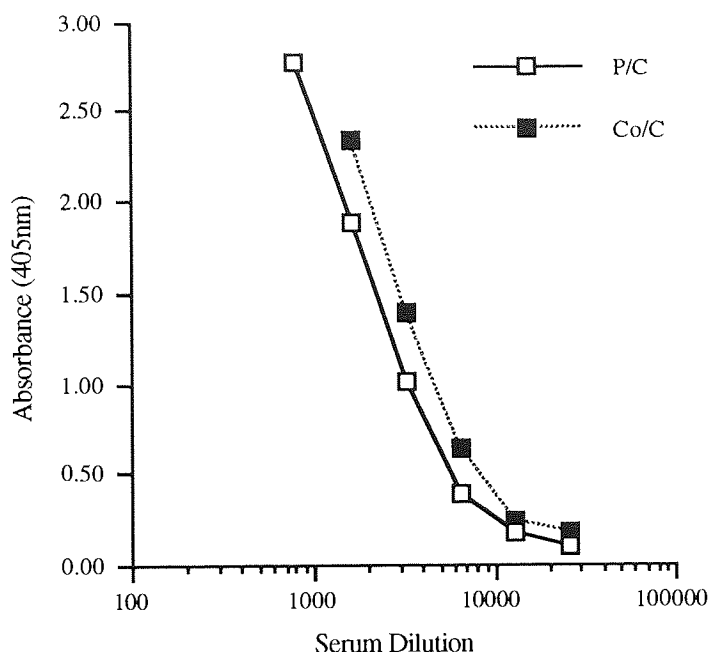
Figure 3.3.1 A: Titres for antisera against an internal peptide of nNOS



Legend to Figure 3.3.1 A

Graph showing the results of an ELISA investigating the recognition of an internal peptide of NOS (P) or a bovine serum albumin conjugate of the peptide (Co) by an antiserum (A) from a rabbit immunised with the peptide.

Figure 3.3.1 B: Titres for antisera against a carboxyl-terminal peptide of nNOS



Legend to Figure 3.3.1 B

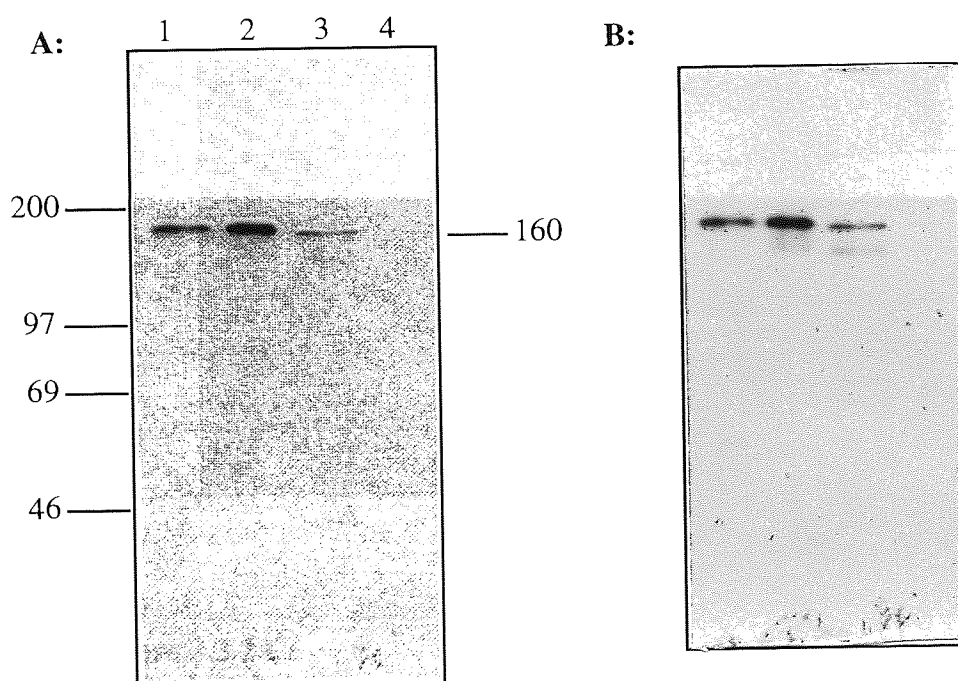
Graph showing the results of an ELISA investigating the recognition of a carboxyl-terminal peptide of nNOS (P) or a bovine serum albumin conjugate of the peptide (Co) by an antiserum from a rabbit immunised with the peptide.

Rabbits developed a high titre of antibodies which bound to the peptides with which the rabbits were immunised. The graphs for both peptides show that when each peptide was presented as a conjugate with bovine serum albumin, the level of recognition was higher than when only a simple peptide was presented. In all cases antibody binding to wells with peptide-albumin conjugate was higher than for wells containing peptide alone. As a result of pilot immunohistochemistry experiments (Chapter 4) the antisera used in immunoblotting were from rabbit A (internal peptide of NOS) and rabbit C (carboxyl-terminal peptide of nNOS), and the ELISA data for these two antisera are shown above.

3.3.2 Immunoblotting with monoclonal antibodies against nNOS and eNOS

The monoclonal anti-nNOS antibody reacted with a 160kDa protein on blots of extracts of rat brain, rat pituitary tumour cells and gastric glandular mucosa but no such band was obtained with an extract of rat intestinal mesentery (Figure 3.3.2 A). A photograph (Figure 3.3.3 B) is provide to allow comparison with the appearance of the scanned image in figure 3.3.2 A. Immunoblotting with fractions of gastric mucosal cells also gave a band at 160kDa in unenriched cells and in a high-density Percoll fraction of cells but a very weak band was evident in a low-density Percoll fraction of cells (Figure 3.3.2 C).

Figures 3.3.2 A and B: Immunoblotting with monoclonal anti-nNOS antibody



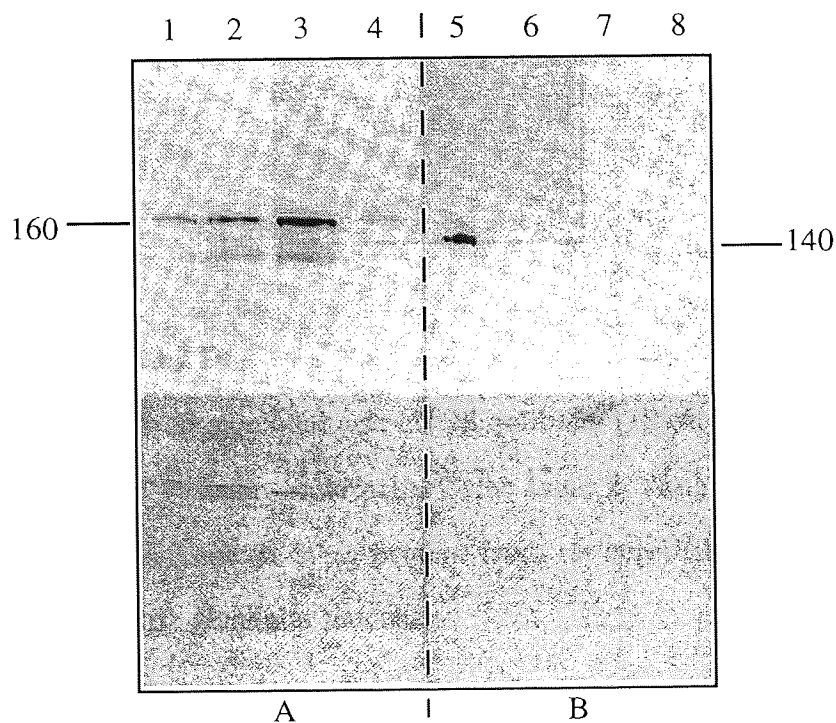
Legends to Figures 3.3.2 A and B

3.3.2 A: Immunoblotting with monoclonal anti-nNOS antibody (1 μ g/ml). Lane 1, 50 μ g protein from rat cerebellum; lane 2, 5 μ g protein from rat pituitary cells; Lane 3, 100 μ g protein from rat gastric glandular mucosa; Lane 4, 100 μ g of protein from rat intestinal mesentery.

3.3.2 B: Photograph of blot shown scanned in 3.3.2 A.

A band of molecular mass 140kDa was obtained when immunoblotting with the anti-eNOS antibody in extracts of human aortic endothelial cells, rat intestinal mesentery, rat cerebellum and rat gastric glandular mucosa (Figure 3.3.2.D). This band was not seen in extracts of any fraction of isolated gastric mucosal cells (Figure 3.3.2 C).

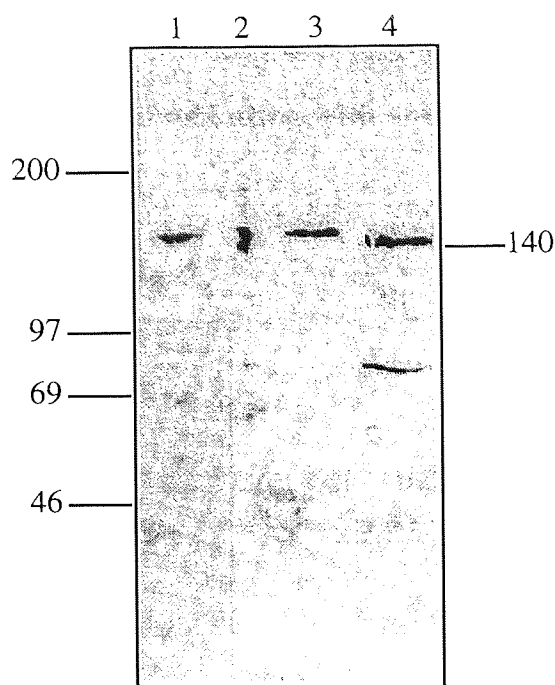
Figure 3.3.2 C: Immunoblotting with monoclonal anti-nNOS and anti-eNOS antibodies



Legend to Figure 3.3.2 C:

Side A, Immunoblotting with monoclonal anti nNOS antibody (1 μ g/ml); Side B, Immunoblotting with anti eNOS antibody (1 μ g/ml). Lanes 1 and 5, 100 μ g of protein from gastric glandular mucosa; Lanes 2 and 6, 100 μ g of protein from unenriched gastric glandular mucosal cells; Lanes 3 and 7, 100 μ g protein from gastric glandular mucosal cells from a high-density Percoll fraction; Lanes 4 and 8, 100 μ g protein from gastric glandular mucosal cells from a low-density Percoll fraction.

Figure 3.3.2 D: Immunoblotting with monoclonal anti-eNOS antibody



Legend to Figure 3.3.2 D:

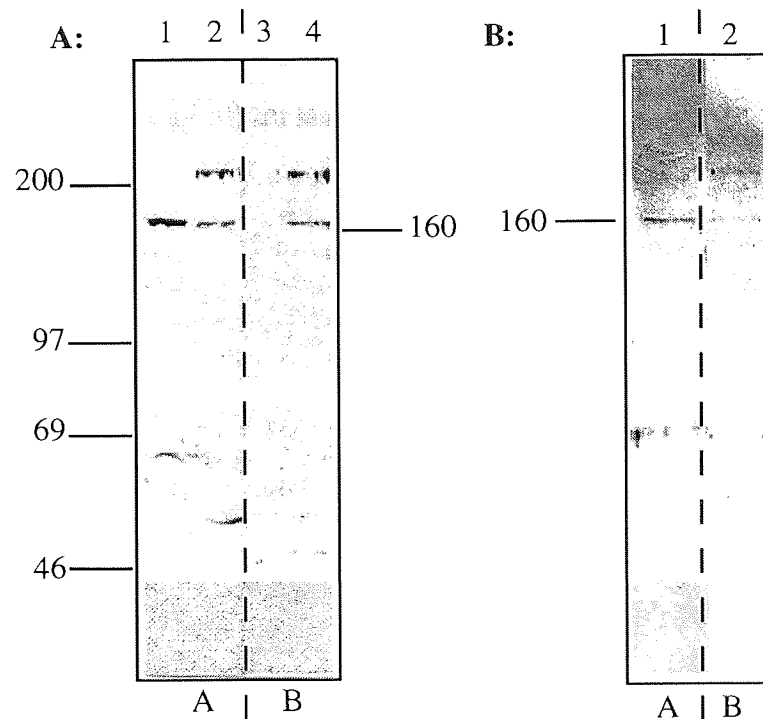
Immunoblotting with monoclonal anti-eNOS antibody (1 μ g/ml). Lane 1, 15 μ g of protein from human vascular endothelial cells; Lane 2, 75 μ g of protein from rat intestinal mesentery; Lane 3, 50 μ g protein from rat cerebellum; Lane 4, 100 μ g protein from rat gastric glandular mucosa.

3.3.3 Immunoblotting of brain and gastric mucosa with the carboxyl-terminal antiserum

The rabbit antiserum raised against the carboxyl-terminal peptide of nNOS reacted with a 160kDa protein on blots of extracts of rat brain (Figure 3.3.3 A) and rat gastric glandular mucosa (Figures 3.3.3 A and 3.3.3 B). The recognition of this band in brain was blocked when peptide was added with the antiserum at a concentration of 20 μ g/ml but peptide at this concentration had little effect on recognition of the band in gastric glandular mucosa (Figure 3.3.3 A). When the peptide was added with the antiserum at a concentration of 100 μ g/ml it was

possible to reduce the intensity of the 160kDa band in gastric glandular mucosa (Figure 3.3.3 B).

Figures 3.3.3 A and B: Immunoblotting with antiserum to carboxyl-terminal peptide of nNOS \pm peptide



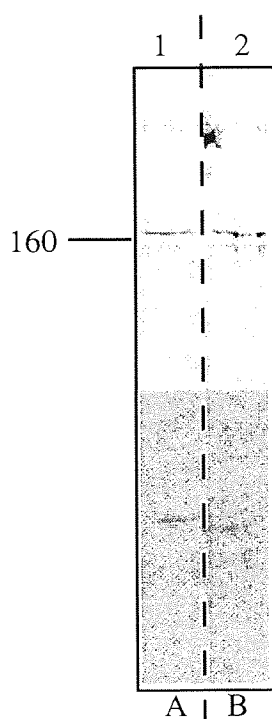
Legend to Figure 3.3.3 A and B

3.3.3 A: Side A, Immunoblotting with antiserum to carboxyl-terminal peptide of nNOS (1/1250). Side B, Immunoblotting with antiserum to carboxyl-terminal peptide of nNOS (1/1250) plus 20 μ g/ml of the peptide. Lanes 1 and 3, 50 μ g of protein from rat cerebellum; Lanes 2 and 4, 100 μ g of protein from rat gastric glandular mucosa.

3.3.3 B: Side A, Immunoblotting with antiserum to carboxyl-terminal peptide of nNOS (1/1250). Side B, Immunoblotting with antiserum to carboxyl-terminal peptide of nNOS (1/1250) plus 100 μ g/ml of the peptide. Lanes 1 and 2, 100 μ g of protein from rat gastric glandular mucosa.

A similar lack of reduction in recognition of the 160kDa band by antiserum was seen with extracts of isolated gastric mucosal cell (Figure 3.3.3 C). An approximately 200kDa band was also recognised by the antiserum in gastric mucosa but this band was not blocked by any concentration of peptide and was not found with the isolated cells (Figure 3.3.3 C).

Figure 3.3.3 C: Immunoblotting with antiserum to carboxyl-terminal peptide of nNOS \pm peptide (20 μ g/ml) on isolated cells

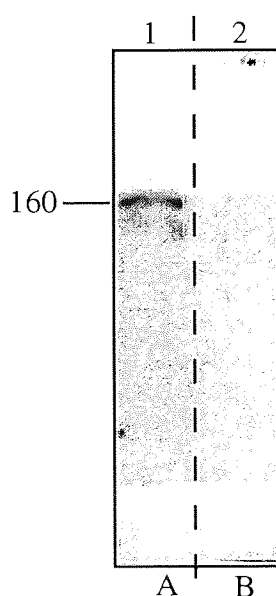


Legend to Figure 3.3.3 C

Side A, Immunoblotting with antiserum to carboxyl-terminal peptide of nNOS (1/1250). Side B, Immunoblotting with antiserum to carboxyl-terminal peptide of nNOS (1/1250) plus 20 μ g/ml of the peptide. Lanes 1 and 2 both contain 100 μ g of protein from unenriched gastric glandular mucosal cells.

A 160kDa band was also recognised in an immunoblot of recombinant rat brain nNOS incubated with the rabbit antiserum against the carboxyl-terminal peptide of nNOS and recognition of this band was blocked when peptide was added with the antiserum at a concentration of 20µg/ml (Figure 3.3.3 D). When inhibition of recognition of the 160kDa band by the presence of the peptide was quantified by densitometric analysis of blots the ability of the peptide to block recognition of the 160kDa band in gastric mucosa was significantly lower ($p<0.001$) than its ability to block the band in brain (Figure 3.3.7 B).

Figure 3.3.3 D: Immunoblotting with antiserum to carboxyl-terminal peptide of nNOS \pm peptide (20µg/ml) on recombinant rat brain NOS

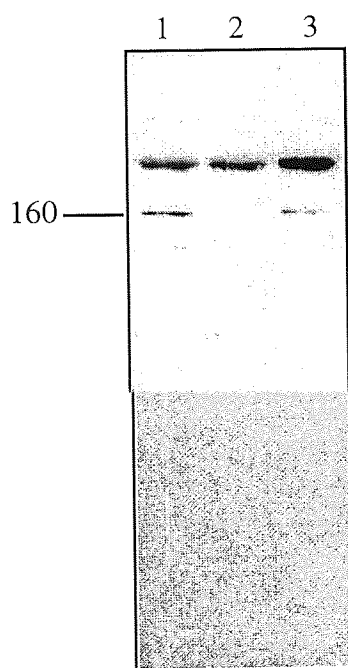


Legend to Figure 3.3.3 D:

Side A, Immunoblotting with antiserum to carboxyl-terminal peptide of nNOS (1/1250). Side B, Immunoblotting with antiserum to carboxyl-terminal peptide of nNOS (1/1250) plus 20µg/ml of the peptide. Lanes 1 and 2 both contain 200ng of rat brain recombinant NOS.

Incubation of the 100,000 x g_{av} supernatant of an extract of gastric mucosa with 2', 5' - ADP agarose followed by centrifugation removed the 160kDa band from the supernatant but not the 200kDa band. Addition of 10mM β -NADPH reduced the ability of ADP agarose to remove the band (Figure 3.3.3 E).

Figure 3.3.3 E: Immunoblotting with antiserum to carboxyl-terminal peptide of nNOS on tissue homogenates showing removal of NOS after 2' ,5' - ADP agarose.



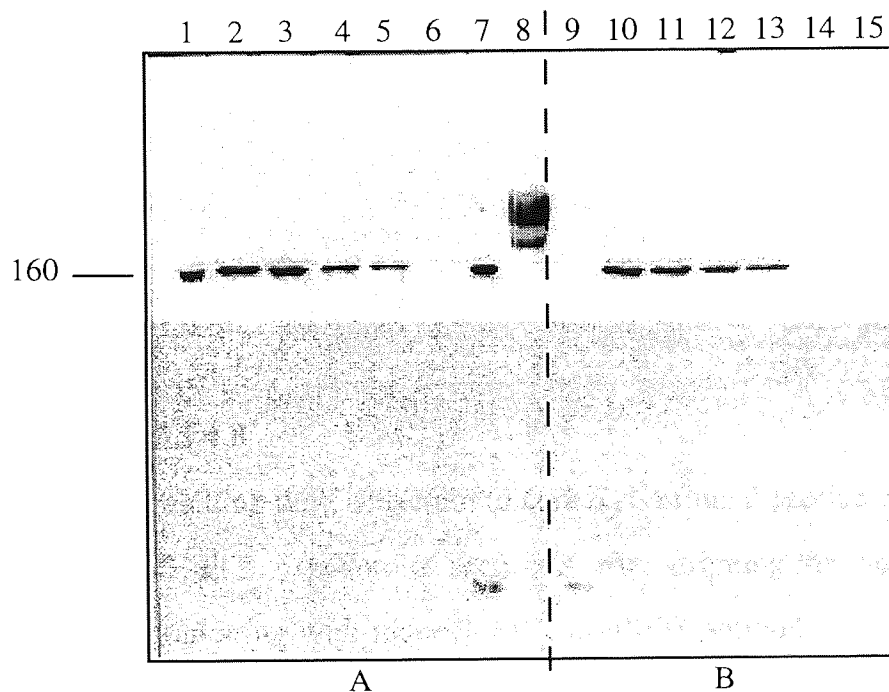
Legend to Figure 3.3.3 E

Immunoblotting with antiserum to carboxyl-terminal peptide of nNOS (1/1250).
Lane 1, 100 μ g of protein from an homogenate of rat gastric glandular mucosa;
Lane 2, 100 μ g of protein from an homogenate of rat gastric glandular mucosa preadsorbed with 2', 5' ADP-agarose; Lane 3, 100 μ g of protein from an homogenate of rat gastric glandular mucosa preadsorbed with 2', 5' ADP-agarose plus 10mM β -NADPH.

3.3.4 Inability of the peptide (20µg/ml) to substantially reduce recognition of the 160kDa band by antiserum was also found with pancreatic samples

A 160kDa band in was also recognised by the carboxyl-terminal antiserum in extracts of rat pancreas and this recognition could not be abolished by addition of the peptide. At all loadings of the pancreas extract at which the 160kDa band is evident the peptide does not substantially block recognition (3.3.4 A).

Figure 3.3.4 A: Immunoblotting with antiserum to carboxyl-terminal peptide of nNOS ± peptide (20µg/ml) on brain and pancreatic samples

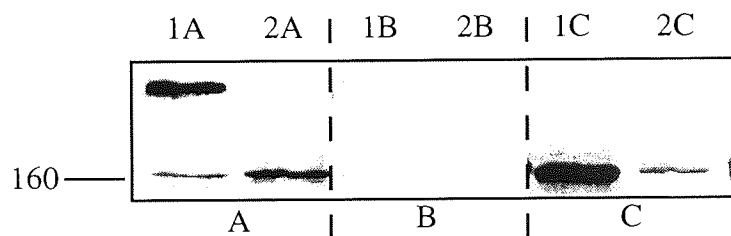


Legend to Figure 3.3.4 A

Side A, Immunoblotting with antiserum to carboxyl-terminal peptide of nNOS (1/1250). Side B, Immunoblotting with antiserum to carboxyl-terminal peptide of nNOS (1/1250) plus 20µg/ml of the peptide. Lanes 1, 7, 9 and 15, 50µg of protein from rat cerebellum; Lanes 2 and 10, Lanes 3 and 11, Lanes 4 and 12, Lanes 5 and 13, Lanes 6 and 14, 100µg, 75µg, 50µg, 25µg and 10µg of protein from rat pancreas respectively. Lane 8, 10µl of rainbow markers (Amersham).

The 160kDa band recognised by the antiserum to the carboxyl-terminal peptide of nNOS in gastric mucosal and pancreas extracts was the same band as was recognised by the monoclonal anti-nNOS antibody since when the antiserum was stripped off an immunoblot of the two extracts the bands recognised by the monoclonal anti-nNOS antibody were at exactly the same positions (Figure 3.3.4 B).

Figure 3.3.4 B: Immunoblotting with antiserum to carboxyl-terminal peptide of nNOS and monoclonal anti-nNOS antibody on gastric mucosal and pancreatic tissue homogenates



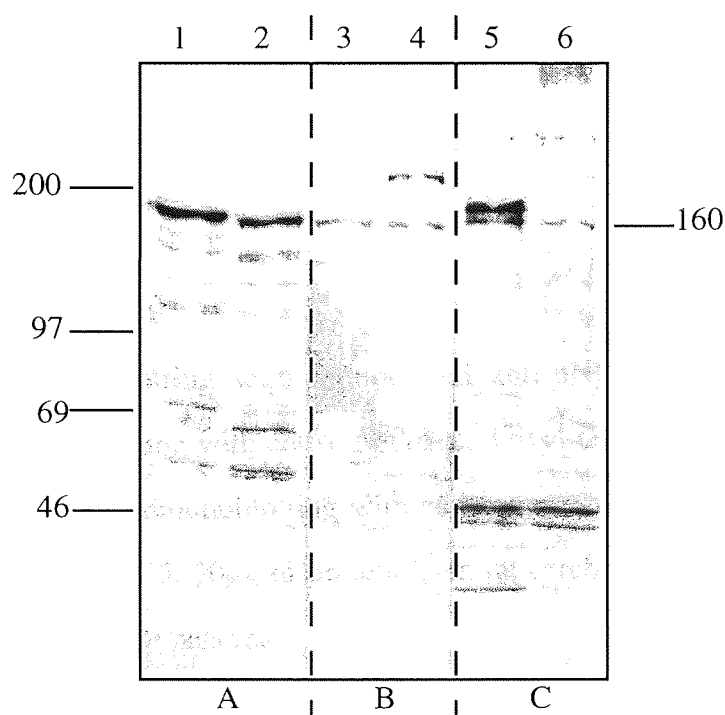
Legend to Figure 3.3.4 B

Section A, Immunoblotting with antiserum to carboxyl-terminal peptide of nNOS (1/1250). Section B, ECL exposure of section A after stripping the membrane. Section C, Immunoblotting with monoclonal anti-nNOS antibody (1 μ g/ml) on Section B. Lane 1, 100 μ g of protein from gastric glandular mucosa; Lane 2 100 μ g of protein from rat pancreas.

3.3.5 An antiserum directed against an internal peptide of NOS recognised a 160kDa Band in samples of brain, gastric mucosa and pancreas

The rabbit antiserum raised against the internal peptide of NOS also recognised a 160kDa band in immunoblots of extracts of rat brain, gastric glandular mucosa and pancreas (Figures 3.3.5 A and B). The brain band was strong and possibly a doublet but the bands seen with gastric mucosa and pancreas were consistently light and in some cases barely detectable.

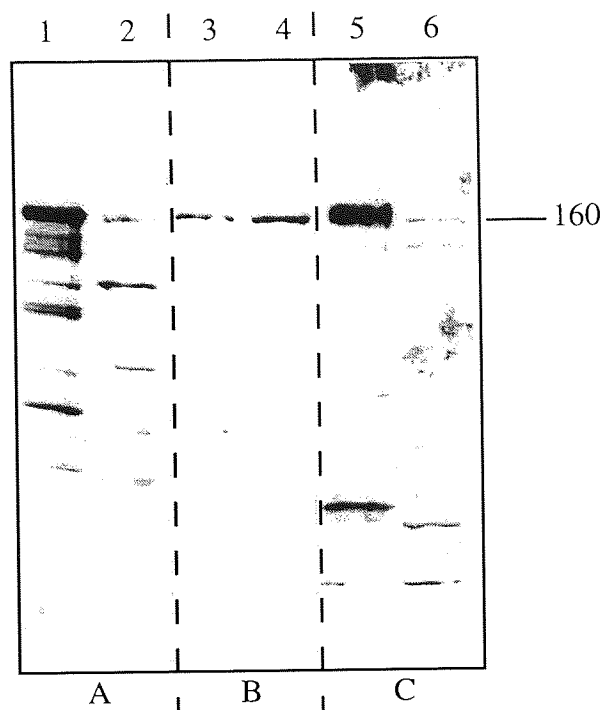
Figure 3.3.5 A: Immunoblot of brain versus gastric mucosa using monoclonal anti-nNOS antibody and anti-peptide antisera



Legend to Figure 3.3.5 A

Section A, Immunoblotting with monoclonal anti-nNOS antibody (1 μ g/ml). Section B, Immunoblotting with antiserum to carboxyl-terminal peptide of nNOS (1/1250). Section C, Immunoblotting with antiserum to internal peptide of NOS (1/500). Lanes 1, 3 and 5, 50 μ g of protein from rat cerebellum; Lanes 2, 4 and 6, 100 μ g of protein from rat gastric glandular mucosa.

Figure 3.3.5 B: Immunoblot of brain versus pancreas using monoclonal anti-nNOS antibody and anti-peptide antisera



Legend to Figure 3.3.5 B

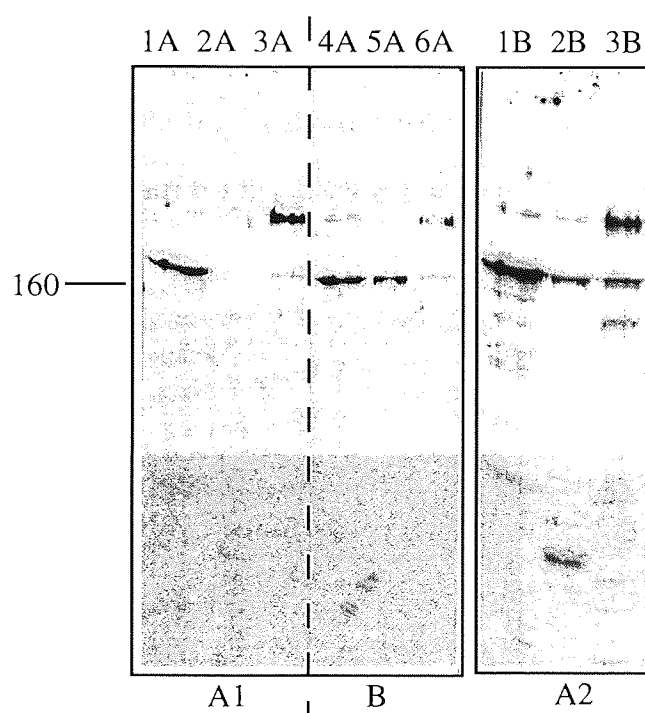
Section A, Immunoblotting with monoclonal anti-nNOS antibody (1 μ g/ml).
 Section B, Immunoblotting with antiserum to carboxyl-terminal peptide of nNOS (1/1250).
 Section C, Immunoblotting with antiserum to internal peptide of NOS (1/500).
 Lanes 1, 3 and 5, 50 μ g of protein from rat cerebellum; Lanes 2, 4 and 6, 100 μ g of protein from rat pancreas.

3.3.6 Effect of pre-adsorption of carboxyl-terminal antiserum on a peptide affinity matrix

Adsorption of the antiserum with the carboxyl-terminal peptide conjugated to an agarose matrix, removed antibodies recognising the 160kDa band in brain extracts but not extracts of pancreas or gastric mucosa. Control antiserum was treated with cysteine-agarose matrix and this antiserum recognised the 160kDa band in all three

extracts (Figure 3.3.6) When the first three lanes of an immunoblot developed using antiserum treated with the peptide-agarose matrix was reprobed using untreated antiserum the brain band showed up as well as the pancreas and gastric mucosal bands, confirming the presence of the protein on the blot (Figure 3.3.6).

Figure 3.3.6: Immunoblotting with antiserum to carboxyl-terminal peptide of nNOS pretreated with a peptide-agarose or a cysteine-agarose affinity matrix



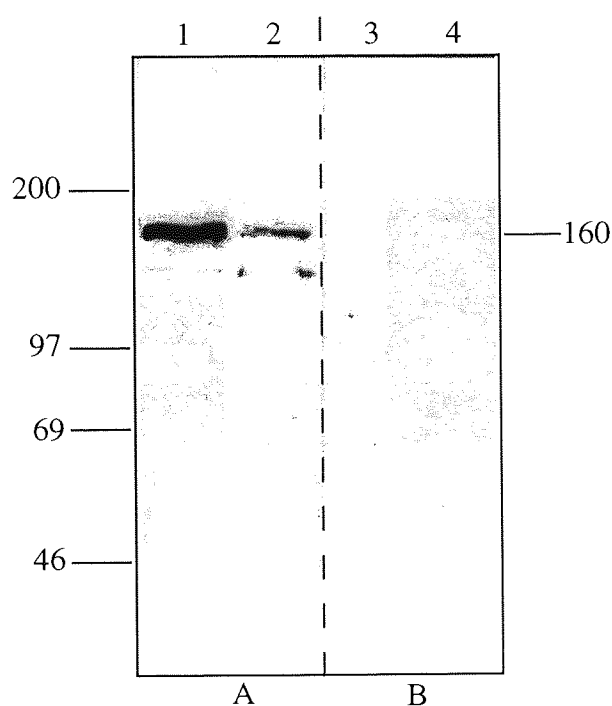
Legend to Figure 3.3.6

Section A1, Immunoblotting with antiserum to carboxyl-terminal peptide of nNOS (1/1250) pre-treated on an agarose matrix conjugated to the peptide. Section B, Immunoblotting with antiserum to carboxyl-terminal peptide of nNOS (1/1250) pre-treated with agarose conjugated to cysteine. Section A2, Immunoblotting of section A1 with whole antiserum to carboxyl-terminal peptide of nNOS (1/1250) after washing of the membrane. Lanes 1 and 4, 100μg of protein from rat pancreas; Lanes 2 and 5, 50μg of protein from rat cerebellum; Lanes 3 and 6, 100μg of protein from rat gastric glandular mucosa.

3.3.7 Investigation into poor reduction of recognition of the 160kDa band by the carboxyl-terminal peptide at 20µg/ml

Investigation of the differing antigenicity of gastric mucosal and brain nNOS could be facilitated by purification of the enzyme. The carboxyl-terminal antiserum recognised a 160kDa protein in gastric mucosal and brain extracts which had been partially purified by affinity chromatography on 2', 5'-ADP agarose, this recognition was prevented in purified samples of both tissues by peptide at a concentration of 20µg/ml (Figure 3.3.7 A).

Figure 3.3.7 A: Immunoblotting with antiserum to carboxyl-terminal peptide of nNOS ± peptide (20µg/ml) using partially purified NOS

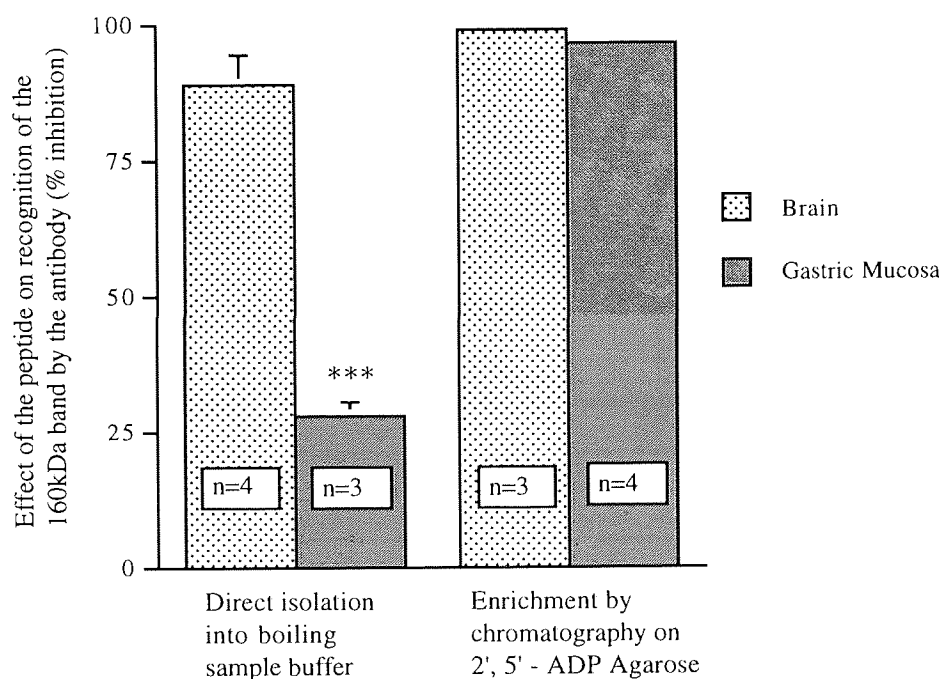


Legend to Figure 3.3.7 A

Side A, Immunoblotting with antiserum to carboxyl-terminal peptide of nNOS (1/1250). Side B, Immunoblotting as Side A plus 20µg/ml of the peptide. Lanes 1 and 3, 10µg of partially purified NOS protein from cerebellum; Lanes 2 and 4, 10µg of partially purified NOS protein from gastric glandular mucosa.

There was no measurable difference (by densitometric analysis) between the ability of the peptide to block recognition of the 160kDa band in partially purified brain or gastric mucosal samples (Figure 3.3.7 B). The enriched material was also recognised in immunoblots by the monoclonal anti-nNOS antibody and by the antiserum directed against the internal peptide (not shown).

Figure 3.3.7 B: Quantification of block by the peptide of recognition of the 160kDa band by the antiserum directed against a carboxyl-terminal peptide of nNOS on crude tissue extracts or partially purified preparations of NOS



Legend to Figure 3.3.7 B

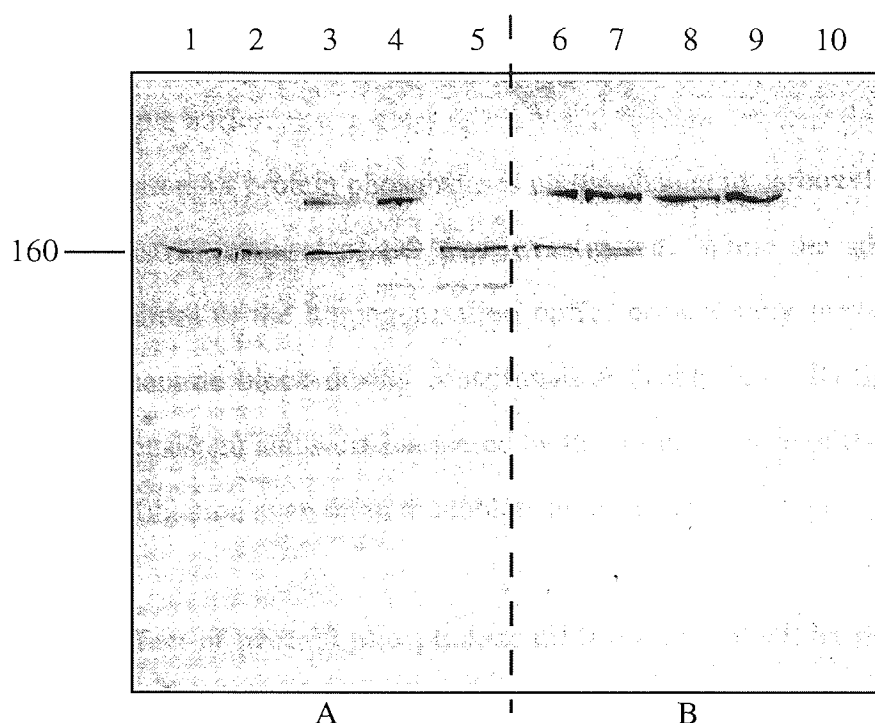
Results are given as means \pm S.E.M with n equal to the number of separate preparations. The effect of the peptide was calculated by densitometric analysis using NIH image. A result of 100% means that peptide completely inhibits recognition by the antibody. ***, $P < 0.001$ for the comparison between brain and gastric mucosa by Student's t test.

The ability of the peptide to block the 160kDa band in gastric mucosa appeared during the time between homogenisation of the tissue and the end of the 30min centrifugation to prepare a 100,000 x g_{av} supernatant . Thus, peptide could not block recognition of the band in gastric mucosa prepared directly into boiling electrophoresis sample buffer, and only occasionally in samples homogenised in purification buffer before preparation in sample buffer (Table 3.3.7 A and Figure 3.3.7 C).

Table 3.3.7 A: Effect of preparation procedures on the ability of the peptide to block the 160kDa band recognised by carboxyl-terminal antiserum in gastric mucosal material

Sample Preparation Method	Number of Different Preparations probed with C-terminal Antiserum (1/1250)	Number of times recognition of 160kDa band could be blocked by peptide (20μg/ml)
Tissue immediately into electrophoresis sample buffer.	10	0
Tissue homogenised in purification buffer then transferred to sample buffer	8	3
100,000 x g_{av} supernatant of homogenate in purification buffer transferred to sample buffer	8	8

Figure 3.3.7 C: Immunoblotting with antiserum to carboxyl-terminal peptide of nNOS \pm peptide (20 μ g/ml) on samples prepared over different time courses



Legend to Figure 3.3.7 C

Side A, Immunoblotting with antiserum to carboxyl-terminal peptide of nNOS (1/1250). Side B, Immunoblotting with antiserum to carboxyl-terminal peptide of nNOS (1/1250) plus 20 μ g/ml of the peptide. Lanes 1 and 6, 100 μ g of protein from gastric glandular mucosa directly into sample buffer; Lanes 2 and 7, 100 μ g of protein from gastric glandular mucosa homogenised in purification buffer and then added immediately to electrophoresis sample buffer; Lanes 3 and 8, 100 μ g of protein from gastric glandular mucosa homogenised in NOS purification buffer, centrifuged at 100,000 \times g_{av} for 30min and then added immediately to electrophoresis sample buffer; Lanes 4 and 9, 100 μ g of protein from gastric glandular mucosa homogenised in purification buffer, centrifuged at 100,000 \times g_{av} for 30min, stored at 4°C for 24h and then added to electrophoresis sample buffer; Lanes 5 and 10, 5 μ g of partially purified (by 2', 5' ADP-agarose) NOS protein from gastric glandular mucosa.

Peptide could however block the recognition of the band in supernatant of a gastric mucosal sample in NOS purification buffer centrifuged at $100,000 \times g_{av}$ for 30min at 4°C and then prepared in sample buffer. It could also block recognition of the band in the same supernatant which had been stored for 24h at 4°C prior to preparation in sample buffer.

The effect of inhibitors of protein phosphatases on the change in carboxyl-terminal antigenicity of gastric mucosal nNOS was investigated. While the addition of phosphatase inhibitors to the homogenisation buffer occasionally prevented the appearance of a peptide block during centrifugation (Table 3.3.7 B) the results obtained were inconsistent and were hampered by the disappearance of the 160kDa band during centrifugation even on immunoblots in the absence of peptide.

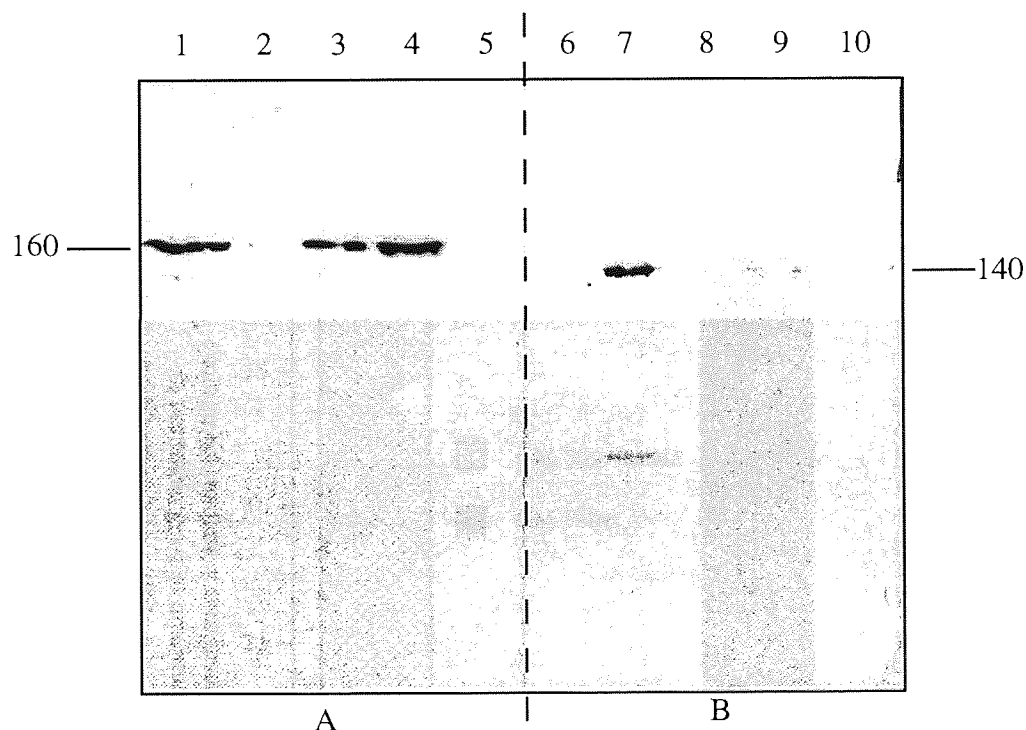
Table 3.3.7 B: Effect of protein phosphatase inhibitors on block by peptide of recognition of the 160kDa band by carboxyl-terminal antiserum in $100,000 \times g_{av}$ supernatant of gastric mucosal homogenates

Inhibitor	Concentration	Number of Times Used and 160kDa Band Present	Number of Times Peptide Block Prevented
Okadaic Acid	0.5 μM	2	1
	1.0 μM	1	0
	1.5 μM	1	0
	10 μM	1	0
Calyculin A	50nM	1	1
NaF	100mM	2	1

3.3.8 Subcellular distribution of NOS protein and activity

Immunoblotting of subcellular fractions of tissue extracts from rat brain and gastric glandular mucosa with the monoclonal antibody to nNOS showed the presence of a protein of molecular mass 160kDa in supernatant from both tissues and in the pellet fraction of brain with little or none of the protein in the gastric mucosal fractions (Figure 3.3.8 A).

Figure 3.3.8 A: Immunoblotting with anti-nNOS and anti-eNOS antibodies on subcellular fractions of tissue homogenates



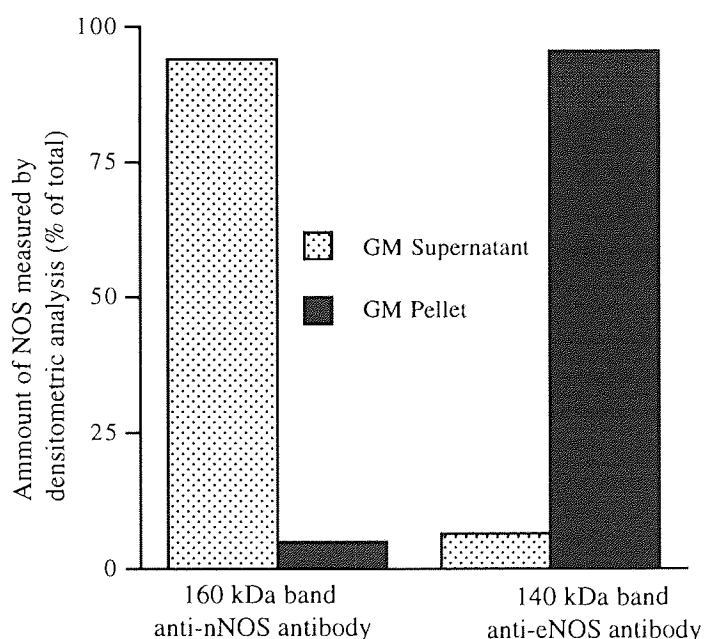
Legend to Figure 3.3.8 A

Side A, Immunoblotting with monoclonal anti-nNOS antibody (1 μ g/ml). Side B, Immunoblotting with monoclonal anti-eNOS antibody (1 μ g/ml). Lanes 1 and 6, 100 μ g of protein from rat gastric glandular mucosal supernatant; Lanes 2 and 7, 100 μ g of protein from rat gastric glandular mucosal pellet; Lanes 3 and 8, 50 μ g of protein from rat cerebellum supernatant; Lanes 4 and 9, 50 μ g of protein from rat cerebellum pellet; Lanes 5 and 10, 10 μ l of rainbow markers (Amersham).

Immunoblotting of the same samples with the monoclonal anti-eNOS antibody gave rise to a band at 140kDa in the pellet fraction of gastric mucosa with little or none of the protein in any of the other samples (Figure 3.3.8 A).

Quantification of the presence of the two proteins recognised by the monoclonal antibodies by densitometric analysis of immunoblots (Figure 3.3.8 B) showed that 93.64 ± 1.48 % of the 160kDa protein in gastric mucosa is found in the supernatant fraction and 95.26 ± 0.59 % of the 140kDa protein in gastric mucosa is found in the pellet fraction.

Figure 3.3.8 B: Amount of nNOS or eNOS in subcellular fractions of tissue homogenates (% of total NOS) measured by densitometric analysis of immunoblots

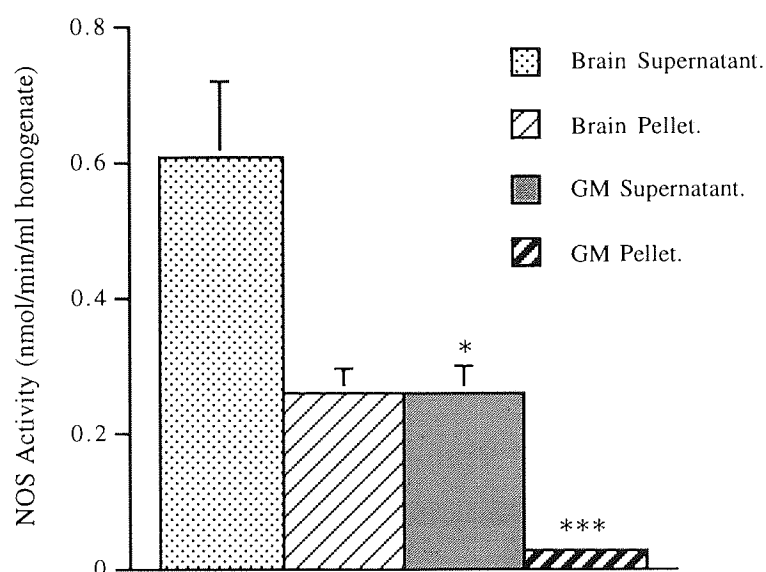


Legend to Figure 3.3.8 B

Results are expressed as % of total NOS present and are given as means \pm S.E.M. n=6 for samples probed with the anti-nNOS antibody and n=4 for samples probed with the anti-eNOS antibody, where n=number of separate preparations. Results were calculated by densitometric analysis using NIH image.

Measurement of NOS activity in subcellular fractions of extracts from rat brain and gastric glandular mucosa showed substantial activity in supernatant and pellet fractions of brain when expressed both per ml homogenate and per mg protein (Figures 3.3.8 C and D). The activity of NOS in both the supernatant and the pellet of gastric mucosa was significantly lower than in respective brain fractions (Figures 3.3.8 C and D).

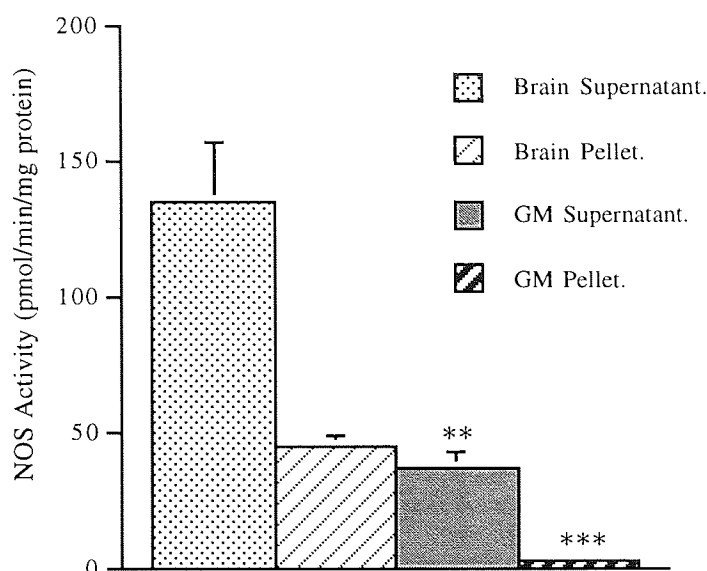
Figure 3.3.8 C: NOS activity in subcellular tissue fractions (nmol/min/ml homogenate)



Legend to Figure 3.3.8 C

Results from NOS assays of supernatant and pellet fractions of rat gastric glandular mucosa (GM) and rat cerebellum (Brain). Results are expressed as nmol/min/ml homogenate and are given as means \pm S.E.M. $n=6$ for all preparations. * and *** indicate a significant difference between brain and gastric mucosa (*, $p<0.05$; ***, $p<0.001$) by student's t-test.

Figure 3.3.8 D: NOS activity in subcellular tissue fractions (nmol/min/mg protein)

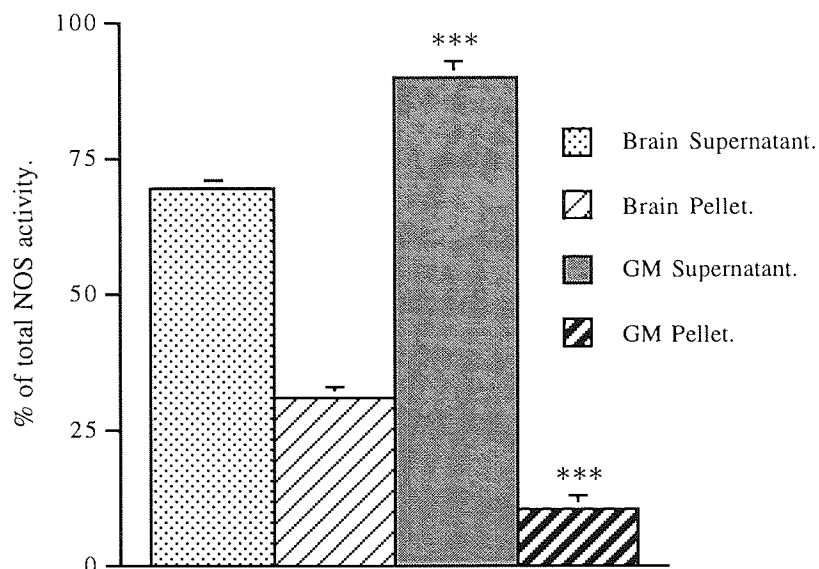


Legend to Figure 3.3.8 D

Results from NOS assays of supernatant and pellet fractions of rat gastric glandular mucosa (GM) and rat cerebellum (Brain). Results are expressed as nmol/min/mg protein and are given as means \pm S.E.M. $n=6$ for all preparations. ** and *** indicate a significant difference between brain and gastric mucosa (**, $p<0.01$; ***, $p<0.001$) by student's t-test.

When the NOS activity in each fraction from both tissue extracts was expressed as a percentage of the total NOS activity (sum of activities expressed per ml homogenate) $69.11 \pm 1.66\%$ of activity was present in the supernatant fraction of brain which was statistically lower ($p<0.001$ by student's t-test)) than the $89.99 \pm 2.95\%$ of NOS activity in the supernatant fraction of gastric mucosa (Figure 3.3.8 E) while $30.89\% \pm 1.66\%$ of activity was in the pellet fraction of brain compared to $10.01 \pm 2.95\%$ of that in the gastric mucosa ($p<0.001$).

Figure 3.3.8 E: NOS activity in subcellular tissue fractions (% of total activity)

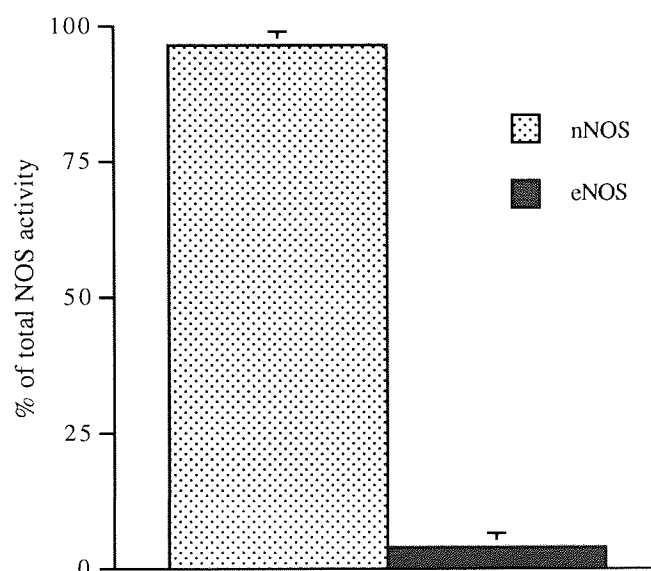


Legend to Figure 3.3.8 E

Results from NOS assays of supernatant and pellet fractions of rat gastric glandular mucosa (GM) and rat cerebellum (Brain). Results are expressed as % of total NOS activity (total activity = pellet activity/ml homogenate + supernatant activity/ml homogenate), and are given as means \pm S.E.M. $n=6$ for all preparations. *** indicates a significant difference between brain and gastric mucosa ($p<0.001$) by student's t-test.

When the proportion of nNOS to eNOS in whole rat gastric mucosa was calculated, the majority of NOS activity ($96.365 \pm 2.44\%$) was clearly due to nNOS (Figure 3.3.8 F)

Figure 3.3.8 F: Proportions of NOS activity in the whole gastric mucosa by the constitutive isoforms of NOS



Legends to Figures 3.3.8 F

Relative NOS activities of nNOS and eNOS in whole rat gastric glandular mucosa calculated from subcellular fraction activity values and corresponding immunoblotting data on NOS content. Results are given as means \pm S.E.M. $n=4$ for both isoforms. The calculation involves solving the following two simultaneous equations for nNOS and eNOS activities:

- 1: Total NOS in supernatant = proportion nNOS in supernatant x nNOS activity
+ proportion eNOS in supernatant x eNOS activity
- 2: Total NOS in Pellet = proportion nNOS in pellet x nNOS activity + proportion
eNOS in pellet x eNOS activity

The assumption is that the activity of eNOS and nNOS is unaffected by subcellular location.

3.4 DISCUSSION

3.4.1 Specificity of antibodies for NOS isoforms

Cross reactivity for a Ca^{2+} -dependent isoform other than the isoform against which they were raised was not evident in any of the antibodies used. The monoclonal nNOS antibody did not cross react with eNOS because no band was produced with an extract of rat mesentery. Faint bands seen below the 160kDa band in extracts from brain, gastric mucosa and pituitary cells could be caused by partial proteolysis of the enzyme during sample preparation. The carboxyl-terminal antiserum was unlikely to cross react with eNOS since the sequence of rat brain NOS against which it was raised is not present in eNOS (Appendix A5) and indeed there was no band in the 140kDa range in extracts from rat cerebellum or gastric mucosa. Further evidence for the ability of the carboxyl-terminal antiserum to specifically recognise nNOS is recognition of a 160kDa band in a sample containing recombinant nNOS which can be blocked by addition of the peptide.

The monoclonal anti-eNOS antibody used in this study has been used by others to detect eNOS in LLC-PK1 cells (McKee et al., 1994), an established source of eNOS (Tracey et al., 1994). Moreover a 140kDa band was detected in an extract from rat mesentery and human vascular endothelial cell lysate, both of which are positive controls for eNOS immunoblotting. The monoclonal anti-eNOS antibody did not cross react with nNOS because immunoblots of extracts from rat cerebellum did not exhibit a band in the 160kDa region.

3.4.2 Isoforms of NOS in the gastric glandular mucosa

The 160kDa protein recognised in stomach by immunoblotting was nNOS because a band of the same molecular weight was recognised by the monoclonal anti-nNOS antibody and the two antipeptide antisera used, all of which were raised against different sequences of nNOS. Further evidence for this band being nNOS is the presence of a band of the same molecular weight recognised by the monoclonal anti-nNOS antibody in rat cerebellar extract and rat pituitary cell lysate, both of

which are positive controls for nNOS. Furthermore, the ability of the carboxyl-terminal peptide to block recognition of the 160kDa band in brain by the antiserum raised against it and, at high concentration, to reduce the intensity of the same band in gastric mucosa indicates that the antiserum specifically recognised nNOS. The adsorption of the 160kDa band from gastric mucosal homogenates by 2', 5' - ADP agarose, coupled with its presence in brain and gastric mucosae samples partially purified for NOS, also points to the protein's identity as nNOS. The results shown here are contradictory to Kugler et al. (1994) who did not detect nNOS in the rat gastric mucosa on immunoblots using an antibody raised against porcine cerebellar NOS (see 3.4.3). The presence of nNOS in cells from a high-density Percoll fraction containing mainly mucus cells is consistent with data from Brown et al. (1992b) who detected the highest level of NOS activity in a high-density Percoll fraction of rat gastric mucosal cells.

The band at approximately 200kDa recognised by the carboxyl-terminal antiserum is likely to be a protein to which the components of the antiserum bind by an interaction which probably does not involve recognition of part, or the whole, of the NOS peptide sequence. Thus the band does not reduce in intensity even when peptide is added at a high concentration with the antibody. The 200kDa band does not seem to be related to nNOS, as for example a precursor, because it is absent from pancreatic and gastric isolated cell extracts which contain nNOS and because it is not removed by 2', 5' - ADP agarose from gastric mucosal homogenates. Consequently it does not appear in a gastric mucosal sample partially purified for NOS. Furthermore, neither the nNOS monoclonal antibody nor the antiserum directed against the internal peptide gave a band at approximately 200kDa with extracts of gastric mucosa.

The band at 140kDa in gastric mucosal extracts was likely to be eNOS given the ability of the antibody to detect eNOS in other tissues (3.4.1). Also the subcellular distribution, mainly particulate, was consistent with the band being eNOS. The presence of eNOS in the cerebellum has been described by others, (Pollock et al.,

1993) and is likely to be explained by eNOS in brain capillaries and in some neurons. No eNOS was present in any fraction of isolated gastric mucosal cells but only in an extract of whole gastric glandular mucosa.

3.4.3 Differences between brain nNOS and gastric mucosal nNOS by immunoblotting

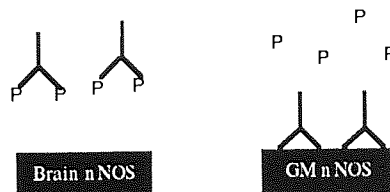
As described in 3.4.2 the 160kDa band is nNOS and the carboxyl-terminal antiserum is known to recognise nNOS. The lack of the ability of the carboxyl-terminal peptide at 20µg/ml to block recognition of this band by the antiserum in gastric mucosal extracts while blocking the band successfully in brain extracts is unlikely to be due to the presence of a protein other than nNOS of the same molecular weight being recognised unspecifically by the antiserum since all of the 160kDa band can be removed from gastric mucosal extracts by pre-incubating with 2', 5'-ADP agarose.

The phenomenon of the lack of the ability of the peptide (20µg/ml) to completely block recognition of nNOS by the carboxyl-terminal antiserum is not unique to gastric mucosa but also occurs with a 160kDa band in an extract of whole pancreas. This band in pancreas is also nNOS since stripping of immunoblots and reprobing of the same samples with the monoclonal anti-nNOS antibody recognised a band in exactly the same position.

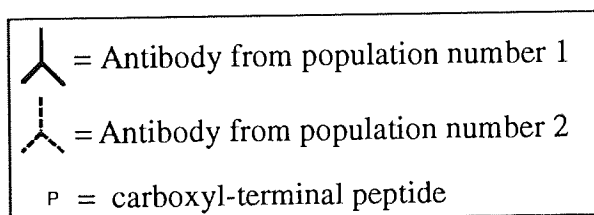
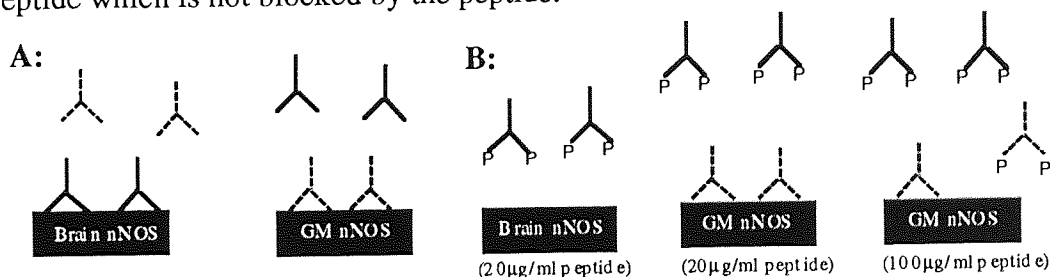
The lack of peptide block in gastric mucosal and pancreatic extracts is not due to differential competition between gastric mucosal nNOS on the blots and peptide for carboxyl-terminal antibodies compared to brain because preadsorption of the antiserum with immobilised peptide on an agarose column should have removed reactive antibodies. Instead this procedure gave the same result as if the peptide had been added to the immunoblot with the antiserum. This suggests the presence of two antibody populations in the carboxyl-terminal antiserum (See Figure 3.4 A, Hypothesis 2). One antibody population recognises the peptide and also the

Figure 3.4: Hypotheses to explain lack of peptide block of recognition by carboxyl-terminal antiserum of gastric mucosal nNOS

Hypothesis 1: Gastric mucosal nNOS has a higher affinity for anti-peptide antibodies than brain nNOS and therefore binds antibody even in the presence of the peptide:



Hypothesis 2: Two populations of antibodies exist in the carboxyl-terminal antiserum, one with a high affinity for the carboxyl-terminal peptide and brain nNOS which is therefore easily blocked by the peptide and the other with a high affinity for gastric mucosal nNOS but with low affinity for the carboxyl-terminal peptide which is not blocked by the peptide.



Legend to Figure 3.4:

Hypothesis 1: Representation of immunoblotting with carboxyl-terminal antiserum plus peptide (20 µg/ml).

Hypothesis 2: A: Representation of immunoblotting with carboxyl-terminal antiserum plus peptide, **B:** Representation of immunoblotting with carboxyl-terminal antiserum plus peptide.

carboxyl-terminal region of nNOS in rat brain, the other population recognises the peptide poorly but recognises another, possibly modified, epitope in the carboxyl terminal region of nNOS in rat gastric glandular mucosa and pancreas. The existence of two populations of antibodies in the antiserum could be explained by the modification of some of the carboxyl-terminal peptide *in vivo* during the immunisation procedure.

The above results suggest a difference between the brain and gastric mucosal forms of NOS in the carboxyl-terminal region. The return of the ability of the peptide to block the 160kDa band in gastric mucosal samples partially purified for NOS and indeed during centrifugation of samples shows that the difference between nNOS from brain and gastric mucosa is unstable. The difference in antigenicity between brain and gastric mucosal nNOS is unlikely to be due to artefactual proteolytic clipping of the carboxyl-terminus during scraping of gastric mucosa before homogenisation with electrophoresis sample buffer since it is difficult to see how this could be reversed during enrichment.

Potential explanations for the difference are a reversible post-translational modification in the carboxyl-terminal region or the existence of an alternatively spliced form of nNOS involving a potential splice site four amino acids from the carboxyl-terminus (Hall et al., 1994). One possible post-translational modification is phosphorylation but results shown here, while suggesting this may be the case, are inconclusive. Nevertheless this explanation is somewhat more attractive than alternative splicing as modifications of this form to make it more like brain nNOS would have to occur during the enrichment procedure.

Heterogeneity has been observed within isoforms of NOS by investigating the primary sequence (Silvagno et al., 1996; Magee et al. 1996) and differing antigenicity between brain and peripheral forms of nNOS may explain the contradictory results concerning the presence of NOS in the pancreas (Worl et al., 1994; Schmidt et al., 1992) and results in this chapter concerning the presence of nNOS in the gastric glandular mucosa compared to a previous study (Kugler et al.,

1994). Differences in antigenicity have also been detected in forms of iNOS but by contrast involve the amino-terminal region (Ringheim et al., 1995).

3.4.4 Subcellular localisation of nNOS in rat gastric glandular mucosa; differences from nNOS in rat brain

The detection of nNOS by the monoclonal anti-nNOS antibody in immunoblots of both supernatant and particulate fractions of rat cerebellum agrees with previous studies which detected NOS activity in the particulate fraction of rat brain, in particular endoplasmic reticulum (Hecker et al., 1994; Hiki et al., 1992). The particulate localisation of eNOS in brain and gastric mucosa is also consistent with previous studies which localised eNOS to membrane fractions in endothelial cells (Forstermann et al., 1991a; Hecker et al., 1991). Densitometric analysis of immunoblots clearly showed that the majority of nNOS in the gastric glandular mucosa was in the soluble fraction while the majority of eNOS was present in the particulate fraction.

Measurement of NOS activity in subcellular fractions mirrored the results shown by immunoblotting, with a substantial proportion of the nNOS activity in the brain being in the particulate fraction while less nNOS activity was detectable in the particulate fraction of gastric glandular mucosa. The presence of NOS activity in the brain particulate fraction validated the assay procedure for detection of particulate NOS activity and therefore the results obtained for gastric mucosal particulate NOS activity. Calculation of relative NOS activity produced by the two constitutive isoforms in whole gastric mucosa showed that the predominant NOS activity was due to nNOS. Since previous studies have suggested that the major role of NO in the gastric mucosa is the maintenance of the microcirculation (Whittle, 1994) this finding is peculiar. The low activity of eNOS in the blood vessels of the gastric mucosa may however be quite sufficient to maintain the microcirculation of the rat stomach in a normal rat while the functions of NO in

other regions and cell types may require more NO production and therefore a higher activity of nNOS.

eNOS is particulate due to post-translational myristoylation and palmitoylation at the amino-terminus which allows it to anchor itself to membrane (Pollock et al., 1992; Lamas et al., 1992). nNOS does not have such a myristoylation site (Bredt et al., 1991) but does have a PDZ motif at the amino-terminus. nNOS which has been described as particulate is so because of binding to proteins via PDZ domains (Brenman et al., 1995 and 1996). nNOS in skeletal muscle is bound to the dystrophin complex on the sarcolemma (Kobzik et al., 1994) and nNOS in the brain binds to other proteins containing PDZ domains. The low level of particulate NOS in the gastric mucosa could be due to a low level of binding proteins or a modification or an alternative splice at the N-terminus making it less likely for protein binding to take place.

3.4.5 Summary

- 1:** Rat gastric glandular mucosa contains two isoforms of NOS: eNOS and nNOS.
- 2:** A difference exists between nNOS from gastric mucosa and nNOS from rat cerebellum in the carboxyl-terminal region of the enzyme. The difference is not restricted to gastric mucosa also being present in pancreatic tissue.
- 3:** nNOS in the rat gastric glandular mucosa is predominantly soluble, while eNOS is predominantly particulate. nNOS is the predominant catalytic activity in gastric mucosa.

CHAPTER 4 - LOCALISATION OF CONSTITUTIVE
NOS IN THE GASTRIC GLANDULAR MUCOSA

4.1 INTRODUCTION

4.1.1 Background

Whereas protein blotting can indicate the presence of NOS within the tissue localisation is best performed by immunocytochemistry. The two constitutive forms of NOS have been localised in a number of tissues and cell-types by immunocytochemistry of tissues sections. A summary of major studies on localisation of NOS is given in tables 4.1 A and 4.1 B.

Table 4.1 A: Summary of major studies localising NOS thought to be the neuronal Form

Tissue	Region	Antibody	Authors
STOMACH	Brush cells in cardiac mucosa (Rat)	Polyclonal antiserum to porcine cerebellar NOS	Kugler et al. (1994)
	Neurons in muscle layer (Guinea Pig)	Polyclonal antiserum to rat cerebellar NOS	Furness et al. (1994)
	Epithelium of forestomach (Rat)	Polyclonal antiserum to rat cerebellar NOS	Schmidt et al. (1992a)
	D-cells in corpus and pyloric regions (Rat)	Polyclonal Antiserum to peptides from rat brain NOS and monoclonal to nNOS	Burrell et al. (1996)
	Isolated chief cells (Guinea Pig)	Polyclonal Antiserum to rat cerebellar NOS	Fiorucci et al. (1995)
PANCREAS	Brush cells (Rat)	Polyclonal antiserum to porcine cerebellar NOS	Kugler et al. (1994)
	B cells in Islets of Langerhans (Rat)	Polyclonal antiserum to rat cerebellar NOS	Schmidt et al. (1992a and b)

Tissue	Region	Antibody/Antiserum	Authors
PANCREAS	Neurons in vascular bundles (Rat)	Polyclonal antiserum to rat cerebellar NOS	Schmidt et al. (1992a)
	Ganglion cells and nerve fibres (rat and human)	Polyclonal antiserum to porcine cerebellar NOS	Worl et al. (1994)
INTESTINE	Neurons in myenteric ganglia and circular muscle of small intestine and colon (Rat)	Polyclonal Antiserum to peptides from rat NOS	Springall et al. (1992) and Alm et al. (1993)
	Neurons in myenteric plexus of colon (Human)	Polyclonal antiserum to porcine cerebellar NOS	Matini et al. (1995)
	Neurons in myenteric plexus and smooth muscle (Human)	Polyclonal antiserum to nNOS	Timmermanns et al. (1994)
	Neurons in myenteric plexus throughout the G.I.T. and submucous plexus in stomach, colon and rectum (Guinea Pig)	Polyclonal antiserum to rat cerebellar NOS	Furness et al. (1994)
	Neurons in myenteric plexus and circular muscle of small intestine (Rat and Guinea Pig)	Polyclonal antiserum to rat cerebellar NOS	Schmidt et al. (1992a) and Llewellyn-Smith et al. (1992)
	Colon columnar epithelial cells (Dog)	Monoclonal anti-nNOS	Torihashi et al. (1996)

Tissue	Region	Antibody/Antiserum	Authors
INTESTINE	Neurons of myenteric and submucosal. ganglia in colon (Dog)	Polyclonal antiserum to rat cerebellar NOS	Ward et al. (1992)
BRAIN/C.N.S	Neurons in cortex and cerebellum (Rat)	Polyclonal antiserum Antisera to peptides from rat nNOS	Springall et al.(1992)
	Neurons in cerebellum, hippocampus and olfactory bulb (Rat)	Polyclonal antiserum to rat cerebellar NOS	Schmidt et al. (1992a) and Bredt et al. (1991)
	Neural elements of spinal cord and dorsal root ganglia. (Rat and Human)	Polyclonal antiserum to peptides from rat NOS and polyclonal antiserum to rat cerebellar NOS	Terenghi et al. (1993)
KIDNEY	Macula Densa	Polyclonal antiserum to rat cerebellar NOS (Rat)	Schmidt et al. (1992a), Wilcox et al. (1992) and Tojo et al. (1993)
LUNG	Bronchial epithelial cells (Rat)	Polyclonal antiserum to rat cerebellar NOS	Schmidt et al. (1992a)
UTERUS	Endometrium (Rat)	Polyclonal antiserum to rat cerebellar NOS	Schmidt et al. (1992a)
HEART	Neural elements in muscle (Rat)	Polyclonal antiserum to rat cerebellar NOS	Schmidt et al. (1992a)

Table 4.1 B: Summary of major studies localising NOS thought to be the endothelial Form

Tissue	Region	Antibody/Antiserum	Authors
INTESTINE	Mucous (goblet) cells in colon (Dog)	Monoclonal anti-eNOS antibody	Torihashi et al. (1996)
	Endothelium and smooth muscle of submucosal. blood vessels in ileum and colon (Rat and Human)	Monoclonal anti-eNOS antibody	Nichols et al. (1994)
BRAIN/C.N.S	Endothelial cells	Monoclonal anti-eNOS antibody	Tomimoto et al. (1994)
KIDNEY	Tubular epithelial cells (LLC-PK ₁)	Monoclonal anti-eNOS antibody	Tracey et al. (1994) and McKee et al. (1994)
	Endothelium of renal artery and small vessels medulla (Bovine and Human)	Monoclonal anti-eNOS antibody.	Pollock et al. (1993)
LUNG	Vascular endothelium in trachea (Human)	Monoclonal anti-eNOS antibody.	Pollock et al. (1993)
PLACENTA	Endothelium of umbilical cord arteries and veins (Human)	Monoclonal anti-eNOS antibody	Myatt et al. (1994)
	Umbilical vein endothelium (Bovine and Human)	Monoclonal anti-eNOS antibody.	Pollock et al. (1993)
AORTA	Endothelium (Bovine)	Monoclonal anti-eNOS antibody.	Pollock et al. (1993)

The main features of this survey are that the constitutive forms of NOS are widely distributed and neither nNOS or eNOS are restricted to neuronal or endothelial cells respectively. For example bronchial epithelial cells were stained by antibodies to nNOS (Schmidt et al. 1992) while renal tubules stained with an antibody to eNOS (McKee et al. 1994). Nevertheless, nNOS is found within neurons and eNOS in the endothelial cells of blood vessels in a wide variety of tissues.

When this study was initiated little histochemical evidence was available about localisation of NOS in the stomach although Ca^{2+} -dependent NOS was known to be present in the gastric mucosa and in isolated gastric mucosal cells (Whittle et al. 1990; Brown et al. 1992b). The major published work mapping NOS by immunohistochemistry (Schmidt et al. 1992) localised nNOS to the epithelium of the forestomach. The morphology of the epithelium of the forestomach is, however, distinct from that of the glandular stomach, the forestomach possessing a stratified squamous epithelium while the epithelium of the gastric glandular mucosa is a simple epithelium consisting of columnar mucous cells. This study does not, therefore, indicate the location of NOS in the mucosal epithelium of other regions of the stomach. Fractionation of gastric mucosal cells by centrifugal elutriation showed that Ca^{2+} -dependent NOS was enriched in a fraction containing cells of medium size with periodic acid-Schiff positive mucous cells being the predominant cell-type (Brown et al. 1992b). These data, however, do not discriminate between mucous epithelial cells and mucous neck cells, as the site of NOS. Nor do they exclude the possibility that NOS may be present in a minor cell population of similar size to the mucous cells. More recent studies (Burrell et al., 1996; Fiorucci et al. 1995) have suggested the presence of nNOS in gastric D cells and chief cells. Finally, Ca^{2+} -independent iNOS has been shown to be present in gastric mucosal cells of rats treated with lipopolysaccharide, but is absent from control animals (Brown et al. 1994).

The aim of this study was therefore to investigate the localisation of the constitutive isoforms of NOS within the rat corpus mucosa in order to have a better

understanding of the involvement of NO in regulation of gastric mucosal integrity and secretory activity.

4.1.2 Practical considerations

4.1.2.1 Choice of localisation procedures

Nitric oxide synthase can be localised in tissue sections in three ways: by *in situ* hybridisation, by NADPH diaphorase staining, and by immunocytochemistry. *In situ* hybridisation detects mRNA by its hybridisation with complementary radio-labelled segments of RNA or DNA. While proving to be a highly effective method (Beesely et al. 1995; Norris et al. 1995), *in situ* hybridisation is a costly and time-consuming technique which may not reflect the level of protein if the message is subjected to translational control and it was therefore not used in this study.

In the presence of β -NADPH, NADPH diaphorase reduces nitroblue tetrazolium salt to a water insoluble nitroblue tetrazolium formazan product. When viewed by light microscopy this product is observed as a blue precipitate. This method of staining does not distinguish between the various isoforms of NOS since all isoforms exhibit NADPH diaphorase activity (Matsumoto et al. 1993; Spessert and Layes 1994). Enzymes other than NOS also exhibit NADPH diaphorase activity although non NOS-associated NADPH diaphorase activity can be affected by fixation conditions (Matsumoto et al. 1993). Despite these reservations NADPH diaphorase staining was used in this study to localise NOS in the gastric mucosa as it allowed a useful comparison with staining produced by immunocytochemistry.

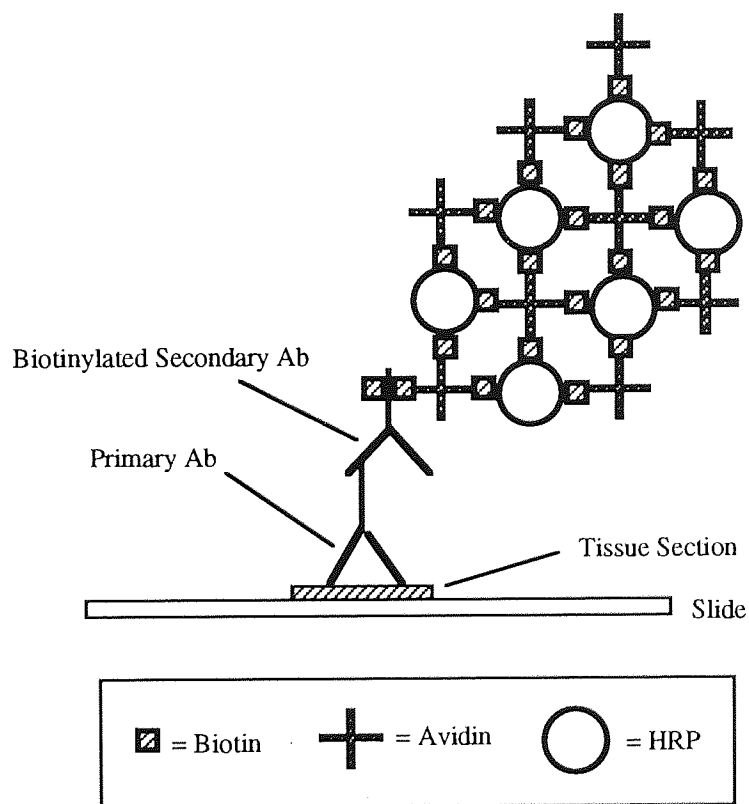
Immunocytochemistry was the main method chosen for localisation of NOS in this study. This technique involves recognition of NOS by antibodies raised against either the whole protein or a peptide sequence from the protein. Binding of the primary antibody must then be detected by further procedures (see 4.1.2.2). Immunocytochemistry is relatively simple to perform and, when using the right antibodies at appropriate concentrations and with appropriate controls, gives highly

specific and selective results. Antibodies used in the characterisation of gastric mucosal NOS (Chapter 3) were used for immunocytochemistry.

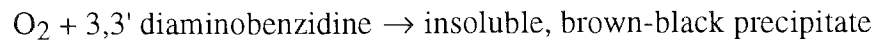
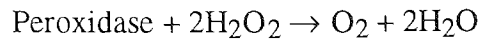
4.1.2.2 Avidin-Biotinylated-Horseradish Peroxidase Complex (ABC) method

The ABC method was chosen for immunocytochemistry in this study. This method is so called because it involves a pre-formed Avidin-Biotin Horseradish Peroxidase(HRP) Complex. The process is illustrated in figure 4.1

Figure 4.1: ABC method of immunocytochemistry



A primary antibody to the antigen of interest is added to the tissue section followed by a biotinylated secondary antibody. Avidin has a very high affinity for biotin (binding is almost irreversible) and the Avidin-Biotin HRP Complex when added to the section binds to the secondary antibody. When a 3,3' diaminobenzidine/urea hydrogen peroxide solution is added to the section, horseradish peroxidase catalyses the following reaction:



The main benefit of the ABC technique over other immunocytochemical detection procedures is the level of amplification produced. With avidin having the ability to bind four molecules of biotin the amount of Avidin-Biotinylated-Horseradish Peroxidase Complex binding to the biotinylated secondary antibody is high and therefore so is the resultant signal produced by the action of horseradish peroxidase on 3,3' diaminobenzidine. Because of the amplification of signal produced by the ABC method the concentration of primary antibody required on the tissue section is low resulting in decreased background staining of the section which is often due to non-specific binding of antibody to the tissue.

4.2.1.3 Fixation of tissue sections

In order to preserve cellular structure and morphology, tissues were subject to one of two fixation procedures. Acetone fixation after sectioning was employed in a major study mapping NOS (Schmidt et al. 1992) and this study also reported that fixation with paraformaldehyde adversely affected the immunoreactivity of nNOS. Fixation in paraformaldehyde may also reduce the intensity of NADPH diaphorase staining (Matsumoto et al. 1993; Spessert and Layes 1994). However fixation with 4% paraformaldehyde prior to cutting sections gives a better quality of preservation and the resulting morphology with this technique is regarded to be superior to that produced by acetone fixation. Matsumoto et al. (1993) also report that NADPH diaphorase activity not related to NOS is abolished by paraformaldehyde fixation. Consequently both procedures were employed.

4.2.1.4 Cutting tissue sections

Tissues to be used for immunocytochemistry and NADPH Diaphorase staining were frozen and sectioned using a cryostat. This technique was chosen over embedding in paraffin wax and cutting using a microtome at room temperature. Embedding in paraffin wax is a harsher, more time-consuming and complex

technique since it involves a lengthy procedure of embedding the tissue, cutting sections then drying and dewaxing them before immunocytochemistry can begin. Cryostat sections are easier to prepare as the procedure involves only freezing of the tissue, embedding and freezing in OCT compound, sectioning and a short drying period of 1-2h, after which sections can either be stained or the slides stored frozen. Antigen preservation is also accepted to be superior in cryostat-fixed sections.

4.2 METHODS

4.2.1 Preparation of histological tissue sections

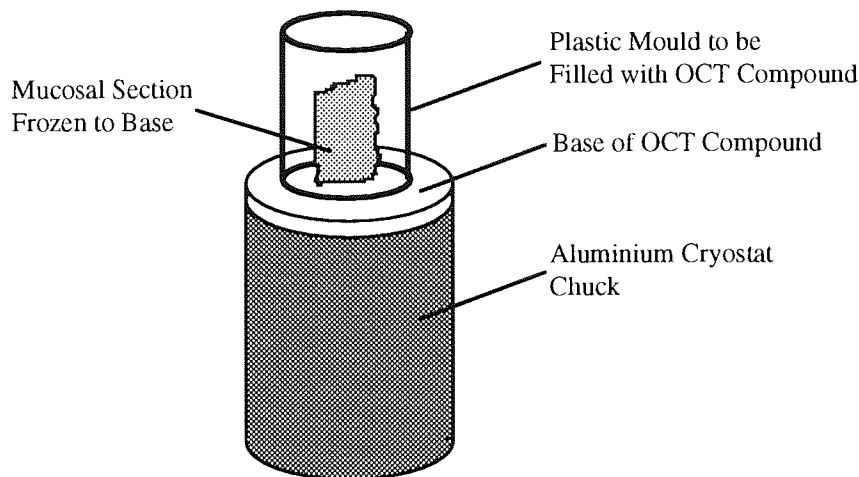
4.2.1.1 Preparation and sectioning of frozen tissue

Samples of stomach, aorta, duodenum and brain were obtained from fed Wistar rats (200-300g) and sections obtained by the following method. Tissues were removed under terminal anaesthesia using sodium pentobarbitone (60mg/kg i.p). The stomach was removed and washed in ice-cold isotonic saline (9g/l NaCl) and square sections (approximately 5 mm x 5 mm) of the dorsal and ventral surfaces of the mid-corpus mucosa were cut with scissors. Tissues to be fixed in acetone were prepared for sectioning in the following way immediately while others were fixed in 4% paraformaldehyde first (see 4.2.1.3). The sections were placed, luminal surface upwards, on top of card covered in aluminium foil and were flash frozen in liquid nitrogen. OCT embedding compound was poured over the sections and the freezing process repeated.

The freezing process for the other tissues was similar. Duodenum was washed out by carefully syringing isotonic saline through the lumen. Blood was washed from the lumen of the aorta by gentle agitation in isotonic saline. The brain was simply rinsed in saline. Duodenum, aorta and brain were all flash frozen in liquid nitrogen but were not covered with OCT compound before mounting.

A base of OCT compound was allowed to freeze on the top of a cryostat chuck. A tissue sample was mounted on the cryostat chuck perpendicular to the top of the chuck. OCT compound was then poured over the tissue, using a cylindrical plastic mould and the chuck was lowered into liquid nitrogen to freeze (see Figure 4.2).

Figure 4.2: Mounting of gastric mucosal tissue on cryostat chuck



The mould was removed leaving a column of OCT compound containing the tissue sample with a very clean smooth surface to enable more easy cutting of sections. The chuck was then fitted into the cryostat, the interior of which was at -20°C . Sections, $10\mu\text{m}$ thick, were then cut and transferred from the cryostat blade onto Superfrost glass slides pre-treated with Vectabond reagent. Vectabond coating of slides increases the adherence of frozen tissue sections to the slides. The slides were then air dried at room temperature for 1-2h. Unfixed tissue sections were then fixed by immersion in acetone at 4°C for 5min and were then allowed to dry. Paraformaldehyde fixed sections (see 4.2.1.3) required no further treatment. Sections were then either stained immediately or slides were wrapped in aluminium foil and stored in polythene bags at -20°C .

4.2.1.2 Preparation of 4% paraformaldehyde

Paraformaldehyde (8g) was added to distilled water (100ml) and the mixture heated to 60°C whilst stirring on a heated magnetic stirrer. At 60°C NaOH (1M) was

added drop-wise until the solution cleared. The solution was then removed from the hot plate and allowed to cool to room temperature. The solution was then diluted with 100ml of 2 x PBS (20mM NaH₂PO₄, 18g/l NaCl, pH 7.5) and cooled to 4°C.

4.2.1.3 Paraformaldehyde fixation

Washed tissue specimens (see 4.2.1.1) were incubated in 4% paraformaldehyde at 4°C for 4h. Tissues were then removed and placed in 10% sucrose in PBS (10mM NaH₂PO₄, 9g/l NaCl, pH 7.5) for 2h at 4°C and then 20% sucrose in PBS at 4°C overnight.

4.2.2 Preparation of gastric mucosal cells for immunocytochemistry

Gastric mucosal cells were isolated as described in section 3.2.6. The cell suspension was diluted to a concentration of 1×10^6 cells per ml and 100µl aliquots were loaded into a cytopsin apparatus and the cells were spun down onto Vectabond-coated glass microscope slides. The slides were then air dried for 1-2h. The cells were fixed by immersing the slides in acetone at 4°C for 5min.

4.2.3 Immunohistochemistry by the ABC method

4.2.3.1 Standard protocol

The ABC procedure was carried out using a Vectastain Elite kit (Vector Laboratories).

Slides were incubated in a humidified chamber to prevent evaporation of reagents. The chamber consisted of a petri dish lined with tissue paper soaked in distilled water. Slides were washed by placing them in an empty Coplin jar, gently pouring PBS over the slides in the jar, emptying, refilling and then standing for the slides to rinse naturally. After each wash the slide around the sections was dried carefully to prevent dilution of the applied reagents. All procedures were carried out at room temperature.

Endogenous peroxidase activity was quenched in the sections by immersing slides in 0.75% (v/v) hydrogen peroxide in methanol for 30min, followed by a 20min wash in PBS. To prevent non-specific binding of antibodies, the sections were then blocked by addition of normal blocking serum (5% v/v goat serum in PBS) and incubated for 20min. Excess serum was then blotted from each section using tissue paper. Primary antibody or an appropriate control, diluted in normal blocking serum was then applied for either 30min or 2h. Slides were then washed for 10min in PBS. The slides were then incubated for 30min with the appropriate biotinylated secondary antibody (anti-rabbit or anti-mouse, 5µg/ml in normal blocking serum) followed by a 10min wash in PBS. Slides were incubated for 30min with ABC reagent (1 of drop reagent A, 1 drop of reagent B in 2.5 ml distilled water) followed by another 10 minute wash in PBS. The ABC reagent was prepared 30 min prior to use to allow the complex to form completely.

The 3, 3'-diaminobenzidine peroxidase substrate was prepared by adding one 3, 3'-diaminobenzidine tablet and one urea/hydrogen peroxide tablet (Sigma fast kit) to 5ml of distilled water and allowing them to dissolve. The slides were then incubated for 5 min with the substrate solution. Slides were then washed for 5min in tap water following which the sections were dehydrated by 3 x 1min changes of ethanol and 3 x 1min changes of xylene. A drop of DPX was then added to the sections on the slide and a coverslip placed on top taking care to avoid bubbles. Slides were then examined using a light microscope.

Serial dilutions of antisera or antibodies were used to discover their optimal concentration which is characterised by maximal specific staining but minimal background staining.

4.2.3.2 Controls

Controls used with antisera were addition of relevant peptide (100µg/ml), replacement by preimmune serum, and removal of secondary antibody. Controls used with monoclonal antibodies were replacement by mouse monoclonal antibody of irrelevant specificity or by mouse IgG at an appropriate concentration. In

addition purified recombinant nNOS from rat brain was used to preadsorb the monoclonal anti-nNOS antibody.

4.2.3.3 Variations to the standard protocol

With the polyclonal anti-nNOS antibody, the use of the Ni-enhanced DAB procedure was investigated. Different times of DAB incubation (5-15min) were used with both the polyclonal anti-nNOS antibody and the monoclonal anti-eNOS antibody.

Trypsin solution (0.01% or 0.1%), prepared from Sigma tablets, was added to paraformaldehyde-fixed sections for 2 or 10 min and washed off as usual with PBS prior to immunocytochemistry with the antiserum to the carboxyl-terminal peptide of NOS in an attempt to unmask hidden epitopes. Keyhole limpet haemocyanin at a concentration of 2mg/ml was used to preadsorb the antiserum to the internal peptide of NOS. A stock solution of keyhole limpet haemocyanin (10mg/ml) was prepared in a buffer containing 31mM NaH₂PO₄, 0.46M NaCl and 41mM Sucrose (pH 7.4).

4.2.4 Staining for NADPH Diaphorase

Tissue sections were stained with a solution containing 50mM Tris.HCl (pH 8.0), 0.2% (v/v) Triton X 100, 0.5 mM nitroblue tetrazolium and 1mM β -NADPH for 15, 30, 45 or 60 min. Control sections were treated with a solution without the β -NADPH. Sections were then dehydrated in ethanol and xylene as with immuno-stained sections and were mounted in DPX under a coverslip and examined using a light microscope.

4.2.5 Photographing tissue sections on slides

Slides were photographed using an Olympus OM-4 camera attached to a Jenamed fluorescence microscope. Exposure settings were automatic with the film speed set at 100 ASA, and with an override used to produce normal exposure, under

exposure by 1/3 stop or over exposure by 1/3 stop. The film used was Kodak Technical Pan which was developed using Kodak Dektol developer.

4.2.6 Enrichment of antibodies in polyclonal antiserum

4.2.6.1 IgG partial purification

5ml of antiserum B was added to 10ml of 60mM Na Acetate solution (pH 4.0) and the pH was adjusted to 4.8. The solution was transferred to a beaker on a magnetic stirrer at room temperature and 0.375ml of caprylic acid was added drop-wise with gentle stirring which was continued for 30min. The solution was then centrifuged at 15°C for 10min at 5000 x g_{av} . The supernatant was removed and dialysed versus 2 x 1l of PBS (0.15M NaCl, 20mM Na₂HPO₄, pH 7.4) at 4°C overnight. The dialysed solution was then removed and transferred to a beaker on a magnetic stirrer and a volume of saturated ammonium sulphate equal to the volume of dialysate was slowly added while stirring gently after which the solution was left at 4°C for 6h. The contents of the beaker were then centrifuged at 4°C for 30min at 3000 x g_{av} . The supernatant was then removed and discarded and the pellet was resuspended in 2.5ml of PBS, transferred to dialysis tubing and dialysed against 3 x 1l of PBS. The dialysate was then removed and made up to 5ml with PBS. This IgG fraction was then either stored frozen or processed for affinity-purification immediately (4.2.5.2).

4.2.6.2 Affinity purification

A purification column was prepared by adding 2ml of SulphoLink coupling gel (Pierce) to a plastic column of 5ml volume. 2mg of the internal peptide of nNOS was dissolved in 2ml of coupling buffer (supplied with kit), the absorbance at 280nm was measured and the peptide solution was added to the column. The column was capped top and bottom and placed on a Luckham Multimix (MM1) roller for 15min to mix gently (40rpm). The column was then placed in a stand, the gel was allowed to settle and the column was then drained and washed with 6ml of

coupling buffer and the absorbance of the mixed eluant at 280nm was measured in order to determine coupling efficiency using the following formula.

$$\text{Coupling efficiency (\%)} = \left(\frac{1 - A_{280} \text{ mixed eluant} \times \text{weight mixed eluant}}{A_{280} \text{ peptide} \times 2} \right) \times 100$$

Non-specific binding sites on the gel were blocked by adding 2ml of 0.5M cysteine solution to the column, capping it top and bottom, mixing on a Luckham Multimix (MM1) roller for 15min at room temperature and allowing the column to stand and settle for 30min after which the column was washed with 16ml of PBS.

The absorbance of the IgG fraction at 280nm was measured. 1ml of the IgG fraction was added to the column and was allowed to run in. The column was capped at the bottom. 1.2ml of PBS was added to the top of the column, the column was capped at the top and was then left for 1h at room temperature for antibody binding to take place. The column was then opened and washed with 6 ml of PBS. This wash was collected in 1ml fractions and their absorbances at 280nm measured. The four fractions with the highest absorbance values were pooled. This pooled column wash was retained and stored frozen for immunocytochemistry.

8ml of Actisep Elution Medium were then passed through the column in order to elute antibodies bound to the peptide, the eluate was collected in 1ml fractions and the absorbance of the fractions at 280nm was measured. The fractions with the highest absorbances were pooled. The pooled eluate was made 1mg/ml by adding an appropriate volume of Bovine Serum Albumin (10mg/ml in PBS containing 0.05% Na Azide). The pooled eluant was then dialysed with 2 x 1l of PBS containing 0.05% Na Azide at 4°C to get rid of the Actisep Elution Medium and was stored frozen for use in immunocytochemistry or ELISA.

4.3 RESULTS

All the results presented in this chapter derive from experiments repeated at least three times.

4.3.1 Antipeptide antisera to nNOS

4.3.1.1 Immunocytochemistry with antisera

Incubation of acetone-fixed sections of corpus mucosa with polyclonal antisera to an internal peptide of nNOS or to a carboxyl-terminal peptide of nNOS stained surface mucosal epithelial cells (Plates 4.3.1 A and 4.3.2 A). The antiserum to the internal peptide of NOS also stained another population of cells in a band along the centre of the mucosa. No specific staining was observed when similar pieces of corpus mucosa were incubated with pre-immune serum collected from appropriate animals prior to the beginning of the immunisation protocol (Plates 4.3.1 B and 4.3.2 B). Staining of the surface mucosal epithelial cells was abolished when corpus mucosal sections were incubated with a polyclonal antiserum plus peptide at a concentration of 100µg/ml (Plates 4.3.1 C and 4.3.2 C). The central band of cells was still stained by the antiserum to the internal peptide of nNOS even in the presence of peptide. Incubation of corpus mucosa with the antiserum to the internal peptide of nNOS plus KLH produced the same pattern of staining as with the antiserum alone (not shown).

Carboxyl-terminal antiserum also recognised myenteric plexus in the duodenum (Plate 4.3.2 D) while controls using pre-immune serum were negative.

Carboxyl-terminal antiserum reacted very poorly with corpus mucosa fixed with 4% paraformaldehyde. Pretreatment of sections with trypsin did not improve the staining by carboxyl-terminal antiserum on paraformaldehyde fixed stomach sections.

4.3.1.2 Affinity purification and immunocytochemistry with affinity purified antiserum.

Affinity purification of the antiserum to the internal peptide of NOS proved ineffective as the eluate did not show any specific staining when added to a section

of corpus mucosa even when added to the section with no dilution. However corpus mucosa incubated with a column wash from the attempted affinity purification stained the central band of cells with no staining at the surface (Plate 4.3.1 D). Coupling efficiency of the internal NOS peptide to the affinity purification column was 93.5% and therefore lack of peptide conjugation was not the reason for poor purification results. An ELISA which used partially purified antiserum (IgG fraction) and affinity purified material to probe for an internal peptide-bovine serum albumin conjugate showed that recognition was approximately 16 x better with the IgG fraction than with the affinity purified antibody (results not shown). This result suggests that antibodies were either inactivated in the affinity purification process or that antibodies bound with such high affinity to the purification column that elution was unsuccessful.

4.3.2 Immunocytochemistry with commercial polyclonal antibody to nNOS

The commercial polyclonal antibody directed against nNOS stained surface mucosal epithelial cells of sections of corpus mucosa fixed in acetone (Plate 4.3.3 A), although staining was not heavy. Staining of the surface did not occur when the antibody was replaced with rabbit IgG (Plate 4.3.3.B). This antibody did not give any bands with either brain or gastric mucosa in immunoblotting experiments (Chapter 3) but stained regions in the hippocampus and cerebellum in brain sections fixed in acetone (Plate 4.3.3 C) while rabbit IgG controls were negative.

4.3.3 Immunocytochemistry with monoclonal antibody to nNOS

The monoclonal antibody to nNOS stained surface epithelial cells in corpus mucosa fixed with acetone (Plate 4.3.4 A) or with 4% paraformaldehyde (Plate 4.3.5 A). Staining of the surface did not occur when similar sections of corpus mucosa were incubated with mouse monoclonal antibody of irrelevant specificity (Plates 4.3.4 B and 4.3.5 D) or when the monoclonal antibody was applied in the presence of purified recombinant rat brain nNOS (Plate 4.3.5 C).

Isolated gastric mucosal cells fixed with acetone, and close to 8µm in diameter, were stained by the monoclonal antibody while larger parietal cells were not stained (Plate 4.3.4 D). The staining of individual cells in corpus mucosa fixed with 4% paraformaldehyde could clearly be seen on enlargement (Plate 4.3.5 B).

The monoclonal antibody to nNOS also recognised neuronal elements in the muscle layers of acetone-fixed duodenum (Plate 4.3.4 C), 4% paraformaldehyde-fixed duodenum (Plate 4.3.5.F) and 4% paraformaldehyde-fixed corpus mucosa (Plate 4.3.5 E).

4.3.4 Immunocytochemistry with monoclonal antibody to eNOS

No obviously specific staining could be seen on corpus mucosa fixed in 4% paraformaldehyde and incubated with the monoclonal anti-eNOS antibody when viewed under low magnification (Plate 4.3.6 A), and in particular there was no staining of the surface epithelial cells. When viewed under higher magnification small blood vessels were evident, probably due to staining of their endothelium by the antibody. Vessels were found in the lower region of the glandular mucosa (Plate 4.3.6 B), near the base of the gastric glands (Plate 4.3.6 C) and in the muscle layer (Plate 4.3.6 D). Staining of vessels was absent when the antibody was replaced by a monoclonal mouse IgG antibody of irrelevant specificity. Endothelium was also stained by the anti-eNOS antibody in 4% paraformaldehyde fixed sections of aorta (Plate 4.3.6 E) but not when the antibody was replaced by mouse IgG (Plate 4.3.6 F). In mucosal sections treated with acetone the antibody directed against eNOS stained fewer blood vessels and again did not stain the mucosal surface.

4.3.5 Immunocytochemistry with antibody to iNOS

No specific staining of the mucosa was observed after acetone-fixed corpus sections were exposed to a mouse monoclonal antibody directed against iNOS

(Plate 4.3.7). The background staining observed with this antibody was quite dark but was uniform across the section.

4.3.6 NADPH Diaphorase staining compared to results obtained with anti-nNOS antibody and anti-mucin antibody

Acetone-fixed corpus mucosa exhibited diaphorase staining at the surface, which extended down into the gastric glands and also staining of some cells at the base of the mucosa (Plate 4.3.8.A). Corpus mucosa fixed in 4% paraformaldehyde showed intense diaphorase staining of the surface mucosal epithelial cells with the remainder of the mucosa staining lightly (Plate 4.3.8 B) and with no differential staining of cells observed deep in the mucosa.

The intense region of diaphorase staining in the paraformaldehyde treated corpus mucosa mirrored the staining produced by the monoclonal anti-nNOS antibody (Plate 4.3.8 C). No nNOS staining was seen of mucous neck, parietal or chief cells in the gastric pits, while NADPH diaphorase staining of tissue fixed in 4% paraformaldehyde was lighter in these regions. An antibody directed against mucin stained the surface of acetone-fixed corpus mucosa with staining descending into the gastric pits.

Plate Series 4.3.1: Immunocytochemistry with antiserum to the internal peptide of nNOS and controls (acetone-Fixed)

Plate 4.3.1 A: Antiserum to the internal peptide of nNOS - Gastric Mucosa

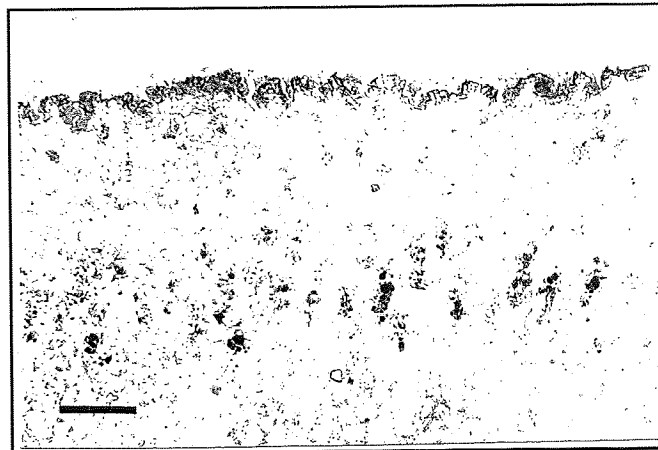


Plate 4.3.1 B: Pre-immune serum - Gastric Mucosa

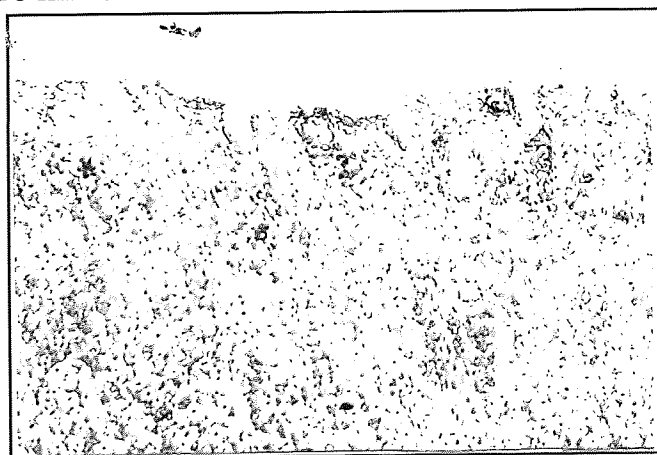


Plate 4.3.1 C: Internal nNOS peptide antiserum + peptide - Gastric Mucosa

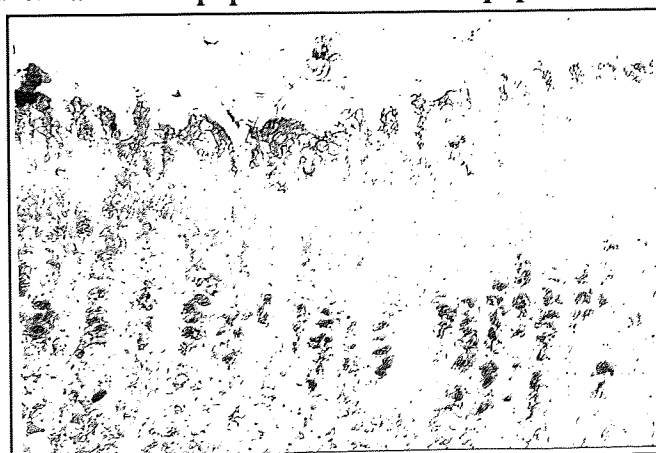
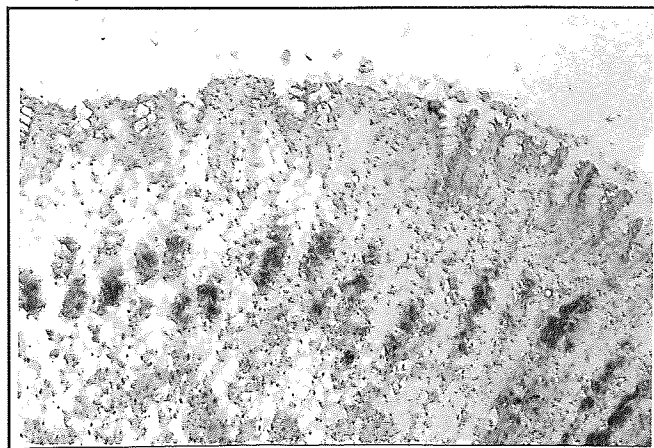


Plate 4.3.1 D: Affinity column wash - Gastric Mucosa



Legends to Plate Series 4.3.1

All plates show acetone-fixed sections (10 μ m) of corpus glandular mucosa stained by the ABC method. The bar in plate 4.3.1 A = 100 μ m and the other plates in the series are of the same magnification.

4.3.1 A: Section incubated with the antiserum to the internal peptide of nNOS (1/160 in normal blocking serum) for 30min at room temperature

4.3.1 B: Section incubated with pre-immune serum (1/160 in normal blocking serum) for 30min at room temperature

4.3.1 C: Section incubated with the antiserum to the internal peptide of nNOS (1/160 in normal blocking serum) and the internal nNOS peptide (100 μ g/ml dilute antiserum solution) for 30min at room temperature. The peptide/antiserum solution was prepared 10 min before addition to the section.

4.3.1 D: Section incubated with column wash (diluted 1:3 with normal blocking serum), from attempted affinity purification of the antiserum to the internal peptide of NOS, for 30min at room temperature

Plate Series 4.3.2: Antiserum to the carboxyl-terminal peptide of nNOS and controls (acetone-fixed)

Plate 4.3.2 A: Carboxyl-terminal antiserum - Gastric Mucosa

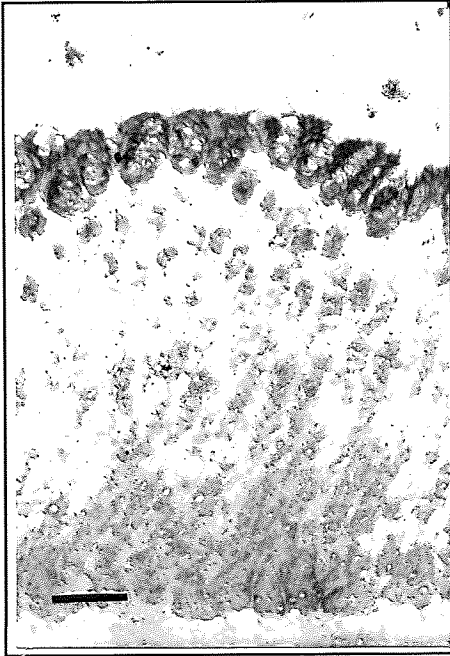


Plate 4.3.2 B: Pre-immune serum - Gastric Mucosa

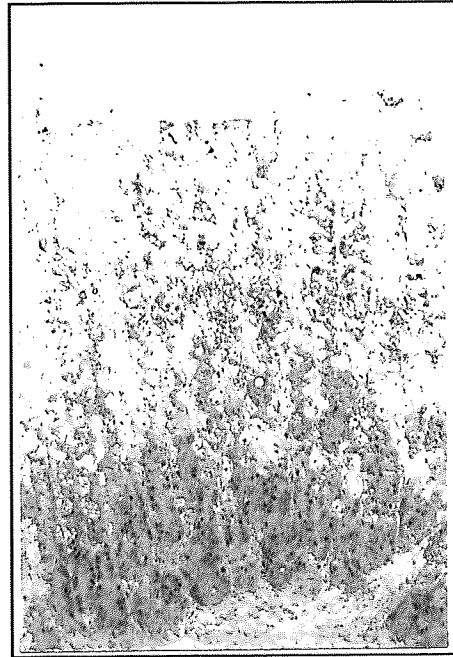


Plate 4.3.2 C: Carboxyl-terminal Antiserum + peptide - Gastric Mucosa

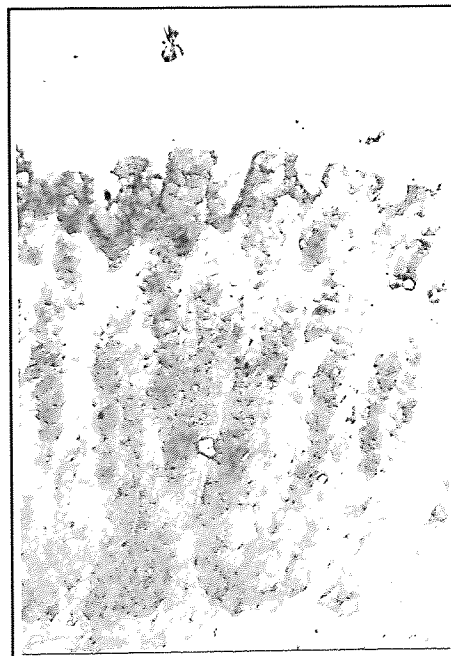
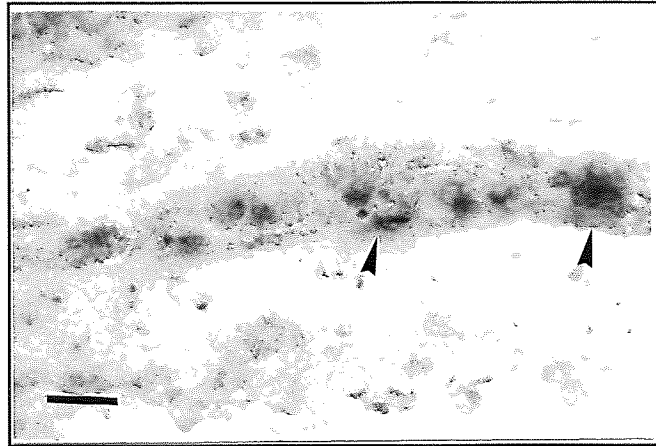


Plate 4.3.2 D: Carboxyl-terminal antiserum - Duodenum



Legends to Plate Series 4.3.2

All plates show acetone-fixed tissue sections (10 μ m) stained by the ABC method. Plates A-C are corpus glandular mucosa and plate D is duodenum. The bar in plate 4.3.2 A = 100 μ m and this magnification refers to plates B and C also. The bar in plate 4.3.2 D = 25 μ m.

4.3.2.A: Section incubated with the antiserum to a carboxyl-terminal peptide of nNOS (1/320 in normal blocking serum) for 30min at room temperature.

4.3.2 B: Section incubated with pre-immune serum (1/320 in normal blocking serum) for 30min at room temperature.

4.3.2.C: Section incubated with the antiserum to a carboxyl-terminal peptide of nNOS (1/320 in normal blocking serum) and the carboxyl-terminal peptide (100 μ g/ml in the diluted antiserum) for 30min at room temperature. The peptide/antiserum solution was prepared 10min before addition to the section.

4.3.2.D: Duodenal muscle layers in section incubated with the antiserum to a carboxyl-terminal peptide of nNOS (1/320 in normal blocking serum)for 30min at room temperature. Arrows indicate myenteric plexus. Longitudinal muscle is at the bottom of the picture.

Plate Series 4.3.3: Polyclonal anti-nNOS antibody, control and validation
(acetone-fixed)

Plate 4.3.3 A: Polyclonal anti-nNOS antibody - Gastric Mucosa

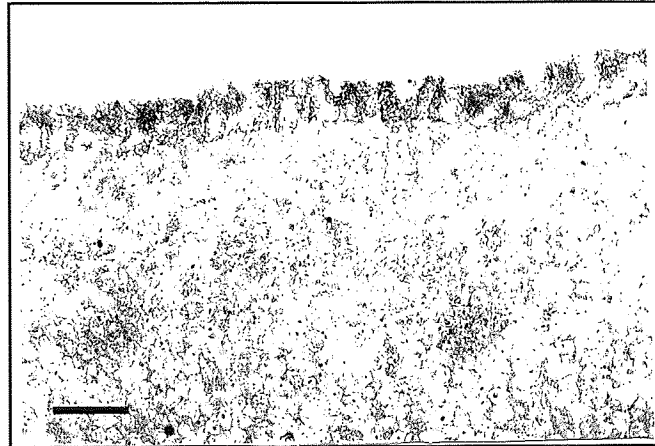


Plate 4.3.3 B: Rabbit IgG - Gastric Mucosa

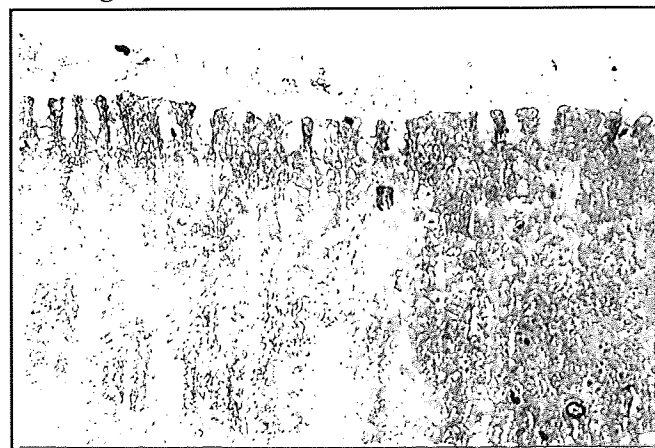
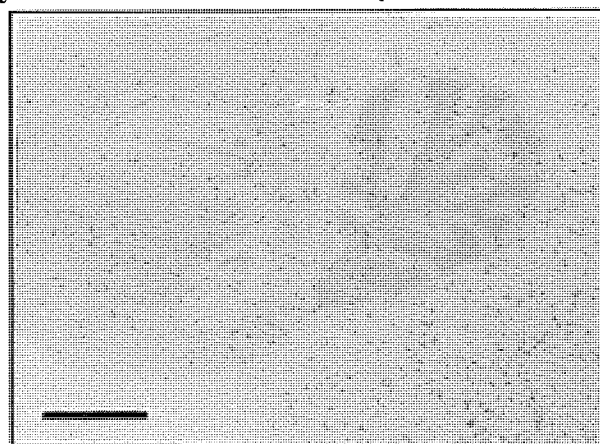


Plate 4.3.3 C: Polyclonal Anti-nNOS antibody - Brain



Legends to Plate Series 4.3.3

All plates shows acetone-fixed tissue sections (10µm) stained by the ABC method.

Plates A and B are corpus glandular mucosa and plate C is brain.

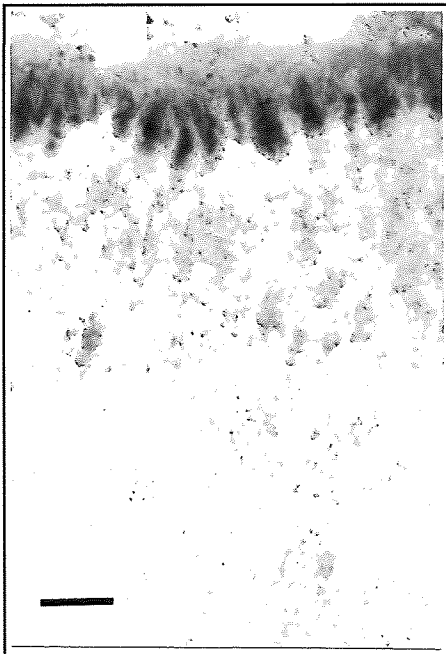
The bar in plate 4.3.3 A = 100µm with the same magnification for B and the bar in 4.3.3 C = 2 mm.

4.3.3 A and B: Sections incubated with polyclonal anti-nNOS antibody (10µg/ml in normal blocking serum) for 30min at room temperature.

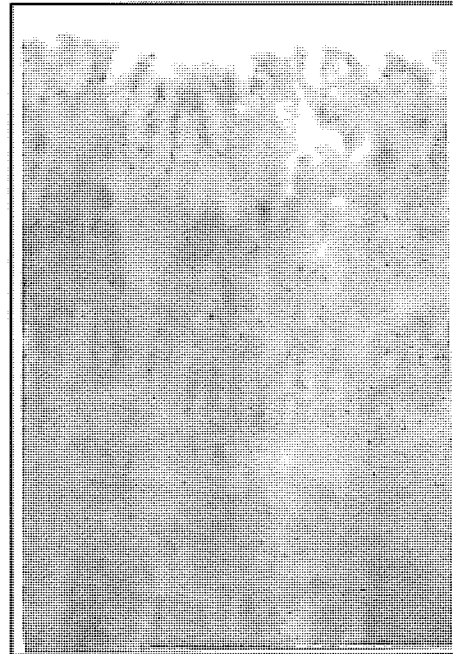
4.3.3 C: Section incubated with rabbit IgG (10µg/ml in normal blocking serum) for 30min at room temperature.

Plate Series 4.3.4: Monoclonal Anti-nNOS antibody and controls (acetone-fixed)

**Plate 4.3.4 A: Monoclonal anti
-nNOS antibody - Gastric Mucosa**



**Plate 4.3.4 B: Mouse IgG
- Gastric Mucosa**



**Plate 4.3.4 C: Monoclonal
anti-nNOS Antibody
- Duodenum**

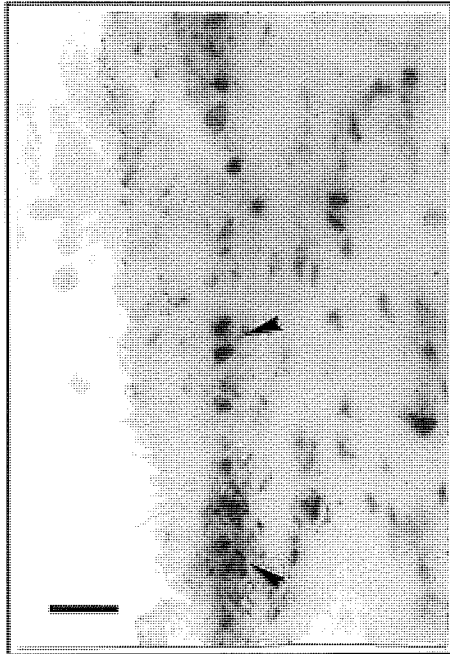
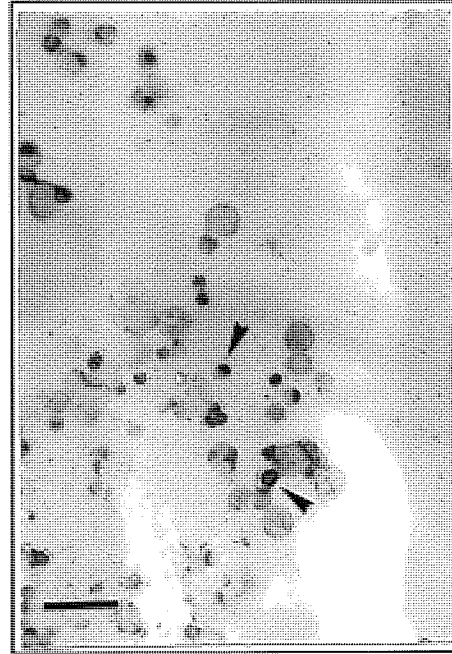


**Plate 4.3.4 D: Monoclonal
anti-nNOS antibody - Isolated
Gastric Mucosal Cells**



Legends to Plate Series 4.3.4

All plates show acetone-fixed tissues stained by the ABC method. Plates 4.3.4 A and B show sections of corpus glandular mucosa (10 μ m), plate 4.3.4 C shows a duodenum section (10 μ m) and plate 4.3.4 D shows isolated cells. The bar in plate 4.3.4 A = 100 μ m with the same magnification for B. In plate 4.3.4 C, the bar = 25 μ m and in plate 4.3.2.4 D, the bar = 50 μ m.

4.3.4 A: Section incubated with monoclonal anti-nNOS antibody (5 μ g/ml in normal blocking serum) for 30min at room temperature.

4.3.4 B: Section incubated with mouse IgG (5 μ g/ml in normal blocking serum) for 30min at room temperature.

4.3.4 C: Duodenal muscle layers in section incubated with monoclonal anti-nNOS antibody (5 μ g/ml in normal blocking serum) for 30min at room temperature. Arrows indicate myenteric plexus. Longitudinal muscle is at left of picture.

4.3.4 D: Cells incubated with monoclonal anti-nNOS antibody (5 μ g/ml in normal blocking serum) for 30min at room temperature. Arrows indicate stained cells.

Plate Series 4.3.5: Monoclonal Anti-nNOS antibody and controls
(paraformaldehyde-fixed)

Plate 4.3.5 A :

Monoclonal anti-nNOS antibody

- Gastric Mucosa

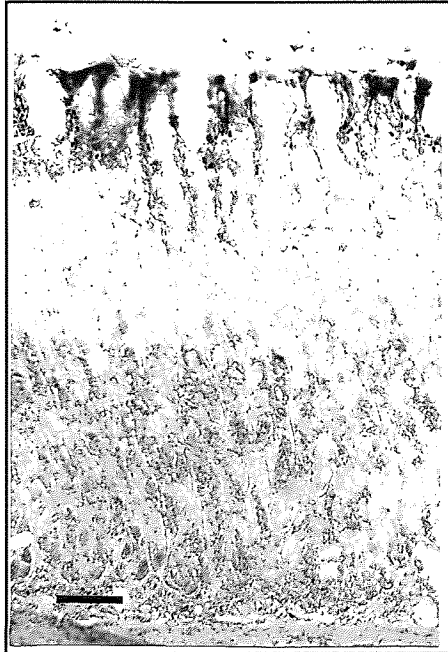


Plate 4.3.5 B:

Monoclonal anti-nNOS antibody

- Gastric Mucosa

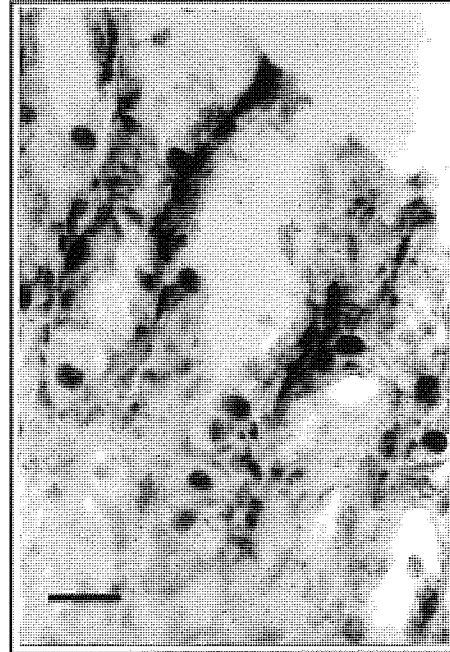


Plate 4.3.5 C: Monoclonal anti-nNOS
antibody + recombinant NOS

- Gastric Mucosa

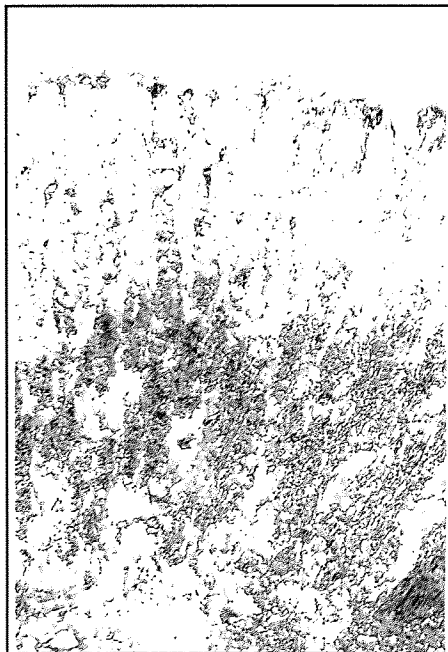


Plate 4.3.5 D:

Mouse IgG

- Gastric Mucosa

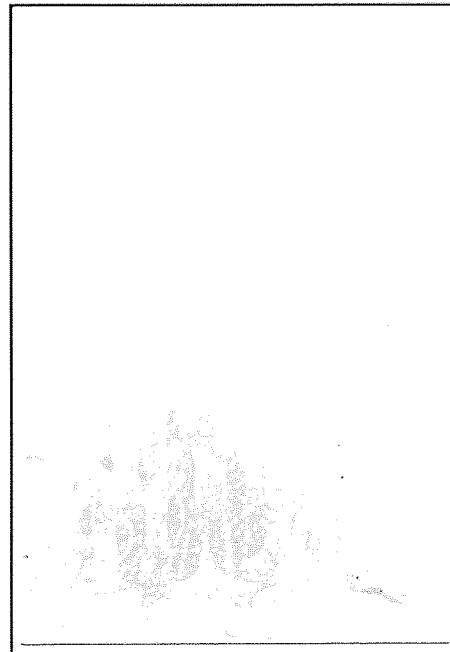
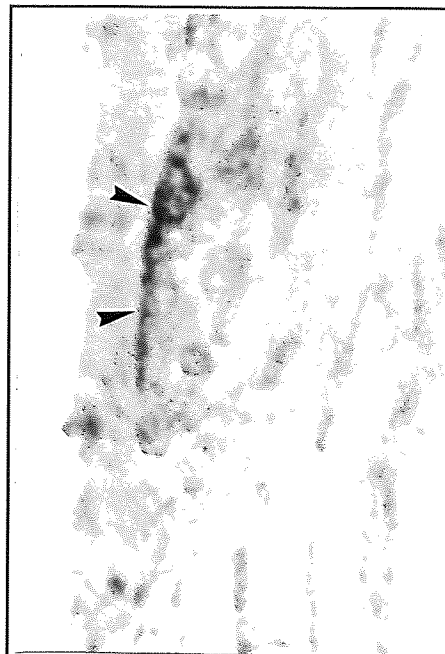


Plate 4.3.5 E: Monoclonal anti-nNOS antibody - Gastric Muscle



Plate 4.3.5 F: Monoclonal anti-nNOS antibody - Duodenum



Legends to Plate Series 4.3.5

All plates show tissue sections (10 μ m) fixed in 4% paraformaldehyde and stained by the ABC method. Plates 4.3.5 A-D are corpus glandular mucosa, Plate 4.3.5 E is corpus muscle and Plate 4.3.5 F is duodenum. In plate 4.3.5 A the bar = 100 μ m with the same magnification in C and D. The bar in plate 4.3.5 B = 25 μ m with the same magnification in F and in plate 4.3.5 E the bar = 25 μ m.

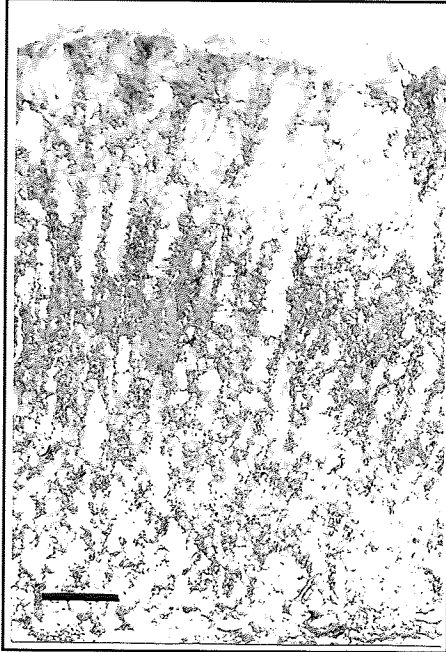
4.3.5 A, B, E and F: Sections incubated with monoclonal anti-nNOS antibody (5 μ g/ml in normal blocking serum) for 30min at room temperature. Arrows in 4.3.5 E indicate neurons. Mucosal side is towards right of picture. Arrows in 4.3.5 F indicate myenteric plexus and longitudinal muscle is at left of picture.

4.3.5.C: Section incubated with monoclonal anti-nNOS antibody plus recombinant nNOS (5 μ g/ml and 10 μ g/ml respectively in normal blocking serum) for 30min at room temperature.

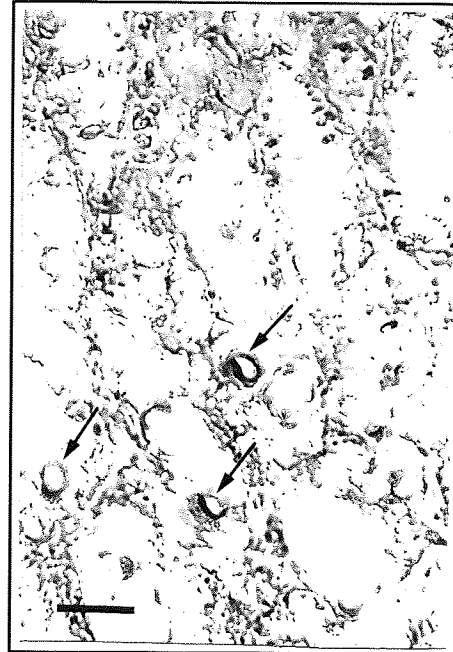
4.3.5.D: Section incubated with mouse IgG (5 μ g/ml in normal blocking serum) for 30min at room temperature.

Plate Series 4.3.6: Anti-eNOS antibody and controls (paraformaldehyde-fixed)

**Plate 4.3.6 A: Anti-eNOS
antibody - Gastric Mucosa**



**Plate 4.3.6 B: Anti-eNOS
antibody - Gastric Mucosa**



**Plate 4.3.6 C: Anti-eNOS
antibody - Gastric Mucosa**

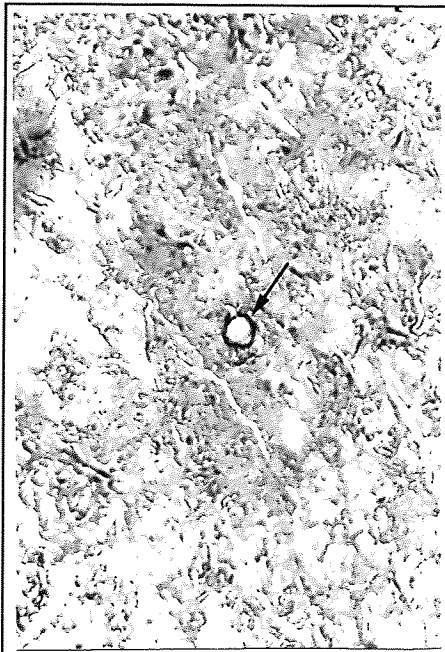


**Plate 4.3.6 D: Anti-eNOS
antibody - Gastric Muscle**

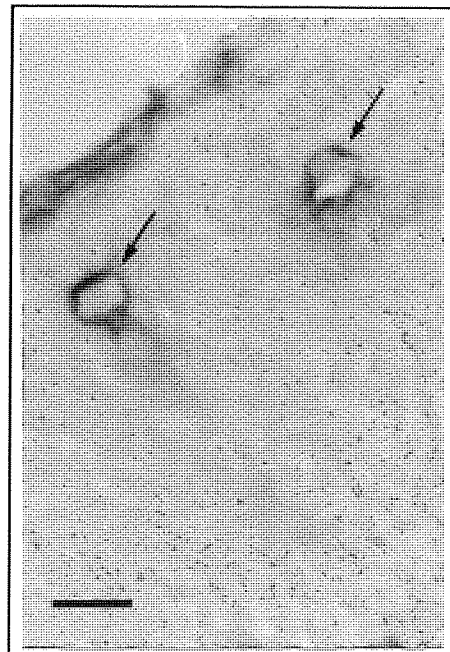


Plate 4.3.6 E: Anti-eNOS

Antibody - Aorta

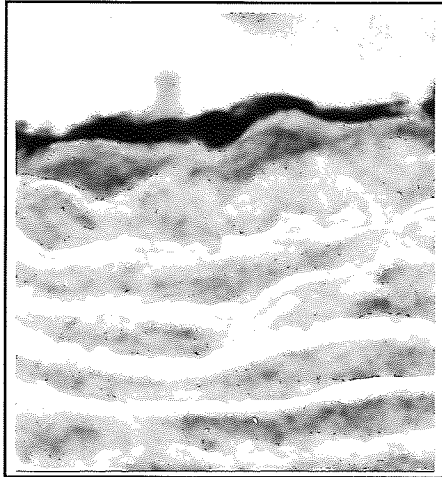
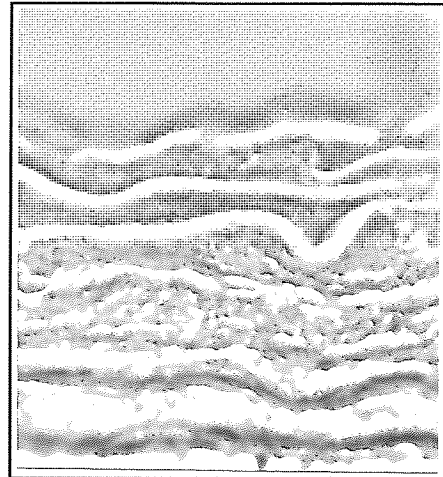


Plate 4.3.6 F: Mouse IgG

- Aorta



Legends to Plate Series 4.3.6

All plates show tissue sections (10 μ m) fixed in 4% paraformaldehyde and stained by the ABC method. Plates 4.3.6 A-D show stomach sections and plates 4.3.6 E and F show aorta sections. The bar in plate 4.3.6 A = 100 μ m and in plates 4.3.6 B and C the bar = 25 μ m. The bar in plate 4.3.6 D = 10 μ m with the same magnification in E and F.

4.3.6 A-D: Sections incubated with anti-eNOS antibody (5 μ g/ml in normal blocking serum) for 30min at room temperature. Arrows in 4.3.5 B-D indicate vessels.

4.3.6 E: Section incubated with anti-eNOS antibody (5 μ g/ml in normal blocking serum) for 2h at room temperature.

4.3.6 F: Section incubated with mouse IgG (5 μ g/ml in normal blocking serum) for 2h at room temperature.

Plate 4.3.7: Anti iNOS antibody



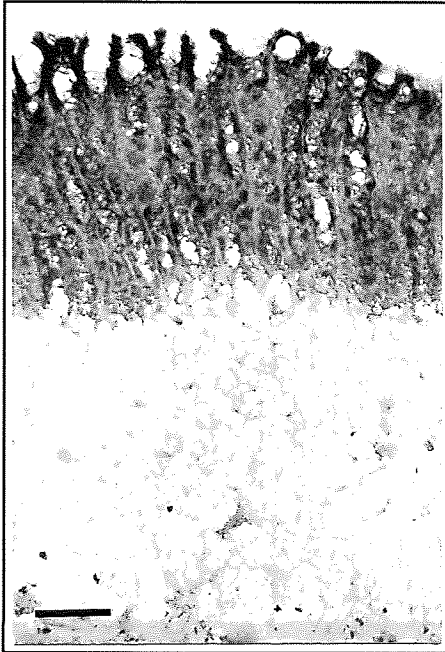
Legend to Plate 4.3.7

Plate series 4.3.7 shows a stomach section fixed in acetone and stained by the ABC method. The bar in plate 4.3.7 =100 μ m.

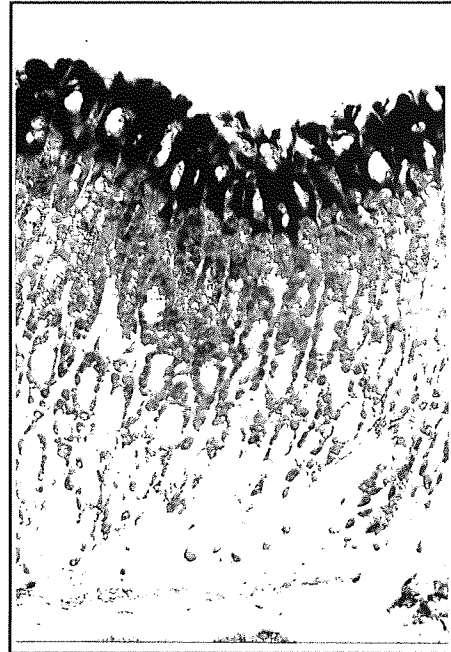
4.3.7: Section incubated with anti-iNOS antibody (10 μ g/ml in normal blocking serum) for 30min at room temperature.

Plate Series: 4.3.8 NADPH Diaphorase staining

**Plate 4.3.8 A :NADPH Diaphorase
on acetone-fixed Gastric Mucosa**



**Plate 4.3.8 B: NADPH
on paraformaldehyde-fixed
Gastric Mucosa**



**Plate 4.3.8 C:
Anti-nNOS monoclonal antibody
- Gastric Mucosa**

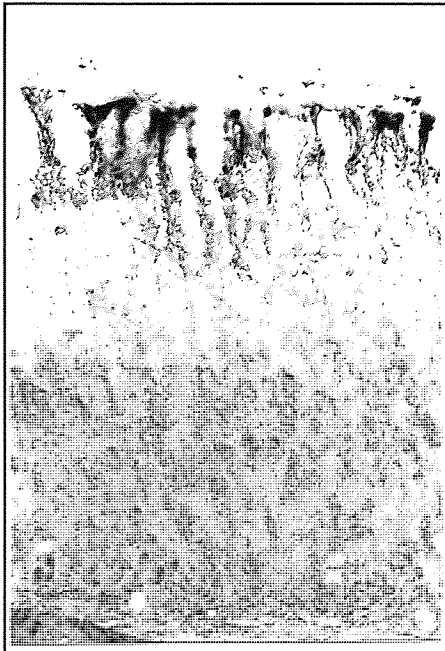
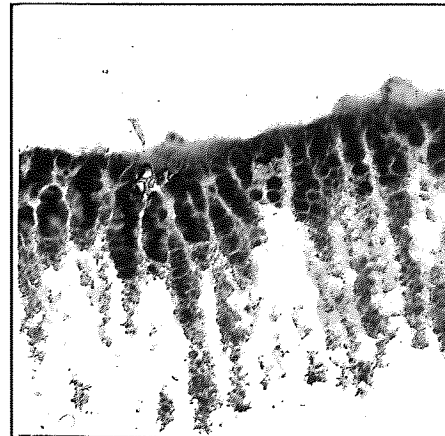


**Plate 4.3.8 D:
Anti-mucin antibody
- Gastric Mucosa**



Legends to Plate Series 4.3.8

All plates show stomach sections (10µm) fixed using either acetone (4.3.8 A and D) or 4% paraformaldehyde (4.3.8 B and C). The bar in plate 4.3.8 A = 100µm with the same magnification in B, C and D.

4.3.8 A and B: Sections stained for NADPH Diaphorase for 30min at 37°C.

4.3.8 C: Section stained by the ABC method, incubated with monoclonal anti-nNOS antibody (5µg/ml in normal blocking serum) for 30min at room temperature.

4.3.8 D: Section stained by the ABC method, incubated with anti-rat gastric mucin antibody (1/2000 in normal blocking serum) for 30min at room temperature.

4.4 DISCUSSION

4.3.1 nNOS in the rat gastric glandular mucosa

The major zone of staining seen in the gastric glandular mucosa with all antibodies directed towards nNOS was the surface mucosal epithelial cells. This staining was recognised to be specific because appropriate negative controls (e.g. preimmune serum) gave no such staining and the staining could be blocked in the case of the antipeptide antisera by the peptides against which they were raised and, in the case of monoclonal anti-nNOS antibody by recombinant rat brain nNOS.

The polyclonal anti-nNOS antibody stained areas in the brain which have been previously described as sites for nNOS i.e. neurons in the hippocampus and cerebellum (see table 4.1). Carboxyl-terminal antiserum stained neuronal structures in the myenteric plexus of the duodenum as did the monoclonal anti-nNOS antibody which also stained neurons in the muscle layer of the stomach, both sites again being well-documented as containing nNOS (see table 4.1). Isolated gastric mucosal cells, of similar diameter to mucous cells (Brown, unpublished) were stained by the monoclonal anti-nNOS antibody which is consistent with a known

high level of NOS enzyme activity in fractions containing such cells (Brown et al. 1992).

A number of other experiments strongly suggest that surface staining derives from the presence of nNOS. In Chapter 3 the carboxyl-terminal antiserum was shown to recognise recombinant nNOS on nitrocellulose confirming its ability to recognise the enzyme. Furthermore both the carboxyl-terminal antiserum and the monoclonal anti-nNOS antibody recognise nNOS in the gastric mucosa by immunoblotting procedures.

The band of stained cells in the centre of the mucosa with the antiserum directed against the internal peptide of nNOS appears to be non-specific and not due to nNOS because these cells were not stained with any of the other antibodies or antisera. A possible explanation for this staining is that the cells of the stained central band contain a protein with an epitope, similar to a sequence from either the peptide against which this antiserum was raised or from KLH, to which the peptide was conjugated for immunisation. When this proposal was tested by experiment the results were unclear. Thus the band did not disappear during immunocytochemistry when the peptide was added to the antiserum or when KLH was added. Affinity purification of the antiserum against the internal peptide of nNOS was attempted to remove the non-specific activity. Although functional antibodies against native gastric mucosal nNOS could not be eluted from the affinity purification, the column wash had the ability to stain this band of cells. This latter result suggests that the reaction did not involve an epitope on the internal peptide.

The staining of the surface cells seen by immunocytochemistry coincided with a region of high NADPH diaphorase activity as clearly demonstrated in Plate series 4.3.8. The slightly different pattern of NADPH diaphorase staining in sections fixed by different methods may be explained by the fixation. Paraformaldehyde fixation may affect the intensity of NADPH diaphorase staining associated with NOS activity (Matsumoto et al. 1993; Tracey et al. 1993) and non-NOS associated

NADPH diaphorase activity can be decreased or abolished in relation to NADPH diaphorase activity associated with NOS (Matsumoto et al., 1993). Because NOS is one of the enzymes which exhibits NADPH diaphorase activity all regions which are positive for NOS should potentially be NADPH diaphorase-positive. NADPH diaphorase staining however does not always indicate the presence of NOS. Thus the region of NADPH diaphorase staining in acetone-fixed corpus mucosa descending into the gastric pits is not likely to be associated with NOS. The pattern of intense staining in paraformaldehyde fixed sections mirrors more closely the staining seen in immunocytochemistry with the weak staining in the rest of the mucosa not corresponding to NOS.

The two different fixation methods used also gave rise to a difference in immunostaining with the carboxyl-terminal antiserum, which only recognised nNOS well in acetone-fixed tissues with only a very slight reaction in paraformaldehyde-fixed tissues. With the monoclonal anti-nNOS antibody staining was seen in tissues fixed by both methods but the quality of preservation observed was much greater in tissues fixed in paraformaldehyde to the extent that individual surface cells could be seen as stained. Paraformaldehyde acts by forming inter- and intra-cellular cross bridges and this process can affect the antigenicity of some proteins and has been reported to decrease the antigenicity of NOS (Schmidt et al. 1992a). It is possible that the monoclonal anti-nNOS antibody recognises an epitope in NOS not affected by fixation while the epitope in NOS recognised by antibodies in carboxyl-terminal antiserum is not available for antibody binding after paraformaldehyde fixation.

The results presented in this study indicating the presence of NOS in surface mucosal epithelial cells do not agree with results published by Burrell et al. (1996) who localised NOS in the human and murine stomach only to somatostatin producing cells or with Fiorucci et al. (1995) who localised NOS in guinea pig isolated chief cells. In this chapter however the results were obtained by using four different antibodies for NOS while Burrell et al. and Fiorucci et al., both only used

used one. Furthermore the antiserum used by Burrell et al. was evaluated by Riveros-Moreno et al. (1993) and found to perform poorly in ELISAs for native nNOS protein. Species differences may also explain the conflicting results.

4.4.2 eNOS in the rat gastric glandular mucosa

The form of NOS present in the surface cells resembles nNOS in its immunoreactivity rather than eNOS as the monoclonal anti-eNOS antibody showed no staining of the surface. eNOS was however detected in small blood vessels of the corpus mucosa which is compatible with an involvement of NOS in the maintenance of gastric mucosal blood flow (Whittle 1994). The staining of the blood vessels due to the presence of eNOS was supported when the endothelium of aorta, a known site of eNOS (Pollock et al. 1993), was shown to stain positively compared to a mouse IgG control. The monoclonal anti-eNOS antibody used has also been shown to detect a band at 140kDa in gastric mucosal extracts (Chapter 3) and has been used successfully by others to detect eNOS in LLC-PK1 cells (McKee et al. 1994) another established source of eNOS (Tracey et al. 1994).

No cross-reactivity was observed with antisera or antibodies to one form of NOS detecting the other form in the sections and this is compatible with results obtained by immunoblotting with gastric mucosal extracts where anti-nNOS antibodies only detected a band of 160kDa and the anti-eNOS antibody a band at 140kDa (Chapter 3).

4.4.3 No evidence of cross reactivity with iNOS

The staining seen with the antibodies directed against eNOS and nNOS is unlikely to be due to cross-reaction with the Ca^{2+} -independent inducible form of iNOS (Cho et al., 1992). Brown et al. (1994) detected no Ca^{2+} -independent NOS activity in gastric mucosa from normal rats. In a corpus mucosa section incubated with anti-iNOS antibody (Plate 4.3.7) background staining was dark but the level of background staining was uniform with no specific staining evident. Finally a cross-

reaction between any iNOS in the gastric mucosa and anti-nNOS or anti-eNOS antibodies would have been visible on immunoblots of gastric mucosal extracts as a band of 130kDa (Cho et al. 1992). No such band was evident (chapter 3).

4.4.4 Potential sites for action of NO in rat stomach

Localisation of nNOS to surface cells of the corpus mucosa indicates that NO, produced intracellularly is likely to be involved in the regulation of mucus secretion from the gastric epithelial cells. NO however can pass easily through cell membranes so NO generated from one cell could modify activity in adjacent cells. Thus activation of NOS in a single mucous cell could conceivably trigger secretory activity in adjacent cells.

The data presented in this chapter together with studies which detected NOS in the stratified squamous epithelium of the forestomach (Schmidt et al. 1992) and in specialised brush or caveolated cells in the cardiac fold (Kugler et al. 1994) suggest the presence of NOS over a large part of the gastric luminal surface. NOS has also been localised in this study in the endothelium of gastric mucosal blood vessels. NOS in the stomach is therefore widespread indicating a variety of roles for NO in gastric secretion and maintenance of gastric mucosal integrity.

4.4.5 Summary

- 1: nNOS in the gastric glandular mucosa has been localised to surface mucosal epithelial cells.
- 2: eNOS in the gastric glandular mucosa has been localised to the endothelium of blood vessels in the mucosal and muscle layers.

CHAPTER 5

ROLE OF NITRIC OXIDE IN CARBACHOL STIMULATED

MUCUS SECRETION IN THE STOMACH

5.1 INTRODUCTION

As described in Chapter 1, mucus is secreted in the gastric glandular mucosa by surface mucous cells to produce a continuous adherent layer of mucus gel over the surface of gastric mucosal epithelium (Allen et al. 1993). This mucus gel layer protects the gastric mucosa from digestion by acid and pepsin (Allen et al. 1993). However, native mucous glycoprotein is slowly broken down by pepsin into lower molecular weight subunits, the surface gel is solubilised and subunits are released into the gastric lumen. The thickness of the surface gel therefore represents a dynamic balance between mucus secretion and its erosion by peptic digestion and shear.

A procedure of sectioning of tissue and measurement of mucus thickness was described by Kerss et al. (1982) and McQueen et al. (1983 & 1984). Short-term changes in the thickness of the gastric mucus gel layer in rats *in vivo* can be used to provide an index of mucus secretion. This technique has the advantages that it is simple and direct, and many measurements can be made on the same piece of mucosa allowing an accurate value of mucus thickness to be calculated.

Mucus secretion can be increased by a number of secretagogues, most notably the muscarinic acetylcholine receptor agonist carbachol (McQueen et al 1984) and prostaglandin E₂ (Bolton et al 1978; Bickel et al. 1981; McQueen et al. 1984). Brown et al. (1992a) showed that the NO donors, SNAP and isosorbide dinitrate administered intragastrically to rats *in vivo* could increase the thickness of the mucus layer, the increase in mucus thickness being similar to the increase reported previously for carbachol (McQueen et al. 1984). Intragastric administration of the cGMP analogue, dibutyl cGMP, also increased the thickness of the mucus layer *in vivo* (Brown et al. 1992a) suggesting that the effect of the NO donors might be due to the release of NO and activation of guanylate cyclase. NO donors and dibutyl cGMP were also shown to enhance the release of mucin from suspensions of isolated gastric mucosal cells *in vitro* (Brown et al. 1993). Furthermore, a cGMP phosphodiesterase inhibitor also enhanced mucin secretion by the isolated gastric

mucosal cells (Brown et al. 1993). The presence of NOS activity in gastric mucosal cells (Chapters 3 and 4) and the above results all suggest a signalling pathway leading from NOS activation and subsequent stimulation of guanylate cyclase by released NO to a cGMP-dependent activation of mucus secretion. The question is, however, whether this pathway actually functions to regulate mucin secretion under the influence of physiological agents in intact tissue. Muscarinic acetylcholine receptor agonists increase intracellular Ca^{2+} in gastric mucosal cells (Seidler and Pfeiffer, 1991) and are therefore reasonable candidates to activate NOS and trigger the proposed pathway leading to mucus secretion. Consequently, the aim of this study was to investigate whether NO was involved in the stimulatory effect of the muscarinic agonist carbachol on the thickness of the adherent mucus gel layer and, therefore by implication the stimulation of gastric mucus secretion.

5.2 METHODS

5.2.1 Administration of drugs to animals

Male Wistar rats (175-225g) which had been deprived of food, but not water, for the previous 18 hours were anaesthetised with sodium pentobarbitone (60mg/kg i.p.). L-NAME (0.4-5.0mg/kg), prepared in sterile isotonic saline (9g/l NaCl), was injected as a bolus into the tail vein. Control animals received saline alone.

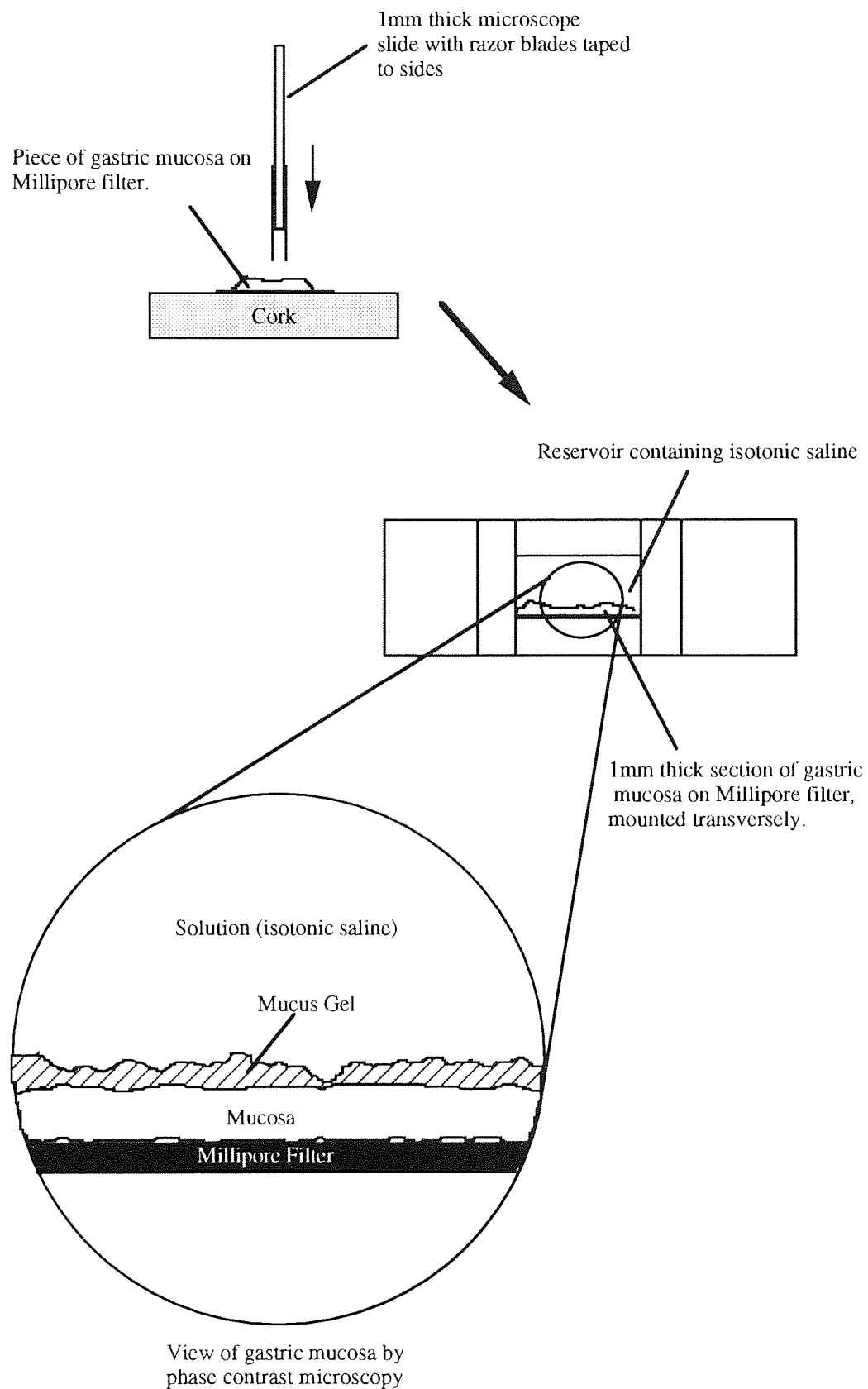
In experiments where the effects of L-arginine and D-arginine on the L-NAME response were investigated to determine the specificity of the action of L-NAME, the L- or D-arginine (100mg/kg) was injected intravenously 5min prior to L-NAME administration. 5min after the intravenous injection of L-NAME the abdomen was opened by a mid-line incision and either sterile isotonic saline (5ml/kg), or sterile saline containing carbachol (150 μ g/kg), or 16, 16-dimethyl prostaglandin E₂ (50 μ g/kg) was injected into the gastric lumen by means of a syringe and a 26 gauge needle which was used to puncture the fore-stomach. The doses of carbachol and 16,16-dimethyl prostaglandin E₂ administered were

established, from pilot and previous experiments (McQueen et al. 1983), to produce maximal effects on increasing the thickness of the mucus gel layer. The abdomen was then stitched up and the animal left on a heated table to maintain its body temperature. The gastric mucosa was exposed to agents for 30 min after which the stomach was removed and placed into ice-cold isotonic saline to be prepared for measurement of gastric mucus thickness.

5.2.2 Measurement of gastric mucus thickness

A "blister" of muscle was produced on the dorsal and ventral surfaces of the mid-corpus mucosa by injection of saline into the wall between the muscle and the mucosa using a 26 gauge needle. The muscle layer was then removed, to prevent "curling" of the section once removed from the stomach, and a circular section of mucosa was cut and placed epithelial surface upwards on a cellulose acetate filter (Millipore). Four sections (i.e. two from the dorsal side two from the ventral side) each 1mm thick and were cut from each stomach using two razor blades taped to either side of a microscope slide (Figure 5.2). Sections were carefully removed from the razor blade and were mounted transversely in isotonic saline in a reservoir mounted on a glass microscope slide and were viewed between 0 and 30min after sectioning under phase contrast using an inverse microscope. The thickness of the mucus layer was determined using an eyepiece graticule, the observer being unaware of the previous treatment of the rat. Three distinct layers were visible on inspection: the bathing solution, the mucus gel layer and the mucosa (Figure 5.2). Measurements were taken every 300µm along the section and mucus thickness was calculated as the arithmetic mean of at least 50 measurements per rat. Measurements were carried out within a 30min time period during which time there was no change in the thickness of the mucus gel layer (Kerss et al, 1982; J.Brown, PhD Thesis)

Figure 5.2 Measurement of gastric mucus thickness

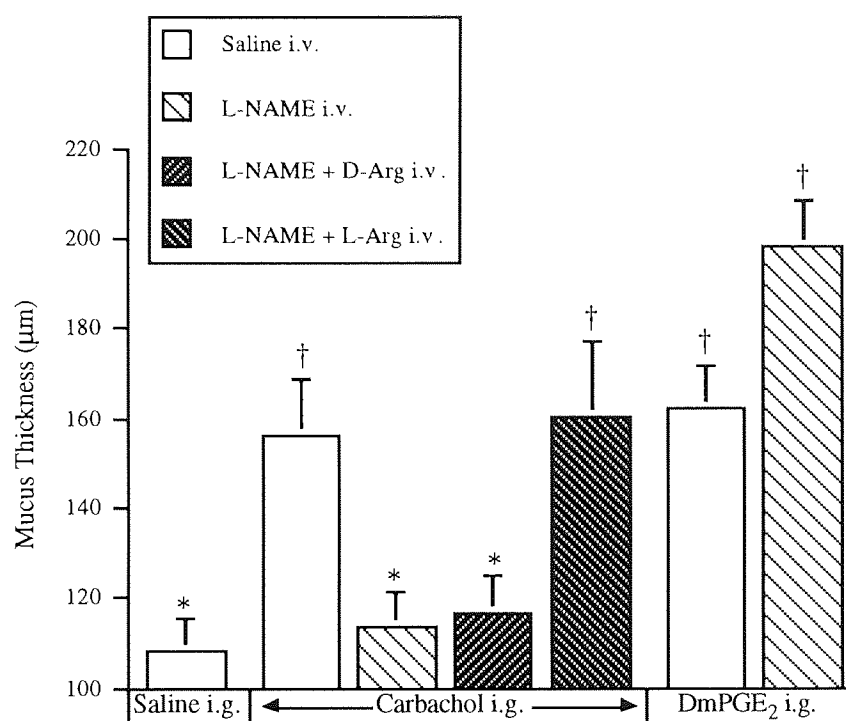


5.3 RESULTS

Comparisons between measurements of mucus thickness made under two different conditions were performed using a Mann-Whitney test and the effects of more than two treatments were analysed by a Kruskal-Wallis test and a non-parametric equivalent of the Newman-Keuls test. These non-parametric tests were used because the distribution of mucus thickness measurements for each animal may depart from normality (Kerss et al. 1982). Statistical tests are described in Appendix A6.

Control mucus thickness in animals injected intragastrically with saline was $108 \pm 7.5 \mu\text{m}$ ($n=6$) which was not different (Mann-Whitney test) from the values obtained from animals which had not been injected at all, $113 \pm 11 \mu\text{m}$ ($n=6$). Intragastric carbachol ($150 \mu\text{g/kg}$) significantly increased ($p < 0.05$) the mucus thickness (Figure 5.3 A). L-NAME ($0.4\text{--}5 \text{mg/kg}$) administered 5min prior to carbachol dose-dependently reduced the stimulation of mucus thickness by carbachol (Figure 5.3 B) and the highest dose of L-NAME completely abolished the effect of carbachol (Figure 5.3 A). There was a significant effect of the dose of L-NAME on the thickness of the mucus gel layer ($p < 0.05$, using a Kruskal-Wallis test). Intravenous administration of L-arginine (100mg/kg) 5min prior to L-NAME prevented the inhibitory action of L-NAME on the response to carbachol but D-arginine had no such effect (Figure 5.3 A). Intravenous administration of L-NAME or L-arginine alone with saline injected intragastrically gave mucus thickness measurements not significantly different from the control results, $128 \pm 9.7 \mu\text{m}$ and $129 \pm 4.7 \mu\text{m}$ respectively. In contrast to the result with carbachol, L-NAME (5mg/kg i.v.) did not inhibit the stimulation of mucus thickness seen after administration of 16,16-dimethyl prostaglandin E_2 ($50 \mu\text{g/kg}$ i.g.)

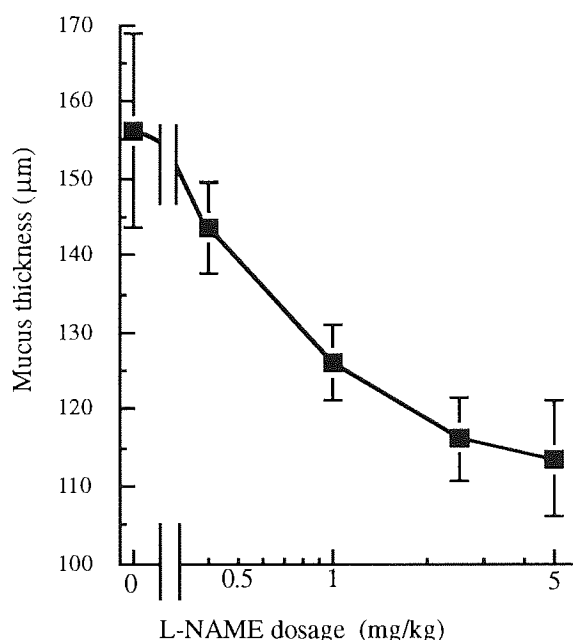
Figure 5.3 A: Mucus thickness in gastric glandular mucosa after administration of various agents.



Legend to Figure 5.3 A

Mucus thickness measurements after administration of saline or a mucus secretagogue i.g. 5min after the administration of saline or L-NAME i.v. In some experiments D- or L-arginine (D-Arg or L-Arg) was administered 5min prior to L-NAME administration. Results are given as means \pm S.E.M. n=6 animals for each treatment. † indicates a significant difference ($p < 0.05$, Kruskal-Wallis test) from basal and * indicates a significant reduction ($p < 0.05$, Kruskal-Wallis test) from the response to the mucus secretagogue in the gastric lumen and saline administered i.v.

Figure 5.3 B: Dose-response curve of the effect of L-NAME on the increase of Mucus Secretion by Carbachol



Legend to Figure 5.3 B

Dose-dependent effect of L-NAME (0.4-5mg/kg) administered i.v. 5min prior to carbachol i.g. (150μg/kg) on the thickness of the mucus gel layer observed 30min after carbachol administration. Results are means \pm S.E.M. from 4-6 rats for each dose. There was a significant effect of the dose of L-NAME on the thickness of the layer of mucus ($p < 0.05$, Kruskal-Wallis test)

5.4 DISCUSSION

The results presented in this study, showing that L-NAME causes a dose-dependent inhibition of the stimulatory effect of carbachol on the thickness of the mucus gel layer in the rat stomach appear to be due to the inhibition of NOS since the effect could be prevented by prior administration of L-arginine, the physiological substrate for NOS (Moncada et al. 1991), but not by the inactive isomer, D-arginine. Thus although L-NAME has been shown in the past to act as an

antagonist at muscarinic acetylcholine receptors (Buxton et al. 1993), the results in this study are not due to this effect. Other effects of L-NAME are the reduction of gastric mucosal blood flow and a rise in blood pressure (Tepperman and Whittle, 1992). However it is unlikely that these effects could have unspecifically interfered with mucus secretion because L-NAME did not affect the increase in mucus layer thickness seen after 16, 16-dimethyl prostaglandin E₂, nor did L-NAME significantly affect the dimensions of the mucus layer in the absence of mucus secretagogues. L-NAME does not directly interfere with gastric acid secretion (Esplugues et al. 1993; Barrachina et al. 1994) which makes it unlikely that the results obtained in this study were caused by changes in acid production. The results in this study suggest that NO is involved in the cholinergic activation of gastric mucus secretion. The results are compatible with reports of stimulation of mucus secretion by NO donors both *in vivo* and *in vitro* (Brown et al. 1993a,b).

Stimulation of the release of mucus by cholinergic agonists is dependent upon intracellular Ca²⁺ (Seidler and Sewing, 1989). Furthermore, cholinergic stimulation has been shown to stimulate release of Ca²⁺ into the cytosol of gastric mucosal epithelial cells (Seidler and Pfeiffer, 1991). nNOS is known to be present in rat gastric glandular epithelial cells (Chapter 3 and 4). Carbachol, by increasing the concentration of intracellular Ca²⁺ may initiate a pathway leading to mucus secretion by activating the Ca²⁺-calmodulin dependent nNOS in the gastric mucosal epithelium. By contrast, the stimulatory effects of prostaglandin E₂ on mucus secretion *in vitro* required neither intra- or extracellular Ca²⁺ (Seidler and Sewing, 1989) and in the present study L-NAME did not inhibit mucus secretion stimulated by 16, 16-dimethyl prostaglandin E₂.

The presence of nNOS in the gastric mucosal epithelium suggests that NO produced in mucous cells affects the secretion of mucus from either the same cell or adjacent cells. However, the origin of NO involved in mucus secretion may also be from sites outside of the epithelial cell. In Chapter 4 eNOS was localised in the vascular endothelium of gastric mucosal blood vessels, thus NO produced by

cholinergic activation of eNOS (Moncada et al. 1991) or other cells might be able to diffuse to mucous cells. In addition, a neuromodulator role of NO (Sander and Ward, 1992), which may influence mucus secretion *in vivo* cannot be excluded although there are few NOS immunoreactive neurons in the rat gastric mucosa (Ekblad et al., 1994). Nevertheless, the simplest explanation of the data is that the direct stimulation of mucus release by carbachol from surface gastric epithelial cells requires NOS to be active.

Summary

- 1:** The stimulation of mucus secretion by carbachol, but not by 16, 16-dimethyl prostaglandin E₂ can be inhibited, dose dependently, by L-NAME.
- 2:** The effect of L-NAME on carbachol stimulated mucus secretion appears to be due to inhibition of NO production because it can be reversed by prior administration of L-arginine but not by D-arginine.

CHAPTER 6
INDUCIBLE NITRIC OXIDE SYNTHASE
IN THE COLON AND SMALL INTESTINE

6.1 INTRODUCTION

6.1.1 Background

NOS activity can be induced in several tissues (Salter et al. 1991) by injection of rats with bacterial lipopolysaccharide(LPS). In most tissues the induced activity was Ca^{2+} -independent (i.e. is not affected by variation in the Ca^{2+} concentration in the assay), suggesting that the increased activity is likely to be due to expression of iNOS (Chapter 1). However, in intestinal tissues a more complex and conflicting picture of NOS induction has been described. Salter et al. (1992) described an increase induced by LPS in NOS activity in ileal whole wall which was partially Ca^{2+} -dependent, these results being mirrored in the caecum. No increase in iNOS activity was seen in the whole wall of the colon after treatment with LPS, activity being totally Ca^{2+} -dependent. After treatment with LPS, Oguchi et al. (1992) observed partial Ca^{2+} -dependence of induced NOS partially purified from rat colon, and Wirthlin et al. (1996) observed partial Ca^{2+} -dependence in NOS activity induced in the whole wall of the rat small intestine. Boughton-Smith et al. (1994) reported an increase in Ca^{2+} -dependent activity in rat colonic muscle after LPS treatment, but in mucosa the increased NOS activity was Ca^{2+} -independent. Intestinal epithelial cells isolated from the small intestine of rats pretreated with LPS (Tepperman et al. 1993; Salzman et al. 1996) showed induction of only Ca^{2+} -independent NOS activity.

The activity of iNOS present in mouse macrophages is independent of Ca^{2+} , probably because calmodulin is tightly bound to the enzyme (Cho et al. 1992). Ribiere et al. (1996) reported that in the presence of a high concentration (5mM) of EGTA in the assay buffer, induced NOS activity can show Ca^{2+} -dependence in extracts of adipose tissue, heart and liver. This effect may possibly be due to the removal of calmodulin caused by chelation of Ca^{2+} by the high concentration of EGTA and is also seen with macrophage iNOS (Stevens-Truss and Marletta. 1994). In this chapter the possibilities that there is a genuine induction of Ca^{2+} -dependent

NOS activity (i.e. nNOS or eNOS) by LPS, or that iNOS may be exhibiting partial Ca^{2+} -dependency are addressed.

6.1.2 Aims

6.1.2.1 Ca^{2+} -dependency of NOS induced in colonic mucosa by LPS

In all studies which have measured NOS activity in intestinal tissue, a Ca^{2+} chelator was present in the homogenisation buffer (see table 6.1).

Table 6.1: Ca^{2+} Chelators in homogenisation buffers used by previous studies

Authors	Chelator present in Homogenisation Buffer	Chelator Concentration (mM)
Oguchi et al. (1992)	EGTA+EDTA	Both 0.5
Salter et al. (1991)	EDTA	1.0
Wirthlin et al. (1996)	EDTA	0.5
Boughton-Smith et al. (1994)	EDTA	1.0
Ribiere et al. (1996)	EDTA	1.5

The first aim of this section therefore, was to examine whether chelation of Ca^{2+} during homogenisation affects subsequent Ca^{2+} -dependency of colonic mucosal inducible NOS. The colonic mucosa was selected because no NOS activity of any type is detectable in tissue from control animals.

6.1.2.2 Ca^{2+} -dependency of NOS in intestinal muscle

The majority of studies investigating induction of NOS in the intestine by LPS have measured NOS activity in the whole wall, and since studies with mucosal cells showed induced NOS to be Ca^{2+} -independent, the second aim of this study was to investigate the activity and Ca^{2+} -dependence of NOS in the intestinal muscle layers of LPS-induced rats.

6.2 METHODS

6.2.1 Induction of NOS activity *in vivo*

Male Wistar rats (200-300g) were anaesthetised using nitrous oxide/halothane gaseous anaesthesia. Lipopolysaccharide (isolated from the cell wall of *E.Coli* 0111:B4; Sigma) was dissolved in sterile saline (0.9% NaCl, w/v) to give a concentration of 3mg/ml. The lipopolysaccharide solution was injected into the tail vein of rats (3mg/kg body weight), while control rats received sterile saline and the animals were allowed to recover from anaesthesia. The animals were left for 4h before again being anaesthetised with sodium pentobarbitone (60mg/kg i.p.) and tissues removed as required.

6.2.2 Assays for NOS activity

6.2.2.1 Ca²⁺-dependency of colonic mucosal NOS - Experiment 1

Colonic mucosa was removed from two rats treated with LPS and was homogenised (2.2.2.2) for 30s on ice at full-speed by using an Ultraturrax homogeniser in homogenisation buffer containing neither calcium chelator nor calcium (Buffer A: 10µg/ml soybean trypsin inhibitor, 10µg/ml leupeptin, 6µg/ml aprotinin, 0.1mg/ml PMSF in 10mM HEPES, 320mM sucrose, 1mM dithiothreitol pH 7.5). Homogenates were pooled and the pooled homogenate was transferred to four microfuge tubes (1ml in each). 100µl total of a mixture of homogenisation buffer A and homogenisation buffer B, which was identical to buffer A but contained 55mM EGTA, was added to each tube to give a range of final EGTA concentrations from 0 to 5mM (see Table 6.2.1). Homogenates were re-homogenised as above and were subject to centrifugation for 20min at 10,000 x *g*_{av} at 4°C following which supernatants were removed and kept on ice until used in the assay.

Table 6.2 A: Variation of EGTA concentration in homogenisation buffer

Tube Number	Volume of Homogenate (ml)	Volume of Buffer A added (μ l)	Volume of Buffer B added (μ l)	Final EGTA concentration (mM)
1	1	100	0	0
2	1	98	2	0.1
3	1	80	20	1
4	1	0	100	5

"Uninhibited", L-NMMA and EGTA assay buffers were prepared using three different assay buffers as a base: normal assay buffer (0.2mM CaCl_2 , see 2.2), Intermediate calcium assay buffer (as normal assay buffer but with 0.34mM CaCl_2) and high calcium assay buffer (as normal assay buffer but with 3.0mM CaCl_2). The final concentrations of constituents were identical to that in the standard assay protocol (Table 2.2). The three types of each assay buffer were added in varying proportions to assay microfuge tubes to give a final volume of 50 μ l and to ensure that free Ca^{2+} concentrations after addition of samples were equal in tubes regardless of the homogenisation buffer in which samples were prepared (143 μ M in uninhibited and L-NMMA assay tubes and 21.7nM in EGTA assay tubes, see Table 6.2 B and C). Concentrations required were calculated by Dr P.J. Hanson using an iterative procedure (Program Complex) to solve the equations for binding of Ca^{2+} and Mg^{2+} to EGTA. $K_A \text{ EGTA} \cdot \text{Mg}^{2+} = 70.858 \text{ M}^{-1}$; $K_A \text{ Ca}^{2+} \cdot \text{EGTA} = 1.2 \times 10^7 \text{ M}^{-1}$.

Volumes of sample added and the methods of stopping the assay and counting citrulline formation were as described for the standard assay protocol (2.2.2)

Table 6.2 B: [EGTA] and [Ca²⁺] values calculated to give an equal free [Ca²⁺] in assay mixtures for homogenates of different [EGTA] - Experiment 1

U/L = uninhibited or L-NMMA assay; E = EGTA assay.

Homog. Buffer	Assay Buffer			Assay Mixture (50μl Assay Buffer + 20μl Homogenate)		
[EGTA] mM	Type	[EGTA] mM	Total [Ca ²⁺] mM	Total [EGTA] mM	Total [Ca ²⁺] mM	Free [Ca ²⁺] mM
0	U/L	0	0.200	0	0.143	0.143mM
	E	1	0.200	0.714	0.143	21.7nM
0.1	U/L	0	0.240	0.02857	0.1715	0.143mM
	E	1	0.208	0.7428	0.1484	21.7nM
1	U/L	0	0.600	0.2857	0.4288	0.143mM
	E	1	0.278	1.000	0.1988	21.7nM
5	U/L	0	2.203	1.4286	1.5733	0.143mM
	E	1	0.601	2.1426	0.429	21.7nM

Table 6.2 C: Variation of [Ca²⁺] in assay buffer - Experiment 1

Homog. Buffer	Assay Buffer					
[EGTA] mM	Type	Volume 0.2mM Ca ²⁺ (μl)	Volume 0.34mM Ca ²⁺ (μl)	Volume 3.0mM Ca ²⁺ (μl)	Total Volume (μl)	Total [Ca ²⁺] mM
0	U/L	50	0	0	50	0.200
	E	50	0	0	50	0.200
0.1	U/L	49.28	0	0.717	50	0.240
	E	47.22	2.77	0	50	0.208
1	U/L	42.85	0	7.15	50	0.600
	E	21.52	28.47	0	50	0.278
5	U/L	14.28	0	35.72	50	2.203
	E	42.85	0	7.15	50	0.601

6.2.2.2 Ca²⁺-dependency of colonic mucosal NOS - Experiment 2

Colonic mucosa from rats pretreated with LPS was homogenised in buffer A used in 6.2.2.1 but with either 0.1mM CaCl₂ or 1mM EDTA added.

Basic assay buffer was then prepared as described in 2.2.2 but not including CaCl₂. 10mM CaCl₂ and 50mM EGTA prepared in basic assay buffer were added to basic assay buffer during preparation of final uninhibited, L-NMMA and EGTA assay buffers in such proportions that the final free Ca²⁺ concentrations after addition of samples were equal in assay tubes regardless of the homogenisation buffer in which the samples were prepared (116μM in uninhibited and L-NMMA assay tubes and 21.7nM in EGTA assay tubes, see Table 6.2 D). Calculations of Ca²⁺ and EGTA concentrations required in assay buffer were again carried out by Dr P.J. Hanson using Program Complex. $K_A \text{ EDTA.Mg}^{2+} = 3.9 \times 10^5 \text{ M}^{-1}$; $K_A \text{ Ca}^{2+}.\text{EDTA} = 3.9 \times 10^7 \text{ M}^{-1}$.

Table 6.2 D: [EGTA] and [Ca²⁺] values calculated to give an equal free [Ca²⁺] in assay mixtures for different Homogenates - Experiment 2

U/L = uninhibited or L-NMMA assay; E = EGTA assay.

Homog. Buffer	Assay Buffer			Assay Mixture (50μl Assay Buffer + 20μl Homogenate)		
	Type	[EGTA] mM	Total [Ca ²⁺] mM	Total [EGTA] mM	Total [Ca ²⁺] mM	Free [Ca ²⁺]
0.1mM CaCl ₂	U/L	0	0.1224	0	0.1159	0.116mM
	E	0.812	0.540	0.58	0.1159	21.7nM
1mM EDTA	U/L	0	0.1224	0	0.3857	0.116mM
	E	2.66	0.540	1.90	0.3857	21.7nM

The concentrations of the other constituents of the assay buffers were identical to the standard assay protocol described in 2.2 and volumes of sample added and the methods of stopping the assay and counting citrulline formation were as described for the standard assay protocol (2.2.2).

6.2.2.3 Assay of NOS activity in intestinal muscles

NOS activity in the muscle layers of colon, jejunum and ileum was measured using the standard assay protocol as described in 2.2.3. Ca^{2+} -independent activity was calculated by subtracting the activity inhibitable by EGTA from the total NOS activity. The Ca^{2+} -dependent activity was the activity inhibitable by EGTA.

6.2.3 Samples for SDS-PAGE

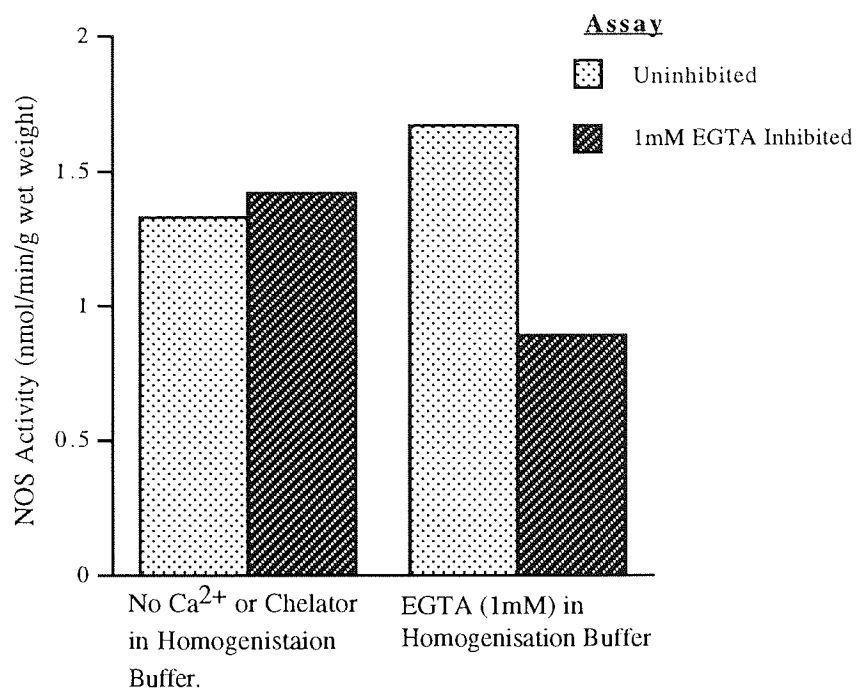
The basic protocol for preparation of samples is given in 2.3.1.1. Modifications are described as appropriate in the results section. The commercial monoclonal anti-iNOS antibody used was raised to a 21kDa fragment of mouse macrophage NOS corresponding to residues 961-1144 (see Appendix A4).

6.3 RESULTS

6.3.1 Ca^{2+} -dependency of colonic mucosal iNOS

Two pilot experiments carried out using version 1 of the NOS assay protocol (6.2.2.2) suggested the appearance of Ca^{2+} -dependency in colonic mucosa from induced animals homogenised in buffer containing EGTA. The first pilot experiment showed that a colonic mucosal sample prepared in the buffer containing 1mM EGTA exhibited Ca^{2+} dependency while a sample prepared in the buffer containing no Ca^{2+} or chelator did not (Figure 6.3.1.A).

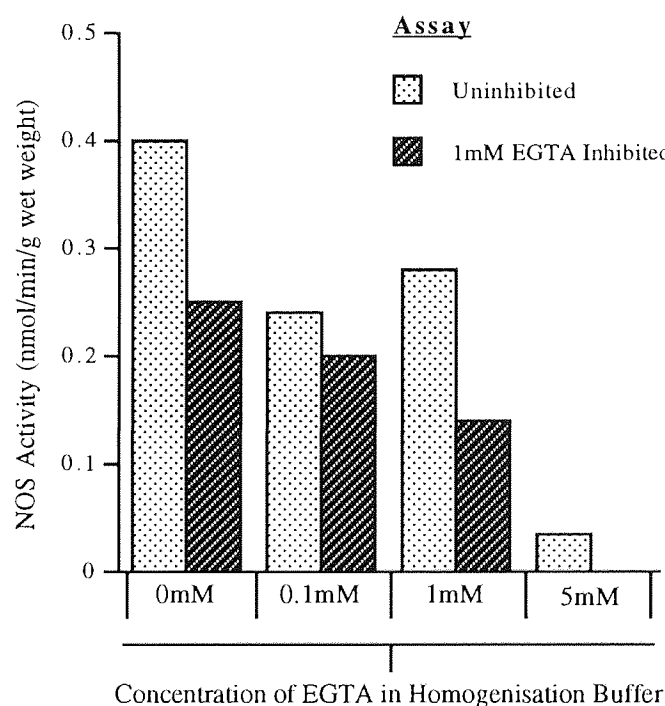
Figure 6.3.1 A : Effect of EGTA in homogenisation buffer on Ca^{2+} -dependency of NOS activity induced by LPS in colonic mucosa



Legend to Figure 6.3.1 A: Assay of NOS Activity in LPS-treated colonic mucosa homogenised in buffer containing either neither Ca^{2+} nor Ca^{2+} chelators or containing 1mM EGTA. Calculated free Ca^{2+} concentration was $143\mu\text{M}$ in uninhibited assay tubes and 21.7nM in EGTA inhibited assay tubes. Results are means of triplicate determinations from a single experiment.

The second pilot experiment showed that the higher the concentration of EGTA in the homogenisation buffer used to prepare a colonic mucosal sample, the lower was the resulting total NOS activity (Figure 6.3.1 B). NOS activity after inhibition by EGTA showed a similar trend.

Figure 6.3.1 B: Effect of EGTA at various concentrations in homogenisation buffer on NOS activity induced by LPS in colonic mucosa

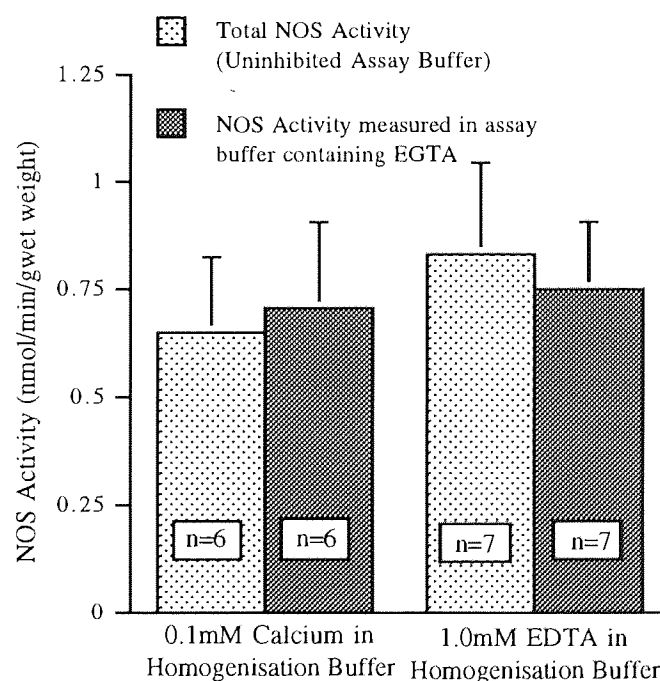


Legends to Figure 6.3.1 B

Assays of total NOS activity or NOS activity after inhibition by 1mM EGTA in colonic mucosa, from rats treated with LPS, homogenised in buffers containing EGTA at various concentrations. Calculated free Ca^{2+} concentration was $143\mu\text{M}$ in uninhibited assay buffer and 21.7nM in assay buffer containing EGTA. Results are from a single experiment involving triplicate determinations under each condition.

Since most authors had used EDTA in their homogenisation buffer (Table 6.1) several experiments were performed with homogenisation in the presence of 0.1mM Ca^{2+} or 1.0mM EDTA. Reduction of the calculated free Ca^{2+} concentration from 116 μM to 21.7nM in the assay produced no change in the NOS activity which was therefore Ca^{2+} -independent whether the homogenisation buffer contained either 0.1mM Ca^{2+} or 1.0mM EDTA (Figure 6.3.1 C; paired t-test between total NOS activity and activity in the presence of EGTA).

Figure 6.3.1 C : Investigation of the effect of the presence of EDTA, during homogenisation, on Ca^{2+} -dependence of NOS Activity in colonic mucosa from rats induced with LPS



Legend to Figure 6.3.1 C:

Results are given \pm S.E.M with n equal to the number of separate preparations. Calculated free Ca^{2+} concentration 116 μM in uninhibited assay buffer and 21.7nM in assay buffer containing EGTA.

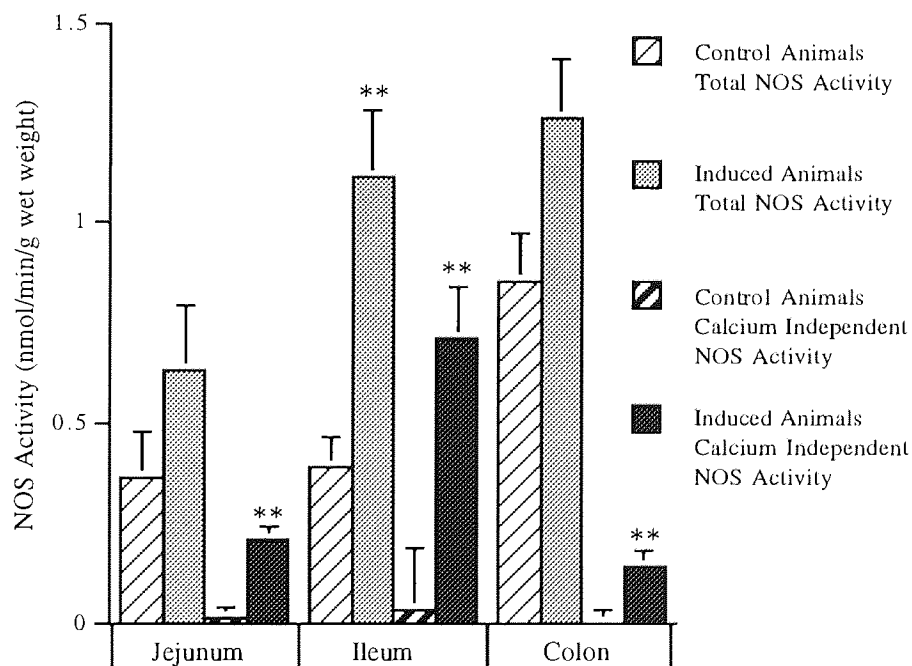
In conclusion the presence of EGTA at 1mM or above but not 1mM EDTA, in the homogenisation buffer appears to cause partial Ca^{2+} -dependency of NOS induced in rat colonic mucosa by LPS.

6.3.2 NOS protein and enzyme activity in muscles of the intestine

6.3.2.1 Presence of iNOS

Ca^{2+} -independent NOS activity was shown to be significantly higher in muscle from jejunum, ileum and colon from rats treated with LPS compared to tissues from

Figure 6.3.2 A: Total and Ca^{2+} -independent NOS activity in muscles of the intestinal tract:



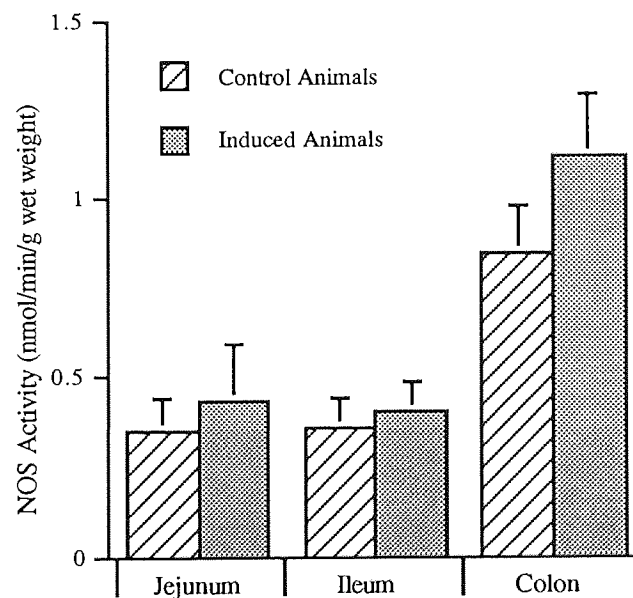
Legend to Figure 6.3.2 A

Results are given \pm S.E.M. n=4 in induced and control jejunum, n=6 in induced and control ileum, n=7 in induced colon and n=6 in control colon (where n=number of separate preparations). ** indicates a significant difference from control (p<0.01) measured by unpaired student's t-test.

control rats (Figure 6.3.2 A). Total NOS activity was found to be higher only in ileum from induced rats compared to tissue from control animals.

Ca²⁺-dependent NOS activity in muscles from the intestine of rats treated with LPS was not found to be significantly different (unpaired t-test) from activity in tissues from control rats (Figure 6.3.2 B).

Figure 6.3.2. B: Ca²⁺-dependent NOS activity in muscles of the intestinal tract

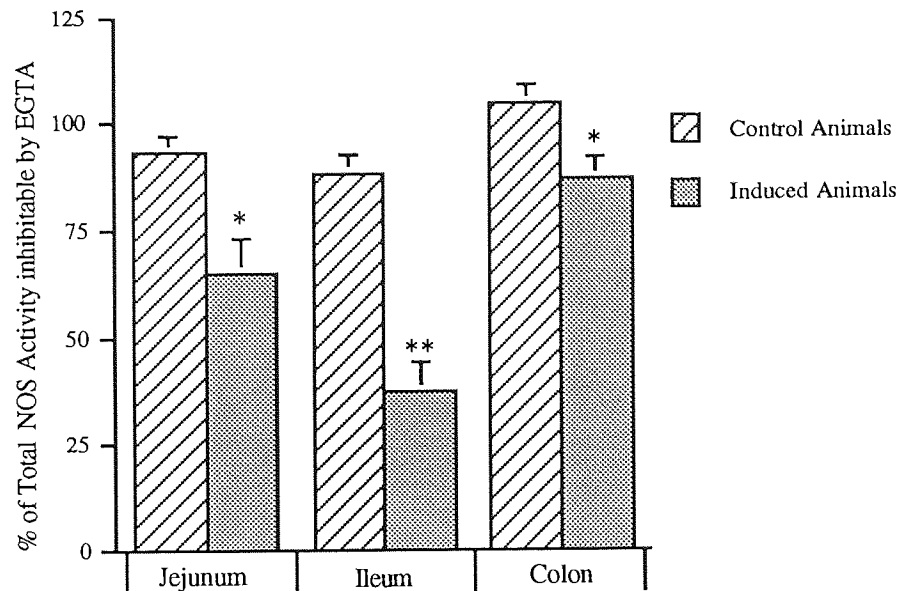


Legend to Figure 6.3.2 B

Results are given \pm S.E.M. n=4 in induced and control jejunum, n=6 in induced and control ileum, n=7 in induced colon and n=6 in control colon (where n=number of separate preparations).

Finally the proportion of total NOS activity found to be Ca²⁺-dependent in intestinal muscles from induced rats was substantially lower in comparison to muscles from control rats (Figure 6.3.2 C).

Figure 6.3.2 C: Proportion of Ca^{2+} -dependent NOS activity in muscles of the intestinal tract:

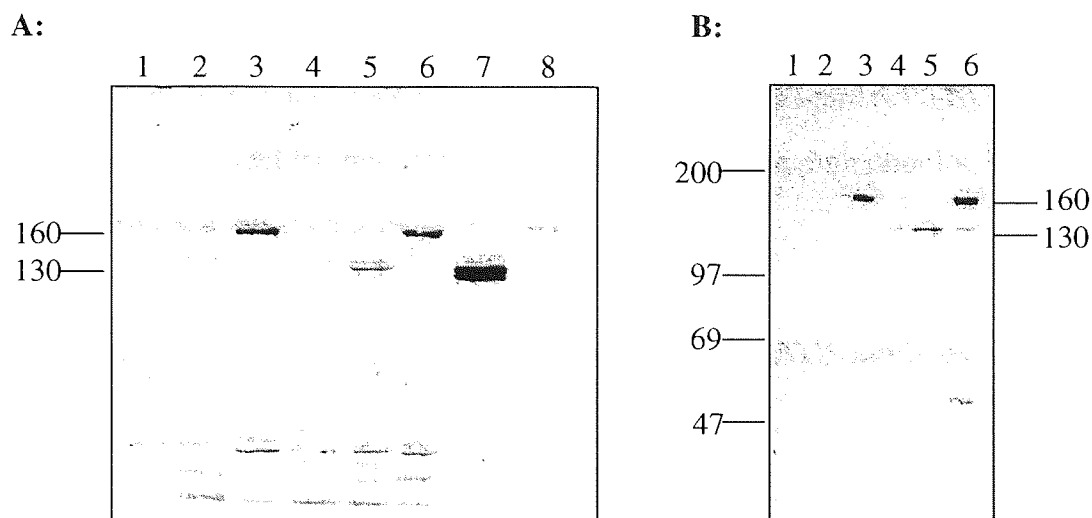


Legend to Figure 6.3.2 C

Results are given \pm S.E.M. $n=4$ in induced and control jejunum, $n=6$ in induced and control ileum, $n=7$ in induced colon and $n=6$ in control colon (where n =number of separate preparations). * and ** indicate a significant difference from control measured by unpaired student's t-test (*, $p<0.05$; **, $p<0.01$).

130kDa bands were detected in immunoblots of jejunal, ileal and colonic muscle extracts from LPS-treated rats with the ileal band being heavier than that from colon or jejunum (Figure 6.2.3 D). No such bands were detected in tissues from control animals. On the same immunoblots a 160kDa band was detected in colon from both induced and control animals, a very light band at 160kDa was detected in an extract of a rat pituitary cell line and a strong 130kDa band was detected in an extract of activated mouse macrophages.

Figure 6.3.2 D: Immunoblotting with monoclonal anti-iNOS antibody



Legend to Figures 6.3.2 D

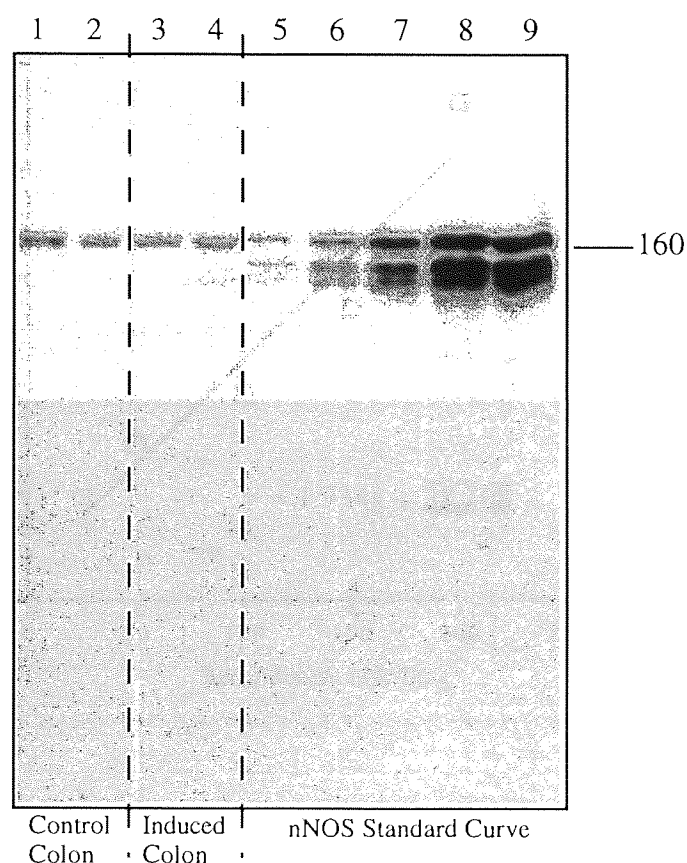
Immunoblotting with monoclonal anti-iNOS antibody (1µg/ml) . Blot A: Lanes 1 and 4, 75µg of protein from rat jejunal muscle; Lanes 2 and 5, 75µg of protein from rat ileal muscle; Lanes 3 and 6, 75µg of protein from rat colonic muscle; Lane 7, 5µg of protein from extracts of mouse macrophages; Lane 8, 5µg of protein from rat pituitary cells. Blot B: Lanes 1 and 4, 100µg of protein from rat jejunal muscle; Lanes 2 and 5, 100µg of protein from rat ileal muscle; Lanes 3 and 6, 100µg of protein from rat colonic muscle. In both blots, muscle protein samples in lanes 1-2 are from control animals and muscle protein samples in lanes 4-6 are from animals treated with LPS.

In conclusion iNOS was present, most prominently in the ileal muscle, but appeared to be Ca²⁺-independent. Thus there was no significant change in Ca²⁺-dependent NOS (Figure 6.3.2 B). Given the previous increase detected in colonic muscle by Boughton-Smith et al. (1994) in response to LPS some immunoblotting experiments were performed (below, 6.3.2 D) to investigate this further.

6.3.2.2 Investigation of possible changes in nNOS in colonic muscle induced by LPS

A 160kDa band was detected in immunoblots of rat colon from both induced and control animals with the monoclonal anti-nNOS antibody (Figure 6.3.2 E). A band of the same molecular mass was detected on the same immunoblot in lanes containing recombinant nNOS.

Figure 6.3.2 E: Immunoblotting with monoclonal anti-nNOS antibody

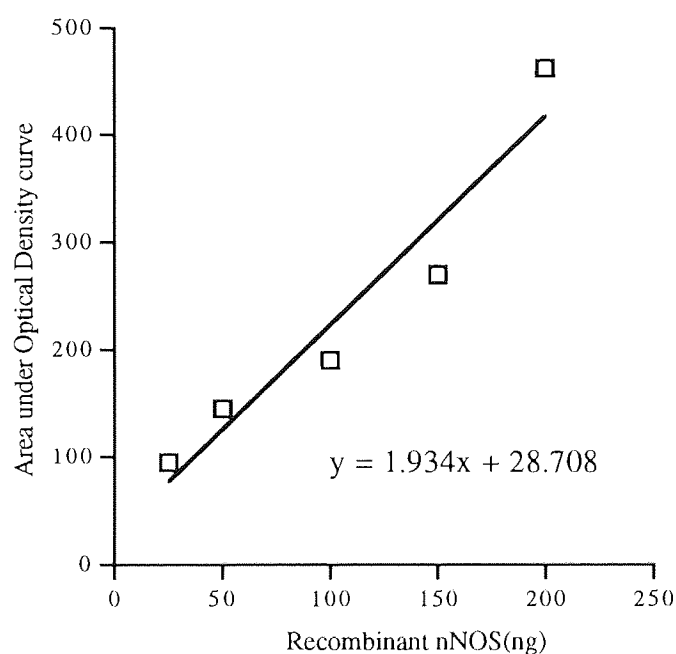


Legend to Figure 6.3.2 E

Immunoblotting with monoclonal anti-nNOS antibody (1 μ g/ml). Lanes 1 and 2, 75 μ g of rat colonic muscle protein from control animals. Lanes 3 and 4, 75 μ g of rat colonic muscle protein from LPS-induced animals. Lanes 5-9, 25, 50, 100, 150 and 200ng of recombinant rat nNOS respectively.

Densitometric analysis of an immunoblot of various loadings of recombinant rat brain NOS (Figure 6.3.2 E) allowed a standard curve of nNOS versus optical density to be constructed (Figure 6.3.2 F) and the content of nNOS in each colon sample on the same immunoblot to be calculated and expressed per mg tissue wet weight (Figure 6.3.2 G). The nNOS content in the colonic muscle was found to be unaffected by LPS treatment (Figure 6.3.2 G).

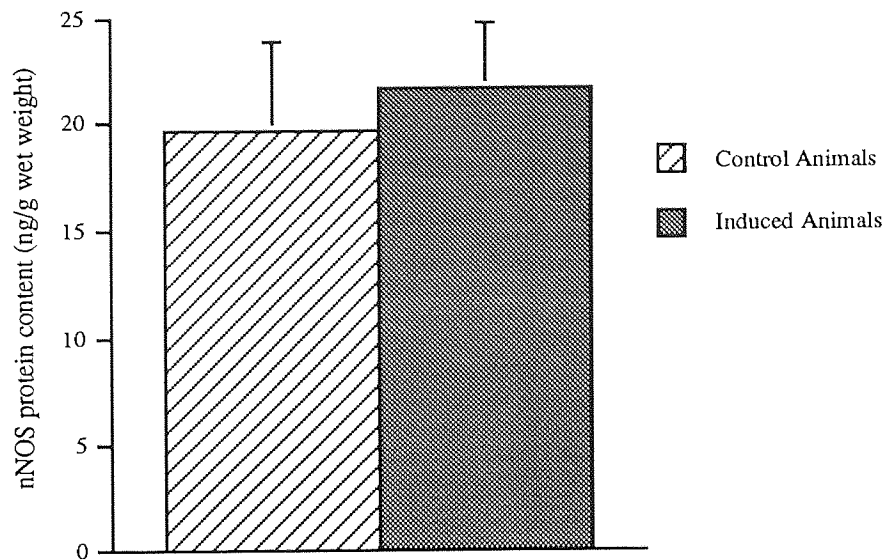
Figure 6.3.2.F: Standard curve for NOS content from immunoblotting



Legend to Figure 6.3.2 F:

Standard curve produced by measuring, by densitometric analysis, the optical density values from of an immunoblot of various loadings of recombinant nNOS probed with the monoclonal anti-nNOS antibody (5 μ g/ml). N.B: only the bands at 160kDa in the standard lane were scanned.

Figure 6.3.2 G: nNOS protein content in colonic mucosa

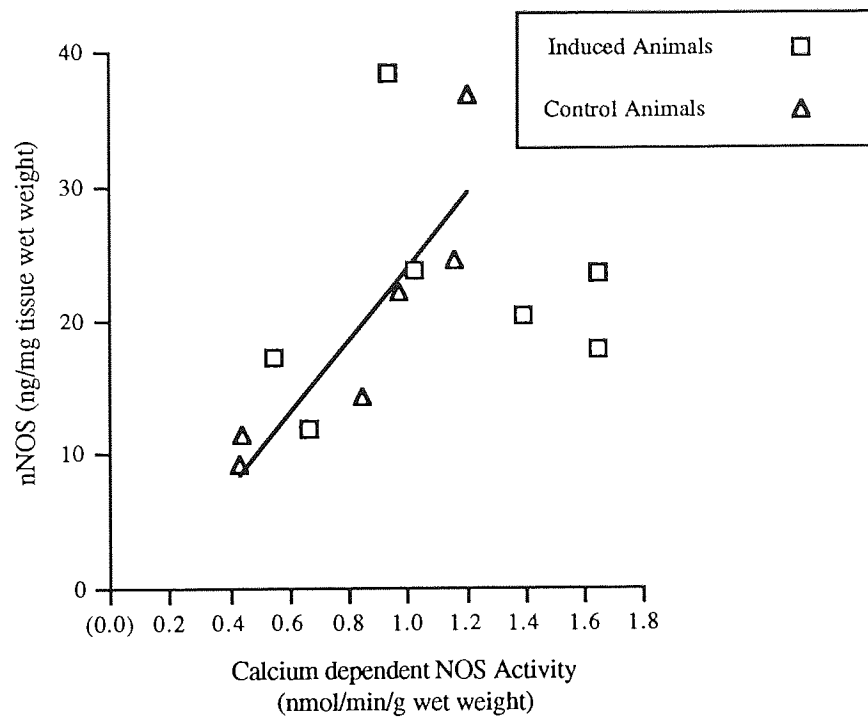


Legend to Figure 6.3.2 G

Results are given \pm S.E.M. $n=6$ in control colon and $n=7$ in induced colon (where n =number of separate preparations. Values for nNOS content were calculated by entering optical density values, from densitometric analysis of colonic muscle samples on an immunoblot probed with the monoclonal anti-nNOS antibody ($1\mu\text{g/ml}$), into the formula obtained for a standard curve of recombinant nNOS on the same immunoblot. nNOS content in each sample was then expressed per mg tissue wet weight as the amount of sample loaded in each well was known.

A plot of nNOS content versus corresponding results for NOS activity per g wet weight (Figure 6.3.2 H) showed that the amount of NOS in colon from control animals correlated with activity ($r=0.90$, p for significant linear correlation= 0.0148) while in colon from LPS treated rats this was not the case ($r=0.102$, $p=0.827$).

Figure 6.3.2 H Correlation of nNOS content with Ca^{2+} -dependent NOS activity in colon

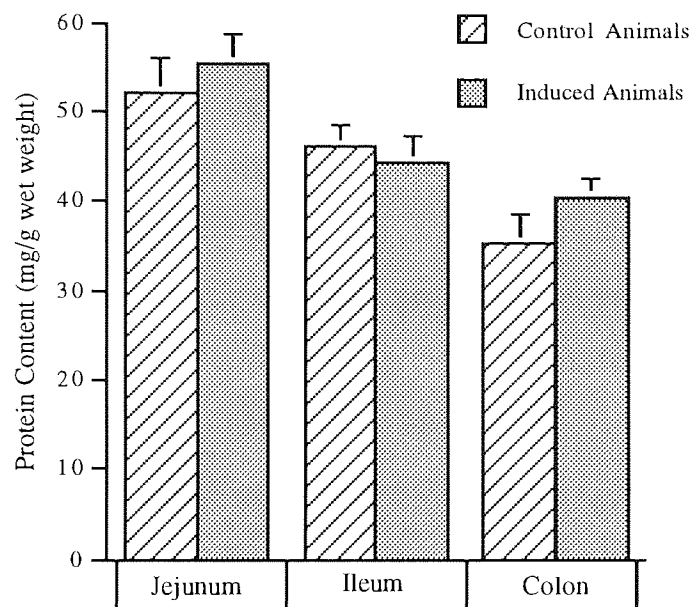


Legend to Figure 6.3.2 H:

Line shown is the line of best fit for values from control animals. Calculation of NOS content was as previously described. No line is drawn for the "induced" samples because there was no significant correlation.

The protein content per g wet weight of intestinal muscles, measured by the BCA assay, was found to be unaffected by LPS (Figure 6.3.2 I).

Figure 6.3.2 I: Protein content in samples of muscles from the intestinal tract



Legend to Figure 6.3.2 I:

Mean protein content values (measured by the BCA assay) with bovine serum albumin as standard and expressed \pm S.E.M. $n=4$ in induced and control jejunum, $n=6$ in induced and control ileum, $n=7$ in induced colon and $n=6$ in control colon (where n =number of separate preparations).

Immunoblots of intestinal muscle samples from either control or LPS induced animals showed no bands when probed with the monoclonal anti-eNOS antibody.

6.4 DISCUSSION

6.4.1 Induced NOS in the rat colonic mucosa

Reports of induction of Ca^{2+} -dependent NOS activity in the intestine are probably not due to the removal of tightly bound calmodulin by treatment with 1mM EDTA during homogenisation since subsequent addition of EGTA to the assay system such as to reduce the calculated free Ca^{2+} concentration from 116 μM to 22nM produced no change in the induced activities. These results are consistent with Boughton-Smith et al. (1994) who, after the above work was completed, detected only Ca^{2+} -independent activity in induced rat colonic mucosa homogenised in a buffer containing 1mM EDTA. The results are also consistent with Williams et al. (1995) who detected no Ca^{2+} -dependence in colon from induced rats even at Ca^{2+} concentrations below 1nM. 1mM EGTA however, may apparently induce partial Ca^{2+} -dependence in the colonic mucosa and was used by Oguchi et al. (1992). At pH 7.4 K_A for Ca.EGTA is $1.2 \times 10^7 \text{M}^{-1}$, and that for Ca.EDTA is $3.9 \times 10^7 \text{M}^{-1}$ added to which Mg^{2+} will reduce by competition Ca^{2+} -binding by EDTA. Free Ca^{2+} may therefore be lower in homogenates with 1mM EGTA and calmodulin dissociation promoted.

6.4.2 Induced NOS in rat intestinal muscle

The results obtained in this study showed that LPS increased Ca^{2+} -independent NOS in all areas of the intestinal muscle examined, ileum showing the greatest increase, while no increase was observed in Ca^{2+} -dependent NOS activity compared to Boughton-Smith et al. (1994) for colonic muscle. The results obtained by immunoblotting mirrored results obtained for Ca^{2+} -independent NOS activity in that a band of 130kDa was recognised in samples of intestine from LPS treated rats by the monoclonal anti-iNOS antibody, the strongest band being seen in the ileal sample. The 130kDa band was likely to be iNOS because a similar band was recognised in a sample from activated mouse macrophages but not in a sample of rat pituitary cells. The 160kDa band recognised in samples of colon and more

lightly in other intestinal samples and rat pituitary cells was likely to be due to cross reactivity of the anti-iNOS antibody with nNOS.

Quantification of nNOS content in colonic muscle samples was likely to be an overestimate of total nNOS content since degradation was evident in samples of recombinant rat brain NOS and only the protein recognised at 160kDa was used to construct the standard curve for NOS content. However, since nNOS content in both induced and control colonic samples on any one immunoblot were calculated from the same standard curve the level of overestimation was the same for both treatments. The amount of immunoreactive nNOS detected in colon after LPS treatment did not increase relative to controls. In LPS treated colonic muscle samples Ca^{2+} -dependent NOS activity was more variable than the amount of NOS and did not correlate with it. The results found by Boughton-Smith et al. (1994) which showed an increase in Ca^{2+} -dependent NOS activity may therefore represent a change in specific activity of nNOS in colonic muscle but not an increase in nNOS protein. It is somewhat unlikely that a change in activity of eNOS could explain the results since no eNOS was detectable by immunoblotting in muscle tissue from induced or control rats and assays of NOS activity were carried out on only the $10,000 \times g_{av}$ supernatant fraction of intestinal muscle samples while eNOS is predominantly particulate.

6.4.3 Summary

1: Ca^{2+} -chelation by 1mM EGTA, but not 1mM EDTA during homogenisation could induce Ca^{2+} -dependency in iNOS induced in the rat colonic mucosa by LPS. Since most workers use 1mM EDTA this finding can not explain previously determined increases in Ca^{2+} -dependent NOS activity induced by LPS in intestinal tissues.

2: Induction of Ca^{2+} -independent iNOS is responsible for the increase in NOS activity seen in rat ileal, jejunal and colonic muscle after LPS administration.

Muscle does not appear to be the site of the putative increased intestinal Ca^{2+} -dependent activity in rats treated with LPS.

3: The specific activity, rather than the amount, of nNOS in the rat colon may be altered by LPS administration.

CHAPTER 7

GENERAL CONCLUSIONS

This thesis has for the first time demonstrated the presence of both constitutive isoforms of NOS in the gastric glandular mucosa. Furthermore, the isoforms have been localised to specific cell types/regions of the gastric glandular mucosa, namely the surface mucosal epithelium (nNOS) and vascular endothelial cells in microvessels (eNOS). Another major finding of this study was that nNOS accounts for the vast majority of NOS activity in the gastric glandular mucosa with eNOS accounting for a minimal proportion. This finding suggests that the role of NO in the maintenance of gastric mucosal integrity could be wider than its effects on the microcirculation (Whittle 1994) and indeed, this thesis has also suggested that NO has a role in maintaining the protective surface mucus-bicarbonate barrier. One explanation for the large difference in the activities of the two constitutive isoforms is that the level of eNOS activity required to maintain the gastric microcirculation at an adequate level is far less than the nNOS activity required elsewhere in the stomach. Another possible explanation is that eNOS is up-regulated during periods of gastric injury when acid-back diffusion may be a problem but in the normal stomach activity is quite low. Measurement of particulate NOS activity and eNOS content by immunoblotting after exposure of the lumen to mild irritants would be one method to investigate this possibility.

The finding that the nNOS found in the gastric glandular mucosa appears to differ in the carboxyl-terminal region from the nNOS isoform in the rat brain is also novel. The modification at the carboxyl-terminus of gastric mucosal nNOS was unstable and since the carboxyl-terminal region involved is not part of the enzyme's active site it is difficult to suggest an obvious function, although either post-translational modification or alternative splicing may be explanations. A substantial amount of nNOS particulate activity was found in the brain but only a very small proportion of gastric mucosal nNOS was found in the pellet fraction. Particulate localisation of nNOS is thought to involve the PDZ domain at the amino terminus, so it is difficult to link the lack of particulate nNOS in the stomach with the difference from brain in the carboxyl-terminal antigenicity. It is possible that

binding proteins analogous to PSD 95 are not expressed in the stomach. While differences between the efficacy of various NOS inhibitors on different isoforms has been studied (Southan and Szabo, 1996), inter-tissue differences have not and a study looking at effectiveness of a range of NOS inhibitors on NOS in brain and gastric mucosal tissue would be useful in this respect. Clearly more work remains to be done on the nature of the differences between the brain and gastric isoforms of nNOS.

The effect of NO on increasing gastric mucus secretion is now clearly established and indeed reports have appeared suggesting that NO also promotes mucus release in lung and small intestine. However, the effect of NO on acid, bicarbonate and pepsin secretion is still not fully understood. In this study nNOS was only localised to the surface mucosal epithelium of the gastric glandular mucosa and not in chief cells, or parietal cells. However, calculations suggest that NO generated from a point source over a few seconds may be active over distances up to and beyond 200 μm (Wood and Garthwaite, 1994). NO released from surface cells could therefore potentially influence the functioning of gastric cells deeper in the mucosa.

The NOS activity induced in the rat intestine by LPS appeared to be due to a typical Ca^{2+} -independent iNOS. By contrast with suggestions in the literature, no evidence was found for a Ca^{2+} -dependent inducible enzyme in the colonic mucosa or an induction of nNOS protein in colonic muscle by LPS treatment although an alteration in Ca^{2+} -dependent nNOS specific activity was suggested in some rats. Whether NO produced by iNOS or some action of LPS can affect nNOS activity remains unclear.

In summary, although the role of NO in the stomach is still not completely understood, the characterisation and localisation of the various isoforms of NOS in the rat gastric glandular mucosa and identification of the role of NO in carbachol-stimulated mucus secretion have significantly advanced understanding of the contribution made by NO-dependent processes to protecting the mucosa of healthy rats. Some evidence of differences in nNOS between brain and gastric mucosa may

be related to tissue-specific functioning of nNOS and need to be further elucidated. In rats treated with lipopolysaccharide changes in intestinal NOS activity were largely or completely due to induction of iNOS. Future work might encompass the localisation of iNOS and the consequences of such induction for the presence and activity of other proteins in the small intestine.

REFERENCES

Allen, A., Flemstrom, G., Garner, A. and Kivlaakso, E (1993) Gastroduodenal mucosal protection. *Physiological Reviews*, 73, 4, 823-857.

Alican, I. and Kubes, P. (1996) A critical role for nitric oxide in intestinal barrier function and dysfunction, *American Journal Of Physiology*, 270, G225-G237.

Alm, P., Larsson, B., Ekbal, E., Sundler, F. and Andersson, K.-E. (1993) Immunohistochemical localisation of peripheral nitric oxide synthase-containing nerves using antibodies raised against synthesised C- and N-terminal fragments of a cloned enzyme from rat brain. *Acta Physiologica Scandinavica*, 148, 421-429.

Amin, A.R., Di Cesare, P.E., Vyas, P., Attur, M., Tzeng, E., Billiar, T.R., Stuchin, S.A. and Abramson, S.B. (1995) The expression and regulation of nitric oxide synthase in human osteoarthritis-affected chondrocytes: Evidence for up-regulated nitric oxide synthase. *Journal of Experimental Medicine*, 182, 2097-2102.

Aoki, E., Takeuchi, I.K. and Shoji, R. (1995) Nitric oxide: An attractive signalling molecule. *Acta Histochemica Cytochemica*, 28, 97-106.

Bandaletova, T., Brouet, I., Bartsch H., Sugimura, T., Esumi, H. and Ohshima, H. (1993) Immunohistochemical localisation of an inducible form of nitric oxide synthase in various organs of rats treated with *Propionibacterium acnes* and lipopolysaccharide. *APMIS*, 101, 330-336.

Barrachina, D., Calatayud, S., Esplugues, J., Whittle, B.J.R., Moncada, S. and Esplugues, J.V. (1994) Nitric oxide donors preferentially inhibit neuronally mediated rat gastric acid secretion. *European Journal of Pharmacology*, 262, 181-183.

Bickel, M. and Kauffman, G.L. (1981) Gastric gel thickness: Effect of distension, 16,16-dimethyl prostaglandin E₂ and carbenoxolone. *Gastroenterology*, 80, 770-775.

Beesley, J.E. (1995) Histochemical methods for detecting nitric oxide synthase. *Histochemical Journal*, 27, 757-769.

Boeckxstaens, G.E., De Man, J.G., Pelckmans, P.A., Cromheeke, K.M., Herman, A.G. and Van Maercke, Y.M. (1993) Ca^{2+} -dependency of the release of nitric oxide from non-adrenergic non-cholinergic nerves. *British Journal of Pharmacology*, 110, 1329-1334.

Bolton, J.P., Palmer, D. and Cohen, M.M. (1978) Stimulation of mucus and non parietal cell secretion by the E_2 prostaglandins. *Digestive Diseases*, 23, 4, 359-364.

Boughton-Smith, N.K., Evans, S.M., Whittle, B.J.R and Moncada, S. (1992) Induction of colonic nitric oxide synthase in a rat model of colitis. *Gastroenterology*, 102, 177-182.

Boughton-Smith, N.K., Evans, S.M., Whittle, B.J.R and Moncada, S. (1993) Induction of nitric oxide synthase in rat intestine and its association with tissue injury. *Agents Actions*, 38, C125-C126.

Boughton-Smith, N.K., Evans, S.M., Hawkey, C.J., Cole, A.T., Balsitis, M., Whittle, B.J.R. and Moncada, S. (1993) Differential changes in nitric oxide synthase activity in ulcerative colitis and Crohns disease. *Lancet*, 342, 338-340.

Boughton-Smith, N.K., Evans, S.M. and Whittle, B.J.R (1994) Characterisation of nitric oxide synthase activity in the rat colonic mucosa and muscle after endotoxin and in a model of colitis. *Agents Actions*, 41, C223-C225.

Bredt, D.S. and Snyder, S.H. (1990) Isolation of nitric oxide synthetase, a calmodulin-requiring enzyme. *Proceedings of the National Academy of Sciences USA*, 87, 682-685.

Bredt, D.S., Glatt, C.E., Hwang, P.M., Fotuhi, M., Dawson, T.M. and Snyder, S.H. (1991) Nitric oxide synthase protein and mRNA are discretely localised in neuronal populations of the mammalian CNS together with NADPH diaphorase. *Neuron*, 7, 615-624.

Bredt, D.S., Hwang, P.M., Glatt, C.E., Lowenstein, C., Reed, R.R. and Snyder, S.H. (1991) Cloned and expressed nitric oxide synthase structurally resembles cytochrome P-450 reductase. *Nature*, 351, 714-718.

Bredt, D.S., Ferris, C.O. and Snyder, S.H. (1992) Nitric oxide synthase regulatory sites-Phosphorylation by cyclic-AMP-dependent protein kinase-identification of flavin and calmodulin binding sites. *Journal of Biological Chemistry*, 267, 16, 10976-10981.

Bredt, D.S. and Snyder, S.H. (1994) Nitric oxide: A physiologic messenger molecule. *Annual Review of Biochemistry*, 63, 175-195.

Brenman, J.E., Chao, D.S., Xia, H., Aldape, K. and Bredt, D.S. (1995) Nitric oxide synthase complexed with dystrophin and absent from skeletal muscle sarcolemma in Duchenne muscular dystrophy. *Cell*, 82, 743-752.

Brenman, J.E., Chao, D.S., Gee, S.H., McGee, A.W., Craven, S.E., Santillano, D.R., Wu, Z., Huang, F., Xia, H., Peters, M.F., Froehner, S.C and Bredt, D.S. (1996) Interaction of nitric oxide synthase with the postsynaptic density protein PSD-95 and α 1-syntrophin mediated by PDZ domains. *Cell*, 84, 757-767.

Brown, J.F., Hanson, P.J. and Whittle, B.J.R. (1992) Nitric oxide donors increase mucus gel thickness in rat stomach. *European Journal of Pharmacology*, 223, 103-104.

Brown, J.F., Hanson, P.J., Whittle, B.J.R. and Moncada, S. (1992) Differential distribution of nitric oxide synthase between cell fractions isolated from the rat gastric mucosa. *Biochemical and Biophysical Research Communications*, 184, 2, 680-685.

Brown, J.F., Keates, A.C., Hanson, P.J. and Whittle, B.J.R. (1993) Nitric oxide generators and cGMP stimulate mucus secretion by rat gastric mucosal cells. *American Journal of Physiology*, 265, G418-G422.

Brown, J.F., Keates, A.C., Hanson, P.J. and Whittle, B.J.R. (1993) The nitric oxide donor S-nitroso-N-acetyl-penicillamine inhibits secretory activity in rat isolated parietal cells. *Biochemical and Biophysical Research Communications*, 195, 1354.

Brown, J.F., Tepperman, B.L., Hanson, P.J. and Whittle, B.J.R. (1994) Lipopolysaccharide induces Ca^{2+} -independent nitric oxide synthase activity in rat gastric mucosal cells. *European Journal Of Pharmacology*, 292, 111-114.

Brune, B. and Lapetina, E.G. (1991) Phosphorylation of nitric oxide synthase by protein kinase-A. *Biochemical and Biophysical Research Communications*, 181, 2, 921-926.

Burrell, M.A., Montuenga, L.M., Garcia, M. and Villaro, A.C. (1996) Detection of nitric oxide synthase (NOS) in somatostatin-producing cells of human and murine stomach and pancreas. *The Journal of Histochemistry and Cytochemistry*, 44, 4, 339-346.

Buxton, I.L.O., Cheek, D., Eckman, D., Westfall, D.P., Sanders, K.M. and Keef, K.D. (1993) N^{G} -nitro L-arginine methyl ester and other alkyl esters of arginine are muscarinic receptor antagonists. *Circulation Research*, 72, 387-395.

Cho, H.J., Xie, Q., Calaycay, J., Mumford, R.A., Swiderek, K.M., Lee, T.D. and Nathan, C. (1992) Calmodulin is a subunit of nitric oxide synthase from macrophages. *Journal of Experimental Medicine*, 176, 599-604.

Dinerman, J.L., Steiner, J.P., Dawson, T.M., Dawson, V. and Snyder, S.H. (1994) Cyclic nucleotide dependent phosphorylation of neuronal nitric oxide synthase inhibits catalytic activity.

Ekblad, E., Mulder, H., Uddman, R. and Sundler, F. (1994) NOS-containing neurons in the rat gut and coeliac ganglia. *Neuropharmacology*, 33, 1323-1331.

Espluques, J.V., Barrachina, M.D., Catalayud, S., Pique, J.M. and Whittle B.J.R. (1993) Nitric oxide mediates the inhibition by interleukin 1- β of pentagastrin-stimulated rat gastric acid secretion. *British Journal of Pharmacology*, 108, 9-10.

Feldman, P.L., Griffith, O.W. and Stuehr, D.J. (1993) The surprising life of nitric oxide. *Chemical and Engineering News*, 71, 51, 26-38.

Fiorucci, S., Distrutti, E., Santucci, L. and Morelli A. (1995) Leukotrienes stimulate pepsinogen secretion from guinea pig gastric chief cells by a nitric oxide-dependent pathway. *Gastroenterology*, 108, 1709-1719.

Fiorucci, S., Distrutti, E., Chiorean, M., Santucci, L., Belia, S., Fano, G., De Giorgio, R., Stanghellini, V., Corinaldesi, R. and Morelli A. (1995) Nitric oxide modulates pepsinogen secretion induced by calcium mediated agonist in guinea pig gastric chief cells. *Gastroenterology*, 109, 1214-1223.

Fiorucci, S., Lanfranccone, L., Santucci, L., Calabro, A., Orsini, B., Federici, B. and Morelli A. (1996) Epidermal growth factor modulates pepsinogen secretion in guinea pig gastric chief cells. *Gastroenterology*, 111, 945-958.

Flemstrom, G.(1994) Gastric and duodenal mucosal secretion of bicarbonate. In: Johnson L.R. (ed), *The Physiology of the gastrointestinal tract*. Raven, New York, 267-294.

Forstermann, U., Schmidt, H.W.W., Pollock, J.S., Heller, M. and Murad, F. (1991) Calmodulin-dependent endothelium derived relaxing factor/nitric oxide synthase activity is present in the particulate and cytosolic fractions of bovine aortic endothelial cells. *Proceedings of the National Academy of Sciences USA*, 78, 1788-1792.

Forstermann, U., Schmidt, H.W.W., Pollock, J.S., Heller, M. and Murad, F. (1991) Enzymes synthesising guanylate cyclase-activating factors in endothelial cells, neuroblastoma cells, and rat brain. *Journal of Cardiovascular Pharmacology*, 17, 30, S57-S64.

Forstermann, U., Gath., I., Schwarz, P., Closs, E.I. and Kleinert, H. (1995) Isoforms of nitric oxide synthase. Properties, cellular distribution and expressional control. *Biochemical Pharmacology*, 50, 9, 1321-1332.

Forstner, J.F. and Forstner, G.G. (1994) Gastrointestinal mucus. In: Johnson L.R. (ed), *The Physiology of the gastrointestinal tract*, Raven, New York, 267-294.

Furness, J.B., Li, Z.S., Young, H.M. and Forstermann (1994) Nitric oxide synthase in the enteric nervous system of the guinea pig: a quantitative description. *Cell and Tissue Research*, 277, 139-149.

Gislason, H., Varhaug, P., Sorbye, H., Waldum, H.L. and Svanes, K. (1996) Role of adenosine and nitric oxide in the hyperemic response to superficial and deep gastric mucosal injury and H⁺ back-diffusion in cats. *Scandinavian Journal of Gastroenterology*, 31, 14-23

Hall, A.V., Antoniou, H., Wang, Y., Cheung, A.H., Arbus, A.M., Olson, S.L, Lu, W.C, Kau, C.-L. and Marsden, P.A. (1994) Structural organisation of the human neuronal nitric oxide synthase gene (NOS1). *The Journal of Biological Chemistry*, 269, 52, 33082-33090.

Hanson, P.J. and Hatt, J.F. (1989) Intracellular signalling and regulation of gastric acid secretion. *Quarterly Journal of Experimental Physiology*, 74, 607-634.

Hecker, M., Walsh, D.T. and Vane, J.R. (1991) on the substrate specificity of nitric oxide synthase. *FEBS Letters*, 294, 221-224.

Hecker, M., Mulsch, A. and Busse, R. (1994) Subcellular localisation and characterisation of neuronal nitric oxide synthase. *Journal of Neurochemistry*, 62, 1524-1529.

Heinemann, A., Jocic, M., Peskar, B.M. and Holzer, P. (1995) Neural mechanism and nitric oxide involved in the cholecystokinin-evoked hyperemia of the rat gastric mucosa. *Gastroenterology*, 108, 4, SS A289.

Heinemann, A., Jocic, M., Peskar, B.M. and Holzer, P. (1996) CCK-evoked hyperemia in rat gastric mucosa involves neural mechanisms and nitric oxide. *American Journal of Physiology*, 270, G253-G258.

Hevel, J.M., White, K.A. and Marletta, M.A. (1991) Purification of the inducible murine macrophage nitric-oxide synthase-Identification as a flavoprotein. *Journal of Biological Chemistry*, 266, 34, 227789-22791.

Hiki, K., Hattori, R., Kawai, C. and Yui, Y. (1992) Purification of insoluble nitric oxide synthase from the rat cerebellum. *Journal of Biochemistry*, 111, 556-558.

Holzer, P., Wachter, Ch., Heinemann, A., Jocic, M., Lippe, I.Th. and Herbert, M.K. (1995) Diverse interactions of calcitonin gene related peptide and nitric oxide in the gastric and cutaneous microcirculation. *Canadian Journal of Physiology and Pharmacology*, 73, 991-994.

Hope, B.T., Michael, G.J., Knigge, K.M. and Vincent, S.R. (1991) Neuronal NADPH diaphorase is a nitric oxide synthase. *Proceedings of the National Academy of Science USA*, 88, 2811-2814.

Huang, P.L., Dawson, T.M., Bredt, D.S., Snyder, S.H. and Fishman, M.C. (1993) Targeted disruption of the nitric oxide synthase gene. *Cell*, 75, 1273-1286.

Ito, S. (1987) Functional Gastric Morphology. In: Johnson L.R. (ed), *The Physiology of the gastrointestinal tract*, Raven, New York, 817-849.

Kerss, S., Allen, A. and Garner, A. (1982) A simple method for measuring thickness of the mucus gel layer adherent to rat, frog and human gastric mucosa: influence of feeding, prostaglandin, N-acetylcysteine and other agents. *Clinical Science*, 63, 187-195.

Kiraly, A., Suto, G. and Tache, Y. (1993) Role of nitric oxide in the gastric cytoprotection induced by central vagal stimulation. *European Journal of Pharmacology*, 240, 299-301.

Kitagawa, H., Takeda, F. and Kohei, H. (1990) Effect of endothelium-derived relaxing factor on the gastric lesion induced by HCl in rats. *Journal of Pharmacology and Experimental Therapeutics*, 253, 3, 1133-1137.

Kobzik, L., Reid, M.B., Bredt, D.S. and Stamler, J.S. (1994) Nitric oxide in skeletal muscle. *Nature*, 372, 546-548.

Konturek, S.J., Brzozowski, T., Majka, J. and Szlachic, A. (1992) Nitric oxide in protection by aluminium-containing antacids. *European Journal of Pharmacology*, 229, 155-162.

Konturek, S.J., Brzozowski, T., Majka, J., Szlachic, A. and Pytko-Polonczyk, J. (1993) Implications of nitric oxide in the action of cytoprotective drugs in the action of the gastric mucosa. *Journal of Clinical Gastroenterology*, 17, S140-S145.

Konturek, S.J., Brzozowski, T., Majka, J., Szlachic, A. and Czarnobilski, K. (1994) Nitric oxide in gastroprotection by sucralfate, mild irritant, and nocloprost. Role of Mucosal blood flow. *Digestive Diseases and Sciences*, 39, 3, 593-600.

Konturek, S.J., Brzozowski, T., Bielanski, W. and Schally, A.V. (1995) Role of endogenous gastrin in gastroprotection. *European Journal of Pharmacology*, 278, 203-212.

Konturek, S.J., Brzozowski, T., Pytko-Polonczyk, J. and Drozdowicz (1995) Comparison of cholecystokinin, pentagastrin, and duodenal oleate in gastroprotection in rats. *Scandinavian Journal of Gastroenterology*, 30, 620-630.

Kubes, P. and Wallace, J.L. (1995) Nitric oxide as a mediator of gastrointestinal injury?- Say it ain't so. *Mediators of inflammation*, 4, 397-405.

Kugler, P., Hofer, D., Mayer, B. and Drenkhahn, D. (1994) Nitric oxide synthase and NADP-linked glucose-6-phosphate dehydrogenase are colocalised in brush cells of rat stomach and pancreas. *The Journal of Histochemistry and Cytochemistry*, 42, 10, 1317-1321.

Hevel, J.M., White, K.A. and Marletta, M.A. (1991) Purification of the inducible murine macrophage nitric-oxide synthase-Identification as a flavoprotein. *Journal of Biological Chemistry*, 266, 34, 227789-22791.

Lamas, S., Marsden, P.A., Li, G.K., Tempst, P. and Michel, T. (1992) Endothelial nitric oxide synthase: Molecular cloning and characterisation of a distinct constitutive enzyme isoform. *Proceedings of the National Academy of Sciences USA*, 89, 6348-6352.

Lazaratos, S., Kashimura, H., Nakahara, A., Fukutomi, H., Osuga, T. and Goto, K. (1995) L-arginine and endogenous nitric oxide protect the gastric mucosa from endothelin-1-induced gastric ulcers in rats. *Journal of Gastroenterology*, 30, 578-584.

Lippe, I.Th. and Holzer, P. (1992) Participation of endothelium-derived nitric oxide but not prostacyclin in the gastric mucosal hyperaemia due to acid back-diffusion. *British Journal of Pharmacology*, 105, 708-714.

Llewellyn-Smith, I.J., Song, Z.-M., Costa, M., Bredt, D.S. and Snyder, S. (1992) Ultrastructural localisation of nitric oxide synthase in guinea-pig enteric neurons. *Brain Research*, 577, 377-342.

Lopez-Belmonte, J., Whittle, B.J.R. and Moncada, S. (1993) The actions of nitric oxide donors in the prevention or induction of injury to the rat gastric mucosa. *British Journal of Pharmacology*, 108, 73-78.

MacNaughton, W.K., Cirino, G. and Wallace, J.L. (1989) Endothelium-derived relaxing factor (nitric oxide) has protective actions in the stomach. *Life Sciences*, 45, 1869-1876.

Magee, T., Fuentes, A.M., Garban., Rajavashisth, T., Marquez, D., Rodriguez, J.A., Rajfer, J. and Gonzalez-Cadavid (1996) Cloning of a neuronal nitric oxide synthase expressed in penis an lower urinary tract. *Biochemical and Biophysical Research communications*, 226, 145-151.

Marletta, M.A. (1993) Nitric oxide synthase structure and mechanism. *The Journal of Biological Chemistry*, 268, 12231-12234.

Marletta, M.A (1994) Nitric oxide synthase: Aspects concerning structure and catalysis. *Cell*, 78, 927-930.

Marsden, P.A., Scappert, K.T., Chen, H.S., Flowers, M., Sundell, C.L., Wilcox, J.N, Lamas, S. and Michel, T. (1992) Molecular cloning and characterisation of human endothelial nitric oxide synthase. *FEBS Letters*, 307, 3, 287-293.

Martinez-Cuesta, M.A., Barrachina, M.D., Pique, J.M., Whittle, B.J.R. and Esplugues, J.V. (1992) The role of nitric oxide and platelet-activating factor in the inhibition by endotoxin of pentagastrin stimulated gastric acid secretion. *European Journal of Pharmacology*, 218, 351-354.

Matini, P., Ibba Manneschi, L., Mayer, B. and Faussone-Pellegrini, M.S. (1995) Nitric oxide producing neurons in the human colon: an immunohistochemical and histoenzymatical study. *Neuroscience Letters*, 193, 17-20.

Matsumoto, T., Nakane, M., Pollock, J.S., Kuk, J.E. and Forstermann, U. (1993) A correlation between soluble brain nitric oxide synthase and NADPH-diaphorase activity is only seen after exposure of the tissue to fixative. *Neuroscience Letters*, 155, 61-64.

McKee, M., Scavone, C. and Nathanson, J.A. (1994) Nitric oxide, cGMP and hormone regulation of active sodium transport. *Proceedings of the National Academy of Science USA*, 91, 12056-12060.

McQueen, S., Hutton, D., Allen, A. and Garner. A. (1983) Gastric and duodenal surface mucus gel thickness: effects of prostaglandins and damaging agents. *American Journal of Physiology*, 245, G388-G393.

McQueen, S., Allen, A. and Garner. A. (1984) Measurement of gastric and duodenal mucus gel thickness. *Mechanisms of Mucosal Protection in the Upper Gastrointestinal Tract* (Raven Press, New York), 215-221.

Merchant, N.B., Dempsey, D.T., Grabowski, M., Rizzo, M. and Ritchie, W.P. (1994) Capsaicin induced gastric mucosal hyperemia: The role of calcitonin gene-related peptide. *Surgery*, 116, 2, 419-425.

Merchant, N.B., Goodman, J., Dempsey, D.T., Milner, R.E. and Ritchie, W.P. (1995) The role of calcitonin gene-related peptide and nitric oxide in gastric mucosal hyperemia and protection. *Journal of Surgical Research*, 58, 344-350.

Michel, T., Li, G.K and Busconi, L. (1993) Phosphorylation and subcellular translocation of endothelial nitric oxide synthase. *Proceedings of the National Academy of Sciences USA*, 90, 13, 6252-6256.

Miller, M.J.S., Zhang, X.-J., Sadowska-Krowicka, H., Chotinaruemol, S., McIntyre, J.A., Clark, D.A. and Bustamante, S.A. (1993) Nitric oxide release in response to gut injury. *Scandinavian Journal of Gastroenterology*, 28, 149-154.

Mobarok Ali, A.T.M (1995) The role of nitric oxide and sulphydryls in gastric mucosal protection induced by sodium chromoglycates in rats. *Journal of Pharmacy and Pharmacology*, 47, 739-743.

Moncada, S., and Higgs, E.A. (1993) Molecular mechanisms and therapeutic strategies related to nitric oxide. *The FASEB Journal*, 9, 1319-1330.

Murad, F., Ishii, K., Forstermann, U., Gorsky, L., Kerwin Jr, J.F., Pollock, J.S. and Heller, M. (1990) EDRF is an intracellular second messenger and autacoid to regulate cyclic GMP synthesis in many cells. In: Nishizuka, Y. (ed) *The Biology and Medicine of Signal Transduction*, Raven, New York, 441-448.

Myatt, L., Brockman, D.E., Eis, A.L.W. and Pollock, J.S. (1993) Immunohistochemical localisation of nitric oxide synthase in the human placenta. *Placenta*, 14, 437-495.

Nakane, M., Mitchell, J., Forstermann, U. and Murad, F. (1991) Phosphorylation by calcium calmodulin-dependent protein kinase-II and protein-kinase-C modulates the activity of nitric oxide synthase. *Biochemical and Biophysical Research Communications*, 180, 3, 1396-1402.

Nathan, C. and Xie, Q.-W. (1994) Regulation of biosynthesis of nitric oxide. *The Journal of Biological Chemistry*, 269, 13725-13728.

Nathan, C. and Xie, Q.-W. (1994) Nitric oxide synthases, rolls, tolls and controls. *Cell*, 78, 915-918.

Nichols, K., Krantis, A. and Staines, W. (1992) Histochemical localisation of nitric oxide-synthesising neurons in the guinea pig intestine. *Neuroscience*, 51, 4, 791-799.

Nichols, K., Staines, W. and Krantis, A. (1993) Nitric oxide synthase distribution in the rat intestine: A histochemical analysis. *Gastroenterology*, 105, 1651-1661.

Nichols, K., Staines, W., Rubin, S. and Krantis, A. (1994) Distribution of nitric oxide synthase activity in arterioles and venules of rat and human intestine. *American Journal of Physiology*, 267, G270-G275.

Nishizaki, Y., Guth, P.H. and Kaunitz, J.D. (1993) Isoprotenerol enhances rat gastric mucosal barrier function in vivo. *Gastroenterology*, 105, 340-346.

Nishizaki, Y., Guth, P.H. and Kaunitz, J.D. (1994) Histamine mediates pentagastrin enhancement of gastric defences. *Gastroenterology*, 106, A149.

Norris, P.J., Charles, I.G., Scorer, C.A. and Emson, P.C. (1995) Studies on the localisation and expression of nitric oxide synthase using histochemical techniques. *Histochemical Journal*, 27, 745-756.

Oguchi, S., Iida, S., Adachi, H., Ohshima, H. and Esumi, H. (1992) Induction of Ca^{2+} /calmodulin-dependent NO synthase in various organs of rats by *Propionobacterium acnes* and lipopolysaccharide treatment. *FEBS*, 308, 1, 22-25.

Ohshima, H., Brouet, I.M., Bandaletova, T., Adachi, H., Oguchi, S., Iida, S., Kurashima, Y., Morishita, Y. and Esumi, H. (1992) Polyclonal antibody against an inducible form of nitric oxide synthase purified from the liver of rats treated with *Propionibacterium acnes* and lipopolysaccharide. *Biochemical and Biophysical Research Communications*, 187, 3, 1291-1297.

Okayama, N., Itoh, M., Joh, T., Miyamoto, T., Takeuchi, T., Moriyama, A. and Kato, T. (1995) Effects of dibutyl guanosine 3', 5'-cyclic monophosphate and sodium nitroprusside in pepsinogen secretion from guinea pig chief cells with respect to intracellular Ca^{2+} . *Biochimica et Biophysica Acta*, 1268, 185-190.

Peskar, B.M., Lambrecht, N., Stroff, T., Respondek, M. and Muller, K-M. (1995) Functional ablation of sensory neurons impairs healing of acute gastric mucosal damage in rats. *Digestive Diseases and Sciences*, 40, 11, 2460-2464.

Pique, J.M, Eplugues, J.V. and Whittle, B.J.R. (1992) Endogenous nitric oxide as a mediator of gastric mucosal vasodilatation during acid secretion. *Gastroenterology*, 102, 168-174.

Podolsky, R.S., Grabowski, M., Milner, R., Ritchie, W.P. and Dempsey, D.T. (1994) Capsaicin-induced gastric hyperemia and protection are NO dependent. *Journal of Surgical Research*, 57, 4, 438-442.

Pollock J.S., Klinghofer, U., Forstermann, U. and Murad, F. (1992) Endothelial nitric oxide is myristylated. *FEBS Letters*, 309, 402-404.

Pollock, J.S., Nakane, M., Buttery, L.D.K., Martinez, A., Springall, D., Polak, J.M., Forstermann, U. and Murad, F. (1993) Characterization and localization of endothelial nitric oxide synthase using specific monoclonal antibodies. *American Journal of Physiology*, 265, C1379-C1387.

Pollock, J.S., Forstermann, U., Tracey, W.R. and Nakane, M.(1995) Nitric oxide synthase isozymes antibodies. *Histochemical journal*, 27, 738-744.

Racmilewitz, Karmeli, K., Eliakim, R., Stalnikowicz, R., Ackerman, Z., Amir, G. and Stamler, J.S. (1994) Enhanced gastric nitric oxide activity in duodenal ulcer patients. *Gut*, 35, 1394-1397.

Ribiere, C., Jaubert, A.M., Gaudiot, N., Sabourault, D., Marcus, M.L., Boucher, J.L., Denis-Henriot, D. and Giudicelli, Y. (1996) White adipose tissue nitric oxide synthase: A potential source for NO production. *Biochemical and Biophysical Research Communications*, 222, 706-712.

Ringheim, G.E. and Pan, J. (1995) Particulate and soluble forms of the inducible nitric oxide synthase are distinguishable at the amino terminus in RAW 264.7 macrophage cells.

Riveros-Moreno, V., Beddell, C. and Moncada, S. (1993) Nitric oxide synthase. Structural studies using antipeptide antibodies. *European Journal of Biochemistry*, 215, 801-808.

Robinson, L.J. and Michel.T. (1995) Mutagenesis of palmitoylation sites in endothelial nitric oxide synthase identifies a novel motif for dual acylation and

subcellular targeting. Proceedings of the National Academy of Sciences USA, 92, 25, 11776-11780.

Ross, M.H. and Romrell (1990), Histology, a text and atlas, 2nd edition, William and Wilkins Baltimore.

Salter, M., Knowles, R.G. and Moncada, S. (1991) Widespread tissue distribution, species distribution and changes in activity of Ca^{2+} -dependent and Ca^{2+} -independent nitric oxide synthases. FEBS, 291, 145-149.

Salzman, A.L., Denenberg, A.G., Ueta, I., O'Connor, M., Linn, S.C. and Szabo, C. (1996) Induction and activity of nitric oxide synthase in cultured human intestinal epithelial monolayers. American Journal of Physiology, 270, G565-G573.

Sanders, K.M., and Ward, S.M. (1992) Nitric oxide as a mediator of nonadrenergic noncholinergic neurotransmission. American Journal of Physiology, 262, G379-G392.

Scherer-Singler, Vincent, S.R., Kimura, H. and McGeer, E.G. (1983) Demonstration of a unique population of neurons with NADPH-diaphorase histochemistry. Journal of Neuroscience Methods, 9, 229-234.

Schmidt, H.H.H.W., Pollock, J.S., Nakane, N., Gordsky, L.D. (1991) Purification of a soluble isoform of guanylyl cyclase-activating factor synthase. Proceedings of the National Academy of Sciences USA, 88, 365-369.

Schmidt, H.H.H.W., Gagne, G.D., Nakane, N., Pollock, J.S., Miller, M.F. and Murad, F. (1992) Mapping of neural nitric oxide synthase suggests frequent co-localisation with NADPH but not with soluble guanylyl cyclase, and novel paraneural functions for nitrinergic signal transduction. The Journal of Histochemistry and Cytochemistry, 40, 10, 1439-1456.

Schmidt, H.H.H.W., Warner, T.D., Ishii, K., Sheng, H. and Murad, F. (1992) Insulin secretion from pancreatic B cells caused buy L-arginine -derived nitrogen oxides. Science, 255, 721.

Schmidt, H.H.H.W., Lohmann, S.M. and Walter, U. (1993) The nitric oxide and cGMP signal transduction system: regulation and mechanism of action. Biophysica Acta, 1178, 153-175.

- Schmidt, H.W.W. and Walter, U. (1994) NO at work. *Cell*, 78, 919-925.
- Seidler, U. and Sewing, K.-Fr. (1989) Ca^{2+} -dependent and -independent secretagogue action on gastric mucus secretion in rabbit mucosal explants. *American Journal of Physiology*, 256, G739-G746.
- Seidler, U. and Pfeiffer, A. (1992) Inositol phosphate formation and $[\text{Ca}^{2+}]_i$ in secretagogue-stimulated rabbit gastric mucous cells. *American Journal of Physiology*, 260, G133-G141.
- Sellers, L.A., Carroll, N.J.H. and Allen, A. (1986) Misoprostol-induced increases in adherent gastric mucus thickness and luminal mucus output. *Digestive Diseases and Sciences*, 31, 2, 91S-95S.
- Sheng, H., Shah, P.K. and Audus, K.L (1996) Sucralfate effects on mucus synthesis and secretion by human gastric epithelium in vitro. *International Journal of Pharmaceutics*, 131, 159-169.
- Silvagno, F., Xia, H. and Bredt, D.S (1996) Neuronal nitric-oxide synthase- μ , an alternative spliced isoform expressed in differentiated skeletal muscle. *The Journal of Biological Chemistry*, 271, 19, 11204-11208.
- Southan, G.J. and Szabo, C. (1996) Selective pharmacological inhibition of distinct nitric oxide synthase isoforms, *Biochemical Pharmacology*, 51, 383-394.
- Spessert, R. and Layes, E. (1994) Fixation conditions affect the intensity but not the pattern of NADPH-diaphorase staining as a marker for neuronal nitric oxide synthase in the rat olfactory bulb. *The Journal of Histochemistry and Cytochemistry*, 42, 10, 1309-1315.
- Springall, D.R., Riveros-Moreno, V., Buttery, L., Merrett, M., Moncada, S. and Polak, J.M. (1992) Immunological detection of nitric oxide synthase(s) in human tissues suggesting different isoforms. *Histochemistry*, 98, 259-266.
- Stainikowicz, R., Karmeli, F. and Rachmilewitz, D. (1995) Morphine protection against ethanol-induced gastric damage-role of nitric oxide and neuropeptides. *Gastroenterology*, 108, 4, SS A225.

- Stamler, J.S. (1994) Redox Signaling: Nitrosylation and related target interactions of nitric oxide. *Cell*, 78, 931-936.
- Stark, M.E. and Szurszewski, J.H. (1992) Role of Nitric oxide in gastrointestinal and hepatic function and disease. *Gastroenterology*, 103, 1928-1949.
- Stuehr, D.J., Cho, H.J., Kwon, N.S., Weise, M.F. and Nathan, C.F. (1991) Purification and characterisation of the cytokine-induced macrophage nitric-oxide synthase-An FAD-containing and FMN-containing flavoprotein. *Proceedings of the National Academy of Sciences of the USA*, 88, 17, 7773-7777.
- Su, Z., Blazing, M.A., Fan, D. and George, S.E. (1995) The calmodulin-nitric oxide synthase interaction. Critical role of the calmodulin latch domain in enzyme activation. *The Journal of Biological Chemistry*, 270, 49, 29117-29122.
- Takahashi, T., and Owyang, C. (1995) Vagal control of nitric oxide and vasoactive intestinal polypeptide release in the regulation of gastric relaxation in the rat. *Journal of Physiology*, 484, 2, 481-492.
- Takeuchi, K., Ohuchi, T., Miyake, H. Sugawara, H. and Okabe, S. (1992) Effects of nitric oxide synthase inhibitors on gastric alkaline secretion in rats. *Japanese Journal of Pharmacology*, 60, 303-305.
- Takeuchi, K., Ohuchi, T., Kato, S. and Okabe, S. (1993) Cytoprotective action of L-arginine against HCl-induced injury in rats: Involvement of nitric oxide? *Japanese Journal of Pharmacology*, 61, 13-21.
- Takeuchi, K., Ohuchi, T., Miyake, H. and Okabe, S. (1993) Stimulation by nitric oxide synthase inhibitors of gastric and duodenal HCO_3^- secretion in rats. *The Journal of Pharmacology and Experimental Therapeutics*, 263, 3, 1512-1519.
- Takeuchi, K., Ohuchi, T. and Okabe, S. (1994) Endogenous nitric oxide in gastric alkaline response in the rat stomach after damage. *Gastroenterology*, 106, 367-374.
- Takeuchi, K., Takehara K., Kaneko, T. and Okabe, S. (1994) Nitric oxide and prostaglandins in regulation of acid secretory response in rat stomach after injury. *The Journal of Pharmacology and Experimental Therapeutics*, 272, 1, 357-363.

Takeuchi, K. and Okabe, S. (1995) Mechanism of gastric alkaline response in stomach after damage. *Digestive Diseases and Sciences*, 40, 865-871.

Tepperman B.L. and Whittle, B.J.R. (1992) Endogenous nitric oxide and sensory neuropeptides interact in the modulation of the rat gastric microcirculation. *British Journal of Pharmacology*, 105, 171-175.

Tepperman B.L., Brown, J.B. and Whittle, B.J.R. (1993) Nitric oxide synthase induction and intestinal epithelial viability in rats. *American Journal of Physiology*, 265, G214-G218.

Tepperman B.L. and Soper B.D. (1993) Effect of neutropenia on gastric mucosal integrity and mucosal nitric oxide synthesis in the rat. *Digestive Diseases and Sciences*, 38, 2056-2061.

Tepperman B.L. and Soper B.D. (1993) Interaction of nitric oxide and salivary gland epidermal growth factor in the modulation of rat gastric mucosal integrity. *British Journal of Pharmacology*, 110, 229-234.

Tepperman B.L. and Soper B.D. (1994). Nitric oxide synthase induction and cytoprotection of rat gastric mucosa from injury by ethanol. *Canadian Journal of Physiology and Pharmacology*, 72, 1308-1312.

Tepperman B.L. and Soper B.D. (1995) Ca^{2+} -mediated damage to rabbit gastric mucosal cells: modulation by nitric oxide. *European Journal of Pharmacology*, 293, 259-266.

Terenghi, G., Riveros-Moreno, V., Hudson, L.D., Ibrahim, N.B.N. and Polak, J.M. (1993) Immunohistochemistry of nitric oxide synthase demonstrates immunoreactive neurons in spinal cord and dorsal root ganglia of man and rat. *Journal of Neurological Sciences*, 118, 34-37.

Tijssen, P. (1987) In: Burdo, R.H. and van Knippenberg, P.H. (eds) *Practice and theory of enzyme immunoassays*, Elsevier, New York.

Timmermans, J.-P., Barbiers, M., Scheuermann, D.W., Bogers, J.J., Adriaensen, D., Fekete, E., Mayer, B., Van Marck, E.A. and Groodt-Lasseel, M.H.A. (1994) Nitric oxide synthase immunoreactivity in the enteric nervous system of the developing human digestive tract. *Cell and Tissue Research*, 275, 235-245.

- Tojo, A., Gross, S.S., Zhang, L., Tisher, C.C., Schmidt, H.H.H.W., Wilcox, C.S. and Madsen, K.M. (1994) Immunocytochemical localisation of distinct isoforms of nitric oxide synthase in the juxtaglomerular apparatus of normal rat kidney. *Journal of the American Society of Nephrology*, 4, 1438-1447.
- Tomimoto, H., Akiguchi, I., Wakita, H., Nakamura, S. and Kimura, J. (1994) Histochemical demonstration of membranous localisation of endothelial nitric oxide synthase in endothelial-cells of the rat-brain. *Brain Research*, 667, 107-110.
- Torihashi, S., Horowitz, B., Pollock, J.S., Ward, S.M., Xue, C., Kobayashi, S. and Sanders, K.M. (1996) Expression of nitric oxide synthase in mucosal cells of the canine colon. *Histochemistry and Cell Biology*, 105, 33-41.
- Tracey, W.R., Pollock, J.S., Murad, F., Nakane, M. and Förstermann, U. Identification of an endothelial-like type III NO synthase in LLC-PK1 kidney epithelial cells.
- Tripp, M.A. and Tepperman, B.L. (1995) Effect of nitric oxide on integrity, blood flow and cyclic GMP levels in the rat gastric mucosa: modulation by sialoadenectomy. *British Journal of Pharmacology*, 115, 344-348.
- Vander, A.J. and Sherman, J.H. and Luciano, D.S. (1990) *Human Physiology: The mechanisms of body function*, 5th edition, McGraw Hill, New York.
- Wallace, J.L., and Bell, C.J. (1995) Gastroduodenal mucosal defense. *Current Opinion in Gastroenterology*, 11, 479-485.
- Ward, S.M., Xue, C., Shuttleworth, C.W., Bredt, D.S., Snyder, S.H. and Sanders, K.M. (1992) NADPH diaphorase and nitric oxide synthase colocalisation in enteric neurons of canine proximal colon. *American Journal of Physiology*, 263, G277-G284.
- Whittle, B.J.R. and Steel, G. (1985) Evaluation of the protection of rat gastric mucosa by a prostaglandin analogue using cellular enzyme marker and histologic techniques. *Gastroenterology*, 88, 315-327.

Whittle, B.J.R. (1990) Role of endogenous nitric oxide in the mechanisms underlying gastric mucosal integrity. In: Moncada, S. and Higgs, E.A. (eds) Nitric oxide from L-arginine: a bioregulatory system, Elsevier Science Publishers, 365-370.

Whittle, B.J.R., Lopez-Belmonte, J. and Moncada, S. (1990) Regulation of gastric mucosal integrity by endogenous nitric oxide: interactions with prostanoids and sensory neuropeptides in the rat. *British Journal of Pharmacology*, 99, 607-611.

Whittle, B.J.R., Lopez-Belmonte, J. and Moncada, S. (1992) Nitric oxide mediates rat mucosal vasodilation induced by intragastric capsaicin. *European Journal of Pharmacology*, 218, 339-341.

Whittle, B.J.R. (1993) Neuronal and endothelium-derived mediators in the modulation of the gastric microcirculation: integrity in the balance. *British Journal of Pharmacology*, 110, 3-17.

Whittle, B.J.R. (1994) Nitric oxide in gastrointestinal physiology and pathology. In: Johnson L.R. (ed), *The Physiology of the gastrointestinal tract*, Raven, New York, 267-294.

Wilcox, C.S., Welch, W.J., Murad, F., Gross, S.S., Taylor, G., Levi, R. and Schmidt, H.H.W. (1992) Nitric oxide synthase regulates glomerular capillary pressure. *Proceedings of the National Academy of Sciences USA*, 89, 11993-11997.

Wood, J. and Garthwaite J. (1994) Models for diffusional spread of nitric oxide: implications for neural nitric oxide signalling and its pharmacological properties. *Neuropharmacology*, 33, 1235-1244.

Worl, J., Wiesand, M., Mayer, B., Greskötter, K.-R. and Neuhuber, W.L. (1994) Neuronal and endothelial nitric oxide synthase immunoreactivity and NADPH-diaphorase staining in rat and human pancreas: influence of fixation. *Histochemistry*, 102, 353-364.

Xie, J., Roddy, P., Rife, T.K., Murad, F. and Young, A.P. (1995) Two closely linked but seperable promoters for human neuronal nitric oxide synthase gene transcription. *Proceedings of the National Academy of Science USA*, 92, 1242-1246.

Yanaka, A., Muto, H., Fukotomi, H., Ito, S. and Silen, W. (1995) Role of nitric oxide in restitution of injured guinea pig gastric mucosa in vitro. *American Journal of Physiology*, 268, G933-G942.

APPENDICES

A1: ABBREVIATIONS

Abbreviation

Meaning

ABC	avidin-biotinylated-horse radish peroxidase complex
BCA	bicinchoninic acid
DAB	3, 3' - diaminobenzidine
dpm	disintegrations per minute
DTT	dithiothreitol
ECL	enhanced chemiluminescence
ELISA	enzyme linked immunosorbant assay
FAD	flavin adenine dinucleotide
FMN	flavin mononucleotide
cGMP	cyclic guanosine monophosphate
GM	gastric mucosa(l)
HRP	horse radish peroxidase
h	hour(s)
KLH	keyhole-limpet haemocyanin
L-NAME	N ^G -nitro-L-arginine methyl ester
L-NMMA	N ^G -monomethyl-L- arginine
L-NNA	N ^G -nitro-L-arginine
LPS	lipopolysacharride
min	minute(s)
NA	not applicable
b-NADPH	b-nicotinamide adenine dinucleotide
NO	nitric oxide
NOS	nitric oxide synthase
PBS	phosphate buffered saline
PMSF	phenylmethyl sulphonyl fluoride
s	second(s)

<u>Abbreviation</u>	<u>Meaning</u>
SDS	sodium dodecyl sulphate
TBS	tris buffered saline
TEMED	N, N, N', N' - tetramethylenediamine
Tris	tris(hydroxymethyl)methylamine
PAGE	polyacrylamide gel electrophoresis

A2: SOURCE OF REAGENTS

<u>Reagent</u>	<u>Supplier</u>
Acrylamide	BDH
D-Arginine	Sigma
L-Arginine	Sigma
2', 5' ADP-Agarose	Sigma
Ammonium persulphate	BDH
Aprotonin	Sigma
Bis-acrylamide	BDH
BCA protein assay reagent kit	Pierce
Bromophenol Blue	Biorad
BSA-fraction V	BDH
CaCl ₂	Sigma
Calmodulin	Sigma
Carbachol	Sigma
Coomassie Blue assay kit	Sigma
L- Cysteine	Sigma
DAB tablets (fast DAB)	Sigma
Dektol Developer (Kodak)	Sigma
Developer (Kodak)	Sigma
16-16 Dimethylprostaglandin E ₂	Sigma

<u>Reagent</u>	<u>Supplier</u>
DOWEX AG W-8	Sigma
DTT	Sigma
ECL Western Blotting Detection Reagents	Amersham
EDTA	Sigma
EGTA	Sigma
FAD	Sigma
Fixer (Kodak)	Sigma
Freunds Adjuvant (complete and incomplete)	Sigma
Glycerol	Sigma
Glycine	BDH
HEPES	BDH
Hisafe II scintillation fluid	Wallac
Leupeptin	Sigma
2-Mercaptoethanol	Sigma
MgCl ₂	Sigma
NaCl	BDH
hNADPH	Sigma
L-NAME	Sigma
L-NMMA	Wellcome
OCT embedding compound	BDH
Pepstatin	Sigma
Percoll	Sigma
PMSF	Sigma
Protein A -alkaline phosphatase	Sigma
Rainbow Markers	Amersham
SDS	BDH
Sodium pentobarbitone	May and Baker
Soybean trypsin inhibitor	Sigma

<u>Reagent</u>	<u>Supplier</u>
Sucrose	BDH
TEMED	BDH
Tetrahydrobiopterin	Sigma
TRIS	BDH
L-Valine	Sigma
Vectastain Elite Rabbit IgG ABC kit	Vector Laboratories
Vectabond	Vector Laboratories

A3: EQUIPMENT

<u>Item</u>	<u>Make and Model</u>
Bench Centrifuge	MSE, Mistral 3000i
Cryostat	Bright, OTF
Electrophoretic Transfer Unit	LKB, 2117 Multiphor II
Freeze Dryer	Modulyo/Edwards
Gel apparatus	Hoefer, SE 600
Homogeniser	Janke and Kunkel, Ultraturrax
Microcentrifuge	Eppendorf, 5414
Microhomogeniser	Janke and Kunkel, Ultraturrax T8
Powerpack	LKB, 2301 Macrodrive 1
Roller	Luckham Multimix MM1
Scintillation Counter	Packard, Tri-Carb 1900TR
Spectrophotometer	Pye Unicam, SP30
Ultracentrifuge	MSE, Superspeed 50
Water Bath	Gallenkamp
Scanner	Agfa, Focus Color

A4: ANIMALS

Male Wistar rats (200-300g body weight) were obtained from Bantin and Kingman (Hull, U.K.) and male rabbits were obtained from Hylyne Rabbits (Statham, U.K.) Animals were fed with a rodent breeder economy diet (Special Diet Services, Witham, UK) and were kept at 20-21°C on a 0800-2000hrs light and 2000-0800hrs dark schedule.

A5: ALIGNED AMINO ACID SEQUENCES IN NOS ISOFORMS

Shown below is an amino acid sequence alignment of nNOS, iNOS and eNOS isoforms. Dots indicate gaps introduced to maintain sequence alignment. Sequences highlighted in bold and underlined are those used to raise either the commercial antibodies used in this thesis or the polyclonal antisera raised in rabbit as described in chapter 2 and 3.

	1					50
iNOS_MOUSE					
iNOS_RAT					
iNOS_HUMAN					
eNOS_BOVIN					
eNOS_HUMAN					
nNOS_HUMAN	MEDHMF GVQQ	IQPNVIS RL	FKRKVG GLGF	LVKERV SKPP	VIISDL IRGG	
nNOS_RAT	MEENTF GVQQ	IQPNVIS RL	FKRKVG GLGF	LVKERV SKPP	VIISDL IRGG	
	51					100
iNOS_MOUSE					
iNOS_RAT					
iNOS_HUMAN					
eNOS_BOVIN					
eNOS_HUMAN					
nNOS_HUMAN	AAEQSGL IQA	GDIILAV NGR	PLVDLSY DSA	LEVLRGI ASE	THVVLIL RGP	
nNOS_RAT	AAEQSGL IQA	GDIILAV NDR	PLVDLSY DSA	LEVLRGI ASE	THVVLIL RGP	
	101					150
iNOS_MOUSE					
iNOS_RAT					
iNOS_HUMAN					
eNOS_BOVIN					
eNOS_HUMAN					
nNOS_HUMAN	EGFTT HLETT	FTGDG TPKTI	RVTQPL GPPT	KAVDLS HQPP	AGKEQ PLAVD	
nNOS_RAT	EGFTT HLETT	FTGDG TPKTI	RVTQPL GPPT	KAVDLS HQPS	ASKDQ SLAVD	


```

151
iNOS_MOUSE.....
iNOS_RAT.....
iNOS_HUMAN.....
eNOS_BOVIN.....
eNOS_HUMAN.....
nNOS_HUMAN GASGPGNGPQ HAYDDGQEAG SLPHANGWPQ APRQDPAKKA TRVSLQGRGE
nNOS_RAT RVTGLGNGPQ HAQGHGQGAG SVSQANG... .VAIDPTMKS TKANLQDIGE

201
iNOS_MOUSE..... .MACPWKFLF KVKSYQSDLK EEKDINNNVK KTPCAVLSPT
iNOS_RAT..... .MACPWKFLF RVKSYQGDLEK EEKDINNNVE KTPGAIPSP
iNOS_HUMAN..... .MACPWKFLF KTKFHQYAMN GEKDINNNVE KAPCATSSPV
eNOS_BOVIN..... .G NLKSVGQEPG PPCGLGLGLG LGLCGKQGPA
eNOS_HUMAN..... .G NLKSVAQEPG PPCGLGLGLG LGLCGKQGPA
nNOS_HUMAN NNELLKEIEP VLSLLTSGSR GVKGGAPAKA EMKDMGIQVD RDLGKSHKP
nNOS_RAT HDELLKEIEP VLSILNSGSK ATNRGGPAKA EMKDTGIQVD RDLGKSHKA

251
iNOS_MOUSEIQDDPKS... ..HQNGSPQL LTGTAQNVPE SLDKLHVT.S TR.....
iNOS_RAT TQDDPKSH.. .KHQNGFPQF LTGTAQNVPE SLDKLYVTPS TR.....
iNOS_HUMAN TQDDLQYHNL SKQQNESQPQ LVETGKKSPE SLVKLDATPL SS.....
eNOS_BOVIN SPAP..... .EPSRA PAPATPHAPD HSPAPNSPTL TRPPEG....
eNOS_HUMAN TPAP..... .EPSRA PASLLPPAPE HSPP..SSPL TQPPEG....
nNOS_HUMAN LPLGVENDRV FNDLWGKGNV PVVLNNPYSE KEQPPTSQKQ SPTKNGSPSK
nNOS_RAT PPLGGDNDRV FNDLWGKDNV PVILNNPYSE KEQSPTSQKQ SPTKNGSPSR

301
iNOS_MOUSE.PQYVRIKNW GSGEILHDTL HHKATSDFTC KSKSCLGSIM NPKSLTRGPR
iNOS_RAT .PQHVRICKNW GNGEIFHDTL HHKATSDISC KSKLCMGSIM NSKSLTRGPR
iNOS_HUMAN .PRHVRIKNW GSGMTFQDTL HHKAKGILTC RSKSCLGSIM TPKSLTRGPR
eNOS_BOVIN .PKFPRVKNW ELGSITYDTL CAQSQQDGPC TPRCCLGSLV LPRKLQTRPS
eNOS_HUMAN .PKFPRVKNW EVGSITYDTL SAQAQQDGPC TPRRCLGSLV FPRKLQGRPS
nNOS_HUMAN CPRFLKVKNW ETEVVLTDTL HLKSTLETGC TEYICMGSIM HPSQ.HARRP
nNOS_RAT CPRFLKVKNW ETDVLTDTL HLKSTLETGC TEHICMGSIM LPSQ.HTRKP

351
iNOS_MOUSEDKPTPLEELL PHAIEFINQY YGSFKEAKIE EHLARLEAVT KEIETTGTQY
iNOS_RAT DKPTPVEELL PQAIEFINQY YGSFKEAKIE EHLARLEAVT KEIETTGTQY
iNOS_HUMAN DKPTPPDELL PQAIEFVNQY YGSFKEAKIE EHLARVEAVT KEIETTGTQY
eNOS_BOVIN PGPPPAEQLL SQARDFINQY YSSIKRSGSQ AHEERLQVEVE AEVASTGTQY
eNOS_HUMAN PGPPPAEQLL SQARDFINQY YSSIKRSGSQ AHEQRLQVEVE AEVAATGTQY
nNOS_HUMAN EDVRTKGQLF PLAKEFIDQY YSSIKRFGSK AHMERLEEVE KEIDTTSTQY
nNOS_RAT EDVRTKDQLF PLAKEFLDQY YSSIKRFGSK AHMDRLEEVE KEIESTSTQY

401
iNOS_MOUSELTDELIFAT KMAWRNAPRC IGRIQWSNLQ VFDARNCSA QEMFQHICRH
iNOS_RAT LTLDELIFAT KMAWRNAPRC IGRIQWSNLQ VFDARSCSA SEMFQHICRH
iNOS_HUMAN LTGDELIFAT KQAWRNAPRC IGRIQWSNLQ VFDARSCSA SEMFEHICRH
eNOS_BOVIN LRESELVFGA KQAWRNAPRC VGRIQWGLQ VFDARDCSSA QEMFTYICNH
eNOS_HUMAN LRESELVFGA KQAWRNAPRC VGRIQWGLQ VFDARDCRS A QEMFTYICNH
nNOS_HUMAN LKDTELIYGA KHAWRNASRC VGRIQWSKLQ VFDARDCTTA HGMFNYICNH
nNOS_RAT LKDTELIYGA KHAWRNASRC VGRIQWSKLQ VFDARDCTTA HGMFNYICNH

451
iNOS_MOUSEILYATNNGNI RSAITVFPQR SDGKHDFRLW NSQLIRYAGY QMPDGTIRGD
iNOS_RAT ILYATNNGNI RSAITVFPQR SDGKHDFRIW NSQLIRYAGY QMPDGTIRGD
iNOS_HUMAN VRYSTNNGNI RSAITVFPQR SDGKHDFRVW NAQLIRYAGY QMPDGSIRGD
eNOS_BOVIN IKYATNRGNL RSAITVFPQR APGRGDFRIW NSQLVRYAGY RQDQGSVRGD
eNOS_HUMAN IKYATNRGNL RSAITVFPQR CPGRGDFRIW NSQLVRYAGY RQDQGSVRGD
nNOS_HUMAN VKYATNKGNI RSAITVFPQR TDGKHDFRVW NSQLIRYAGY KHRDGSSTLGD
nNOS_RAT VKYATNKGNI RSAITVFPQR TDGKHDFRVW NSQLIRYAGY KQPDGSSTLGD

```

501 550
iNOS_MOUSEAATLEFTQLC IDLGWKPRYG RFDVLPPLVLQ ADGQDPEVFE IPPDLVLEVT
iNOS_RAT PATLEFTQLC IDLGWKPRYG RFDVLPPLVLQ AHGQDPEVFE IPPDLVLEVT
iNOS_HUMAN PANVEFTQLC IDLGWKPKYG RFDVVPPLVLQ ANGRDPELFE IPPDLVLEVA
eNOS_BOVIN PANVEITELC IQHGWTPGNG RFDVLPPLLLQ APDEAPELFEV LPPELVLEVP
eNOS_HUMAN PANVEITELC IQHGWTPGNG RFDVLPPLLLQ APDEPELFL LPPELVLEVP
nNOS_HUMAN PANVQFTEIC IQQGWKPPRG RFDVLPPLLLQ ANGNDPELFQ IPPELVLELP
nNOS_RAT PANVQFTEIC IQQGWKAPRG RFDVLPPLLLQ ANGNDPELFQ IPPELVLEVP

551 600
iNOS_MOUSEMEHPKYEFQ ELGLKWYALP AVANMLLEVQ GLEFPACPFN GWYMGTEIGV
iNOS_RAT MEHPKYEFQ ELGLKWYALP PVANMLLEVQ GLEFPACPFN GWYMGTEIGV
iNOS_HUMAN MEHPKYEFR ELELKWYALP AVANMLLEVQ GLEFGPCPFN GWYMGTEIGV
eNOS_BOVIN LEHPTLEWFA ALGLRWYALP AVSNMLLEIG GLEFSAAPFS GWYMSTEIGT
eNOS_HUMAN LEHPTLEWFA ALGLRWYALP AVSNMLLEIG GLEFPAAPFS GWYMSTEIGT
nNOS_HUMAN IRHPKFEWFK DLALKWYGLP AVSNMLLEIG GLEFSACPFS GWYMGTEIGV
nNOS_RAT IRHPKFDWFK DLGLKWYGLP AVSNMLLEIG GLEFSACPFS GWYMGTEIGV

601 650
iNOS_MOUSERDFCDTQRYN ILEEVGRRMG LETHTLASLW KDRVTEINV AVLHSFQKQN
iNOS_RAT RDFCDTQRYN ILEEVGRRMG LETHTLASLW KDRVTEINA AVLHSFQKQN
iNOS_HUMAN RDFCDVQRYN ILEEVGRRMG LETHKLASLW KDQAVVEINI AVIHSFQKQN
eNOS_BOVIN RNLCDPHRYN ILEDVAVCMD LDTRTTSSLW KDKAAVEINL AVLHSFQKQAK
eNOS_HUMAN RNLCDPHRYN ILEDVAVCMD LDTRTTSSLW KDKAAVEINV AVLHSYQKQAK
nNOS_HUMAN RDYCDNSRYN ILEEVAKKMN LDMRKTSSLW KDQALVEINI AVLYSFQSDK
nNOS_RAT RDYCDNSRYN ILEEVAKKMD LDMRKTSSLW KDQALVEINI AVLYSFQSDK

651 700
iNOS_MOUSEVTIMDHHTAS ESFMKHMONE YRARGGCPAD WIWLVPVSG SITPVFQHEM
iNOS_RAT VTIMDHHTAS ESFMKHMONE YRARGGCPAD WIWLVPVSG SITPVFQHEM
iNOS_HUMAN VTIMDHHSAA ESFMKYMONE YRSRGGCPAD WIWLVPMSG SITPVFQHEM
eNOS_BOVIN VTIVDHHAAT VSFMKHLDNE QKARGGCPAD WAWIVPPISG SLTPVFQHEM
eNOS_HUMAN VTIVDHHAAT ASFMKHLNE QKARGGCPAD WAWIVPPISG SLTPVFQHEM
nNOS_HUMAN VTIVDHHSAT ESFIKHMENE YRCRGGCPAD WAWIVPPMSG SITPVFQHEM
nNOS_RAT VTIVDHHSAT ESFIKHMENE YRCRGGCPAD WAWIVPPMSG SITPVFQHEM

701 750
iNOS_MOUSELNYVLSPFYY YQIEPWKTHI WQNEKL.RPR RREIRFRVLV KVVFFASMLM
iNOS_RAT LNYVLSPFYY YQIEPWKTHI WQDEKL.RPR RREIRFTVLV KAVFFASVLM
iNOS_HUMAN LNYVLSPFYY YQVEAWKTHV WQDEKR.RPK RREIPLKVLV KAVLFACMLM
eNOS_BOVIN VNYILSPAFR YQDPWPWKGSA TKGAGITRKKTFKEVA NAVKISASLM
eNOS_HUMAN VNYFLSPAFR YQDPWPWKGSA AKGTGITRKKTFKEVA NAVKISASLM
nNOS_HUMAN LNYRLTPSFE YQDPWNTHV WKGTNGTPTK RRAIGFKKLA EAVKFSAKLM
nNOS_RAT LNYRLTPSFE YQDPWNTHV WKGTNGTPTK RRAIGFKKLA EAVKFSAKLM

751 800
iNOS_MOUSERKVMASRVRA TVLFATETGK SEALARDLAT LFSYAFNTKV VCMDQYKAST
iNOS_RAT RKVMASRVRA TVLFATETGK SEALARDLAA LFSYAFNTKV VCMEQYKANT
iNOS_HUMAN RKTMASRVRA TILFATETGK SEALAWDLGA LFSCAFNPKV VCMDKYRLSC
eNOS_BOVIN GTLMAKRVKA TILYASETGR AQSYAQQQGR LFRKAFDPRV LCMDEYDVVS
eNOS_HUMAN GTVMAKRVKA TILYGSETGR AQSYAQQQGR LFRKAFDPRV LCMDEYDVVS
nNOS_HUMAN GQAMAKRVKA TILYATETGK SQAYAKTLCE IFKHAFDAKV MSMEYDIDVH
nNOS_RAT GQAMAKRVKA TILYATETGK SQAYAKTLCE IFKHAFDAKA MSMEYDIDVH

801 850
iNOS_MOUSELEEEQLLLHV TSTFGNGDCP SNGQTLKKS L FMLRELNH...
iNOS_RAT LEEEQLLLHV TSTFVNGDCP SNGQTLKKS L FMMKELGH...
iNOS_HUMAN LEEERLLLHV TSTFGNGDCP GNKEKLKKS L FMLKELNN...
eNOS_BOVIN LEHEALVLV TSTFGNGDPP ENGESFAAAL MEMSGPYNSS PRPEQHKS YK
eNOS_HUMAN LEHETLVLV TSTFGNGDPP ENGESFAAAL MEMSGPYNSS PRPEQHKS YK
nNOS_HUMAN LEHETLVLV TSTFGNGDPP ENGEKFGCAL MEMRHP...N SVQEERKS YK
nNOS_RAT LEHEALVLV TSTFGNGDPP ENGEKFGCAL MEMRHP...N SVQEERKS YK

851 900

iNOS_MOUSE.....TFRYAVF GLGSSMYPQF
iNOS_RAT.....TFRYAVF GLGSSMYPQF
iNOS_HUMAN.....KFRYAVF GLGSSMYPRF
eNOS_BOVIN IRFNSVSCSD PLVSSWRRKR KESSNTDSAG ALGTLRF CVF GLGSRAYPHF
eNOS_HUMAN IRFNSISCS D PLVSSWRRKR KESSNTDSAG ALGTLRF CVF GLGSRAYPHF
nNOS_HUMAN VRFNSVSSYS DSQKSSG DGP DLRDNFESAG PLANVRFSVF GLGSRAYPHF
nNOS_RAT VRFNSVSSYS DSRKSSG DGP DLRDNFESTG PLANVRFSVF GLGSRAYPHF

901 950

iNOS_MOUSECAFAHDIDQK LSHLGASQLA PTGEGDELSG QEDAFRSWAV QTFRACETF
iNOS_RAT CAFAHDIDQK LSHLGASQLA PTGEGDELSG QEDAFRSWAV QTFRACVFP
iNOS_HUMAN CAFAHDIDQK LSHLGASQLT PMGEGDELSG QEDAFRSWAV QTFKAACETF
eNOS_BOVIN CAFARAVDTR LEELGGERLL QLGQGDDEL CG QEEAFRGWAK AAFQASCETF
eNOS_HUMAN CAFARAVDTR LEELGGERLL QLGQGDDEL CG QEEAFRGWAK AAFQACETF
nNOS_HUMAN CAFGHA VDTL LEELGGERIL KMREGDEL CG QEEAFRTWAK KVFKAACDV F
nNOS_RAT CAFGHA VDTL LEELGGERIL KMREGDEL CG QEEAFRTWAK KVFKAACDV F

951 1000

iNOS_MOUSEDVRSKHHIQI PKR..FTSNA TWEPEQYRLI QSPEPLDLNR ALSSIHAKNV
iNOS_RAT DVRSKH CIQI PKR..YTSNA TWEPEQYKLT QSPESLDL NK ALRSIHAKNV
iNOS_HUMAN DVRGKQHIQI PKL..YTSNV TWDPHHYRLV QDSQPLDL SK ALSSMHAKNV
eNOS_BOVIN CVGEEAK..A AAQDIFSPKR SWKRQRYRLS TQAEGLQLLP GLIHVHRRKM
eNOS_HUMAN CVGEDAK..A AARDIFSPKR SWKRQRYRLS AQAEGQLLP GLIHVHRRKM
nNOS_HUMAN CVGDDVNIEK ANNSLISNDR SWKRNFRLT FVAEAPELTQ GLSNVHKRV
nNOS_RAT CVGDDVNIEK PNNLSLISNDR SWKRNFRLT YVAEAPDLTQ GLSNVHKRV

1001 1050

iNOS_MOUSEFTMRLKSQQN LQSEKSSRTT LLVQLTFEGS RGPSYLPGEH LGIFPGNQTA
iNOS_RAT FTMRLKSLQN LQSEKSSRTT LLVQLTFEGS RGPSYLPGEH LGIFPGNQTA
iNOS_HUMAN FTMRLKSRQN LQSPTSSRAT ILVELSCEDG QGLNYLPGEH LGVCPGNQPA
eNOS_BOVIN FQATVLSVEN LQSSKSTRAT ILVRLDTAGQ EGLQYQPGDH IGICPPNRP G
eNOS_HUMAN FQATIRSVEN LQSSKSTRAT ILVRLDTGGQ EGLQYQPGDH IGVCPPNRP G
nNOS_HUMAN SAARLLSRQN LQSPKSSRST IFVRLHTNGS QELQYQPGDH LGVFPGNHED
nNOS_RAT SAARLLSRQN LQSPKFSRST IFVRLHTNGN QELQYQPGDH LGVFPGNHED

1051 1100

iNOS_MOUSELVQGILERVV DCPTPHQTV C LEVLDESG...SYWVKD KRLPPCSLSQ
iNOS_RAT LVQGILERVV DCSSPDQTV C LEVLDESG...SYWVKD KRLPPCSLRQ
iNOS_HUMAN LVQGILERVV DGPTPHQTV R LEDLDESG...SYWVSD KRLPPCSLSQ
eNOS_BOVIN LVEALLSRVE DPPPPTESVA VEQL.EKGSP GGPPPSWVRD PRLPPCTLRQ
eNOS_HUMAN LVEALLSRVE DPPAPTEPVA VEQL.EKGSP GGPPPGWVRD PRLPPCTLRQ
nNOS_HUMAN LVNALIERLE DAPPVNQMV K VELLEERNTA LGVISNWTDE LRLPPCTIFQ
nNOS_RAT LVNALIERLE DAPPANHVVK VEMLEERNTA LGVISNWKDE SRLPPCTIFQ

1101 1150

iNOS_MOUSEALTYFLDITT PPTQLQLHKL ARFATDETDR QRLEALCQ.P SEYNDWKFSN
iNOS_RAT ALTYFLDITT PPTQLQLHKL GRFATEETHR QRLEALCQ.P SEYNDWKFSN
iNOS_HUMAN ALTYS PDITT PPTQLLLQKL AQVATEEPER QRLEALCQ.P SEYSKWKF TN
eNOS_BOVIN ALTFFLDITS PPSRLLRLL STLAEEPSEQ QELETLSQDP RRYE EWK WFR
eNOS_HUMAN ALTFFLDITS PPSQLLRLL STLAEEPSEQ QELETLSQDP RRYE EWK WFR
nNOS_HUMAN AFKYLDITT PPTPLQLQOF ASLATSEKEK QRLLVLSKGL QEYEEWKW GK
nNOS_RAT AFKYLDITT PPTPLQLQOF ASLATNEKEK QRLLVLSKGL QEYEEWKW GK

1151 1200

iNOS_MOUSENPTFLEVLEE FPSLVPAAF LLSQLPILKP RYYSISSSQD HTPSEVHLTV
iNOS_RAT NPTFLEVLEE FPSLRVPAAF LLSQLPILKP RYYSISSSQD HTPSEVHLTV
iNOS_HUMAN SPTFLEVLEE FPSLRVSAGF LLSQLPILKP RFYYSISSRD HTPTEIHLTV
eNOS_BOVIN CPTLLEVLEQ FPSVALPAPL LLTQLPLLQ P RYYSVSSAPN AHPGEVHLTV
eNOS_HUMAN CPTLLEVLEQ FPSVALPAPL LLTQLPLLQ P RYYSVSSAPS THPGEIHLTV
nNOS_HUMAN NPTIVEVLEE FPSIQMPATL LLTQLSLLQ P RYYSISSSPD MYPDEVHLTV
nNOS_RAT NPTMVEVLEE FPSIQMPATL LLTQLSLLQ P RYYSISSSPD MYPDEVHLTV

1250

1201

iNOS_MOUSEAVVTYRTRDG QGPLHHGVCS TWIRNLKPQD PVPCFVRSVS GFQLPEDPSQ
iNOS_RAT AVVTYRTRDG QGPLHHGVCS TWIRNLKPED PVPCFVRSVS GFQLPEDPSQ
iNOS_HUMAN AVVTYHTGDG QGPLHHGVCS TWLNSLKPQD PVPCFVRNAS AFHLPEDPSH
eNOS_BOVIN AVLAYRTQDG LGPLHYGVCS TWLSQLKTGD PVPCFIRGAP SFRLPPDPYV
eNOS_HUMAN AVLAYRTQDG LGPLHYGVCS TWLSQLKPGD PVPCFIRGAP SFRLPPDPSL
nNOS_HUMAN AIVSYRTRDG EGPIHHGVCS SWLNRIQADE LVPCFVRGAP SFHLPRNPQV
nNOS_RAT AIVSYHTRDG EGPVHHGVCS SWLNRIQADD VVPCFVRGAP SFHLPRNPQV

1300

1251

iNOS_MOUSEPCILIGPGTG IAPFRSFWQO RLHDSQHKGL KGRMSLVFG CRHPEEDHLY
iNOS_RAT PCILIGPGTG IAPFRSFWQO RLHDSQHRGL KGRMTLVFG CRHPEEDHLY
iNOS_HUMAN PCILIGPGTG IVPFRSFWQO RLHDSQHKGV RGRMTLVFG CRRPDEDHIY
eNOS_BOVIN PCILVGPGTG IAPFRGFWE RLHDIESKGL QPAPMTLVFG CRCSQLDHLIY
eNOS_HUMAN PCILVGPGTG IAPFRGFWE RLHDIESKGL OPTPMTLVFG CRCSQLDHLIY
nNOS_HUMAN PCILVGPGTG IAPFRSFWQO RQFDIQHKGM NPCPMVLVFG CRQSKIDHIY
nNOS_RAT PCILVGPGTG IAPFRSFWQO RQFDIQHKGM NPCPMVLVFG CRQSKIDHIY

1350

1301

iNOS_MOUSEQEEMQEMVRK RVLFQVHTGY SRLPGKPKVY VQDILQKOLA NEVLSVLHGE
iNOS_RAT QEEMQEMVRK GVLQVHTGY SRLPGKPKVY VQDILQKELA DEVFSVLHGE
iNOS_HUMAN QEEMLEMAQK GVLHAVHTAY SRLPGKPKVY VQDILRQOLA SEVLRVLHKE
eNOS_BOVIN RDEVQDAQER GVFGVLTAF SREPDPKTY VQDILRTELA AEVHRVLCLE
eNOS_HUMAN RDEVQNAQOR GVFGVLTAF SREPDPKTY VQDILRTELA AEVHRVLCLE
nNOS_HUMAN REETLQAKNK GVFRELYTAY SREPDPKPKY VQDILQEQLA ESVYRALKEQ
nNOS_RAT REETLQAKNK GVFRELYTAY SREPDRPKKY VQDVLQEQLA ESVYRALKEQ

1400

1351

iNOS_MOUSEQGHLYICGDV RMARDVATTL KKLVAATKLN SEEQVEDYFF QLKSOQRYHE
iNOS_RAT QGHLYVCGDV RMARDVATTL KKLVAATKLN SEEQVEDYFF QLKSOQRYHE
iNOS_HUMAN PGHLYVCGDV RMARDVAHTL KQLVAATKLN NEEQVEDYFF QLKSOQRYHE
eNOS_BOVIN RGHMFVCGDV TMATSVLQTV QRILATEGDM ELDEAGDVIG VLRDQORYHE
eNOS_HUMAN RGHMFVCGDV TMATSVLQTV QRILATEGDM ELDEAGDVIG VLRDQORYHE
nNOS_HUMAN GGHYVCGDV TMAADVLKAI QRIMTQQGKL SAEDAGVFIS RMRDDNRYHE
nNOS_RAT GGHYVCGDV TMAADVLKAI QRIMTQQGKL SEEDAGVFIS RLRDDNRYHE

1446

1401

iNOS_MOUSEDIFGAVFSYG AKKGSALEEP KATRL.....
iNOS_RAT DIFGAVFSYG AKKGNTLEEP KGTRL.....
iNOS_HUMAN DIFGAVFPYE AKKDRVAVQP SSLEMSAL.. ..
eNOS_BOVIN DIFGLTLRTQ EVTSRIRTQS FSLQERHLRG AVPWAFDPPG PDTPGP *
eNOS_HUMAN DIFGLTLRTQ EVTSRIRTQS FSLQERHLRG AVPWAFDPPG SDTNSP *
nNOS_HUMAN DIFGVTLRTI EVTNRLRSES IAFIEESKKD TDE.VFSS.. ..
nNOS_RAT DIFGVTLRTY EVTNRLRSES IAFIEESKKD ADE.VFSS.. ..

* human and bovine eNOS sequences carry on for approximately 80 more amino acids which are not shown here (carboxyl-terminal sequence is not clearly sequenced in eNOS).

A6: STATISTICAL TESTS USED TO COMPARE MUCUS THICKNESS

RESULTS

Kruskal-Wallis Test

Analysis of mucus thickness results to investigate whether significant differences exist between results obtained from different treatments was carried out using the Kruskal-Wallis test, often called an analysis of variance by ranks.

Table A6 A: Rank values assigned for Kruskal-Wallis test

Treatment	Rank Values for Separate Experiments						Rank Sums
Control	1	3	11	12	17	19	63
Control + L-NAME	2	14	22	25	29	31	123
Carbachol	16	18	35	38	44	34	185
Carbachol + L - NAME	4	7	10	13	15	28	77
Carbachol + L - NAME + D-Arg	5	6	9	20	23	26	89
Carbachol + L - NAME + L-Arg	8	27	30	32	40	48	185
DmPGE ₂	21	24	36	37	39	42	199
DmPGE ₂ + L - NAME	33	41	43	45	46	47	255

Mean mucus thickness values from single experiments for eight treatments were assigned rank numbers and rank sums were calculated for each treatment (Table A6 A). The Kruskal-Wallis statistic (H) was calculated using the following equation where N=Total number of rank values; R_i =sum of the ranks; n_i =number of observations in each group; k=number of treatments; N=total number of observations; i=group number:

$$H = \frac{12}{N(N+1)} \sum_{i=1}^k \frac{R_i^2}{n_i} - 3(N+1)$$

The value for H calculated for the mucus results was 28.17 which when compared to a statistical table showed a significance of $p < 0.001$, indicating a significant difference between groups.

Non-parametric equivalent of the Newman-Keuls Test

To determine between which of the treatments significant differences occur a non-parametric equivalent of the Newman-Keuls test was employed. Rank sums from the Kruskal-Wallis test were placed in ascending order (see Figure A6 B). Comparisons were made between treatment groups by first calculating the difference between the rank sums of the two groups. The standard error between the groups was then calculated using the following formula where n = number of observations in each treatment group; p = range of rank sums delimited in the comparison:

$$S.E. = \sqrt{\frac{n(np)(np+1)}{12}}$$

A statistic, q, was then calculated by dividing the difference of rank sums for a particular comparison with the standard error. The q value was then compared to a statistical table in order to discover if the difference between the two treatment compared was significant.

Table A6 B: Rank sums placed in ascending order for non-parametric equivalent of the Newman-Keuls test

Treatment	Rank of Rank Sums	Rank sums
Control	1	63
Carbachol + L-NAME	2	77
Carbachol + L-NAME + D-Arginine	3	89
Control + L-NAME	4	123
Carbachol	5	185*
Carbachol + L-NAME + L-Arginine	6	185*
DmPGE ₂	7	199
DmPGE ₂ + L-NAME	8	255

* These two rank sums are equal and were therefore placed in order according to the mean mucus values for these treatments (carbachol > carbachol + L-NAME + L-Arginine).

A7: PUBLICATIONS RESULTING FROM THIS WORK

Papers

Price, K. J., Hanson, P. J. & Whittle B. J. R. (1994). Stimulation by carbachol of mucus gel thickness in rat stomach involves nitric oxide. *European Journal of Pharmacology*, 263, 199-202.

Price, K. J., Hanson, P. J. & Whittle B. J. R. (1996) Localisation of constitutive isoforms of nitric oxide synthase in rat gastric glandular mucosa. *Cell and Tissue Research*, 285, 157-163.

Abstracts

Brown, J. F., Price, K. J., Williams, J. M., Hanson, P. J. & Whittle B. J. R. (1995). Localisation and properties of nitric oxide synthase in rat gastric mucosa. *Gastroenterology*, 108, A955.

Williams, J. M., Price, K. J. & Hanson, P. J. (1995). Investigation of the calcium dependency of nitric oxide synthase induced in rat colonic mucosa by intravenous lipopolysaccharide. *Biochemical. Society Transactions*, 23, 455 S.

Price, K. J., Hanson, P. J., Byrne, C. R. & Whittle B. J. R. (1995). Nitric oxide synthase in the rat gastric mucosa: isoforms, localisation, and regulation. *Endothelium* 3, S103.

Price, K. J. and Hanson, P. J. (1996) Gastric mucosal nitric oxide synthase: A neuronal form with an unstable modification close to the carboxyl-terminus. *FEBS Abstracts* 24, 94.